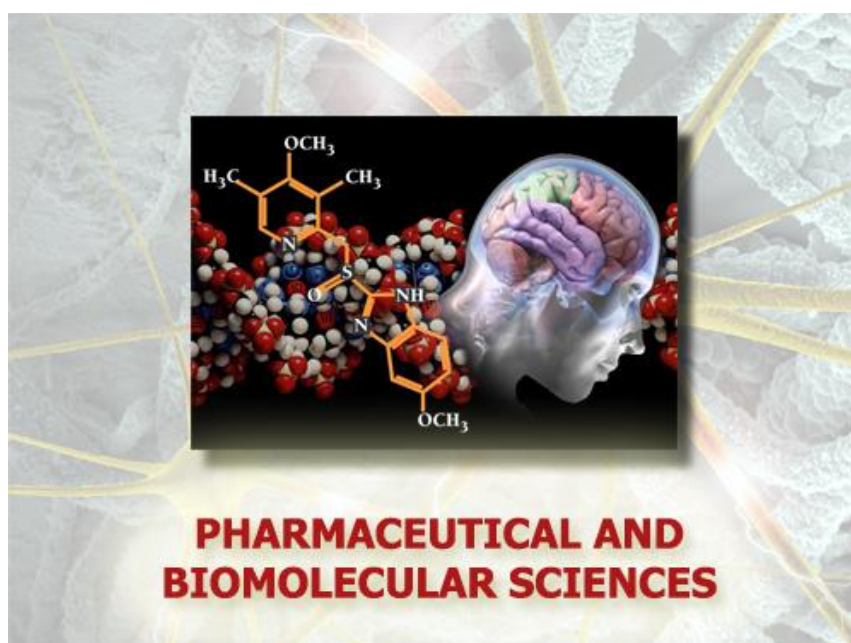


**Università degli Studi di Torino**



**Scuola di Dottorato in  
Scienze della Natura e Tecnologie Innovative**

**Dottorato in  
Scienze Farmaceutiche e Biomolecolari  
(XXXIV ciclo)**



**Process intensification  
for extraction and sustainable conversion  
of biomass derived compounds**

**Candidate: Francesco Mariatti  
Tutor: Prof. Giancarlo Cravotto  
Co-Tutor: Prof. Silvia Tabasso**



**Università degli Studi di Torino**



**Dottorato in Scienze Farmaceutiche e Biomolecolari**

**Tesi svolta presso il Dipartimento di Scienza e Tecnologia del  
Farmaco**

**CICLO: XXXIV**

**TITOLO DELLA TESI:** Process intensification for extraction and sustainable conversion of biomass derived compounds

**TESI PRESENTATA DA:** Francesco Mariatti

**TUTOR:** Prof. Giancarlo Cravotto

**CO-TUTOR:** Prof.ssa Silvia Tabasso

**COORDINATORE DEL DOTTORATO:** Prof.ssa Roberta Cavalli

**ANNI ACCADEMICI:** 2018/2021

**SETTORE SCIENTIFICO-DISCIPLINARE DI AFFERENZA:** CHIM/06



## SUMMARY

AIM AND PREFACE .....	1
1. INTRODUCTION: CIRCULAR AND SUSTAINABLE BIO BASED ECONOMY .....	3
1.1. CIRCULAR ECONOMY (CE) .....	4
1.2. BIOREFINERY: THE CIRCULAR BIO-BASED ECONOMY .....	6
1.2.1. Biorefinery: feedstocks .....	7
1.2.1.1. Second generation biomasses .....	8
1.2.2. The role of green chemistry in biorefinery development .....	10
1.2.3. Biorefinery: towards old and new products .....	11
1.2.4. New green “smart” technologies for biorefinery development .....	14
1.2.4.1. Microwave heating .....	14
1.2.4.2. Ultrasound irradiation .....	17
1.2.5. Focus: green extractions as preliminary step for biorefinery .....	18
1.3. REFERENCES .....	22
2. MONOSACCHARIDES PRODUCTION FROM TOMATO-PLANT RESIDUES FOR MIXED-CULTURE FERMENTATION .....	25
2.1. INTRODUCTION .....	26
2.1.1. Alternatives to conventional petroleum-based plastics .....	26
2.1.2. Alternatives to conventional petroleum-based plastics: polyhydroxyalkanoates ...	26
2.1.2.1. Polyhydroxyalkanoates: properties and applications .....	27
2.1.2.2. Polyhydroxyalkanoates: industrial aspects .....	28
2.1.2.2.1. Feedstocks for nutritional medium .....	30
2.1.2.2.2. Microbial culture selection: advantages/limitations of pure microbial cultures and mixed microbial cultures .....	31
2.1.2.2.3. PHA extraction and recovery .....	31
2.2. RESULTS AND DISCUSSION .....	33
2.2.1. Post-harvest tomato plant (PHTP) for monosaccharides production .....	33
2.2.2. PHTP-derived monosaccharides fermentation with mixed microbial culture .....	40
2.3. CONCLUSIONS .....	47
2.4. EXPERIMENTAL .....	48
2.5. REFERENCES .....	52
3. PRODUCTION OF 5-(HYDROXYMETHYL)FURFURAL HALOGENATED DERIVATIVES .....	55
3.1. INTRODUCTION .....	56
3.1.1. 5-(hydroxymethyl)furfural .....	56
3.1.2. 5-(halomethyl)furfurals: hydrophobic analogues of 5-HMF .....	59
3.2. RESULTS AND DISCUSSION .....	64
3.2.1. Multimode MW reactor and LiBr·nH <sub>2</sub> O + HBr (dil.) .....	66
3.2.2. Monomode MW reactor and LiBr·nH <sub>2</sub> O + HBr (dil.) .....	69

3.2.3. Monomode MW reactor and HBr (conc.).....	70
3.2.4. Multimode MW reactor and HBr (conc.).....	71
3.2.5. CMF production from cellulose and biomass PHTP .....	78
3.3. CONCLUSIONS.....	80
3.4. EXPERIMENTAL .....	82
3.5. REFERENCES.....	86
4. SUSTAINABLE VALORISATION OF LIGNINS .....	88
4.1. INTRODUCTION .....	89
4.1.1. Lignin: structure and composition .....	89
4.1.2. Lignin in biorefinery processes.....	90
4.1.3. Biomass pre-treatments for lignin recovery/isolation.....	91
4.1.4. Oxidative valorisation of lignin .....	92
4.2. RESULTS AND DISCUSSION .....	96
4.2.1. Sustainable microwave-assisted aerobic oxidation of tomato plant waste into bioaromatics and organic acids .....	96
4.2.2. Sustainable microwave-assisted aerobic oxidation of lignins from grape stalks into bioaromatics and long chain fatty acids .....	102
4.3. CONCLUSIONS.....	109
4.4. EXPERIMENTAL .....	110
4.5. REFERENCES.....	112
5. COCOA BY-PRODUCT VALORISATION: A BIOREFINERY APPROACH.....	115
5.1. INTRODUCTION .....	116
5.1.1. Cocoa pod husk composition .....	117
5.1.2. Secondary metabolites from cph: polyphenols .....	118
5.2 RESULTS AND DISCUSSION .....	121
5.2.1 cocoa pod husk extraction.....	121
5.2.2. Valorisation of residual husk .....	127
5.3. CONCLUSIONS.....	130
5.4. EXPERIMENTAL .....	131
5.5. REFERENCES.....	134
6. CYCLIC ACETALS PRODUCTION FROM RENEWABLE DIOLS AND POLYOXYMETHYLENE PLASTIC WASTE .....	136
6.1. INTRODUCTION .....	137
6.1.1. Recycling processes for plastic wastes .....	137
6.1.1.1. Microwave-assisted plastic waste recycling .....	138
6.1.2. Polyoxymethylene: production and recycling.....	139
6.1.3. C2-C4 diols production from renewable feedstocks.....	140
6.2. RESULTS AND DISCUSSION .....	142
6.2.1. Metal triflate catalysts.....	143

6.2.2. Solid-acid catalysts .....	148
6.2.2.1. Zeolites .....	148
6.2.2.2. Ion exchange resins .....	152
6.3. CONCLUSIONS .....	156
6.4. EXPERIMENTAL .....	157
6.5. REFERENCES .....	159
GENERAL CONCLUSIONS .....	160
APPENDIX .....	161
ACKNOWLEDGEMENTS .....	162





*“One can see from space how the human race has changed the Earth.  
Nearly all of the available land has been cleared of forest and is now used for agriculture or  
urban development.  
The polar icecaps are shrinking, and the desert areas are increasing.  
At night, the Earth is no longer dark, but large areas are lit up.  
All of this is evidence that human exploitation of the planet is reaching a critical limit.  
But human demands and expectations are ever-increasing.  
We cannot continue to pollute the atmosphere, poison the ocean, and exhaust the land.  
There isn’t any more available.”*

Stephen Hawking, physicist.

*“Orbiting Earth in the spaceship, I saw how beautiful our planet is.  
People, let us preserve and increase this beauty, not destroy it!”*

Yuri Alekseevič Gagarin, cosmonaut and first human in space.

*“A chi cambia strada,  
a chi ha il coraggio di esitare,  
a chi arriva ultimo, e così vince”*

*“To those who change their way,  
to those who have the courage to hesitate,  
to whoever arrives last, and so wins”*

Roberto Mercadini, from his book “Bomba Atomica”



## AIM AND PREFACE

Environmental issues dealing with the accumulation of wastes deriving from anthropic activities began to emerge in 1940s and are nowadays recognised from scientific community as one of main cause of concern for the future of humanity. In 2018 the amount of waste generated in the EU by all economic activities and household was estimated to be 2337 million tonnes, of which 101.7 million tonnes were classified as hazardous (+11.9% respect to 2010). 54.6% of the total waste was subjected to recovery operations such as recycling, backfilling or energy recovery while the remaining 45.5% was landfilled, incinerated without energy recovery or otherwise disposed (source: EUROSTAT)<sup>1</sup>.

At the same time, the increasing scarcity and progressive depletion of non-renewable resources is emerging as one of the most troubling dilemmas of our century, causing high resource volatility prices and problems on supply chains.

Furthermore, the intensive use of fossil resources for energy and materials production has led to severe pollution consequences due to the emissions of greenhouse gasses, seriously endangering the survival of mankind. As stated in the 6th Assessment Report of the Intergovernmental Panel on Climate Change (2021): “It is unequivocal that human influence has warmed the atmosphere, ocean and land. Widespread and rapid changes in the atmosphere, ocean, cryosphere and biosphere have occurred”<sup>2</sup>. This makes the so called “decarbonization” of our society the main priority for a sustainable future.

Consequently, the demand of alternative, cheap, abundant, sustainable, and renewable feedstocks is increasing every year in industrialized and developing countries. A possible candidate for such needs can be found in residual lignocellulosic biomasses, mainly composed of secondary metabolites, cellulose, hemicellulose and lignin. This huge amount of materials produced every year around the world, is usually disposed without any further valorisation. Despite that, owing to their abundance and chemical complexity, residual lignocellulosic biomasses are under investigation as sustainable and renewable source of platform-chemicals for industrial applications. This is leading to the development of the new concept of biorefinery intended as an innovative approach that exploits various biomass feedstocks and sustainable technologies to produce biofuels, bioenergy and bio-based chemicals.

The biorefinery approach, that aims to produce economic value from complete exploitation of lignocellulosic wastes, is consistent with the new economic model of “circular economy” which is expected to overcome the old linear model “take-make-consume-dispose” trough the continuous recirculation of energy and materials in a closed loop minimising waste production.

To achieve the goal of a cleaner and sustainable production the use of non-conventional technologies is crucial. Efficiency enhancement, time and energy savings can result through the adoption of novel enabling technologies opening the way for new sustainable development models.

In the frame of these considerations, the present thesis aims to set up environmental-friendly processes for the complete valorisation of all the biomass components by means of non-conventional technologies such as microwaves and ultrasound.

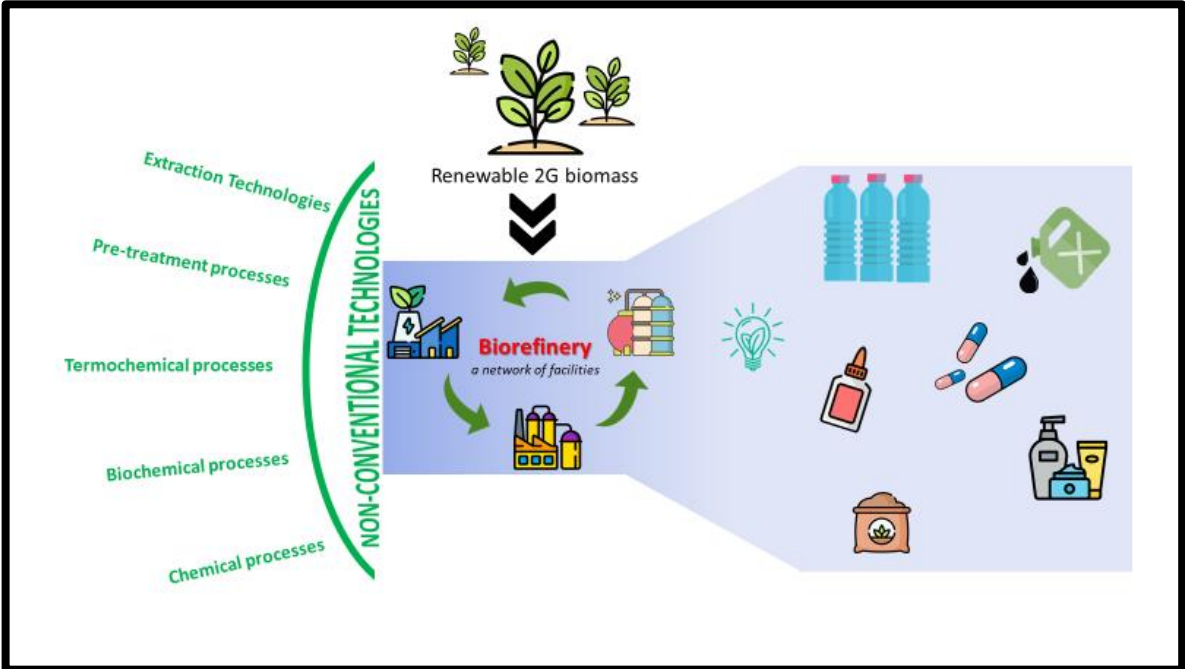
Sustainability, waste reduction and waste valorisation are the guidelines of this work.

Coherently with circular economy principles and biorefinery guidelines illustrated in the introduction, different strategies for second-generation biomasses valorisation will be discussed.

In chapter 2 cellulose and hemicellulose contained in biomass are converted into monosaccharides by means of microwave-assisted acid hydrolysis. Such monosaccharides are further used as substrate for mixed microbial culture fermentation towards polyhydroxyalkanoates, a class of sustainable biobased and biodegradable plastics. Chapter 3 illustrates the conversion of cellulose and biomass into halogenated derivatives of platform molecule 5-hydroxymethylfurfural, namely 5-brominemethylfurfural and 5-chloromethylfurfural. Different microwave technologies and reaction environments are investigated, aiming to maximise sustainability and efficiency of the process. Chapter 4 explores different approaches for lignin valorisation towards platform molecules, in particular bio-aromatics, organic acids and long chain fatty acids. Catalyst free microwave assisted oxidation reactions are reported both directly on raw biomass and on already extracted lignin. The first part of chapter 5 illustrates secondary metabolites (polyphenols) recovery from cocoa industry by-products (cocoa pod husk) by means of microwave assisted subcritical water extraction. In the second part the protocol is extended and integrated by converting the cocoa pod husk residues resulting from extraction into 5-brominemethylfurfural following the optimised procedure described in chapter 3. This is an attempt to confirm the feasibility of biorefinery approach that states the integration of different protocols and technology for full biomass valorisation. In chapter 6, polyoxymethylene plastic residues are recycled and converted into cyclic acetals with the addition of biobased and bioderived renewable diols. The protocol is optimised by cheap catalysts and low reaction times and aims to demonstrate the possibility to include biorefinery products in a chemical recycling protocol.

- (1) [https://ec.europa.eu/eurostat/statistics-explained/index.php?title=Waste\\_statistics](https://ec.europa.eu/eurostat/statistics-explained/index.php?title=Waste_statistics).
- (2) <https://www.ipcc.ch/report/ar6/wg1/>.

# 1. INTRODUCTION: CIRCULAR AND SUSTAINABLE BIO BASED ECONOMY



## 1.1. CIRCULAR ECONOMY (CE)

In March 2021 the European Commission presented a resolution regarding the “new circular economy action plan” as fundamental part of the European Green Deal<sup>1</sup>. The aim of European Green Deal is “to transform the EU into a modern, resource-efficient and competitive economy, ensuring: no net *emissions of greenhouse gases by 2050, economic growth decoupled from resource use, and no person and no place left behind*”<sup>2</sup>.

CE is proposed as a sustainable alternative to the actual predominant linear economic system “take-make-consume-throw away”. Such old and outdated approach derives from the early days of industrialisation: resources and raw materials are extracted from the environment and transformed into goods and products through labour and energy, subsequently they are used by the consumer and finally are discarded.

Linear economy presents several criticalities due to inefficient management of non-renewable resources:

- a high quantity of resources is lost during the production chains
- material recovery at the end-of-life of an item is usually inefficient
- during production chain a high quantity of energy is incorporated into a product (especially in the early stage of resource extraction), but when such product is discarded at the end of his life cycle such energy is lost
- losses in ecosystem services (i.e. benefits provided from the ecosystem that are essential for human well-being)

Such criticalities are negatively impacting the stability of economies (increasing the uncontrolled and unpredictable rise of resources prices due to their scarcity) and endangering the preservation of natural ecosystems<sup>3</sup>.

To overcome these critical issues CE is proposed as an industrial model that is restorative by intention and design. Products and materials are highly valued through reusing, repairing, refurbishing and recycling<sup>4</sup>, in a virtuous cycle that aims to maximise waste reduction and minimise resources losses<sup>5</sup> (Figure 1).

Geissdoerfer et al.<sup>6</sup> in 2017 proposed a comprehensive definition of CE as: “*regenerative system in which resource input and waste, emission, and energy leakage are minimised by slowing, closing, and narrowing material and energy loops. This can be achieved through long-lasting design, maintenance, repair, reuse, remanufacturing, refurbishing, and recycling*”

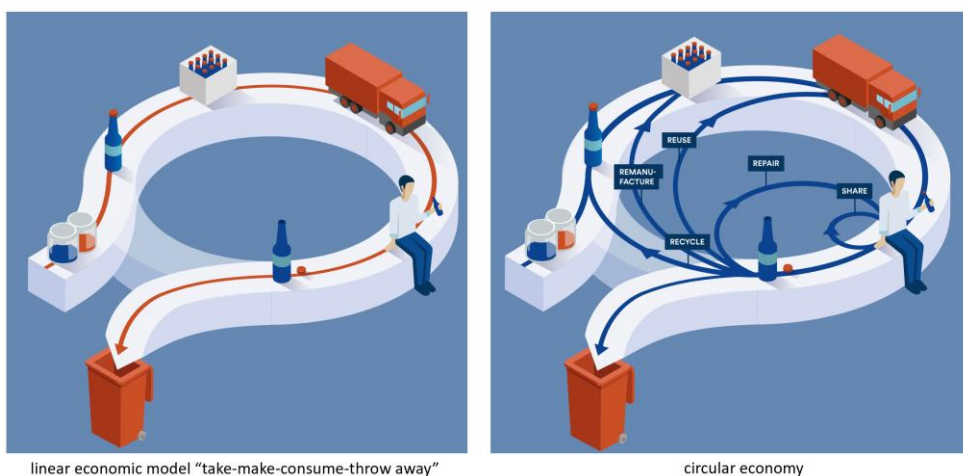


Figure 1: Linear economy and circular economy

According to the description reported in “towards the circular economy” report from the Ellen Macarthur Foundation<sup>3</sup> CE can be graphically represented by two complementary loops as reported in picture. The first loop is for “biological” materials and the second one is for “technical” materials; consumer and user are respectively at the centre of each cycle. The two loops are accompanied by the three main principles of CE (Figure 2)<sup>7,5</sup>.

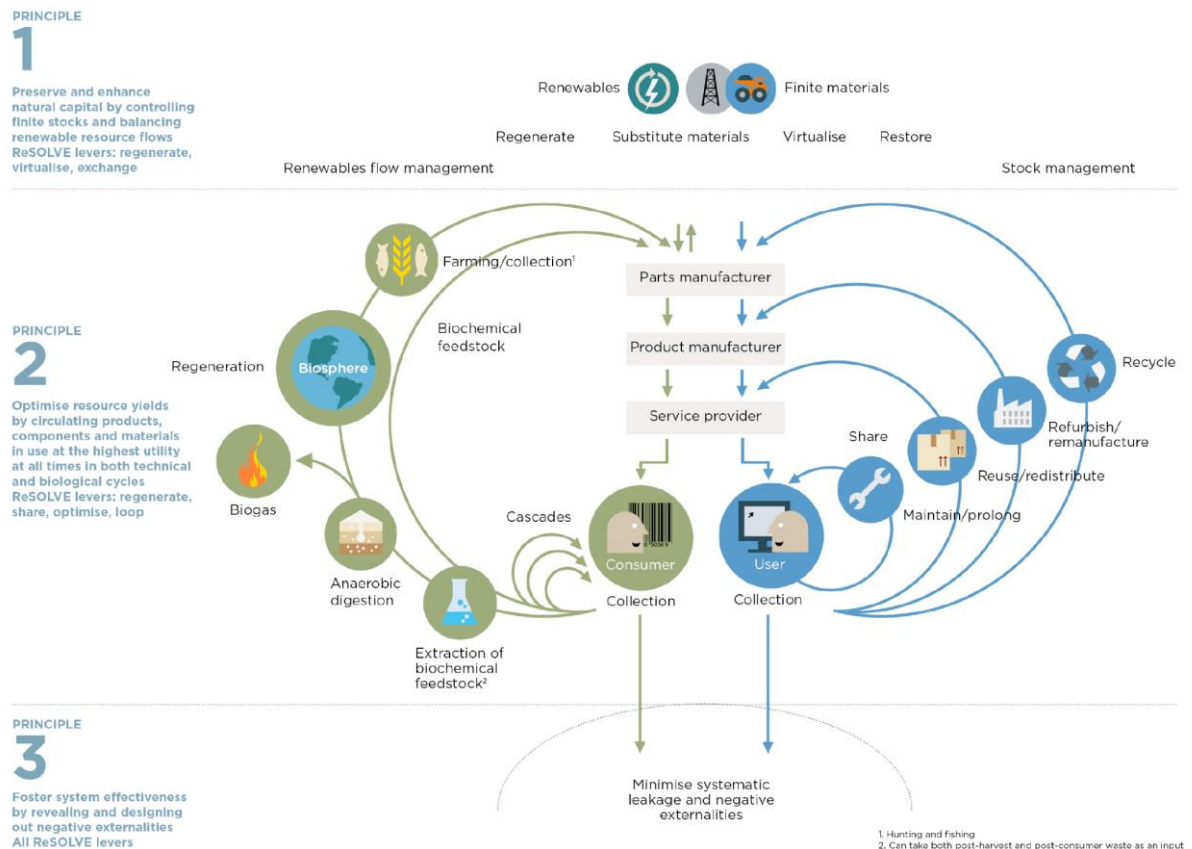


Figure 2: Graphical representation of CE (Ellen Macarthur Foundation)

This new approach favours high added value creation from every industrial process. By-products and wastes recovery and valorisation towards new products are highly promoted. In other words, the waste produced in a certain process should be valorised by using it as raw material for another process<sup>8</sup>.

CE advantages can be summarized as:

- reduction of the pressure on the environment (through reduction of resources depletion)
- enhancement of raw material supply
- competitiveness
- innovation
- economic growth and creation of new jobs<sup>5</sup>

Despite that, a shared and definitive description of CE nowadays is still missing. The need for a clear and shared definition remains mandatory for CE development, being functional to define and overcome barriers that oppose to its development.

This broad concept is recognised to be widely different from other attempts to reduce energy and material consumption.

After a critical analysis of literature works Prieto-Sandoval et al. described CE as<sup>9</sup>:

*“The circular economy is an economic system that represents a change of paradigm in the way that human society is interrelated with nature and aims to prevent the depletion of resources,*

*close energy and materials loops, and facilitate sustainable development through its implementation at the micro (enterprises and consumers), meso (economic agents integrated in symbiosis) and macro (city, regions and governments) levels. Attaining this circular model requires cyclical and regenerative environmental innovations in the way society legislates, produces and consumes.”*

Such definition clearly states the need to develop CE at three levels:

1. The micro-level: firm-specific initiatives through reduction, reuse, recycle for energy, raw materials and waste minimisation,
2. The meso-level: inter-firm initiatives devoted to cross-chain and cross-sector collaborations (i.e. eco-industrial parks, where businesses and industries can cooperate in a shared property to more efficiently use resources),
3. The macro-level: initiatives operated by governments and policymakers to favour CE development.

These three levels are independent and at the same time strictly connected since macro-level initiatives can strongly impact meso- and micro-level initiatives, and micro-level initiatives can unlock future meso-level initiatives<sup>10</sup>.

Grafström and Aasma<sup>10</sup> reported four main barriers to full CE development:

1. Technological barriers: lack of product design for remanufacturing, recycle and reuse at the end of product's lifecycle. Moreover, waste separation technologies and infrastructures are still far from effective and appropriate development;
2. Market barriers: difficulties in CE business models funding, high investment costs and still low virgin material prices;
3. Institutional and regulatory barriers;
4. Social barriers: lack of consumer awareness, weak cooperation throughout supply chain and resistant company culture.

Above mentioned barriers are strictly connected and the removing of one of these barriers can produce a cascade effect of disentanglement, allowing CE progress and worldwide diffusion.

## **1.2. BIOREFINERY: THE CIRCULAR BIO-BASED ECONOMY**

According to the above-mentioned definition of CE formulated by Prieto-Sandoval et al., energy and materials should circulate in a closed loop preventing depletion of non-renewable resources and reducing waste to zero. From this perspective the dependence on non-renewable fossil resources should be heavily reduced or eliminated in favour of renewable substrates. Actual refineries for fuels and chemicals production are based on petroleum, which is neither renewable nor environmentally friendly. Therefore the new concept of biorefinery emerged as a *“strategic mechanism for the realization of a circular bioeconomy”*<sup>11</sup>. As the refinery generates pure chemicals from non-renewable petroleum, the same principle can be transposed to biorefineries whose purpose is the production of pure chemicals and energy from renewable biomasses<sup>12</sup>. Coherently with CE principles, waste biomasses from agriculture, food industry, forestry, aquaculture and households should circulate in a closed loop becoming the input of new production processes for fuels and products instead of being disposed in landfills or environment.

In other words, the biorefinery could answer to the two main needs of CE: continuous recirculation of materials and progressive reduction on non-renewable resources dependence<sup>13</sup>.

As already mentioned, the input of biorefinery is biomass: an abundant and chemically complex raw material that through a series of complex chemical, physical and biotechnological



operations can be fractionated and separated in its main components, and subsequently converted into products. Prior being subjected to these operations, biomasses can also undergo preliminary extraction protocols aiming to recover high added value chemicals such as fragrances, flavouring agents, food-related products, and nutraceuticals<sup>14,15</sup>. Modern biorefineries are expected to develop as a series of different size facilities (a network of facilities) rather than a unique large plant. In such bio-industrial systems, the residue of a certain facility becomes the input of another facility, and so on, allowing the complete exploitation of all biomass' components, coherently with CE definition<sup>15</sup>.

To achieve the goal of an almost complete valorisation of all biomass' components, a combination of several operations and technologies is required, as summarised below<sup>15,16</sup>:

- Extraction technologies for preliminary high added value compounds recovery,
- Pre-treatment processes for feedstocks size reduction and component separations (usually applied prior to subsequent conversion steps),
- Thermochemical processes such as gasification, pyrolysis, liquefaction, hydrothermal processing for conversion into energy and products,
- Biochemical processes such as fermentation and anaerobic digestion,
- Chemical processes for the transformation of feedstocks components into chemical compounds

Extraction technologies for valuable product recovery prior to any other operation, are expected to give a significant contribution in financial returns. Biochemical processes are characterised by low temperatures and high selectivity but also by long times, low space-time yields and difficult downstream operations. From the other side, thermochemical/chemical processes are extremely fast but characterised by low selectivity and high temperatures. In integrated biorefineries combination of biochemical and thermochemical/chemical processes is considered fundamental since they complement each other<sup>17</sup>.

### 1.2.1. Biorefinery: feedstocks

In integrated biorefineries, fuels, chemicals and materials are sustainably produced from renewable biomasses. Thanks to this approach, the substitution of existing products with new recyclable, biodegradable, bio-based alternatives can be promoted<sup>18</sup>.

Feedstocks for biorefinery can have different origins:

1. Agriculture (with dedicated crops and/or agricultural residues)
2. Forestry
3. Industries (process residues) and households (municipal wastes)
4. Aquaculture

Biomasses can be classified in three “generations” (Table 1):

<b>1<sup>st</sup> generation biomasses (1G)</b>	Derived from edible biomasses (starch, seeds)
<b>2<sup>nd</sup> generation biomasses (2G)</b>	Derived from lignocellulosic residual biomasses
<b>3<sup>rd</sup> generation biomasses (3G)</b>	Derived from aquatic carbohydrates

Table 1: The three generations of biomasses

Such classification was commonly used for biofuels and bioethanol, but it can be generally applied for biorefinery feedstocks, independently from the targeted product.

Exploitation of 1G biomasses can led to several ethical, political, and environmental concern, due to the competition of such cultures with food-dedicated cultures, and therefore

exploitation of raw biomasses from agricultural waste or non-food crops (2G) arose as more ethical and sustainable option.

Indeed, 1G biomasses are mainly composed by seeds and grains, while 2G biomasses are derived from a wide variety of agricultural and industrial wastes that do not imply ethical concerns. Moreover, 2G biomasses are intended to be entirely exploited in biorefinery processes while in 1G biomasses, only a small portion is used as feedstock (only grains and seeds). 2G biomasses use is therefore considered more coherent with CE principle of by-products/waste exploitation.

Detailed scheme of the three biomasses generations is reported in Table 2<sup>19</sup>:

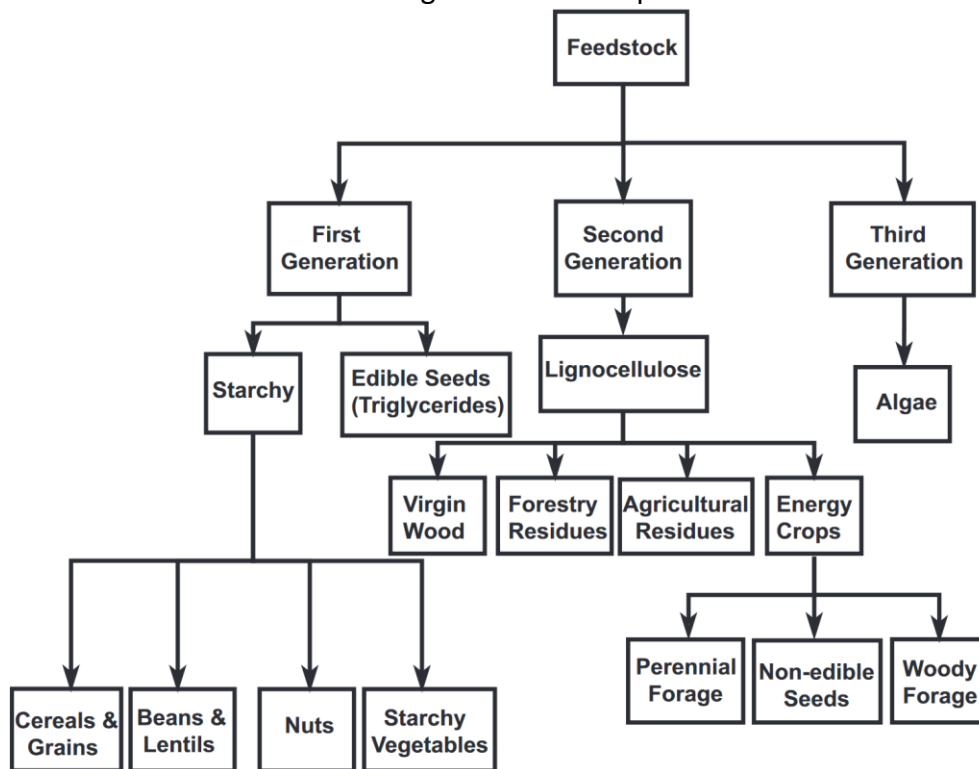


Table 2: Detailed scheme of the three generation of biomasses<sup>19</sup>

One of the crucial challenges of biorefinery relies in the availability and supply of feedstock. Coherent biomass supply will be a fundamental step in the complete development of biorefinery systems. Nowadays several criticalities are still to be overcome being the supply chain of biomasses still in the early stage and therefore highly fragmented, uncoordinated and inconstant. Moreover, also homogeneity in feedstock will be a crucial challenge, being some chemical and biochemical valorisation protocols extremely sensible to feedstock composition changes. Moisture content, long term storage and transportation of biomasses, still represent fundamental points to be considered for large scale biorefinery feasibility and worldwide diffusion<sup>20</sup>.

#### 1.2.1.1. Second generation biomasses

Lignocellulosic residual biomasses are considered promising feedstock for modern biorefineries: every year billions of tons of agricultural residues are produced around the globe, but the major part is usually discarded or incinerated. Moreover, dedicated crops compatible with low-quality soils (not suitable for food crops) can be exploited and included in 2G biomass class, as well as industrial wastes, forestry wastes and municipal solid wastes.

Thus enormous advantages in exploitation of such feedstock rely in their worldwide availability and low price.<sup>21</sup>

Lignocellulosic biomass is composed by two main fractions: a carbohydrate (or polysaccharide) fraction (comprising cellulose and hemicellulose) and a lignin fraction. Such components are arranged in a complex, non-uniform, three-dimensional structure. Relative abundance of constituents and overall resulting structure are highly dependent on biomass type.

During its growth, plant produces primary and secondary walls, characterised by different compositions and role:

- Primary wall is composed of high amounts of pectin and hemicellulose and lower quantity of cellulose,
- Secondary wall is essentially composed of high quantities of cellulose, hemicellulose, and lignin.

Cellulose is the main constituents of plant cell walls (from 30 to 50% of the whole plant). It is a long chain, linear homo-polymer polysaccharide of cellobiose (glucose disaccharide), linked through  $\beta$ -1,4 glycosidic bond. Due to the high number of -OH groups, hydrogen bonds can be formed in the same chain or vicinal chains. Moreover, Van der Waals forces can be established improving cellulose high tensile strength. Cellulose can be characterised by two crystallinity domains: amorphous (low crystallinity) and crystalline. As result the highest is the crystallinity of cellulose, the highest will be its recalcitrance to any treatment.

Cellulose microfibrils are strictly connected with hemicellulose and covered by lignin.

Hemicellulose (15-35% of the whole biomass) is amorphous, random, branched polysaccharide composed by different hexose and pentose such as xylose, glucose, mannose, galactose and arabinose. According to the types of substituent hemicelluloses are classified as xyloglucans, xylans, mannans or galactans. It presents lower polymerisation degree if compared with cellulose. Being more amorphous than cellulose, hemicellulose is more susceptible to various treatments such as chemical or thermal hydrolysis. Hemicellulose role in plants, is to link cellulose and lignin yielding an extremely rigid structure, resistant to chemical treatments. Lignin is the second-most abundant natural polymer (10-20% of whole biomass); it is composed by aromatic units and is the most recalcitrant component of lignocellulosic biomass.

All the constituents previously described are reported to be capable of producing high-added value products<sup>22,23,24</sup>.

The limitation in the use of lignocellulose as raw material in biorefineries is due to the high rigidity and recalcitrance that can led to difficulties in its constituent separation, depolymerisation and conversion. Indeed 1G (starch) hydrolysis is reported to be easier if compared with cellulose hydrolysis.

Schematic representation of biomass structure together with main classes of products that can be achieved from its constituents are reported in Figure 3<sup>23,24</sup>

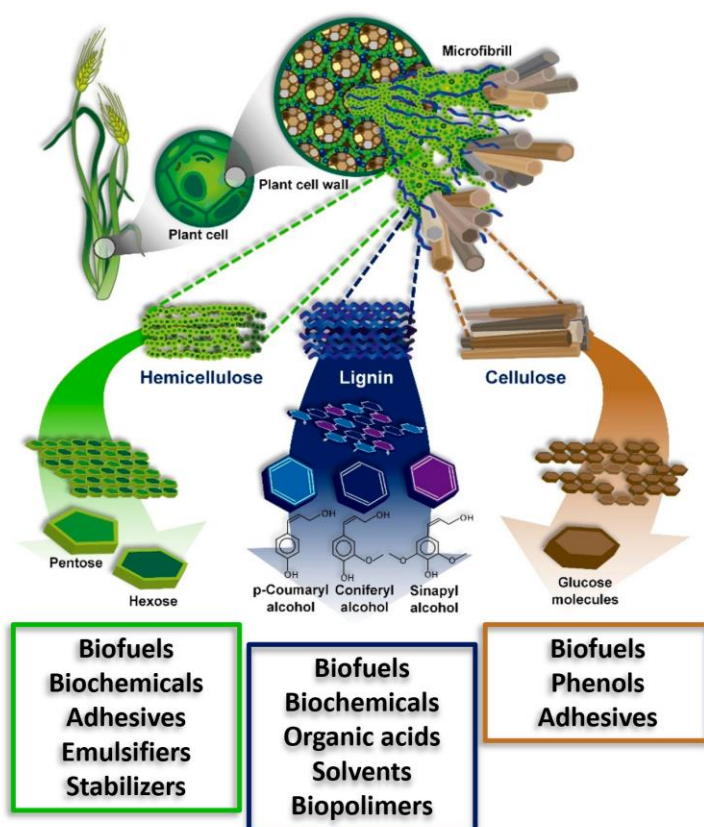


Figure 3: Schematic representation of biomass structure

### 1.2.2. The role of green chemistry in biorefinery development

A general definition of green and sustainable chemistry can be formulated as: *“Green chemistry is the design, development, and implementation of chemical products and processes that reduce or eliminate the use and generation of hazardous substances”* Such definition is the summary of the so called 12 principles of green chemistry, formulated in 1998 by P.T. Anastas and J.C. Warner<sup>25</sup> (Figure 4).

As can be guessed, green chemistry principles are one of the main driving forces for biorefinery: integration of green chemistry principles in the biorefinery concept is expected to be the key for a real and effective biorefinery development. Reduction in energy requirements, operation time and waste generation, together with an increase in resource efficiency, are needed for full application of the biorefinery concept in the frame of CE. Moreover, biorefinery products should be non-toxic, recyclable or easily biodegradable. Clean processes that start from non-polluting, sustainable, low-price feedstocks and lead to (new) environmentally friendly products, seems nowadays hardly attainable, but a crucial role will be played by the adoption of new and sustainable technologies. Many industrial processes are expected to be replaced by new technology introduction that aim to reduce at zero the environmental footprints. As a consequence, not only the process but also the products should be rethought in a sustainable way<sup>26,17</sup>. Only when such objectives will be achieved, biorefinery will be considered competitive with actual oil-based refineries.



Figure 4: The 12 principles of green chemistry<sup>25</sup>

### 1.2.3. Biorefinery: towards old and new products

Despite biofuels production will remain a fundamental goal, also chemicals production will be an important feature of biorefinery. Integration of both biofuels and chemicals production from 2G biomasses is expected to provide better return on investment because of the high added value of chemicals, if compared with fuels.

In other words, biorefineries should incorporate in their portfolio products both biofuels and chemicals to be competitive and economically feasible.

Conversion of lignocellulosic feedstocks to chemical products, intermediates, or building blocks is the least developed and most challenging of biorefinery operations. Indeed, lack of conversion technologies together with an over-abundance of possible target products are the two main obstacles for full biorefinery development.

A definitive group of primary chemicals and secondary intermediates has yet to be definitively defined: potential targets include a combination of molecules already present in the market as product of “conventional” chemistry and new “alternative” molecules derived from lignocellulosic.

In 2004 the US Department of Energy (DOE) released a list of 15 fundamental molecules derived from carbohydrate fractions of biomasses that were expected to become the main carbohydrates derivatives in biorefinery development (Table 3)<sup>27</sup>. Moreover, a second report was released dealing with product classes deriving from lignin (Table 4)<sup>28</sup>.

Succinic, fumaric and malic acids
2,5-Furan dicarboxylic acid
3-Hydroxypropionic acid
Aspartic acid
Glucaric acid
Glutamic acid
Itaconic acid
Levulinic acid
3-Hydroxybutyrolactone
Glycerol
Sorbitol
Xylitol/arabinitol

Table 3: 15 fundamental molecules derived from carbohydrate fractions of biomasses according to DOE<sup>27</sup>

Syngas products
Hydrocarbons
Phenols
Oxidized products
Macromolecules

Table 4: Main product classes derived from lignin fraction of biomasses according to DOE<sup>28</sup>

The two lists were drawn up aiming to provide guidelines for future research, taking into consideration technologic, economic, market and industrial viability factors.

The lists were widely revised and updated in following years<sup>29</sup> highlighting progresses, criticalities and success due to the ever-growing research in the field. Indeed, few years later the publication of DOE list, Bozell and Petersen<sup>29</sup> revised the carbohydrate list (Table 5), defining new products and opportunities from carbohydrate fractions and highlighting that, being in the early stage of development, DOE's list should be considered a dynamic list rather than a definitive concept.

Ethanol
Furans
Furfural
5-hydroxymethylfurfural
FDCA
Glycerol and derivatives
Bio-hydrocarbons
Isoprene
Bio-hydrocarbons
Lactic acid
Succinic acid
Hydroxypropionic acid/aldehyde
Levulinic acid
Sorbitol
Xylitol

Table 5: Fundamental molecules derived from carbohydrate fractions of biomasses according to Bozell and Petersen<sup>29</sup>

More recently (2018) an updated and detailed investigation was provided by Kohli et al.<sup>30</sup> describing platform chemicals derivable from lignocellulose and possible chemicals that can be achieved from such platform molecules (Figure 5).

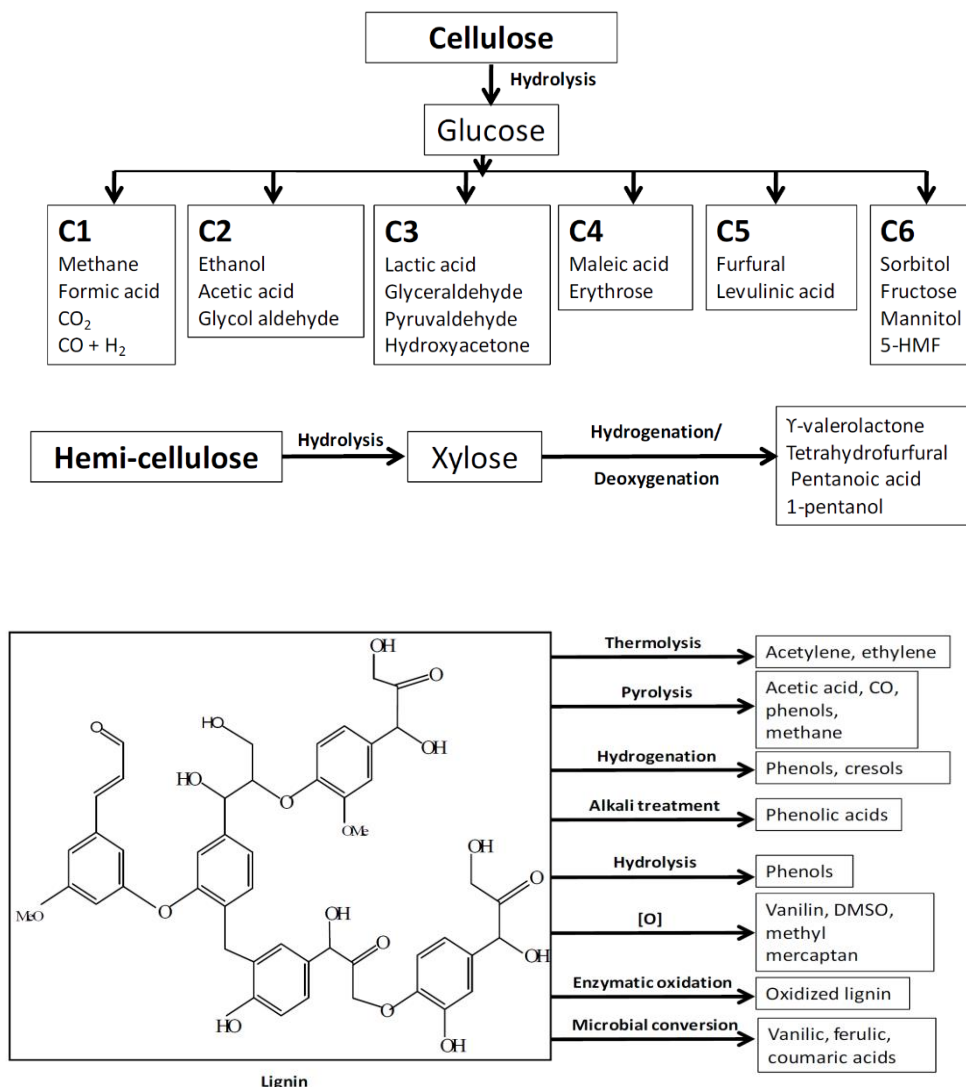


Figure 5: Fundamental molecules derivable from lignocellulose according to Kohli et al.<sup>30</sup>

As previously discussed, the inclusion of chemicals in the portfolio of biorefinery products could increase its economic competitiveness, adding twice the commercial value compared with energy and fuels. Building blocks for plastic materials can be derived from biomasses or replaced with biomass-derived alternatives (as in the case of bisphenol A, that can be replaced with lignin-derived phenols).

Bioplastics, pharmaceuticals (such as antioxidants, vitamins and probiotics), surfactants and food additives can be considered among the main products of biorefinery together with energy and biofuels, as described by Andrade et al.<sup>56</sup> and reported in Figure 6

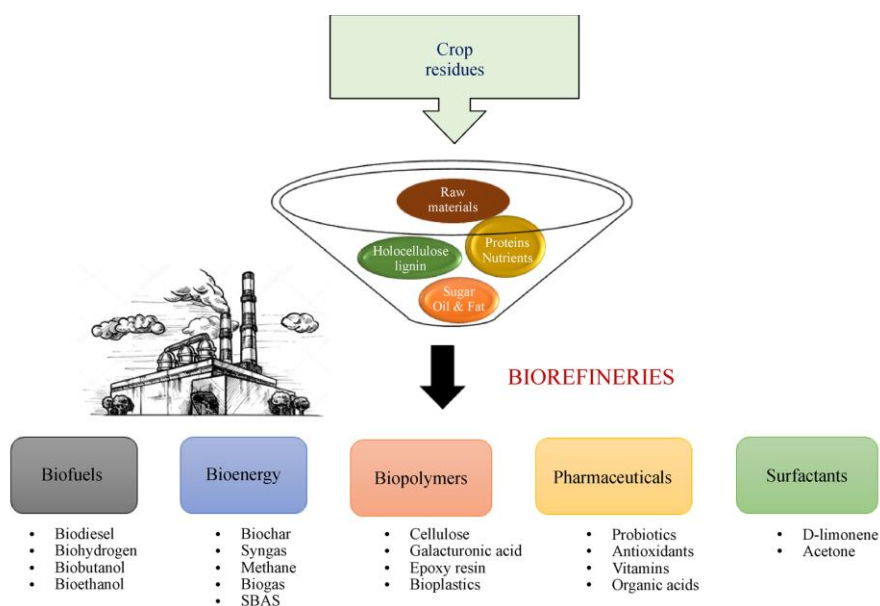


Figure 6: Biorefinery products and their applications

#### 1.2.4. New green “smart” technologies for biorefinery development

Development of new technologies is a crucial step for massive diffusion of biorefinery, aiming to reduce energy consumption and improve the overall process performances. Several promising non-conventional technologies have been developed in recent years for extractions, treatment, and pre-treatment of 2G/3G biomasses. As previously described, biomass’ recalcitrance can therefore be overcome by means of such technologies.

The terms “smart” and “non-conventional” can be used since such technologies possess one or more of subsequent features that makes them a valid alternative to conventional processes: energy-efficiency, quickness, zero-waste, non-hazardous, environmentally friendly (or “green”), easy scalable, low cost, versatile, combinable with other “smart” processes, not requiring use of other chemicals than water<sup>31</sup>. Efficiency in raw material exploitation is the core concept that should make “green”, “smart”, “non-conventional” technologies extremely competitive against conventional processes. Such technologies can be defined, in agreement with Stankiewicz and Moulijn,<sup>32</sup> as process intensification technologies, i.e. any innovative apparatus, technology or technique that can offer reduction in equipment-size/production-capacity ratio, energy consumption and waste generation.

##### 1.2.4.1. Microwave heating

###### Microwave heating theory

Microwaves (MW) are non-ionising electromagnetic radiations in the wavelength range from 1mm to 1m. Their frequency range is comprised between 300MHz and 300GHz. In scientific and industrial applications two frequencies are allowed: 2.45GHz (in lab-scale reactors) and 915MHz (in industrial-scale equipment).

Absorbing materials are materials that can interact with electromagnetic radiation generating heat. Such materials are often defined as “high dielectric-loss materials” or “loss dielectrics”<sup>33</sup>. In MW heating, heat can be generated through two different mechanisms:

- Ionic conduction, where ions migrate following the changes of oscillating field. This generates friction (and so, heat) in solvent and moving ions.



- Dipole rotation, where molecular dipoles tend to align with oscillating field. When molecules fail to align they start a vibrating movement that produces friction and so, heat.

Generated heat depends on the  $\tan\delta$  factor (or dissipation factor) that is described by the following equation:

$$\tan\delta = \frac{\varepsilon^{ii}}{\varepsilon^i}$$

where  $\varepsilon^{ii}$  is defined “dielectric loss” that takes in account the efficiency of microwave conversion into heat, and  $\varepsilon^i$  is the tendency of material to adsorb microwave energy, defined dielectric constant.

High  $\tan\delta$  means high heat generation and high heating rate of the material<sup>33,34</sup>.

MW heating has demonstrated better heating performances in respect to conventional heating. Indeed, conventional conductive heating is slow and characterised by slow energy transfer, being related to thermal conductivity of the media. As shown in picture Figure 7<sup>35</sup> when conductive heating is applied, the sample is heated from the surface to the bulk, and a temperature gradient from the outside to the inside of the sample is established.

From the other hand, when microwave heating is applied, sample is rapidly and homogeneously heated (bulk heating) with a heat gradient reversed respect to conductive heating. Such heating dynamic can't be reproduced by conventional heating techniques and allows the reaction to proceed uniformly in the reaction vessel, resulting in higher yields, milder reaction conditions, and faster reaction times<sup>35,36</sup>.

Some “thermal” effects and features have been identified, influencing and boosting MW heating performances:

Overheating is characterised by heating of polar liquids that can reach temperatures above their boiling point thanks to the bulk heating since the boiling nuclei are formed at the surface of the liquid.

Hot spots can be formed in irradiated sample. At microscopic level, certain zones can show higher temperature respect to the overall macroscopic temperature of the sample. Such conditions are reported to boost reactions conversion, reaching up to 100-200°C higher temperatures than the macroscopic temperature.

Selective heating deals with the ability of different materials to absorb or not MW radiations. Two different solvents (e.g. biphasic solvent systems) can be simultaneously irradiated reaching different temperatures in the two solvents, according to their dielectric properties<sup>36</sup>.

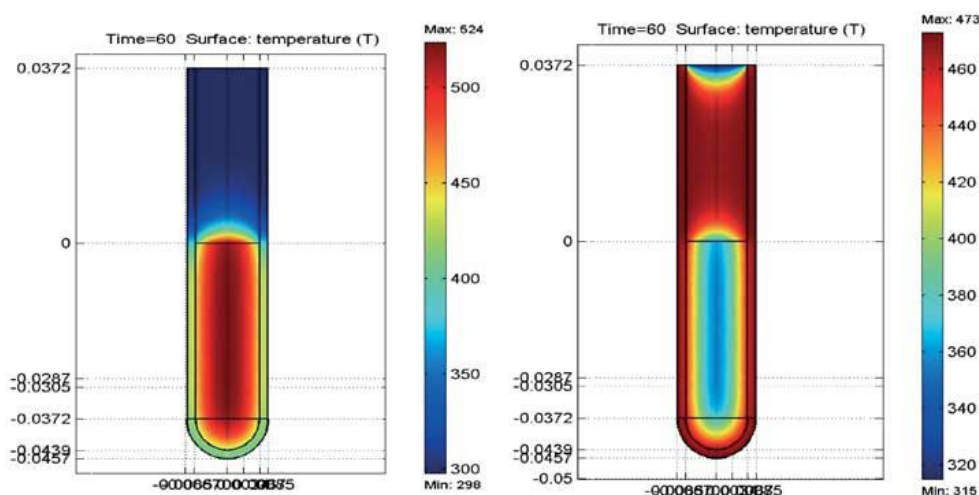


Figure 7: Bulk heating and conductive heating<sup>35</sup>

### Microwave apparatuses configurations

Independently from the configuration, in all MW apparatuses, radiation is usually generated from the magnetron. Subsequently, MW should be transported to the cavity where samples/reactants are located. This can be achieved through proper waveguides or antennas.

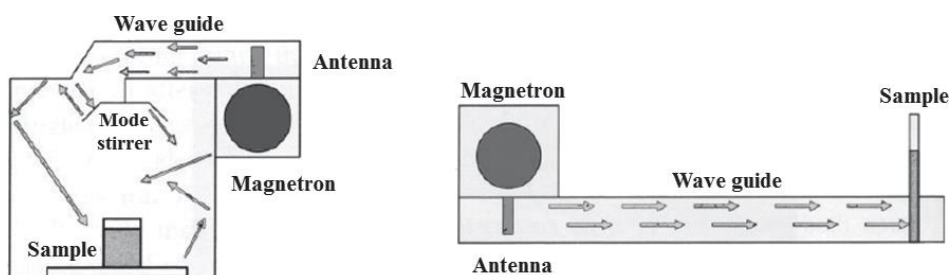


Figure 8: Multimode MW reactor (left) and monomode MW reactor (right)

MW reactors can be grouped in two categories according to the reaction cavity (Figure 8):

- Monomode MW reactors.

In monomode configuration, radiation from the magnetron is directly conveyed to the sample trough the waveguide. Waveguide is designed in a way that cause wave to reflect cophasally thus forming a standing wave with only one wave mode. Radiation penetrates the sample from one side and sample is placed in a small cavity located at the end of the waveguide<sup>37,38</sup>.

- Multimode MW reactors

In multimode configuration radiation from the magnetron passes through a waveguide and enters in a large reaction cavity where one or more samples can be placed. Inside the reaction cavity radiation is reflected by cavity's wall resulting in different wave modes (three-dimensional stationary pattern of standing waves, called modes). Samples are therefore irradiated from every side<sup>37</sup>.

Multimode reactors present the undoubted advantage of allowing to perform simultaneous reactions (more than one sample can be placed in the reaction chamber) or big-scale reactions (high volume of the sample). Monomodal reactors can work only on small-scale and, according to their configuration, a more homogeneous distribution of energy is believed to insist on the sample<sup>39</sup>.

### Microwave heating in 2G biorefinery

Proficient use of MW irradiation in lignocellulosic biomass treatment was reported in past decades. Two approaches can be identified: thermochemical (pyrolysis) and solvolysis.

- Thermochemical processes usually involve pyrolysis at high temperatures (above 400°C) yielding bio-oil, bio-gas and bio-char. MW-assisted treatments are considered valuable alternative to conventional pyrolysis being fast, targeted and energy-efficient<sup>40</sup>.  
During MW assisted pyrolysis biopolymers are deconstructed resulting in liquefaction or gasification of the lignocellulosic matrix. Biofuels and chemicals are produced.
- Solvolysis process involves lower temperatures allowing the hydrolysis of lignocellulosic biomass. Biomass' constituents are therefore depolymerised to produce sugars and value added chemicals<sup>40</sup>.

### 1.2.4.2. Ultrasound irradiation

#### Ultrasound irradiation theory

Ultrasound (US) are sound waves comprised in the range from 20kHz to 10MHz. Propagation of ultrasonic waves in liquid media produces a series of compressions (positive pressure) and expansions (negative pressure) cycles. When negative pressure exceeds certain level (the so-called cavitation threshold) attractive forces of the liquid are overcome and micro-bubbles are formed (nucleation). In other words, nucleation and bubble formation takes place when the rarefaction cycle has enough energy to overcome solvent intermolecular bound. Once the bubbles are formed, an expansion process takes place (rectified diffusion) increasing the dimension of the bubbles themselves. Vapor and/or gas from surrounding media enters the bubbles being subsequently released when the bubbles collapse once a critical dimension of the bubbles is reached. Such a violent collapse (acoustic cavitation) generates local temperatures around 5000K and pressures around 200bar<sup>33,41,42</sup> (Figure 9).

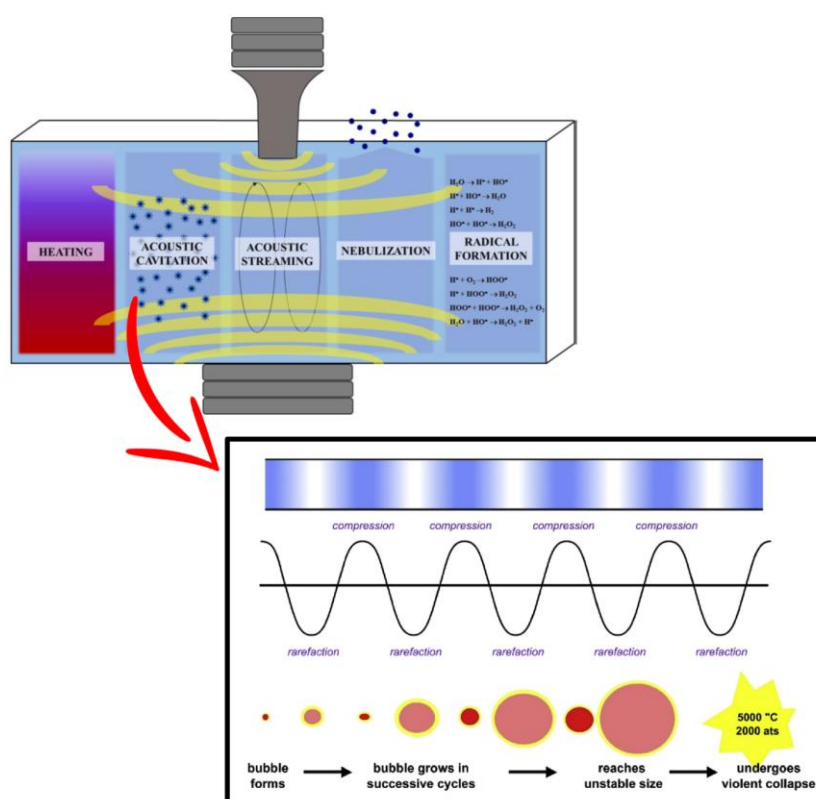


Figure 9: Ultrasound irradiation and his effects<sup>33,34</sup>

Physical and chemical effects are induced in the liquid media when US are applied: acoustic cavitation, heating, acoustic streaming, and nebulisation.

During acoustic cavitation, as results of bubble implosion microjets, shockwaves and micro flow are produced intensifying fluids transport and mass transfer. Moreover, radicals can be formed during bubble collapse at certain values of energy and frequency<sup>41</sup>. According to these considerations, US can be proficiently used both in biomass pre-treatments and biomass conversion to value-added products.

#### Ultrasound irradiation in 2G biorefinery

Most of lignocellulosic biomass pre-treatments (alkaline or acid hydrolysis, extrusion, biological treatments) focused on biomass' component separation/fragmentation usually involve the use of large amounts of reagents, long treatment times and harsh temperature and pressure conditions. As a consequence, pre-treatments require further development to

make them more environmental-friendly and less expensive. The use of US can strongly contribute to reach this aim. Indeed, an increase in efficiency can be achieved thanks to turbulence, micro jets, micro level mixing, and shock waves that makes the biomass more prone to subsequent treatments by increasing its solubility and component accessibility<sup>41</sup>.

#### **1.2.5. Focus: green extractions as preliminary step for biorefinery**

As already discussed, extraction of high added value molecules can be performed as a preliminary step in biorefinery systems.

Traditional extraction methodologies involve the use of solvents. Extraction process can be summarised in four steps:

- (1) The solvent penetrates the matrix
- (2) The solvent dissolves targets molecules
- (3) Solute molecules diffuse out of the matrix
- (4) Solute molecules are recovered

More in detail, when solvent contacts the matrix a solvent layer is created around the matrix particles. Considering that matrix particles are usually dry, a swelling process immediately takes place: particles expand and change their shape from a very irregular shape to a more regular shape that can be ideally assimilated to a sphere. During the swelling step, solvent enters in the matrix while solute molecules exit from matrix into the solvent. At a certain point the swelling reaches its maximum and solvent mobility around the particle is reduced by forming a stagnant layer. In the second stage of extraction, solute molecules diffuse from the matrix particles through the stagnant layer and in the third stage they diffuse from stagnant layer to the bulk solvent. Stagnant layer will negatively impact the extraction by reducing diffusion process by acting as a barrier, reducing extraction efficiency. Moreover being water, ethanol and methanol the most used solvents in plant extraction, high quantity of hydrogen bonds are formed among the solvent and the -OH and -O groups of the plant structure, increasing adhesion of the stagnant layer around matrix particles and resulting in a more improved barrier effect that reduce diffusion process<sup>43</sup>.

Starting from the green chemistry definition, in 2012 Chemat et al., proposed a suitable definition of green extraction: "Green Extraction is based on the discovery and design of extraction processes which will reduce energy consumption, allows use of alternative solvents and renewable natural products, and ensure a safe and high quality extract/product"<sup>44</sup>.

Moreover, similarly to what happened for green chemistry, 6 principles for green extractions were formulated:

- Principle 1: Innovation by selection of varieties and use of renewable plant resources.
- Principle 2: Use of alternative solvents and principally water or agro-solvents.
- Principle 3: Reduce energy consumption by energy recovery and using innovative technologies.
- Principle 4: Production of co-products instead of waste to include the bio- and agro-refining industry.
- Principle 5: Reduce unit operations and favour safe, robust and controlled processes.
- Principle 6: Aim for a non-denatured and biodegradable extract without contaminants.

It can be concluded that "Green Extraction" is a novel approach that produces high quality extracts by means of sustainable, alternative solvents, exploiting renewable plant resources. The role of non-conventional green technologies is therefore crucial: microwave-assisted extraction and ultrasound-assisted extraction technologies can provide a substantial contribution in green extraction development.

Several different green extraction technologies have been developed, such as: Pressurized liquid extraction (PLE), Subcritical water extractions (SWE), Supercritical fluid extraction (SFE), Ultrasound-assisted extractions (UAE), Microwave-assisted extractions (MAE), Pulsed electric field assisted extraction (PEF) and High-voltage electric discharge (HVED).

The features of the main green extraction technologies (MAE, SWE and UAE) used in this thesis are described below.

Microwaves in green extractions (microwave-assisted extractions)

Microwave assisted extractions can provide higher yields in lower times, compared to conventional extractions, thanks to the combination of heat and mass gradient that proceeds in the same direction, from the bulk to the walls of the extracting vessel (and therefore from the inside to the outside of vegetal matrix cells)<sup>45</sup> (Figure 10).

Extraction processes in solvent microwave assisted extractions (MAE) consist of several consecutive steps:

- solvent diffuses into the vegetal matrix and solubilizes target compounds
- solubilized target compounds diffuse from the inside to the surface of the matrix
- either natural or forced convection drives the solute to migrate from matrix surface to the bulk solvent<sup>45</sup>.

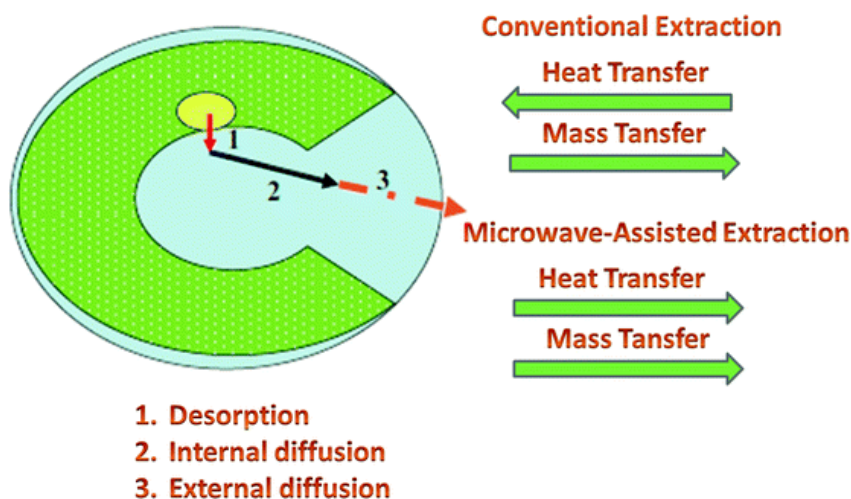


Figure 10: MAE vs conventional extraction<sup>45</sup>

Plant tissues can undergo disruption thus improving extraction yields: indeed water naturally present in cells is heated, leading to cell wall expansion and rupture from the inside, facilitating the release of intracellular compounds.

Reduction of matrix particle size can improve MAE results exposing higher surface area to the solvent. Solvent should be selected depending on its ability to absorb MW: high dielectric solvents such as water, methanol or ethanol are considered perfect solvents for MAE while low MW adsorbents solvents can be coupled with small quantities of water or ethanol to substantially improve extraction results. When MAE is performed, particular care should also be devoted in accurate temperature control, since excessive heating can lead to target degradation<sup>45</sup>.

When MAE is performed using water at temperature above its boiling point, extraction can be defined as subcritical water (SWE) microwave assisted extractions (or MASWE).

Being abundant, safe, cheap and non-toxic, water is considered the best environmentally friendly solvent. Unfortunately due to its highly hydrogen-bonded structure, and high polarity

water at room temperature is unsuitable for medium- and low-polar molecules extraction, indeed its dielectric constant ( $\epsilon$ ) at 25°C is equals to 78<sup>46,47</sup>.

By heating water over its boiling point and applying moderate pressure to keep it in condensed state, properties of water can be tuned for medium- and low-polar molecules extraction<sup>48,49</sup>. Indeed,  $\epsilon$  decreases gradually with temperature increase, from 100 °C to 374 °C (the critical point of water). At 250 °C, water reaches an  $\epsilon$  value of 27, very close to  $\epsilon$  of ethanol (24) and methanol (33) (Figure 11). Such temperature-driven  $\epsilon$  reduction, allows water to behave like organic solvents, thus favouring less polar compounds to dissolve<sup>46,47,49</sup>.

Together with temperature increase, other physicochemical properties of water undergo important modifications, such as surface tension and viscosity decrease, and diffusivity increases. Such phenomena result in improved mass transfer and matrix wetting, favouring penetration of water in the matrix<sup>50,51</sup>.

Major drawbacks of this enhanced extraction performances are represented by degradation of thermo-labile molecules and loss of selectivity (due to severe extraction conditions, several co-extractives can be recovered together with targeted molecules).

Aiming to avoid excessive co-extractive recovery the extraction condition should be properly optimised: more polar compounds are usually extracted at lower temperatures, and less polar compounds can be extracted at higher temperatures<sup>52,53</sup>.

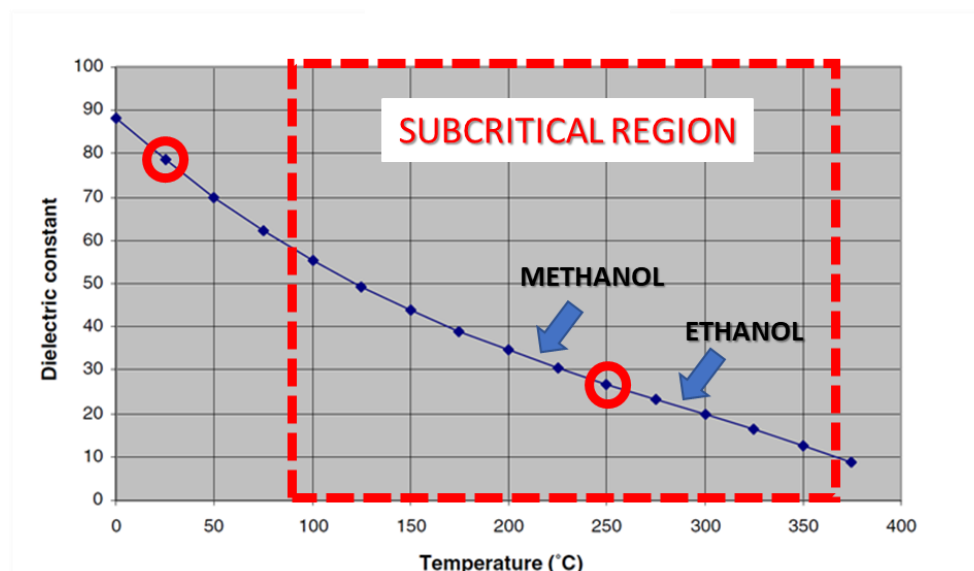


Figure 11: Dielectric constant of water in function of temperature

#### Ultrasound irradiation in green extractions (ultrasound-assisted extractions)

During ultrasound-assisted extractions (UAE), the collapse of bubbles created in the solvent by US source, forms high velocity micro-jets<sup>33,42</sup>. Micro-jets impact the surface of the vegetal matrix resulting in enhancement of mass-transfer, mixing, and diffusion of the target molecules from the matrix to the bulk solvent<sup>33,54</sup> (Figure 12).

Moreover, physical effects can be exerted on vegetal matrices by ultrasound, including fragmentation, erosion, destruction/detexturation of plant structure, sonocapillary effect and sonoporation.

By combination of aforementioned effects, extractions can be intensified by ultrasound trough<sup>55</sup>:

1. Reduction of solvent used
2. Reduction of unit operations
3. Reduction of extraction time

4. Reduction in energy consumption
5. Improvement of security and safety (by use of safer solvents such as simple water)
6. Reduction of overall environmental impact of extraction protocol.

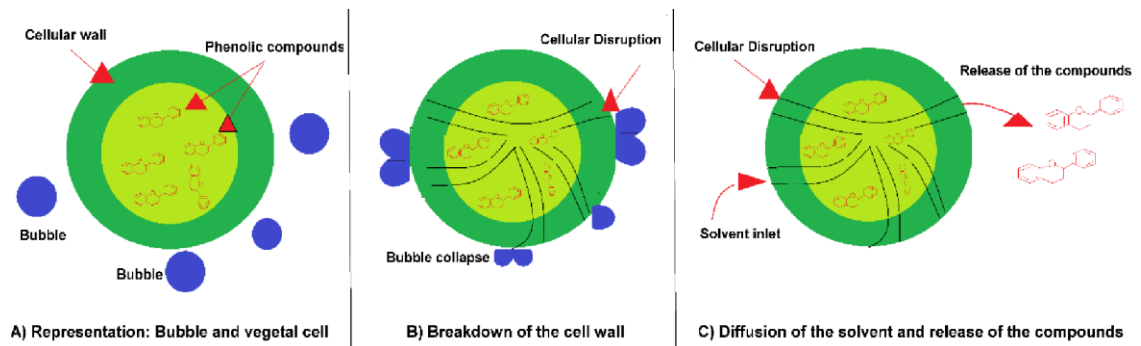


Figure 12: Mechanism of UAE<sup>54</sup>

### 1.3. REFERENCES

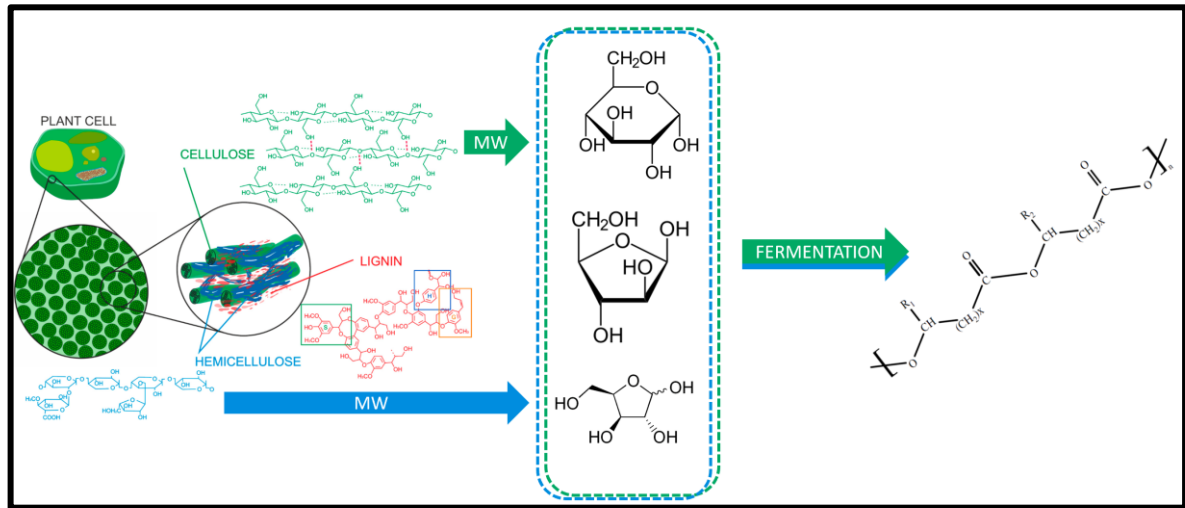
- (1) [https://Ec.Europa.Eu/Commission/Presscorner/Detail/En/Ip\\_20\\_420](https://Ec.Europa.Eu/Commission/Presscorner/Detail/En/Ip_20_420).
- (2) [https://Ec.Europa.Eu/Info/Strategy/Priorities-2019-2024/European-Green-Deal\\_en](https://Ec.Europa.Eu/Info/Strategy/Priorities-2019-2024/European-Green-Deal_en).
- (3) Ellen MacArthur Foundation: Towards the Circular Economy Report.
- (4) <https://Www.Europarl.Europa.Eu/Thinktank/Infographics/Circulareconomy/Public/Index.Html>.
- (5) Didier, B. Closing the Loop: New Circular Economy Package. 9.
- (6) Geissdoerfer, M.; Savaget, P.; Bocken, N. M. P.; Hultink, E. J. The Circular Economy – A New Sustainability Paradigm? *J. Clean. Prod.* **2017**, *143*, 757–768. <https://doi.org/10.1016/j.jclepro.2016.12.048>.
- (7) Camacho-Otero, J.; Boks, C.; Pettersen, I. Consumption in the Circular Economy: A Literature Review. *Sustainability* **2018**, *10* (8), 2758. <https://doi.org/10.3390/su10082758>.
- (8) Garcia-Muiña, F.; González-Sánchez, R.; Ferrari, A.; Settembre-Blundo, D. The Paradigms of Industry 4.0 and Circular Economy as Enabling Drivers for the Competitiveness of Businesses and Territories: The Case of an Italian Ceramic Tiles Manufacturing Company. *Soc. Sci.* **2018**, *7* (12), 255. <https://doi.org/10.3390/socsci7120255>.
- (9) Prieto-Sandoval, V.; Jaca, C.; Ormazabal, M. Towards a Consensus on the Circular Economy. *J. Clean. Prod.* **2018**, *179*, 605–615. <https://doi.org/10.1016/j.jclepro.2017.12.224>.
- (10) Grafström, J.; Aasma, S. Breaking Circular Economy Barriers. *J. Clean. Prod.* **2021**, *292*, 126002. <https://doi.org/10.1016/j.jclepro.2021.126002>.
- (11) Ubando, A. T.; Felix, C. B.; Chen, W.-H. Biorefineries in Circular Bioeconomy: A Comprehensive Review. *Bioresour. Technol.* **2020**, *299*, 122585. <https://doi.org/10.1016/j.biortech.2019.122585>.
- (12) Kamm, B.; Kamm, M. International Biorefinery Systems. *Pure Appl. Chem.* **2007**, *79* (11), 1983–1997. <https://doi.org/10.1351/pac200779111983>.
- (13) Leong, H. Y.; Chang, C.-K.; Khoo, K. S.; Chew, K. W.; Chia, S. R.; Lim, J. W.; Chang, J.-S.; Show, P. L. Waste Biorefinery towards a Sustainable Circular Bioeconomy: A Solution to Global Issues. *Biotechnol. Biofuels* **2021**, *14* (1), 87. <https://doi.org/10.1186/s13068-021-01939-5>.
- (14) Ragauskas, A. J.; Williams, C. K.; Davison, B. H.; Britovsek, G.; Cairney, J.; Eckert, C. A.; Jr, W. J. F.; Hallett, J. P.; Leak, D. J.; Liotta, C. L.; Mielenz, J. R.; Murphy, R.; Templer, R.; Tschaplinski, T. The Path Forward for Biofuels and Biomaterials. *SCIENCE* **2006**, *311*, 7.
- (15) Cherubini, F. The Biorefinery Concept: Using Biomass Instead of Oil for Producing Energy and Chemicals. *Energy Convers. Manag.* **2010**, *51* (7), 1412–1421. <https://doi.org/10.1016/j.enconman.2010.01.015>.
- (16) Menon, V.; Rao, M. Trends in Bioconversion of Lignocellulose: Biofuels, Platform Chemicals & Biorefinery Concept. *Prog. Energy Combust. Sci.* **2012**, *38* (4), 522–550. <https://doi.org/10.1016/j.pecs.2012.02.002>.
- (17) Clark, J. H.; Luque, R.; Matharu, A. S. Green Chemistry, Biofuels, and Biorefinery. *Annu. Rev. Chem. Biomol. Eng.* **2012**, *3* (1), 183–207. <https://doi.org/10.1146/annurev-chembioeng-062011-081014>.
- (18) Sheldon, R. A. Biocatalysis and Biomass Conversion: Enabling a Circular Economy. *Philos. Trans. R. Soc. Math. Phys. Eng. Sci.* **2020**, *378* (2176), 20190274. <https://doi.org/10.1098/rsta.2019.0274>.
- (19) Bardhan, S. K.; Gupta, S.; Gorman, M. E.; Haider, M. A. Biorenewable Chemicals: Feedstocks, Technologies and the Conflict with Food Production. *Renew. Sustain. Energy Rev.* **2015**, *51*, 506–520. <https://doi.org/10.1016/j.rser.2015.06.013>.
- (20) Singhvi, M. S.; Gokhale, D. V. Lignocellulosic Biomass: Hurdles and Challenges in Its Valorization. *Appl. Microbiol. Biotechnol.* **2019**, *103* (23–24), 9305–9320. <https://doi.org/10.1007/s00253-019-10212-7>.
- (21) Lodz University of Technology, Faculty of Biotechnology and Food Sciences, Institute of Fermentation Technology and Microbiology, Department of Spirit and Yeast Technology Wolczanska 171/173, PL-90-924 Lodz, Poland; Robak, K.; Balcerek, M.; Lodz University of Technology, Faculty of Biotechnology and Food Sciences, Institute of Fermentation Technology and Microbiology, Department of Spirit and Yeast Technology Wolczanska 171/173, PL-90-924 Lodz, Poland. Review of Second-Generation Bioethanol Production from Residual Biomass. *Food Technol. Biotechnol.* **2018**, *56* (2). <https://doi.org/10.17113/ftb.56.02.18.5428>.
- (22) Zheng, Y.; Zhao, J.; Xu, F.; Li, Y. Pretreatment of Lignocellulosic Biomass for Enhanced Biogas Production. *Prog. Energy Combust. Sci.* **2014**, *42*, 35–53. <https://doi.org/10.1016/j.pecs.2014.01.001>.
- (23) Haq, I.; Qaisar, K.; Nawaz, A.; Akram, F.; Mukhtar, H.; Zohu, X.; Xu, Y.; Mumtaz, M.; Rashid, U.; Ghani, W.; Choong, T. Advances in Valorization of Lignocellulosic Biomass towards Energy Generation. *Catalysts* **2021**, *11* (3), 309. <https://doi.org/10.3390/catal11030309>.
- (24) Hernández-Beltrán, J. U.; Hernández-De Lira, I. O.; Cruz-Santos, M. M.; Saucedo-Luevanos, A.; Hernández-Terán, F.; Balagurusamy, N. Insight into Pretreatment Methods of Lignocellulosic Biomass to Increase



- Biogas Yield: Current State, Challenges, and Opportunities. *Appl. Sci.* **2019**, *9* (18), 3721. <https://doi.org/10.3390/app9183721>.
- (25) Anastas, P. T.; Warner, J. C. *Green Chemistry: Theory and Practice*, Oxford University Press: New York, 1998, p.30.
- (26) Morais, A. R.; Bogel-Lukasik, R. Green Chemistry and the Biorefinery Concept. *Sustain. Chem. Process.* **2013**, *1* (1), 18. <https://doi.org/10.1186/2043-7129-1-18>.
- (27) Werpy, T.; Petersen, G. *Top Value Added Chemicals from Biomass: Volume I -- Results of Screening for Potential Candidates from Sugars and Synthesis Gas*; DOE/GO-102004-1992, 15008859; 2004; p DOE/GO-102004-1992, 15008859. <https://doi.org/10.2172/15008859>.
- (28) Holladay, J. E.; White, J. F.; Bozell, J. J.; Johnson, D. *Top Value-Added Chemicals from Biomass - Volume II—Results of Screening for Potential Candidates from Biorefinery Lignin*; PNNL-16983, 921839; 2007; p PNNL-16983, 921839. <https://doi.org/10.2172/921839>.
- (29) Bozell, J. J.; Petersen, G. R. Technology Development for the Production of Biobased Products from Biorefinery Carbohydrates—the US Department of Energy’s “Top 10” Revisited. *Green Chem.* **2010**, *12* (4), 539. <https://doi.org/10.1039/b922014c>.
- (30) Kohli, K.; Prajapati, R.; Sharma, B. Bio-Based Chemicals from Renewable Biomass for Integrated Biorefineries. *Energies* **2019**, *12* (2), 233. <https://doi.org/10.3390/en12020233>.
- (31) Zollmann, M.; Robin, A.; Prabhu, M.; Polikovskiy, M.; Gillis, A.; Greiserman, S.; Golberg, A. Green Technology in Green Macroalgal Biorefineries. *Phycologia* **2019**, *58* (5), 516–534. <https://doi.org/10.1080/00318884.2019.1640516>.
- (32) Stankiewicz, A. I.; Moulijn, J. A. Process Intensification: Transforming Chemical Engineering. 13.
- (33) Vinatoru, M.; Mason, T. J.; Calinescu, I. Ultrasonically Assisted Extraction (UAE) and Microwave Assisted Extraction (MAE) of Functional Compounds from Plant Materials. *TrAC Trends Anal. Chem.* **2017**, *97*, 159–178. <https://doi.org/10.1016/j.trac.2017.09.002>.
- (34) Chan, C.-H.; Yusoff, R.; Ngoh, G.-C.; Kung, F. W.-L. Microwave-Assisted Extractions of Active Ingredients from Plants. *J. Chromatogr. A* **2011**, *1218* (37), 6213–6225. <https://doi.org/10.1016/j.chroma.2011.07.040>.
- (35) Schanche, J.-S. Microwave Synthesis Solutions from Personal Chemistry. *Mol. Divers.* **2003**, *7* (2–4), 291–298. <https://doi.org/10.1023/B:MODI.0000006866.38392.f7>.
- (36) de la Hoz, A.; Díaz-Ortiz, Á.; Moreno, A. Microwaves in Organic Synthesis. Thermal and Non-Thermal Microwave Effects. *Chem Soc Rev* **2005**, *34* (2), 164–178. <https://doi.org/10.1039/B411438H>.
- (37) Nüchter, M.; Müller, U.; Ondruschka, B.; Tied, A.; Lautenschläger, W. Microwave-Assisted Chemical Reactions. *Chem. Eng. Technol.* **2003**, *26* (12), 1207–1216. <https://doi.org/10.1002/ceat.200301836>.
- (38) Patil, N. G.; Benaskar, F.; Rebrov, E. V.; Meuldijk, J.; Hulshoff, L. A.; Hessel, V.; Schouten, J. C. Microwave Setup Design for Continuous Fine-Chemicals Synthesis. *Chem. Eng. Technol.* **2014**, *37* (10), 1645–1653. <https://doi.org/10.1002/ceat.201400118>.
- (39) Blackwell, H. E. Out of the Oil Bath and into the Oven—Microwave-Assisted Combinatorial Chemistry Heats Up. *ORGANOCHEM 5*.
- (40) Hassan, S. S.; Williams, G. A.; Jaiswal, A. K. Emerging Technologies for the Pretreatment of Lignocellulosic Biomass. *Bioresour. Technol.* **2018**, *262*, 310–318. <https://doi.org/10.1016/j.biortech.2018.04.099>.
- (41) Flores, E. M. M.; Cravotto, G.; Bizzi, C. A.; Santos, D.; Iop, G. D. Ultrasound-Assisted Biomass Valorization to Industrial Interesting Products: State-of-the-Art, Perspectives and Challenges. *Ultrason. Sonochem.* **2021**, *72*, 105455. <https://doi.org/10.1016/j.ultsonch.2020.105455>.
- (42) Wen, C.; Zhang, J.; Zhang, H.; Dzah, C. S.; Zandile, M.; Duan, Y.; Ma, H.; Luo, X. Advances in Ultrasound Assisted Extraction of Bioactive Compounds from Cash Crops – A Review. *Ultrason. Sonochem.* **2018**, *48*, 538–549. <https://doi.org/10.1016/j.ultsonch.2018.07.018>.
- (43) Saleh, I. A.; Vinatoru, M.; Mason, T. J.; Abdel-Azim, N. S.; Aboutabl, E. A.; Hammouda, F. M. A Possible General Mechanism for Ultrasound-Assisted Extraction (UAE) Suggested from the Results of UAE of Chlorogenic Acid from *Cynara Scolymus* L. (Artichoke) Leaves. *Ultrason. Sonochem.* **2016**, *31*, 330–336. <https://doi.org/10.1016/j.ultsonch.2016.01.002>.
- (44) Chemat, F.; Vian, M. A.; Cravotto, G. Green Extraction of Natural Products: Concept and Principles. *Int. J. Mol. Sci.* **2012**, *13* (7), 8615–8627. <https://doi.org/10.3390/ijms13078615>.
- (45) *Microwave-Assisted Extraction for Bioactive Compounds*; Chemat, F., Cravotto, G., Eds.; Food Engineering Series; Springer US: Boston, MA, 2013. <https://doi.org/10.1007/978-1-4614-4830-3>.
- (46) Smith, R. M. Extractions with Superheated Water. *J. Chromatogr. A* **2002**, *975* (1), 31–46. [https://doi.org/10.1016/S0021-9673\(02\)01225-6](https://doi.org/10.1016/S0021-9673(02)01225-6).
- (47) Teo, C. C.; Tan, S. N.; Yong, J. W. H.; Hew, C. S.; Ong, E. S. Pressurized Hot Water Extraction (PHWE). *J. Chromatogr. A* **2010**, *1217* (16), 2484–2494. <https://doi.org/10.1016/j.chroma.2009.12.050>.

- (48) Bursać Kovačević, D.; Barba, F. J.; Granato, D.; Galanakis, C. M.; Herceg, Z.; Dragović-Uzelac, V.; Putnik, P. Pressurized Hot Water Extraction (PHWE) for the Green Recovery of Bioactive Compounds and Steviol Glycosides from *Stevia Rebaudiana* Bertoni Leaves. *Food Chem.* **2018**, *254*, 150–157. <https://doi.org/10.1016/j.foodchem.2018.01.192>.
- (49) Herrero, M.; Cifuentes, A.; Ibanez, E. Sub- and Supercritical Fluid Extraction of Functional Ingredients from Different Natural Sources: Plants, Food-by-Products, Algae and Microalgae A Review. *Food Chem.* **2006**, *98* (1), 136–148. <https://doi.org/10.1016/j.foodchem.2005.05.058>.
- (50) Plaza, M.; Marina, M. L. Pressurized Hot Water Extraction of Bioactives. *TrAC Trends Anal. Chem.* **2019**, *116*, 236–247. <https://doi.org/10.1016/j.trac.2019.03.024>.
- (51) Plaza, M.; Turner, C. Pressurized Hot Water Extraction of Bioactives. *TrAC Trends Anal. Chem.* **2015**, *71*, 39–54. <https://doi.org/10.1016/j.trac.2015.02.022>.
- (52) Ibañez, E.; Kubátová, A.; Señoráns, F. J.; Cavero, S.; Reglero, G.; Hawthorne, S. B. Subcritical Water Extraction of Antioxidant Compounds from Rosemary Plants. *J. Agric. Food Chem.* **2003**, *51* (2), 375–382. <https://doi.org/10.1021/jf025878j>.
- (53) Ko, M.-J.; Cheigh, C.-I.; Chung, M.-S. Relationship Analysis between Flavonoids Structure and Subcritical Water Extraction (SWE). *Food Chem.* **2014**, *143*, 147–155. <https://doi.org/10.1016/j.foodchem.2013.07.104>.
- (54) Medina-Torres, N.; Ayora-Talavera, T.; Espinosa-Andrews, H.; Sánchez-Contreras, A.; Pacheco, N. Ultrasound Assisted Extraction for the Recovery of Phenolic Compounds from Vegetable Sources. *Agronomy* **2017**, *7* (3), 47. <https://doi.org/10.3390/agronomy7030047>.
- (55) Chemat, F.; Rombaut, N.; Sicaire, A.-G.; Meullemiestre, A.; Fabiano-Tixier, A.-S.; Abert-Vian, M. Ultrasound Assisted Extraction of Food and Natural Products. Mechanisms, Techniques, Combinations, Protocols and Applications. A Review. *Ultrason. Sonochem.* **2017**, *34*, 540–560. <https://doi.org/10.1016/j.ultsonch.2016.06.035>.
- (56) M. C. Andrade, C. de Oliveira Gorgulho Silva, L. R. de Souza Moreira, E. X. Ferreira Filho Crop residues: applications of lignocellulosic biomass in the context of a biorefinery. *Front. Energy.* **2021** <https://doi.org/10.1007/s11708-021-0730-7>

## 2. MONOSACCHARIDES PRODUCTION FROM TOMATO-PLANT RESIDUES FOR MIXED-CULTURE FERMENTATION



## 2.1. INTRODUCTION

### 2.1.1. Alternatives to conventional petroleum-based plastics

Problems dealing with accumulation of non-biodegradable plastics in landfills and environment are one of the main challenges of our century. Moreover, depletion of fossil fuels has led to the need for new alternative biodegradable, bioresourced, sustainable polymers<sup>1,2</sup>. As highlighted by Tarrahi et al.<sup>1</sup>, when talking about bioresourced/biodegradable polymers, some terms should be clarified:

- Some bioresourced plastics are both renewable and biodegradable.
- Some bioresourced plastics are not biodegradable.
- Some fossil-based plastics are biodegradable.
- Some plastics are a mixture of bioresourced and fossil-based plastics and are partially biodegradable
- Majority of conventional fossil-based plastics are neither biodegradable nor renewable

Such concepts and some examples, can be graphically visualised according to European Bioplastics<sup>3</sup> in the scheme below (Figure 1):

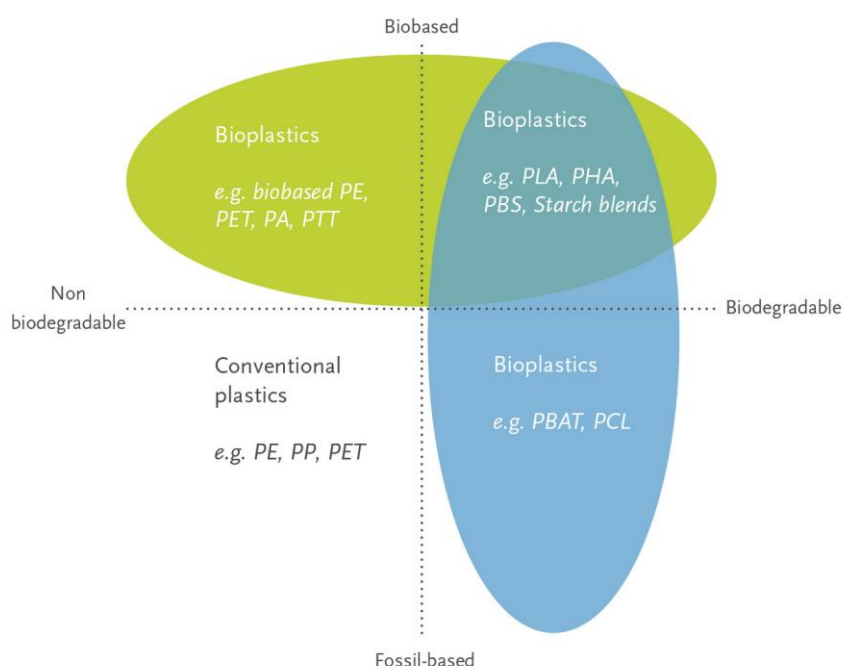


Figure 1: Conventional plastics and bioplastics classification

### 2.1.2. Alternatives to conventional petroleum-based plastics: polyhydroxyalkanoates

As both biodegradable and bioresourced polymers, polyhydroxyalkanoates (PHAs), can be considered a valuable alternative to conventional, non-biodegradable, fossil-based plastics. PHAs are a class of polyesters produced through fermentation by numerous bacteria as energy and carbon storage compounds. PHAs can be produced in nutrient-limiting conditions, characterised by carbon excess and low nitrogen and/or phosphate concentrations. In some bacteria PHAs production was observed also in absence of nutrient-limiting condition<sup>2,4,5</sup>. PHAs are accumulated inside cells as discrete, water insoluble cytoplasmic inclusions<sup>4</sup>, composed by esterified hydroxyacids monomers<sup>6</sup>. When carbon source is depleted, PHAs can be depolymerised in cells to produce carbon and/or energy<sup>4</sup>.

Wide varieties of bacteria both Gram negative and Gram positive (such as *Pseudomonas*, *Bacillus*, *Ralstonia*, *Aeromonas*, *Rhodobacter*) and some Archea are able to synthesise PHAs<sup>6</sup>.

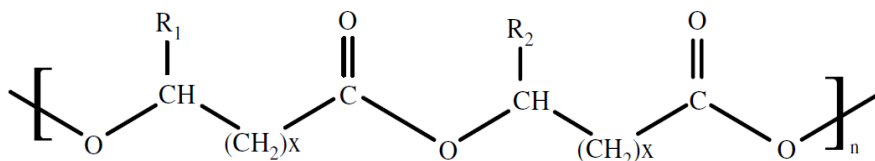


Figure 2: General PHA structure

PHAs can be produced by more than 300 microbial species in various forms: homopolymer, co-polymer, block co-polymer or blends depending on fermentation substrate, fermentation conditions and bacterial strain type<sup>7</sup>.

PHAs monomers are connected through ester linkages and each monomer presents a side chain (R) that is usually a linear, saturated alkyl group (but also unsaturated and/or branched alkyl groups can be found)<sup>5</sup>.

PHAs can be classified into three groups, according to the number of carbon atoms in their monomers:

- Short chain length (SCL), presenting less than 5 carbon atoms
- Medium chain length (MCL), presenting from 5 to 14 carbon atoms
- Long chain length (LCL), presenting more than 14 carbon atoms<sup>2</sup>

Some bacteria can synthesise PHAs containing both SCL and MCL monomers.

More than 150 PHAs have been recorded up to now, characterised by different properties with different potential applications<sup>5</sup>. Moreover, PHAs' side chains can be further modified by introducing functional groups aiming to modify their physical and chemical properties and extend their application range<sup>4</sup>. Such modifications are mainly intended to introduce functional groups that are difficult to directly incorporate through biological routes. Several procedures have been investigated such as chlorination, carboxylation, epoxidation/crosslinking, grafting, thiolation, esterification and metallization (Figure 3)<sup>8</sup>.

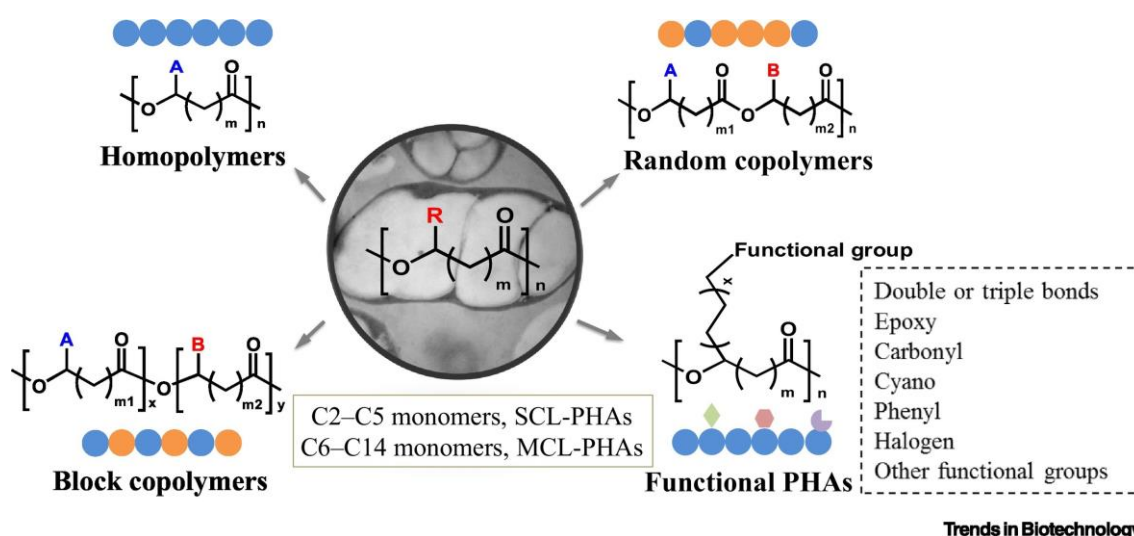


Figure 3: PHAs classification, according to Tan et al.

### 2.1.2.1. Polyhydroxyalkanoates: properties and applications

PHAs are considered valuable alternatives to petroleum-based polymers because of their properties that are similar to synthetic polymers like polypropylene or polystyrene<sup>4</sup>. Such

properties are strictly related to bacterial species involved in their production and overall fermentation conditions.

PHAs are thermoplastic polymers that can be processed in different phase states (solution, emulsion, powder, melt). SCL PHAs are stiff and brittle, characterised by high degree of crystallinity (in the range 60-80%), while MCL PHAs are flexible and elastic polymers with low crystallinity (in the range 20-25%), low tensile strength, high elongation to break, glass transition temperature below room temperature and low melting temperatures<sup>9</sup>.

Polymer	Melting temperature (°C)	Glass transition temperature (°C)	Tensile strength (MPa)	Tensile modulus (GPa)	Elongation to break (%)
P(3HB)	177	4	40	3.5	6
P(4HB)	60	-50	104	0.149	1000
P(3HB-co-16%4HB)	152	-8	26	N.D	444
P(3HB-co-20%3HV)	145	-1	32	1.2	50
P(3HB-co-17%3HHx)	120	-2	20	0.173	850
P(3HO-co-12%3HHx)	61	-35	9	0.008	380
Polypropylene	176	-10	38	1.7	400
Polyurethane	195	20	38	0.004	550

ND: Not detected; P(3HB): Poly(3-hydroxybutyrate); P(4HB): PHA: Polyhydroxyalkanoate; Poly(4-hydroxybutyrate); P(3HB-co-16%4HB): Poly (3-hydroxybutyrate-co-16% 4-hydroxybutyrate); P(3HB-co-20%3HV): Poly (3-hydroxybutyrate-co-20% 3-hydroxyvalerate); P(3HB-co-17%3HHx): Poly (3-hydroxybutyrate-co-17% 3-hydroxyhexanoate); P(3HO-co-12%3HHx): Poly (3-hydroxyoctanoate-co-12%3-hydroxyhexanoate). Several reports have demonstrated variation of the measured values, hence an average value has been quoted.

Table 1: Properties of some PHAs, according to Valappil et al.

In Table 1, different PHAs together with their properties are reported and compared with polypropylene and polyurethane<sup>10</sup>.

As already mentioned, PHAs properties can vary widely depending on PHA type and production conditions. Such variability makes PHAs extremely flexible materials that can be exploited for several applications such as disposable plastics, biofuels, 3D printing and biomedical materials, high quality textiles, agricultural mulch films.

Hydrophobicity, gas barrier properties and nontoxicity make PHAs promising materials for packaging purposes. Moreover, due to their biocompatibility coupled with mechanical properties, PHAs can be used for 3D printing of human implants and biomedical applications in general (heart valves, bone replacements, nerve conduits)<sup>11</sup>.

#### 2.1.2.2. Polyhydroxyalkanoates: industrial aspects

Despite microbial plastics are considered a valuable alternative to petroleum-based plastics, limitations to their wide diffusion are still to be solved. Of course, PHA are both biosourced and biodegradable, but life cycle assessment (LCA) studies showed higher carbon footprint for PHAs respect to petroleum-based plastics: indeed, upstream and downstream processes for PHAs production are characterised by high energy and chemicals consumption.

Moreover, both upstream and downstream processes nowadays are not economically sustainable<sup>12</sup>: PHAs average price can range from 4 to 5€/kg, while petrochemical polymers have costs lower than 1€/kg<sup>13</sup>. Despite several efforts have been made to reduce production costs, nowadays only few companies reached PHAs production in commercial scale (Table 2<sup>35</sup>).

Company	PHA type	Current Capacity (tons in 2020)	Expansion plans Expected capacity (tons in 2025)
Danimer Scientific	PHBH	8.000 + 2.000	20.000 + 2.000
Kaneka Corporation	PHBH	5.000	5.000 +20.000
Newlight	PHB	5.000	23.000
RWDC	PHBH	5.000	105.000
TianAn	PHBV, P3H4B	2.000	10.000

Table 2: industrial PHAs production

Several prerequisites are mandatory before industrialisation of PHAs production, such as strain selection and/or development (wild type or recombinant bacteria), shake flask studies, lab and pilot-scale fermenter investigations and industrial scale-up tests (Figure 4)<sup>5</sup>.

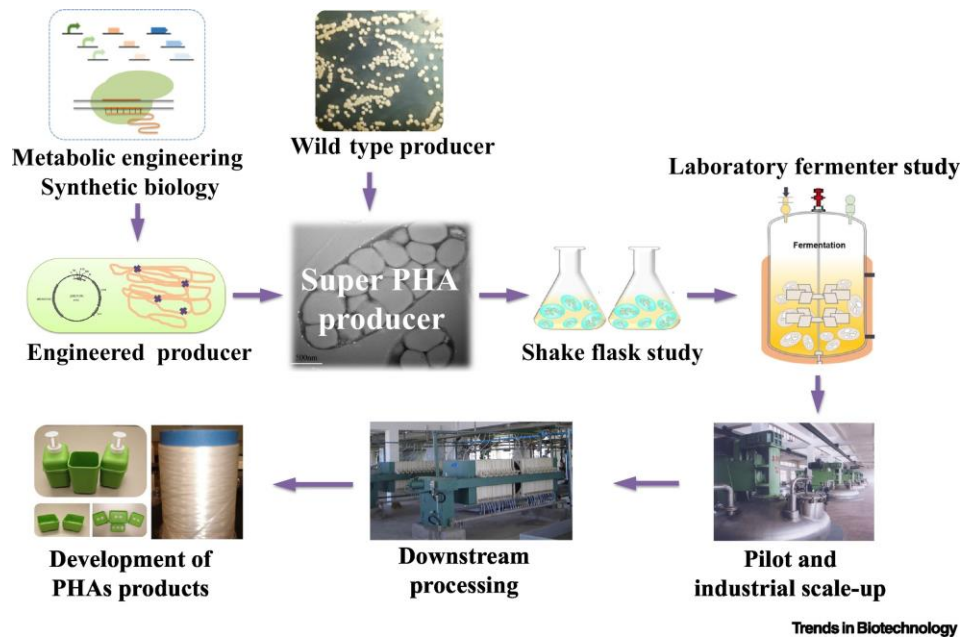


Figure 4: Overall procedure for PHAs production process industrialisation (Tan et al.)

More into detail, an overall flowchart of PHA production process is reported in Figure 5: the nutritional medium with selected feedstock is prepared and selected strain is added. Subsequently, after pre-culture, fermentation starts in a bioreactor. Once the fermentation is completed, PHAs-rich cells are recovered, dried, and subjected to PHA extraction. PHA extraction usually involves use of solvents and requires high amounts of energy, negatively impacting the overall costs and LCA of the process. Moreover, also the choice of nutritional medium feedstock has enormous impact on overall production costs (up to 50% of overall costs)<sup>14</sup>.

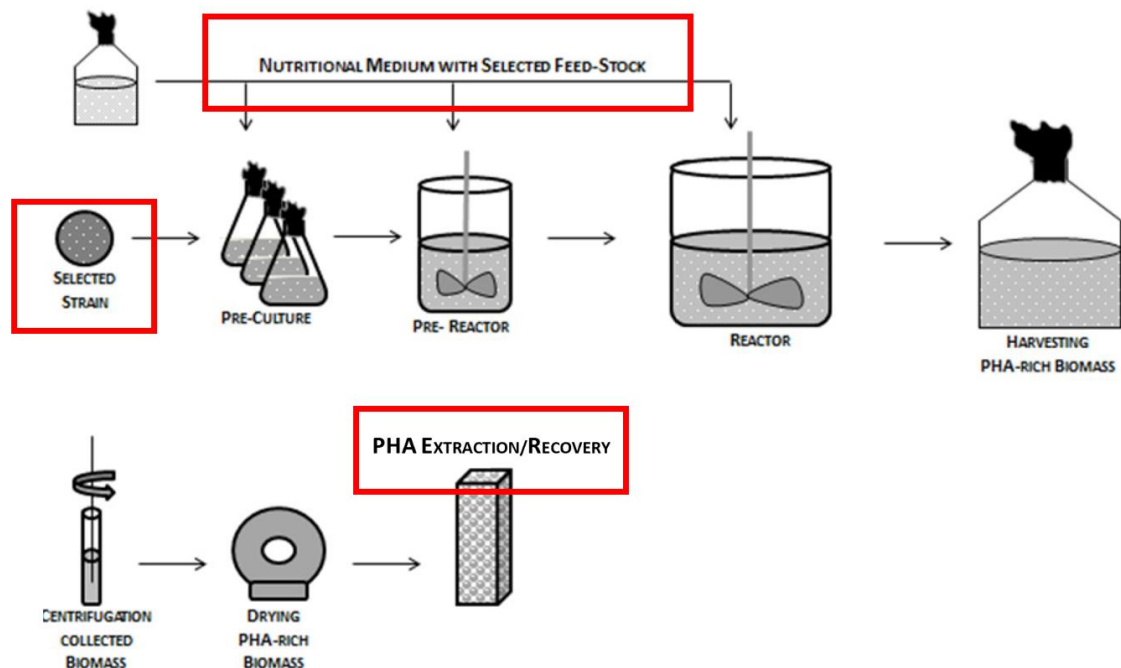


Figure 5: Operative steps for PHAs production (adapted from Koller et al.)

In summary, both nutritional medium feedstock selection, microbial culture selection and downstream processing for PHA recovery/extraction require to be implemented to achieve environmental and economic sustainability (highlighted in red in Figure 5).

Furthermore aiming to enhance productivity also microbial cultures require particular attention in selection of high efficiency species<sup>15</sup>.

Considering the above, it is also important to note that PHA structure, properties and characteristics can widely vary according to the strategies adopted in every step of the production protocol<sup>16</sup>.

#### 2.1.2.2.1. Feedstocks for nutritional medium

As already mentioned, relevant part of overall PHAs production costs is related to nutritional medium feedstocks. Pure sugars are commonly involved in PHA production studies and represent one of the main obstacles to commercial success of PHAs being estimated that an average of 3 tonnes of sugars are required to achieve 1 ton of PHA. From a circular economy point of view, exploitation of alternative feedstock could boost sustainability both from an economical and carbon footprint point of view<sup>14</sup>. Use of waste feedstocks could also avoid ethical problems with land consumptions for non-food dedicated cultures. Consequently, waste feedstocks can be selected as alternative substrates, being rich in organic matter and readily available in high quantities.

Different waste feedstocks have been investigated: industrial wastes (such as mill effluents from palm oil, wastes from wood, paper and biodiesel industry), agricultural and food derived wastes, municipal solid wastes and animal derived wastes<sup>7</sup>.

Steady supply of low-value biomasses (2G feedstocks) are estimated to be around 150 billion tonnes per year globally,<sup>14</sup> making them interesting candidates as feedstock for PHA production.

As reviewed by Sawant et al.,<sup>17</sup> most of works reported in literature using biomass-derived polysaccharides, involve a step of chemical and/or enzymatic hydrolysis. The aim is to produce



simple sugars from carbohydrates fractions such as glucose, fructose, xylose, etc..., to be used as carbon source for microbial fermentation<sup>18</sup>. For instance, rice husk hydrolysate produced through acid hydrolysis and steam treatment was used as broth for *Bacillus mycoides* DFC1 fermentation yielding PHB and 3HB-co-3HV<sup>19</sup>. Xylose-rich sugar maple hydrolysate produced through sulphuric acid treatment was successfully used for *B. cepacia* ATCC 17759 fermentation, yielding PHB<sup>20</sup>. Furthermore, Silva et al.<sup>21</sup> extensively reviewed PHA production from xylose fermentation, highlighting the huge amount of xylose that can be recovered as by-product from bio-ethanol production. According to the authors, the bio-ethanol production from glucose and the PHA production from xylose can be integrated in a biorefinery-based system, being both glucose and xylose derivable from the same feedstock: sugarcane bagasse.

#### **2.1.2.2.2. Microbial culture selection: advantages/limitations of pure microbial cultures and mixed microbial cultures**

In Table 2, the most world relevant commercial PHAs producers are reported. In most cases, pure microbial cultures (PMC) are employed. PMC advantages are:

- high PHA accumulation levels in cells (above 80% of cell dry weight)
- high cell densities that can be achieved during fermentations.

Despite that, PMC present several limitations, due to sterility requirements (characterised by high energy requirements and constant contamination risks) and high substrate price (due to the need of high purity substrates)<sup>12,13</sup>.

Such issues can be avoided in part or at all by employing mixed microbial cultures (MMC). MMC consist of a set of known and/or unknown microbial groups<sup>22</sup>. MMC presenting similar intracellular PHA accumulation and accumulation rates can be considered a promising alternative to PMC but relevant challenges remain in downstream processing due to difficulties in PHA extraction, recovery and purification, that can impact negatively on the overall production costs even more than in PMC case<sup>12</sup>. Despite that, MMC advantages respect to PMC are described below.

- Absence of sterility requirements allows lower energy consumption for sterilisation operations (with sensible reduction of production costs)<sup>23</sup>
- Stability, robustness and tolerance to complex substrates: due to the presence of different microorganisms, MMC can maintain their functions when external or internal perturbations occur. Moreover, variations of substrate composition can be well tolerated thanks to the alternative metabolic pathways offered by the members of the microbial community. This flexibility makes MMC perfect candidates when complex feedstocks are used<sup>24</sup>.
- Performance improvement: typical inhibition due to accumulation of by-products can be lowered or avoided in MMC thanks to the presence of species able to degrade such side products<sup>24</sup>.

#### **2.1.2.2.3. PHA extraction and recovery**

Downstream processing for PHA extraction/recovery is reported to be a critical step in PHA production. Indeed, part of the production costs are due to high energy consumption and use of non-recyclable chemicals during this phase<sup>16,25</sup>. Moreover, the chemicals involved in PHA recovery are often toxic, thus negatively impacting the sustainability of the whole production protocol.

Problems dealing with PHA extraction/recovery from cells are amplified when dealing with MMC, that are reported to be more recalcitrant to cell-hydrolysis/rupture than PMC<sup>12,16</sup>.

Different conventional approaches are reported for PHA extraction/recovery:

- Acid cells hydrolysis followed by solvent extraction
- Strong oxidant cells treatment (for cell rupture) followed by solvent extraction<sup>16</sup>
- Lyophilization followed by solvent extraction (widely used in industrial-scale productions usually from PMC)<sup>25</sup>

Chlorinated solvents are the most used solvents, posing serious problems due to their hazardousness.

As a consequence, it can be said that during the downstream processing two critical points can be individuated: the cell rupture for PHA release and the PHA solubilisation for recovery. Several investigations have been reported involving alternative extraction technologies and solvents: fast MW irradiation was investigated by Bocaz-Beltrán et al.<sup>25</sup> for cells rupture with good PHA recovery efficiency comparable with conventional methods. Ethylic esters were recently investigated as non-toxic solvents for PHA recovery by Alfano et al.<sup>26</sup>, and dimethyl carbonate was successfully applied for the same purpose by Samorì et al.<sup>27</sup>.

## 2.2. RESULTS AND DISCUSSION

The aim of the work described in this chapter was to produce monosaccharides (MSC) through MW-assisted acid hydrolysis of 2G biomass. MSC so produced were used as sustainable and cheap substrate for MMC fermentation toward PHA.

Tomato-plant residues (post-harvest tomato plant, PHTP) were used as starting feedstock for MSC production in microwave reactor.

### 2.2.1. Post-harvest tomato plant (PHTP) for monosaccharides production

#### PHTP hydrolysis

PHTP overall chemical composition was investigated through NREL-derived protocol<sup>28</sup> (see chapter 1). Organic fraction accounts for 78% wt., while inorganic fraction accounts for 22% wt. Complete characterisation of PHTP is reported in Table 3.

Components	% wt.
<b>OVERALL ORGANIC FRACTION</b>	<b>78</b>
<i>Lipids, resins, catechols, tannins, proteins, fulvic acids</i>	3
<i>Cellulose</i>	39
<i>Hemicellulose, sugars</i>	21
<i>Lignin</i>	15
<b>INORGANIC FRACTION</b>	<b>22</b>

Table 3: Complete characterisation of PHTP

Cellulose/hemicellulose acid hydrolysis is usually performed using concentrated or diluted mineral acids such as HCl or H<sub>2</sub>SO<sub>4</sub>. Carbohydrate hydrolysis is a fundamental step for monosaccharides and other platform chemicals production. Cellulose is a biopolymer composed of glucose units, connected through  $\beta$ -1-4 glycosidic bonds. Acid hydrolysis proceeds through breakage of such  $\beta$ -1-4 glycosidic bonds towards glucose or oligosaccharides<sup>29</sup>. Glucose, xylose, mannose and galactose are the main sugars produced through cellulose/hemicellulose hydrolysis<sup>30</sup>.

Previously reported investigations for PHTP MW-assisted hydrolysis led to 52% wt. yield monosaccharides (62% wt. conversion), at 150°C, using 1N HCl, in only 2 minutes (Table 4, entry 8)<sup>31</sup>.

Entry	HCl (mol L <sup>-1</sup> )	T (°C)	Conversion (%)	Yield (%) <sup>32</sup>	
				LA	MSC
1	12	225	80	58	0
2	5	225	79	60	0
3	1	225	78	63	0
4	0.5	225	74	51	0
5	0.1	225	67	0	49
6	1	60	30	0	11
7	1	100	30	0	30
8	1	150	62	0	52
9	1	190	81	61	0
10	1	250	80	56	0
11 <sup>b</sup>	1	225	73	59	0
12 <sup>c</sup>	12	Reflux	50	5	20

<sup>a</sup> Reaction conditions: PHTP/HCl solution = 1/10 (w/v), 2 min MW, N<sub>2</sub> pressure (40 bar). <sup>b</sup> PHTP/HCl solution = 1/5 (w/v). <sup>c</sup> Conventional heating: PHTP/HCl solution = 1/10 (w/v), 2 h.

Table 4: PHTP hydrolysis (Tabasso et al.)

The reaction was performed in the same conditions using 60g PHTP as starting material. At the end of the hydrolysis, the crude was filtrated on paper filter under vacuum to separate unconverted solid PHTP fraction from liquid acid MSC-rich fraction. Unconverted PHTP was dried and weighted in order to calculate the conversion trough the formula:

$$\text{Conversion (\% wt.)} = \frac{\text{PHTP (g)} - \text{Unconverted PHTP (g)}}{\text{PHTP (g)}} * 100$$

63.45 wt.% conversion was achieved: this result is coherent with previously reported data for PHTP hydrolysis.

Liquid acid MSC-rich fraction presented a pH value around 1.

Adequate neutralisation of liquid acid MSC fraction was therefore mandatory before exploitation of the product for microbial fermentation. Simple neutralisation trough alkali addition was not possible because of the salt formation during neutralisation process.

Excessive salt presence in the final product was considered highly undesirable because the subsequent fermentation step requires a salt-controlled environment.

For this reason, different ion-exchange resins were tested and combined, aiming to achieve neutralised MSC solution with low salt content.

#### Weak-base anion exchange resin neutralisation: single resin treatment

Weak base anion exchange resin treatment was selected as a valuable approach for hydrolysate neutralisation: such resins are characterised by macroporous styrene-divinylbenzene structure supporting tertiary amine group. Tertiary amine is capable of adsorbing strong acids thanks to the free electron pair of the amine, as reported in the scheme below (Figure 6):

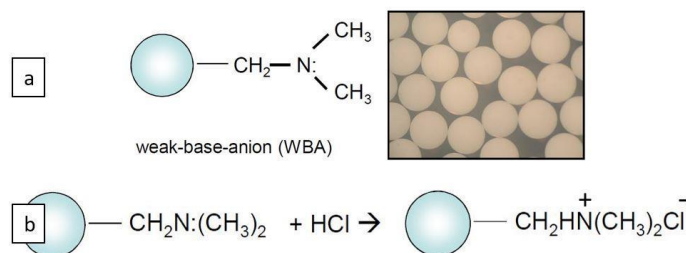


Figure 6: Weak-base anion resin operating mechanism

Dow Amberlite IRA96 weak base anion exchange resin was selected, and proper volume was estimated according to resin's exchange capacity.

Liquid acid MSC-rich fraction was therefore passed through a column filled with resin.

At the end of the treatment, recovered fraction showed a pH of 9: this value contrasted with expectations, indeed pH around 7 was expected.

Such value can be due to the presence in the hydrolysate of inorganic salts, released during hydrolysis by PHTP.

A subsequent recirculation of solution trough the same resin finally led the solution to reach pH 7.3.

Water was removed trough freeze drying and yield (%), moisture, inorganic and organic content of the product were determined (Table 5).

Organic (% wt.)	Inorganic (% wt.)	Moisture (% wt.)
49,50	33,19	17,31

Table 5: Moisture, organic and inorganic content of MSC from single resin treatment

$$\text{Yield (\% wt.)} = \frac{\text{Organic content in recovered product (g)}}{\text{Organic content in PHTP (g)}} * 100 = 29.0$$

Despite the good yield, the inorganic content in the product was considered excessive for further application as fermentation substrate for PHA production.

Such non-negligible quantity of salts in the product can be due to the ashes originally present in PHTP and solubilised during hydrolysis reaction, that were not retained by the resin.

#### Strong-acid cation and weak-base anion exchange resin neutralisation: double resin treatment

Aiming to remove both PHTP-derived salts and HCl, a treatment involving strong-acid cation exchange resin coupled with weak-base anion exchange resin was investigated.

Dow Amberlite IRA96 weak base anion exchange resin and Amberlite IR120 strong acid cation resin were used.

Appropriate volumes were estimated according to each resin's exchange capacity.

The process is illustrated in Figure 7:

1. hydrolysate was passed through the strong-acid cation exchange resin, where salts cations are exchanged with H<sup>+</sup>,
2. subsequently hydrolysate was passed through weak-base anion exchange resin, where acids are adsorbed by tertiary amine groups.

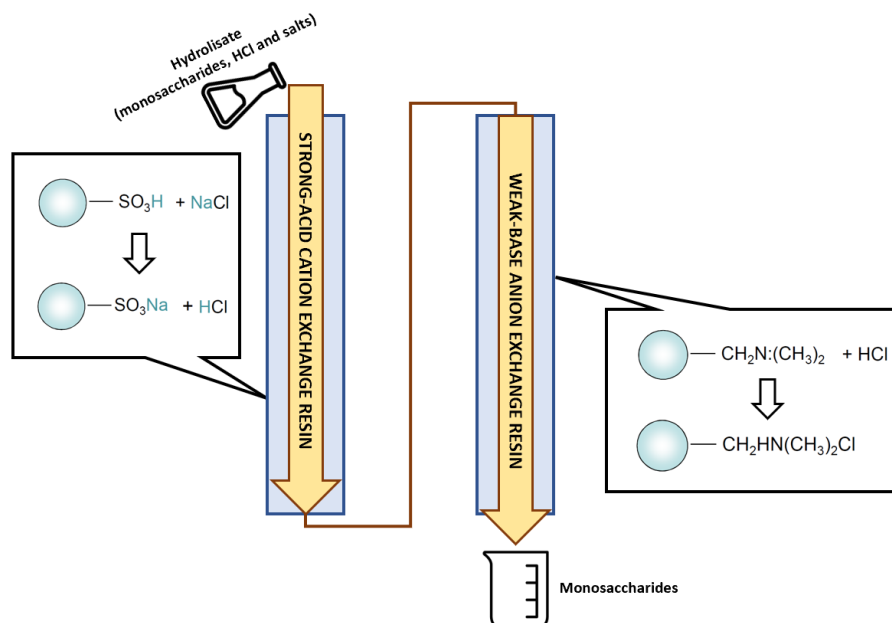


Figure 7: Double resin treatment

Treatment was tested on hydrolysate derived from 2g PHTP and pH 7.5 solution was recovered at the end of the whole protocol. Neutralised solution was freeze dried and yield (%), moisture, inorganic and organic content of the product were determined (Table 6):

<b>Organic (%wt.)</b>	<b>Inorganic (%wt.)</b>	<b>Moisture (%wt.)</b>
74.52	0	25.48

Table 6: Moisture, organic and inorganic content of MSC from double resin treatment

$$Yield (\% \text{ wt.}) = \frac{\text{Organic content in recovered product (g)}}{\text{Organic content in PHTP (g)}} * 100 = 15.7$$

Unfortunately, MSC yield was substantially decreased if compared with single weak-base cation exchange resin treatment (15.7% wt. vs 29.0% wt.).

Yield reduction can be due to MSC adsorption on both resins involved in the protocol.

Such hypothesis was confirmed during resin regeneration step: the regeneration off stream GC-MS analysis showed the presence of monosaccharides.

Despite that, the product was completely free of any inorganic component, thus making this protocol worth of scaling-up tests. Moreover, GC-MS qualitative analysis showed no relevant differences in MSC composition respect to the ones achieved in single treatment with weak-base cation exchange resin.

A scaling-up of the process was therefore performed, from 2g PHTP to 20g PHTP (same reaction conditions), with a hydrolysate volume to be treated on resins of 800mL.

Again, final product was completely ash-free. MSC yield was similar to the yield achieved in small-scale experiment (Table 7).

<b>Organic (%wt.)</b>	<b>Inorganic (%wt.)</b>	<b>Moisture (%wt.)</b>
67.75	0	32.25

Table 7: Moisture, organic and inorganic content of MSC from double resin treatment (first scale-up)

$$Yield (\% \text{ wt.}) = \frac{\text{Organic content in recovered product (g)}}{\text{Organic content in PHTP (g)}} * 100 = 16.7$$

Considering the low MSC yield and the high amount of MSC needed for further microbial fermentations, a second scale-up of the treatment was performed. 60g PHTP were hydrolysed, with a final volume of 2.4L hydrolysate to be treated on resin. In such case, an automatic system equipped with a peristaltic pump was used for resin treatment, as illustrated in Figure 8.

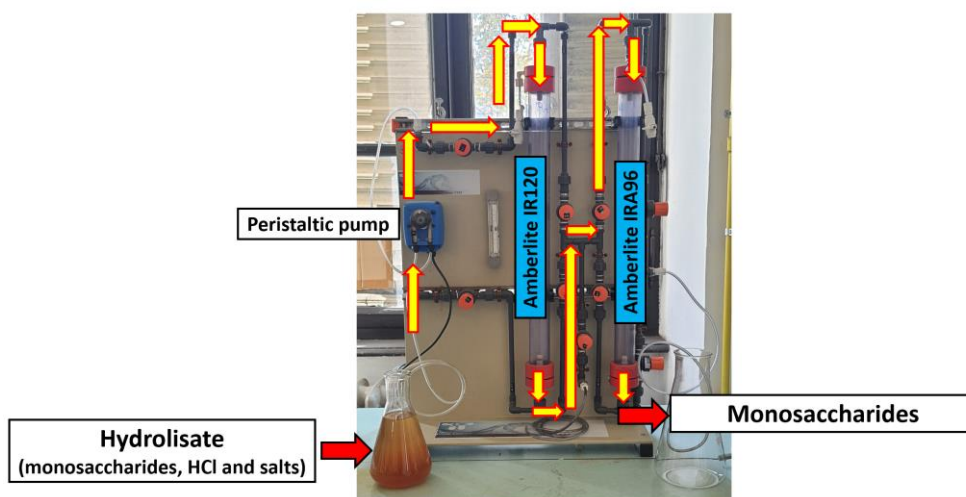


Figure 8: Automatic system for resin treatment

Neutralised solution was freeze dried and moisture, inorganic and organic content of the product were determined (Table 8)

Organic (%wt.)	Inorganic (%wt.)	Moisture (%wt.)
58.95	2.34	39.49

Table 8: Moisture, organic and inorganic content of MSC from double resin treatment (second scale-up)

A little amount of inorganic salts was detected in the final product but this was considered acceptable for the further fermentation step.

The whole protocol (hydrolysis 60g PHTP + resin treatment) was therefore repeated 5 times in order to recover enough monosaccharides for subsequent fermentation experiments. At the end of every repetition, resins were regenerated with proper volumes of 2M HCl and 1M NaOH solutions.

MSC so produced were collected and the overall yield, moisture, inorganic and organic content of the final product were determined (Table 9):

Organic (%wt.)	Inorganic (%wt.)	Moisture (%wt.)
75.78	7.81	16.40

Table 9: Moisture, organic and inorganic content of MSC from double resin treatment (5 treatments)

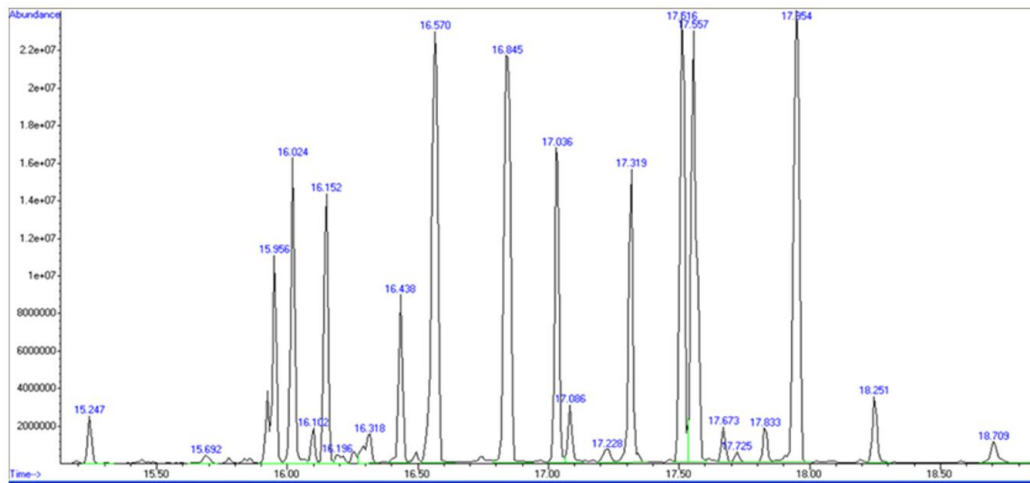
Again, a little quantity of ashes in the product was detected but this was still considered acceptable.

$$Yield (\% wt.) = \frac{\text{Organic content in recovered product (g)}}{\text{Organic content in PHTP (g)}} * 100 = 26.3$$

Surprisingly, the overall yield achieved after 5 repetitions was higher (+10%) respect to what previously observed. This increase in yield can be probably ascribed to the improvement of resin performances after some cycles of exchange-regenerations.

GC-MS qualitative analysis was performed and results are reported in Figure 9a and Table 10:

**a**



**b**

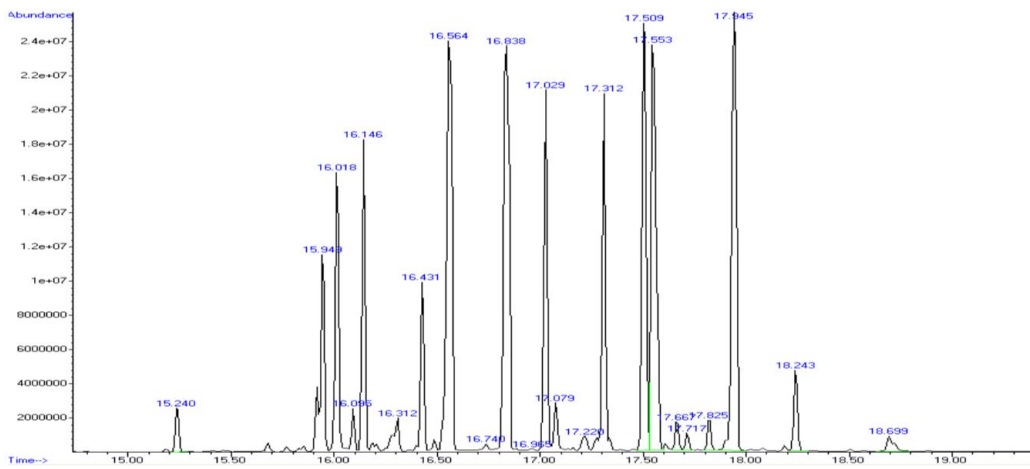


Figure 9: GC-MS spectrum of MSC



#	R.T. (min)	% of total GC area	Monosaccharides	MS Quality %
1	15.247	0.86%	meso-Erythritol	87
2	15.692	0.24%	Galactopyranose	43
3	15.956	4.82%	$\beta$ -D-(-)-Ribopyranose D-Ribose	91 91
4	16.024	5.60%	l-Mannopyranose	90
5	16.102	0.65%	D-(-)-Lyxofuranose D-(-)-Ribofuranose (isomer 2)	91 91
6	16.152	4.57%	$\beta$ -D-(-)-Ribopyranose $\alpha$ -D-Arabinopyranose D-Arabinopyranose (isomer 2)	91 91 91
7	16.196	0.33%	Arabinose	94
8	16.318	1.10%	D-(-)-Ribofuranose (isomer 2)	91
9	16.438	3.10%	L-(+)-Rhamnopyranose L-Mannose	87 91
10	16.57	12.62%	d-(+)-Xylose $\beta$ -D-(+)-Xylopyranose	93 91
11	16.845	13.39%	alpha.-D-(-)-Lyxopyranose $\beta$ -D-(+)-Xylopyranose D-Altrose	91 91 91
12	17.036	6.84%	$\beta$ D-Glucopyranose $\alpha$ -D-Mannopyranose $\beta$ -d-Galactopyranose D-Mannopyranose	91 91 91 91
13	17.086	1.11%	$\beta$ D-Galactofuranose D-(+)-Talofuranose (isomer 2) D-Allofuranose	91 91 91
14	17.228	0.48%	$\beta$ D-Galactofuranose	89
15	17.319	5.82%	$\alpha$ -D-Galactopyranose Talose $\alpha$ -D-Mannopyranose	91 91 91
16	17.516	10.17%	D-Mannopyranose $\beta$ -D-Glucopyranose $\alpha$ -D-Glucopyranose	93 91 91
17	17.557	11.23%	D-(+)- galactopyranose B-D-allopyranose Talose	91 91 91
18	17.673	0.67%	D-Mannitol D-(+)-Galactose D-Glucose	90 87 90
19	17.725	0.22%	D-(+)-Talofuranose (isomer 2)	72
20	17.833	0.76%	Galacturonic acid D-Glucose	93 93
21	17.954	13.32%	$\beta$ -D-Glucopyranose $\alpha$ -D-Mannopyranose	91 91
22	18.251	1.41%	D-(+)-Galacturonic acid	91
23	18.709	0.72%	Myo-Inositol Inositol	97 93

Table 10: Qualitative analysis of MSC

According to the GC-MS analysis, the main monosaccharides detected were glucose, galactose, mannose xylose and lyxose. No impurities were detected. The GC-MS was compared with analogous GC-MS of monosaccharides recovered before the resin treatment (Figure 9b) and no relevant differences in qualitative profile were detected.

### 2.2.2. PHTP-derived monosaccharides fermentation with mixed microbial culture

#### Pre-culture

Fermentative protocol with PHTP-derived MSC was performed in cooperation with the Department of “Scienza Applicata e Tecnologia” (DISAT) of the Politecnico di Torino.

A mixed microbial culture (MMC) derived from dairy industry was used in the protocol for shake flask fermentation study. The protocol applied was derived from a work by Khardenavis et al.<sup>32</sup>

A preliminary pre-culture step was planned, in order to select and increase the number of PHA-producing species in MMC.

Two 200mL pre-cultures were performed in 500mL Erlenmeyer flasks, in a swing plate (150rpm) at 30°C. Biomass growth medium was formulated to reach a C/N ratio equals to 50, optimal for PHA production and accumulation from MMC. Acetic acid was used during this stage as carbon source. Detailed biomass growth medium composition is reported in Table 11.

<b>Biomass growth medium</b>	
<b>Component</b>	<b>Concentration (g/L)</b>
CH <sub>3</sub> COOH	20
(NH <sub>4</sub> ) <sub>2</sub> HPO <sub>4</sub>	0.754
K <sub>2</sub> HPO <sub>4</sub>	1
MgSO <sub>4</sub> *7H <sub>2</sub> O	0.4
Trace element	1mL

<b>Trace element composition</b>	
<b>Component</b>	<b>Concentration (mg/mL)</b>
Na <sub>2</sub> SO <sub>4</sub>	25
FeSO <sub>4</sub> *7H <sub>2</sub> O	25
MnSO <sub>4</sub> *H <sub>2</sub> O	3.077
ZnSO <sub>4</sub> *7H <sub>2</sub> O	4.40
CuSO <sub>4</sub> *5H <sub>2</sub> O	0.79
CaCl <sub>2</sub> *2H <sub>2</sub> O	73.4

Table 11: MMC growth medium

In each flask 180mL of growth medium were added, together with 20mL MMC (10% overall volume). Pre-culture was performed up to 140hours and OD260 and pH were recorded approx. every 20/24 hours. In Figure 10 OD260 and pH vs time graph is reported:

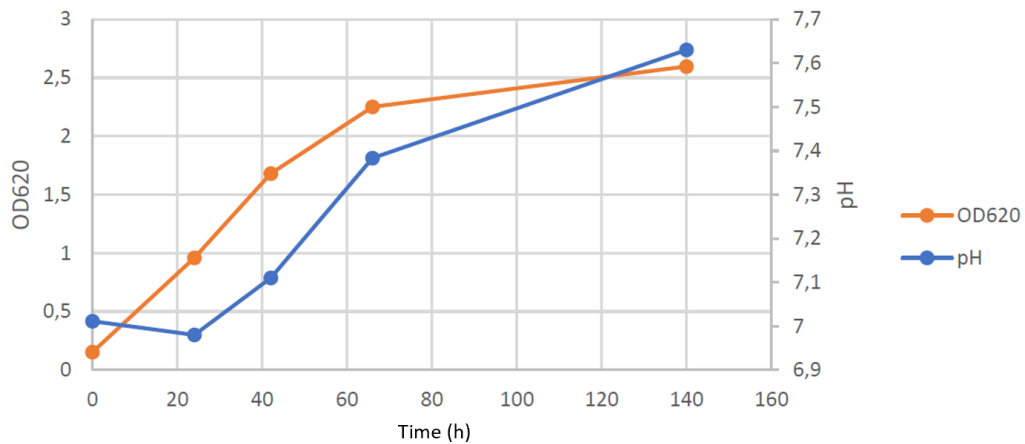


Figure 10: OD260 and pH vs time (pre-culture)

Pre-culture reached the stationary phase after about 140 hours and therefore appropriate aliquots of MMC for subsequent shake flask fermentation were recovered at 69 hours in correspondence of the exponential growth phase.

### Shake flask fermentation

Shake-flask fermentation was therefore performed by adding the appropriate volume of MMC from pre-culture to a biomass growth medium formulated as previously described, but with PHTP-derived monosaccharides as C source instead of acetic acid.

Since quantitative composition of pentoses and hexoses contained in PHTP-derived MSC was unknown, the growth medium was formulated to present a C/N ratio from 40 to 50.

A battery of 5 flasks was prepared, aiming to investigate microbial growth, quantity of PHA produced, PHA yield, and pH every 24 hours (Figure 11).



Figure 11: MMC flask fermentation of MSC

At the end of the fermentation, cellular biomass was recovered, dried and extracted by means of conventional extraction protocol using NaClO for cell rupture and chloroform for PHA recovery as reported in experimental section.

PHA yield was expressed through the formula:

$$PHA \text{ yield } (\%) = \frac{\text{recovere PHA weight (g)}}{\text{dry cellular biomass weight (g)}} * 100$$

Results are reported in Table 12 and graphically reported in Figure 12 and 13.

Flask	0	1	2	3	4	5
Time (h)	0	24	48	72	96	168
pH	7.0	6.1	5.1	4.8	4.8	4.8
Dry cellular biomass weight (g)	0	0.434	0.569	0.849	0.845	0.7946
Recovered PHA (g)	0	0.67	0.082	0.344	0.289	0.1991
PHA yield (%)	0	15.4	14.4	40.5	34.2	25.1

Table 12: Results of shake flask fermentation experiments

Stationary phase was reached after 72 hours. Indeed, pH and dry cellular biomass weight remain constant after 72 hours (Figure 12). Moreover, the amounts of recovered PHAs reach the maximum value in correspondence of this time (Figure 13), with a PHA yield of 40.5%. It should be noted that after the stationary phase is reached, recovered PHA (and PHA yield) dramatically decreased, probably due to their consumption by MMC that used it as energy and carbon source once MSC in growth medium were depauperated during the growth phase.

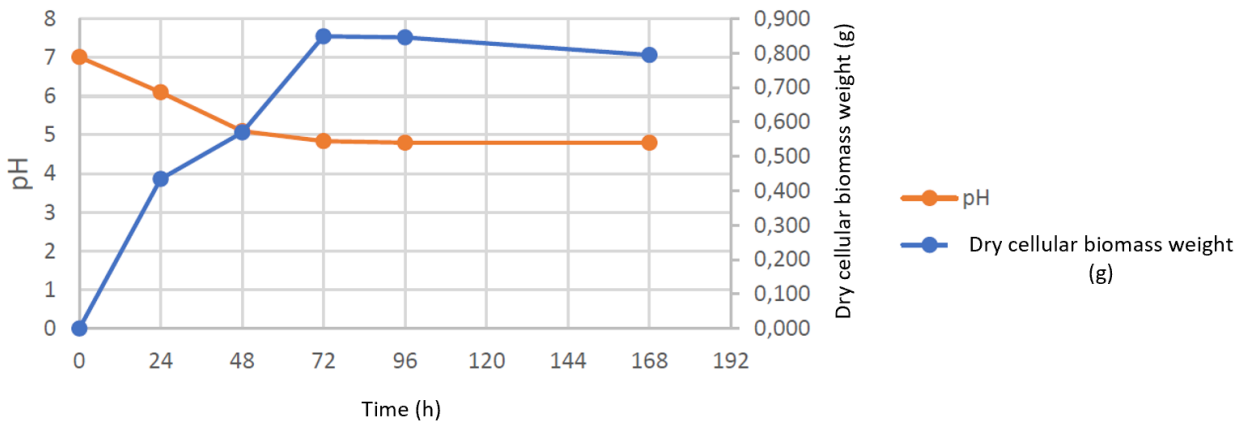


Figure 12: pH and dry cellular biomass weight vs time

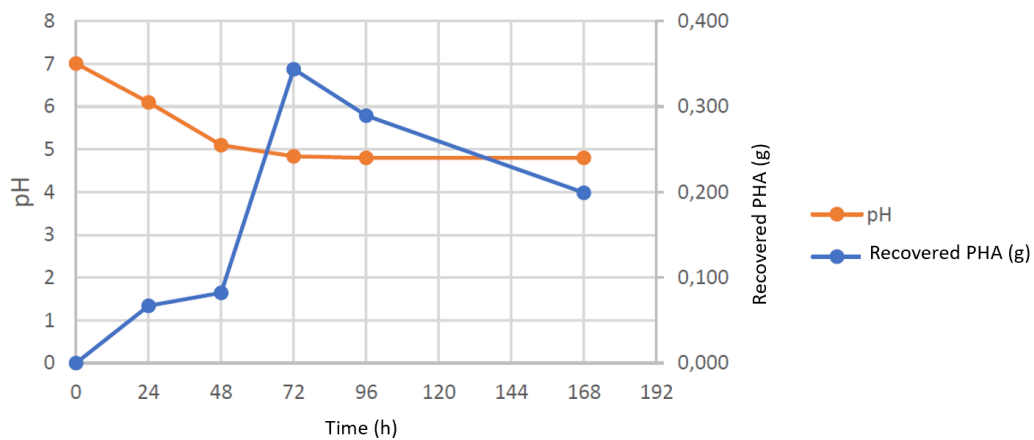


Figure 13: pH and dry cellular biomass weight vs time

### PHA characterisation

FT-IR analysis of recovered PHA was performed and compared with literature-reported spectra (PHA achieved from *Pseudomonas putida*)<sup>33</sup> (Figure 14 and Table 13).

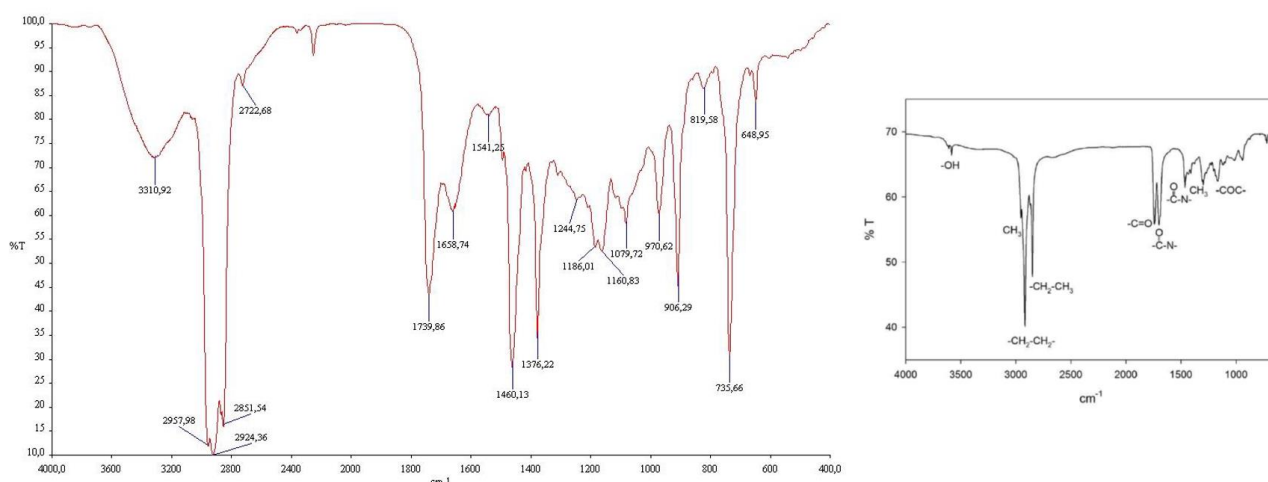


Figure 14: FTIR spectra of extracted PHA (red) and FTIR spectra achieved from *Pseudomonas putida*<sup>33</sup> (black)

<b>cm<sup>-1</sup></b>	<b>Vibrational mode</b>	<b>Functional group</b>	<b>Details</b>
3310.92	Stretching	-OH	Polymer terminal group
2957.98	Asymmetric stretching	-CH <sub>3</sub>	Side chain
2924.36	Asymmetric stretching	-CH <sub>2</sub> -	Side chain valerate
2851.54	Symmetric stretching	-CH <sub>3</sub>	Side chain
1739.86	Stretching	C=O	Ester bond: "PHA marker band"
1658.74	Stretching	-CO-N-	Bacterial intracellular amide
1541.25	Bending	N-H	Protein amide
1460.13	Stretching	-CO-N-	Bacterial intracellular amide
1376.22	Bending	-CH <sub>3</sub>	Terminal -CH <sub>3</sub> groups
1244.75	Asymmetric stretching	-P=O	Phosphodiester backbone of nucleic acids
1160.83 -648.95	Stretching	C-O e C-C	Vibrations of the amorphous phase

Table 13: FTIR bands assignment of PHA according to literature

In recorded FT-IR spectra, the PHA marker band was detected at 1739.36 cm<sup>-1</sup>.

The presence of some impurities, related to DNA and protein residues was also detected.

Moreover, the peak at 2924.36 cm<sup>-1</sup>, referred to side chain -CH<sub>2</sub>- could indicate the presence of valerate monomer in the polymer.

<sup>1</sup>H-NMR analysis was performed and compared with literature<sup>34</sup>. Despite the presence of impurities was confirmed by the spectra, it was possible to appreciate the presence of both valerate and butyrate monomers in the product, thus allowing the hypothesis that the recovered PHA was a copolymer Poly(hydroxi-*butyrate-co*-hydroxy-*valerate*) (Figure 15 and Table 14).

Chemical Shift ( $\delta$ , ppm)	Functional group
0.84	-CH <sub>3</sub> (5)
1.28	-CH <sub>3</sub> (4')
1.57	-CH <sub>2</sub> (4)
2.25 – 2.34	-CH <sub>2</sub> (2,2')
5.34	-CH (3,3')

Table 14: Chemical shift of <sup>1</sup>H-NMR analysis of extracted PHA

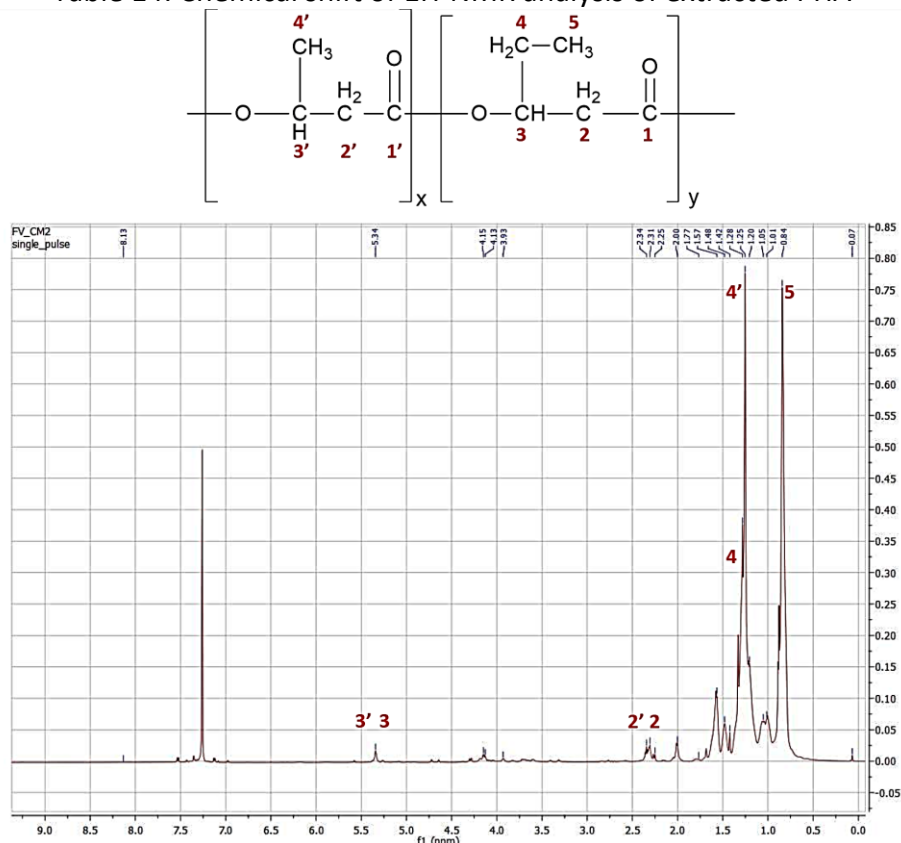


Figure 15: <sup>1</sup>H-NMR analysis of extracted PHA

### Non-conventional PHA extractions

Aiming to improve the sustainability of the extraction protocol, some preliminary, qualitative experiments were conducted using US for cell breakage and 2-Methyltetrahydrofuran (2-MeTHF) for PHA recovery.

Initially, US were coupled to chloroform extraction to verify their efficiency in cell lysis for PHA release.

Dry cellular biomass was suspended in water and CHCl<sub>3</sub> was added. The system was sonicated for 15 minutes and at the end of the treatment the chloroform phase was recovered. The procedure was repeated twice. At the end of the protocol FTIR analysis was performed on recovered PHA.

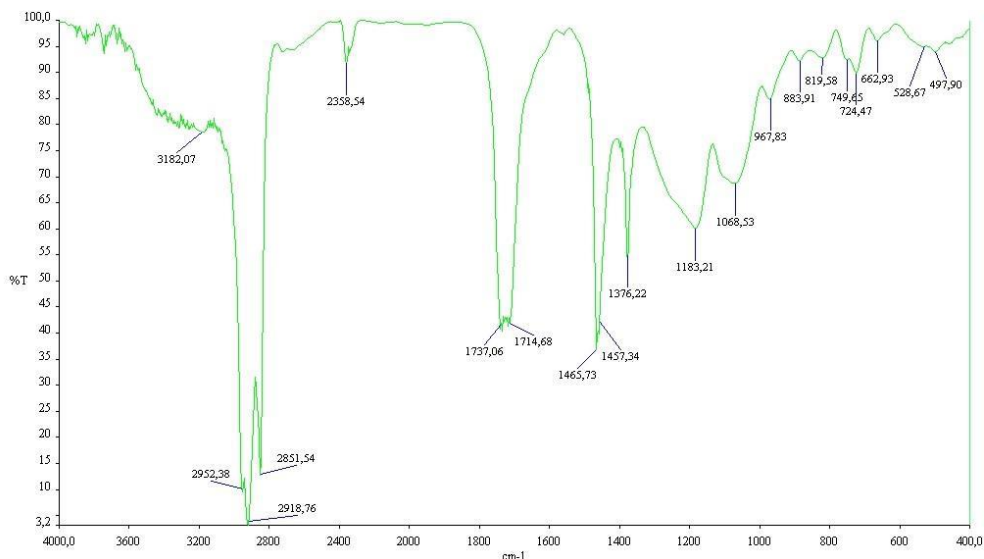


Figure 16: FTIR analysis of PHA extracted using US+CHCl<sub>3</sub> extraction

By comparing the FTIR spectra of PHA extracted with US + CHCl<sub>3</sub> (Figure 16) with PHA extracted using NaClO + CHCl<sub>3</sub> (Figure 14), it can be noted the absence of bands at 1658.74 cm<sup>-1</sup>, 3310.92 cm<sup>-1</sup>, 1541.25 cm<sup>-1</sup> and 1244.75 cm<sup>-1</sup> ascribed to the presence of impurities. Therefore, it can be hypothesised that US can reduce the presence of impurities in the product.

A second experiment using NaClO with 2-MeTHF as the extraction solvent was conducted, aiming to investigate the substitution of chloroform with a green solvent. Extracted PHA was qualitatively characterised using FTIR: showing the presence of some impurities. Despite such criticalities the use of 2-MeTHF was considered worth of further investigations (Figure 17).

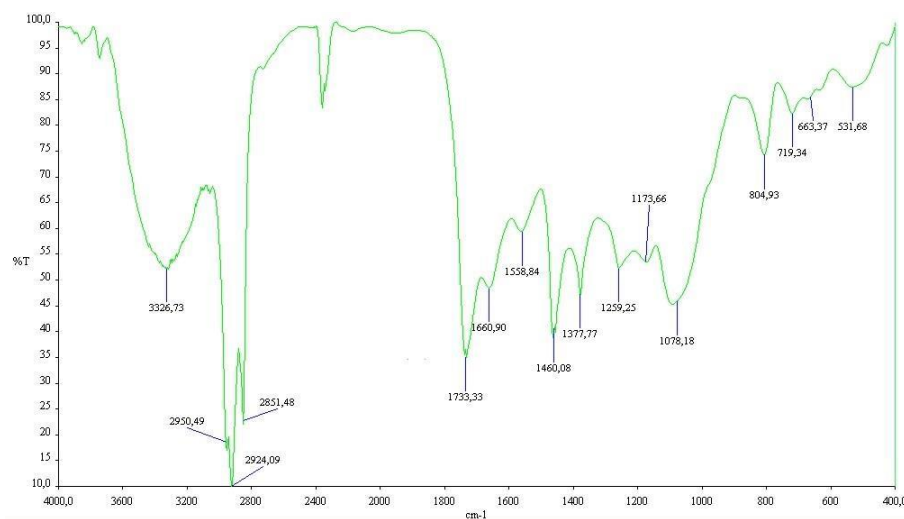


Figure 17: FTIR analysis of PHA extracted using NaClO+2-MeTHF

Finally, 2-MeTHF was used for US-assisted extraction: dry cellular biomass was suspended in water and 2-MeTHF was added. The system was sonicated for 15 minutes and at the end of the treatment an emulsion was formed. Such emulsion was left to rest for 48h aiming to recover at least a little fraction of the organic fraction for FTIR qualitative analysis (Figure 18).

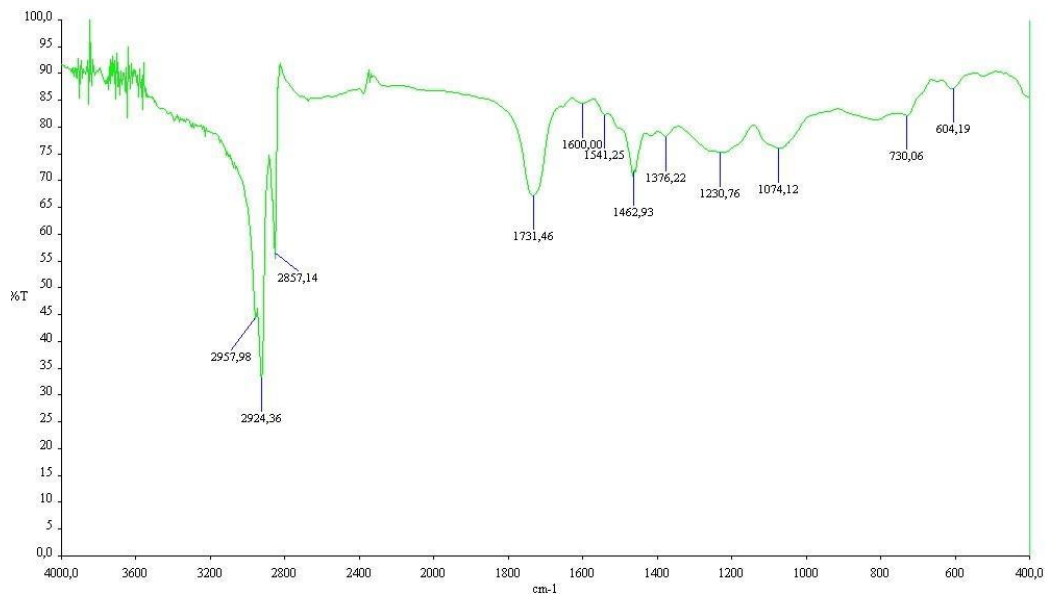


Figure 18: FTIR analysis of PHA extracted using US+2-MeTHF

The absence of impurities bands was confirmed also in this case, but several issues still remain to be solved due to the emulsion formation that makes PHA quantitative recovery extremely difficult.



## 2.3. CONCLUSIONS

In this chapter monosaccharides were produced from biomass PHTP and subsequently used as fermentation substrate for mixed microbial culture towards polyhydroxyalkanoates. The whole protocol was developed trying to reduce typical limitation of actual polyhydroxyalkanoates production strategies, aiming to improve sustainability and integrating it with waste valorisation principles typical of biorefinery:

- Monosaccharides were sustainably produced from cost-effective renewable 2G PHTP waste biomass. Thanks to microwave irradiation, fast hydrolysis reaction was scaled-up from few grams to 60 grams without any issue. Resin treatment allowed pure monosaccharides recovery with low inorganic content (7.81%). A reduction in yield was observed when resin treatments were performed (52% yield without resin treatment, 29% single resin treatment, 26% double resin treatment), suggesting that resin can partially adsorb monosaccharides. Unfortunately, this limitation could negatively impact the application of the whole protocol at industrial level. A future improvement of this step can be beneficial in maximising the quantity of monosaccharides recovered. This could be achieved by reducing the quantity of acid involved in the hydrolysis and consequently in the volume of resin needed for neutralisation. Reduction of acid involved in hydrolysis could be beneficial also from an environmental and economic perspective.
- Mixed microbial culture derived from dairy industry waste was exploited for shake-flask fermentation, allowing to set up a simple protocol with no sterility requirements and good polyhydroxyalkanoates yields (around 40% after 72hours of fermentation). According to NMR and FTIR analyses, recovered product was characterised as Poly(hydroxi-*butyrate-co-hydroxy-valerate*).
- Despite some impurities, polyhydroxyalkanoates were recovered with good yields and some preliminary experiments for green and sustainable polyhydroxyalkanoates extraction were performed using US and 2-MeTHF, avoiding the use of harmful substances such as chloroform and NaClO involved in downstream processing of cells. Further experiments are needed to improve the protocol, aiming to increase the yield of the recovered product.

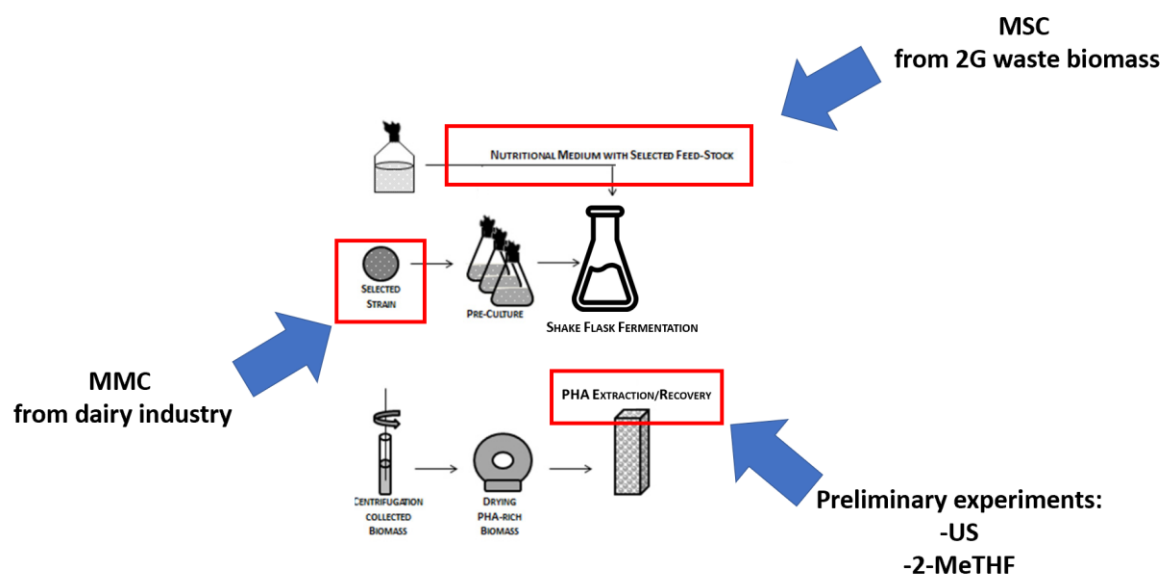


Figure 19: Conclusions

## 2.4. EXPERIMENTAL

### Reagents

All reagents and solvents, unless otherwise specified, were purchased from Sigma-Aldrich and used without further purification.

### NREL-derived protocol

NREL-protocol for chemical characterisation of CPH and RCPH was performed following the procedure illustrated by Genevini et al.

### *Moisture, inorganic and organic CPH/RCPH content evaluation*

CPH/RCPH moisture content was estimated by gravimetric analysis by placing approx. 200mg of raw biomass for 24hours at 80°C in a furnace muffler (Gelman Instrument Company, Ann Arbor, MI, USA).

Inorganic content was subsequently determined by gravimetric analysis, increasing the furnace muffler temperature to 650°C and exposing the biomass at such temperature for 4hours. At the end of the process inorganic ashes are recovered.

Results are expressed as %W of CPH and RCPH.

### *Organic fraction chemical characterisation*

Organic fraction chemical characterisation was performed through subsequent fractionation steps.

- Fraction I: organic extraction of lipids, resins, catechols, tannins, part of proteins and part of fulvic acids.

Approx. 5g CPH/RCPH were placed in a 500mL flat bottom flask and 250mL of a benzene:ethanol 50:50 (s/l ratio 1g to 50mL) was added to the flask. The system was left at room temperature under stirring for 2 hours.

At the end of the extraction, biomass was filtered through sintered glass filter (por.4) and dried at 45°C in ventilated oven. Difference between

-Fraction II: hemicellulose, part of proteins, sugars and part of fulvic acids.

### PHTP hydrolysis

The hydrolysis reaction was carried out in a multimode MW-reactor (SynthWave, Milestone) using HCl 1N.

Nitrogen pressure (40 bar) was added to the reactor to keep aqueous HCl in liquid state.

PHTP was added in 40mL specific vial (2g), or directly in the reactor vessel (20-60g).

The reaction was conducted at 150°C for 2 minutes, with biomass/liquid ratio equal to 1:10 wt./v. To reach the set temperature, an 8-minute ramp was applied.

The reaction crude was then filtered on paper under vacuum with a Buchner funnel and the residual solid was washed with distilled water.

### Weak-base anion exchange resin neutralisation: single resin treatment

Resin Dow Amberlite IRA96 is characterized by an exchange capacity of 1.25 eq/L and a service flow rate ranging from 5 to 40 bed volumes (BV) of resin per hour (BV / h).

The quantity of resin involved in the treatment was calculated according to the quantity of HCl used for the hydrolysis reaction and according to the exchange capacity of the resin (plus an excess of 25%).

The resin was packed in a glass column and the hydrolysate was fed with a service flow rate of 20 BV/h. Subsequently, a volume of distilled water equal to 2BV was passed through the column for washing (service flow rate 20 BV/h).

Hydrolysate and washing were recovered, being rich in MSC.

At the end of the treatment the exhaust resin was regenerate using 1N NaOH solution, with a proper flow rate to guarantee a minimum contact time of 30 minutes.

Proper volume of regenerant NaOH 1N was calculated according to the resin's exchange capacity (plus an excess of 25%). The resin was then washed with distilled water (3BV).

#### Strong-acid cation and weak-base anion exchange resin neutralisation: double resin treatment

In double resin treatment, hydrolysate was fed to the strong-acid cation exchange resin column and subsequently to the weak-base anion exchange resin column.

Proper quantities of resins were calculated, considering the volume of hydrolysate and their exchange capacity (plus an excess of 25%):

1. Amberlite IR120H: exchange capacity of 1.8 eq/L and service flow rate ranging from 5 to 40 BV/h
2. Amberlite IRA96: exchange capacity of 1.25 eq/L and service flow rate ranging from 5 to 40 BV/h

Resins were packed in glass column or in an automated double column system provided with peristaltic pump (Tecnoimpianti Water Treatment)

Hydrolysate was fed to the first resin (strong acidic) with a service flow rate of 20 BV / h. Subsequently, a volume of distilled water equal to 2BV was passed through the column for washing. Hydrolysate and washing were recovered, and fed to the second resin (weak basic) with a service flow rate of 20 BV / h. Subsequently, a volume of distilled water equal to 2BV was passed through the column for washing.

At the end of the double treatment neutral hydrolysate was recovered and freeze dried in a *Telstar Lyotest freeze-drier* (-70°C, 80 mbar) to achieve pure MSC.

#### MSC Ponderal analysis

Freeze-dried MSC were subjected to ponderal analysis for moisture, inorganic and organic content determination.

Approx. 150mg MSC were placed into porcelain crucible and left in muffle at 100°C overnight for moisture content determination. Subsequently, the crucible was heated in muffle at 650°C for the inorganic content determination.

#### MSC GC-MS analysis

GC-MS analyses were conducted on an Agilent 6890 GC (Agilent Technologies - USA), connected to an Agilent Network 5973 mass detector, using a MEGA-5 MS column (30 m capillary column, 0.25 mm and film thickness of 0.25 µm).

The temperature program was performed as follows:

- initial maintenance in isotherm for 5 minutes at 65°C,
- ramp 10°C / minute up to 100°C
- isotherm at 100°C for 1 minute,
- ramp 20°C / minute up to 230°C
- isotherm 230°C for 1 minute,
- ramp 20°C / minute up to 300°C
- isotherm at 300°C for 5 minutes.

Split injection 1:20, injector temperature 250 ° C, detector temperature 280 ° C. Carrier gas: He.

Before injection MSC were derivatised using BSTFA (N,O-Bis(trimethylsilyl)trifluoroacetamide): 10mg MSC were dissolved in 1mL pyridine and 0.250mL BSTFA were added. The system was

heated at 60°C under stirring for 45min. The identification of the individual monosaccharides was performed on the basis of GC-MS chromatograms using Library MS NIST 05

#### Pre-culture

The pre-culture was settled in 500 mL flask. 180mL *Khardenavis*<sup>32</sup> growth medium (Table 11) were added to the flask (acetic acid was used as carbon source) together with 20mL inoculum. The flask was stirred in a Thermo Scientific MaxQ 6000 thermostat at 150rpm, 30°C, 0-140h. Activated carbon filters were used to close the flasks. Bacterial growth was monitored using the spectrophotometer (Perkin Elmer Lambda 465), reading the optical density at 620 nm (OD620) and monitoring the pH.

#### Shake flask fermentation

The fermentation was settled in 5 flasks (500 mL) stirred in a Thermo Scientific MaxQ 6000 thermostat at 150 rpm, 30°C, 0-168h. *Khardenavis*<sup>32</sup> growth medium was used (Table 11) using MSC (20g/L, considering only the organic fraction of the product) as carbon source. 20mL inoculum were kept from the pre-culture (69h) and added to the flasks. Activated carbon filters were used to close the flasks. The flasks were sequentially recovered and analysed (one flask every 24h from 0 to 96 plus an extra flask at 168h).

#### Cellular biomass recovery

The content of each flask (growth medium + cellular biomass) was centrifuged at 4100 rpm for 10 minutes and the precipitate (cellular biomass) was washed twice with distilled water. Recovered cellular biomass was dried in an oven at 60 °C for 72 hours.

#### Conventional PHA extraction

The PHAs were recovered from cellular biomass using sodium hypochlorite for cell lysis and chloroform for PHA extraction with NaClO/CHCl<sub>3</sub> 1/1. 10mL of NaClO and 10mL of CHCl<sub>3</sub> were added in a 45mL Falcon tube to the cellular biomass and stirred with magnetic stirrer for 90min. At the end of the extraction step, the crude was centrifuged at 3600 rpm for 10 minutes: a clear separation between aqueous and solvent phase was observed with a cell debris layer at the interface. Chloroform fraction, rich in PHA, was recovered by means of a Pasteur pipette and placed in a 15mL tube. Chloroform was evaporated by gentle nitrogen flux and the recovered PHA quantity was determined gravimetrically.

#### Non-conventional PHA extractions

-US + CHCl<sub>3</sub>

Cell lysis was carried out with US Hainertec generator (Suzhou) Co., Ltd, (20KHz, 500W).

1. Cell biomass was placed in a glass vial (40 mL) and 20mL of distilled water were added;
2. sonication was carried out for 15 minutes,
3. the suspension obtained at the end of the sonication was transferred to 45 mL Falcon tube and 10 mL of CHCl<sub>3</sub> were added,
4. the system was then stirred on a magnetic plate for 30 minutes to allow PHA extraction in the organic phase.

At the end of the extraction step, the crude was centrifuged at 3600 rpm for 10 minutes: a clear separation between aqueous and solvent phase was observed with a cell debris layer at

the interface.  $\text{CHCl}_3$  fraction, rich in PHA, was recovered by means of a Pasteur pipette and placed in a 15mL falcon.  $\text{CHCl}_3$  was evaporated by gentle nitrogen flux and the recovered PHA quantity was determined gravimetrically.

- NaClO + 2-MeTHF

The extraction involving NaClO and 2-MeTHF was performed as described for conventional extraction

-US + 2-MeTHF

Cell lysis was carried out with US Hainertec generator (Suzhou) Co., Ltd, (20KHz, 500W).

1. Cell biomass was placed in a glass vial (40 mL) and 20mL of distilled water were added together with 10mL 2-MeTHF
2. sonication was carried out for 15 minutes,
3. the suspension obtained at the end of the sonication was transferred to 45 mL Falcon tubes,
4. the system was then stirred on a magnetic plate for 30 minutes to further improve PHA extraction in 2-MeTHF phase. A stabile emulsion was observed.
5. the system was transferred into a separation funnel and left to rest 48h,
6. part of 2-MeTHF was recovered and evaporated in rotary evaporator to recover extracted PHA,
7. recovered PHA quantity was determined gravimetrically.

#### FTIR analysis of PHA

The IR analyses of PHAs were carried out with the Perkin Elmer BX FT-IR System spectrometer through the film casting method: PHA dissolved in chloroform was deposited on an infrared transparent window. Chloroform was evaporated and the window was placed in the instrument.

#### $^1\text{H-NMR}$ analysis of PHA

All NMR spectra were recorded with a Jeol 600 ECZ R instrument at 25 °C using  $\text{CdCl}_2$  as a solvent.

## 2.5. REFERENCES

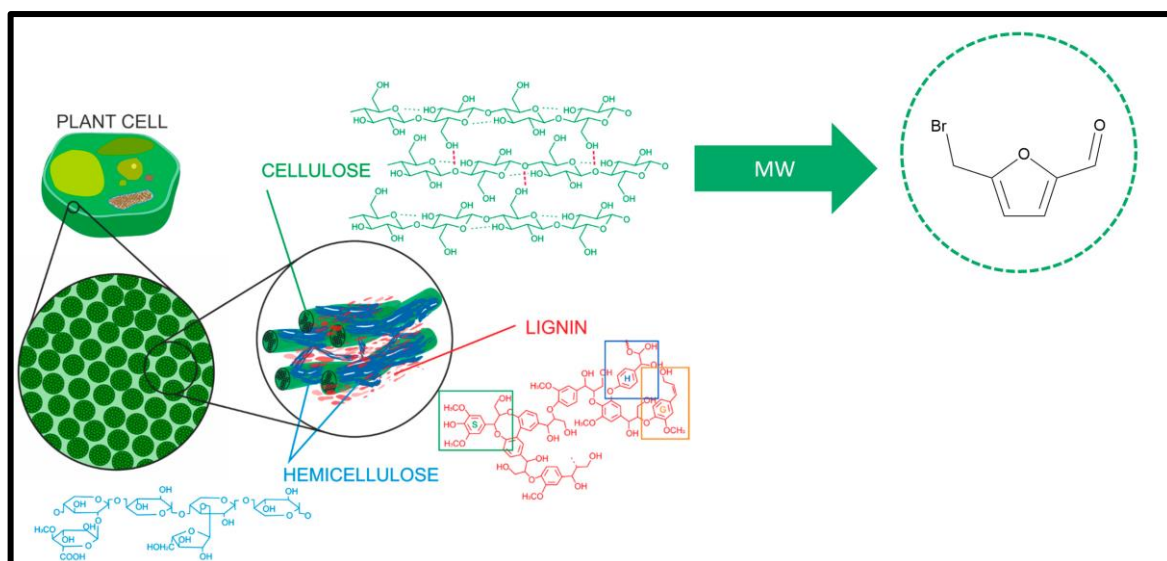
- (1) Tarrahi, R.; Fathi, Z.; Seydibeyoğlu, M. Ö.; Doustkhah, E.; Khataee, A. Polyhydroxyalkanoates (PHA): From Production to Nanoarchitecture. *Int. J. Biol. Macromol.* **2020**, *146*, 596–619. <https://doi.org/10.1016/j.ijbiomac.2019.12.181>.
- (2) Raza, Z. A.; Abid, S.; Banat, I. M. Polyhydroxyalkanoates: Characteristics, Production, Recent Developments and Applications. *Int. Biodeterior. Biodegrad.* **2018**, *126*, 45–56. <https://doi.org/10.1016/j.ibiod.2017.10.001>.
- (3) <https://www.european-bioplastics.org/bioplastics/>.
- (4) Możejko-Ciesielska, J.; Kiewisz, R. Bacterial Polyhydroxyalkanoates: Still Fabulous? *Microbiol. Res.* **2016**, *192*, 271–282. <https://doi.org/10.1016/j.micres.2016.07.010>.
- (5) Riaz, S.; Rhee, K. Y.; Park, S. J. Polyhydroxyalkanoates (PHAs): Biopolymers for Biofuel and Biorefineries. *Polymers* **2021**, *13* (2), 253. <https://doi.org/10.3390/polym13020253>.
- (6) Philip, S.; Keshavarz, T.; Roy, I. Polyhydroxyalkanoates: Biodegradable Polymers with a Range of Applications. *J. Chem. Technol. Biotechnol.* **2007**, *82* (3), 233–247. <https://doi.org/10.1002/jctb.1667>.
- (7) Pakalapati, H.; Chang, C.-K.; Show, P. L.; Arumugasamy, S. K.; Lan, J. C.-W. Development of Polyhydroxyalkanoates Production from Waste Feedstocks and Applications. *J. Biosci. Bioeng.* **2018**, *126* (3), 282–292. <https://doi.org/10.1016/j.jbiosc.2018.03.016>.
- (8) Raza, Z. A.; Riaz, S.; Banat, I. M. Polyhydroxyalkanoates: Properties and Chemical Modification Approaches for Their Functionalization. *Biotechnol. Prog.* **2018**, *34* (1), 29–41. <https://doi.org/10.1002/btpr.2565>.
- (9) Volova, T.; Kiselev, E.; Nemtsev, I.; Lukyanenko, A.; Sukovatyi, A.; Kuzmin, A.; Ryltseva, G.; Shishatskaya, E. Properties of Degradable Polyhydroxyalkanoates with Different Monomer Compositions. *Int. J. Biol. Macromol.* **2021**, *182*, 98–114. <https://doi.org/10.1016/j.ijbiomac.2021.04.008>.
- (10) Valappil, S. P.; Misra, S. K.; Boccaccini, A. R.; Roy, I. Biomedical Applications of Polyhydroxyalkanoates, an Overview of Animal Testing and *in Vivo* Responses. *Expert Rev. Med. Devices* **2006**, *3* (6), 853–868. <https://doi.org/10.1586/17434440.3.6.853>.
- (11) Tan, D.; Wang, Y.; Tong, Y.; Chen, G.-Q. Grand Challenges for Industrializing Polyhydroxyalkanoates (PHAs). *Trends Biotechnol.* **2021**, *39* (9), 953–963. <https://doi.org/10.1016/j.tibtech.2020.11.010>.
- (12) Pagliano, G.; Galletti, P.; Samorì, C.; Zaghini, A.; Torri, C. Recovery of Polyhydroxyalkanoates From Single and Mixed Microbial Cultures: A Review. *Front. Bioeng. Biotechnol.* **2021**, *9*, 624021. <https://doi.org/10.3389/fbioe.2021.624021>.
- (13) Sabapathy, P. C.; Devaraj, S.; Meixner, K.; Anburajan, P.; Kathirvel, P.; Ravikumar, Y.; Zabed, H. M.; Qi, X. Recent Developments in Polyhydroxyalkanoates (PHAs) Production – A Review. *Bioresour. Technol.* **2020**, *306*, 123132. <https://doi.org/10.1016/j.biortech.2020.123132>.
- (14) Vigneswari, S.; Noor, M. S. M.; Amelia, T. S. M.; Balakrishnan, K.; Adnan, A.; Bhubalan, K.; Amirul, A.-A. A.; Ramakrishna, S. Recent Advances in the Biosynthesis of Polyhydroxyalkanoates from Lignocellulosic Feedstocks. *Life* **2021**, *11* (8), 807. <https://doi.org/10.3390/life11080807>.
- (15) Koller, M.; Salerno, A.; Muhr, A.; Reiterer, A.; Chiellini, E.; Casella, S.; Horvat, P.; Braunegg, G. Whey Lactose as a Raw Material for Microbial Production of Biodegradable Polyesters. In *Polyester*; Saleh, H. E.-D., Ed.; InTech, 2012. <https://doi.org/10.5772/48737>.
- (16) Samorì, C.; Abbondanzi, F.; Galletti, P.; Giorgini, L.; Mazzocchetti, L.; Torri, C.; Tagliavini, E. Extraction of Polyhydroxyalkanoates from Mixed Microbial Cultures: Impact on Polymer Quality and Recovery. *Bioresour. Technol.* **2015**, *189*, 195–202. <https://doi.org/10.1016/j.biortech.2015.03.062>.
- (17) Sawant, S. S.; Salunke, B. K.; Tran, T. K.; Kim, B. S. Lignocellulosic and Marine Biomass as Resource for Production of Polyhydroxyalkanoates. *Korean J. Chem. Eng.* **2016**, *33* (5), 1505–1513. <https://doi.org/10.1007/s11814-016-0019-4>.
- (18) Al-Battashi, H. S.; Annamalai, N.; Sivakumar, N.; Al-Bahry, S.; Tripathi, B. N.; Nguyen, Q. D.; Gupta, V. K. Lignocellulosic Biomass (LCB): A Potential Alternative Biorefinery Feedstock for

- Polyhydroxyalkanoates Production. *Rev. Environ. Sci. Biotechnol.* **2019**, *18* (1), 183–205. <https://doi.org/10.1007/s11157-018-09488-4>.
- (19) Narayanan, A.; Sajeev Kumar, V. A.; Ramana, K. V. Production and Characterization of Poly (3-Hydroxybutyrate-Co-3-Hydroxyvalerate) from *Bacillus Mycoides* DFC1 Using Rice Husk Hydrolyzate. *Waste Biomass Valorization* **2014**, *5* (1), 109–118. <https://doi.org/10.1007/s12649-013-9213-3>.
- (20) Pan, W.; Perrotta, J. A.; Stipanovic, A. J.; Nomura, C. T.; Nakas, J. P. Production of Polyhydroxyalkanoates by *Burkholderia Cepacia* ATCC 17759 Using a Detoxified Sugar Maple Hemicellulosic Hydrolysate. *J. Ind. Microbiol. Biotechnol.* **2012**, *39* (3), 459–469. <https://doi.org/10.1007/s10295-011-1040-6>.
- (21) Silva, L. F.; Taciro, M. K.; Raicher, G.; Piccoli, R. A. M.; Mendonça, T. T.; Lopes, M. S. G.; Gomez, J. G. C. Perspectives on the Production of Polyhydroxyalkanoates in Biorefineries Associated with the Production of Sugar and Ethanol. *Int. J. Biol. Macromol.* **2014**, *71*, 2–7. <https://doi.org/10.1016/j.ijbiomac.2014.06.065>.
- (22) *Applications of Biotechnology in Traditional Fermented Foods*; National Academies Press: Washington, D.C., 1992; p 1939. <https://doi.org/10.17226/1939>.
- (23) Serafim, L. S.; Lemos, P. C.; Albuquerque, M. G. E.; Reis, M. A. M. Strategies for PHA Production by Mixed Cultures and Renewable Waste Materials. *Appl. Microbiol. Biotechnol.* **2008**, *81* (4), 615–628. <https://doi.org/10.1007/s00253-008-1757-y>.
- (24) Mixed Microbial Cultures for Industrial Biotechnology: Success, Chance, and Challenges. In *Industrial Biocatalysis*; Grunwald, P., Ed.; Jenny Stanford Publishing, 2014; pp 241–274. <https://doi.org/10.1201/b17828-9>.
- (25) Bocaz-Beltrán, J.; Rocha, S.; Pinto-Ibieta, F.; Ciudad, G.; Cea, M. Novel Alternative Recovery of Polyhydroxyalkanoates from Mixed Microbial Cultures Using Microwave-assisted Extraction. *J. Chem. Technol. Biotechnol.* **2021**, *96* (9), 2596–2603. <https://doi.org/10.1002/jctb.6802>.
- (26) Alfano, S.; Lorini, L.; Majone, M.; Sciubba, F.; Valentino, F.; Martinelli, A. Ethylic Esters as Green Solvents for the Extraction of Intracellular Polyhydroxyalkanoates Produced by Mixed Microbial Culture. *Polymers* **2021**, *13* (16), 2789. <https://doi.org/10.3390/polym13162789>.
- (27) Samorì, C.; Basaglia, M.; Casella, S.; Favaro, L.; Galletti, P.; Giorgini, L.; Marchi, D.; Mazzocchetti, L.; Torri, C.; Tagliavini, E. Dimethyl Carbonate and Switchable Anionic Surfactants: Two Effective Tools for the Extraction of Polyhydroxyalkanoates from Microbial Biomass. *Green Chem.* **2015**, *17* (2), 1047–1056. <https://doi.org/10.1039/C4GC01821D>.
- (28) Genevini, P.; Adani, F.; Villa, C. Rice Hull Degradation by Co-Composting with Dairy Cattle Slurry. *Soil Sci. Plant Nutr.* **1997**, *43* (1), 135–147. <https://doi.org/10.1080/00380768.1997.10414722>.
- (29) Kelly J. Dussan; Debora D.V. Silva; Elisangela J. C. Moraes; Priscila V. Arruda; Maria G.A. Felipe. Dilute-Acid Hydrolysis of Cellulose to Glucose from Sugarcane Bagasse. *Chem. Eng. Trans.* **2014**, *38*, 433–438. <https://doi.org/10.3303/CET1438073>.
- (30) Świątek, K.; Gaag, S.; Klier, A.; Kruse, A.; Sauer, J.; Steinbach, D. Acid Hydrolysis of Lignocellulosic Biomass: Sugars and Furfurals Formation. *Catalysts* **2020**, *10* (4), 437. <https://doi.org/10.3390/catal10040437>.
- (31) Tabasso, S.; Montoneri, E.; Carnaroglio, D.; Caporaso, M.; Cravotto, G. Microwave-Assisted Flash Conversion of Non-Edible Polysaccharides and Post-Harvest Tomato Plant Waste to Levulinic Acid. *Green Chem* **2014**, *16* (1), 73–76. <https://doi.org/10.1039/C3GC41103F>.
- (32) Khardenavis, A.; Sureshkumar, M.; Mudliar, S.; Chakrabarti, T. Biotechnological Conversion of Agro-Industrial Wastewaters into Biodegradable Plastic, Poly  $\beta$ -Hydroxybutyrate. *Bioresour. Technol.* **2007**, *98* (18), 3579–3584. <https://doi.org/10.1016/j.biortech.2006.11.024>.
- (33) Gumel, A. M.; Annuar, M. S. M.; Heidelberg, T. Biosynthesis and Characterization of Polyhydroxyalkanoates Copolymers Produced by *Pseudomonas Putida* Bet001 Isolated from Palm Oil Mill Effluent. *PLoS ONE* **2012**, *7* (9), e45214. <https://doi.org/10.1371/journal.pone.0045214>.
- (34) Bhattacharyya, A.; Saha, J.; Haldar, S.; Bhowmic, A.; Mukhopadhyay, U. K.; Mukherjee, J. Production of Poly-3-(Hydroxybutyrate-Co-Hydroxyvalerate) by *Haloferax Mediterranei* Using Rice-Based Ethanol Stillage with Simultaneous Recovery and Re-Use of Medium Salts. *Extremophiles* **2014**, *18* (2), 463–470. <https://doi.org/10.1007/s00792-013-0622-9>.

(35) Paving the way for biobased materials, A roadmap for the market introduction of PHAs Karin Molenveld, Wouter Post, Stephan Falcão Ferreira, Guy de Sévaux and Maud Hartstra.  
<https://doi.org/10.18174/561676>



### 3.PRODUCTION OF 5-(HYDROXYMETHYL)FURFURAL HALOGENATED DERIVATIVES



### 3.1. INTRODUCTION

#### 3.1.1. 5-(hydroxymethyl)furfural

5-(hydroxymethyl)furfural (5-HMF) is a platform molecule whose importance is unanimously recognized by scientific community. 5-HMF is considered one of the few petroleum-based chemicals that can also be readily produced from renewable sources and plays an important role as starting point of many synthetic pathways for resin, fuel additives, pharmaceuticals, and other products<sup>1</sup>.

5-HMF can be produced, as depicted in Figure 1, from 2<sup>nd</sup> generation lignocellulosic biomasses through:

- cellulose hydrolysis to glucose,
- isomerization of glucose to fructose,
- fructose dehydration to 5-HMF.

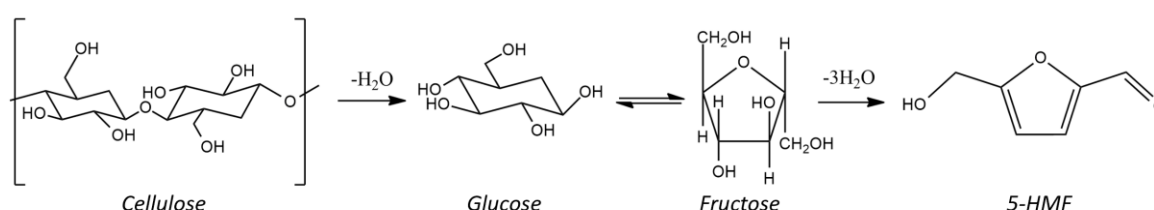


Figure 1: General 5-HMF production from cellulose

Several approaches for 5-HMF production have been investigated using different feedstocks: fructose, glucose, starch and low-cost lignocellulosic 2G waste biomasses<sup>1,2</sup>.

When fructose is used as feedstock two possible reaction pathways have been identified involving acyclic or cyclic intermediates (Figure 2):

- Cyclic pathway proceeds by dehydration of ring-closed fructose at the C2–OH position, yielding 2-(hydroxymethyl)-5-(hydroxymethylene)-tetrahydrofuran-3,4-diol (HMHMTD). HMHMTD is subsequently dehydrated to 4-hydroxy-5-(hydroxymethyl)-4,5-dihydrofuran-2-carbaldehyde (HHMDHC) which, again, is dehydrated to finally form 5-HMF.
- Acyclic pathway involves the open-ring fructose that is dehydrated to 3-deoxyglucos-2-ene (DGE). DGE is transformed into 3-deoxyglucosone (DGO) which is dehydrated to 3,4-deoxyglucosene (DGS) and finally to 5-HMF.

When glucose is used as feedstock, isomerisation to fructose occurs through 1,2-endiol mechanism or 1,2-hydride shift mechanism. Subsequently the cyclic pathway is considered the most relevant. Isomerisation reaction from glucose to fructose is considered the rate determining step, making conversion of glucose to 5-HMF slower and less efficient if compared with fructose (Figure 2). Despite this, glucose is usually preferred to fructose because of its low price and high availability<sup>3,4</sup>.

Despite some non-catalytic systems have been applied<sup>5</sup>, most of 5-HMF production reaction systems involves the use of catalysts because of their positive contribution to hydrolysis, isomerisation and dehydration reactions. Indeed Bronsted acid catalysts are reported to favour hydrolysis and dehydration reactions while Lewis acid catalysts are reported to favour isomerisation reactions<sup>3</sup>.

Bronsted acids can ease hydrolysis and dehydration. Indeed, catalyst can protonate carbohydrate's oxygen atom of glycosidic bond favouring hydrolysis. Moreover, fructose dehydration can be favoured: proton attaches to C2 -OH group enhancing water elimination.

The intermediate formed can further re-arrange to enol form that finally dehydrates to 5-HMF. By the other hand Lewis acids can catalyse isomerisation from glucose to fructose easing ring opening of glucose<sup>6</sup>. Combination of Bronsted and Lewis acids can be a valuable strategy to improve 5-HMF production boosting all the steps involved in reaction mechanism.

Two main classes of catalysts can be defined<sup>3</sup>:

1. Homogeneous catalysts, such as organic acids, mineral acids, metal chlorides, metal triflates, ionic liquids.
2. Heterogeneous catalysts, such as acidic resins, acidic zeolites, metal oxides, acidulated metal oxides, metal phosphates, heteropolyacid salts, functionalized silicas, functionalized clays, coordination polymers and carbonaceous acids.

Heterogeneous catalysts are considered more promising in term of future industrialisation, being tuneable, easy to be recovered and recyclable<sup>3</sup>.

Since temperature plays a pivotal role in 5-HMF production a crucial role is also recognised to heating system employed. Microwave heating is therefore considered a promising approach to favour 5-HMF formation from carbohydrates: reaction time reduction, yield improvement and side-reaction reduction are fundamental characteristics of MW technology that can show positive influence<sup>6</sup>.

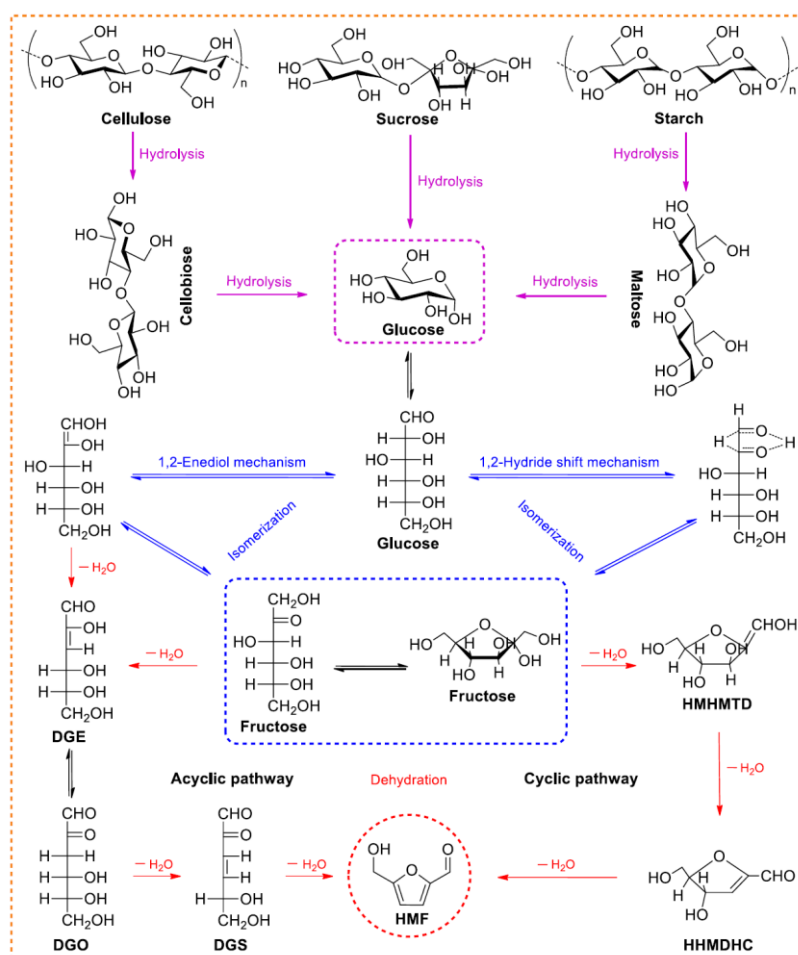


Figure 2: Detailed reaction pathway for 5-HMF production from carbohydrates, glucose and fructose<sup>3</sup>

5-HMF is a furanic compound presenting a tremendous synthetic potential according to the presence of three functional groups: a furan ring, an aldehyde and a hydroxymethyl group.

By modifications of one or more functional groups, a wide variety of products can be achieved. A comprehensive review of 5-HMF derived products according to its functional group modifications was reported in 2021 by Dutta (Figure 3)<sup>7</sup>

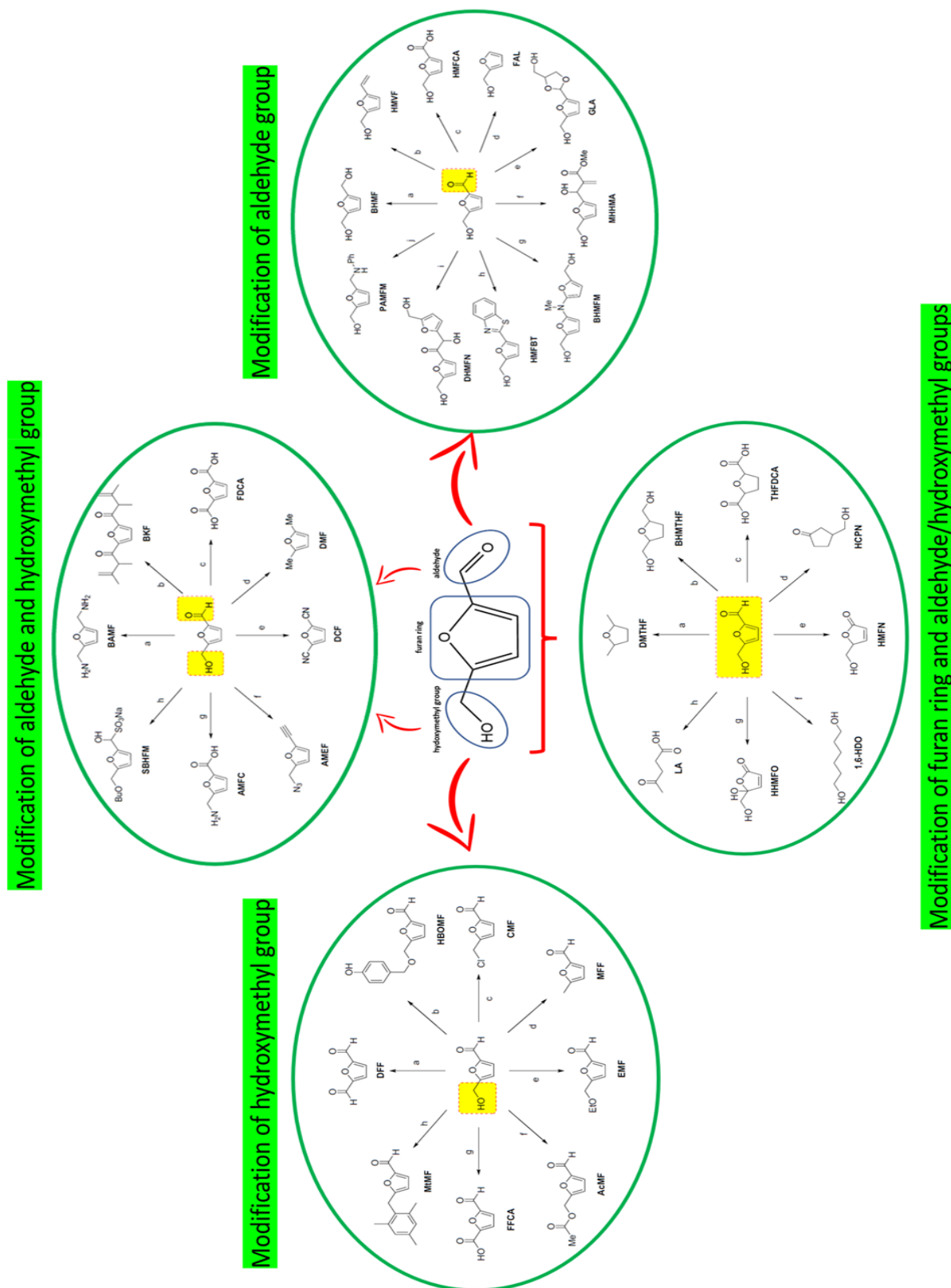


Figure 3: 5-HMF derived products (adapted from Dutta<sup>7</sup>)

Due to this enormous synthetic potential 5-HMF has been referred as the “sleeping giant of sustainable chemistry” but despite a high volume of studies involving 5-HMF, it is still not

competitive with fossil resources. The delay in “awaken” of the “sleeping giant” is due to specific limitations:

- Obstacles to the industrial-scale production: actual synthesis strategies are characterised by low yields and selectivity, high cost of solvents and catalysts, difficulties in catalysts regeneration and difficulties in isolation/purification.
- Low chemical stability: due to his high reactivity, 5-HMF is unstable and strongly susceptible to hydrolysis, forming levulinic acid and other by-products like insoluble humins, derived from oligomerisation and polymerisation of 5-HMF. Moreover, high content of oxygen in the molecule makes its isolation and purification quite complicate<sup>8</sup>.

Such behaviour negatively impacts both the synthesis stage, the long-term storage of the molecule and the transformation of 5-HMF into other chemicals<sup>9</sup>.

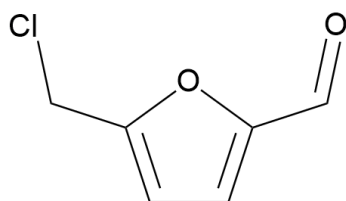
### 3.1.2. 5-(halomethyl)furfurals: hydrophobic analogues of 5-HMF

As already mentioned, 5-HMF production is characterised by several limitations that act as a barrier to its industrialisation and commercialisation.

In recent times 5-(halomethyl)furfurals were investigated as valuable alternatives to 5-HMF.

Both 5-chloromethylfurfural (CMF) and 5-brominemethylfurfural (BMF) were considered.

5-(halomethyl)furfurals can be directly produced from carbohydrates fractions of lignocellulosic biomasses with satisfactory yields. Moreover, being hydrophobic, 5-(halomethyl)furfurals can be easily extracted from aqueous solution with common organic



solvents<sup>10</sup>.

Figure 4: CMF

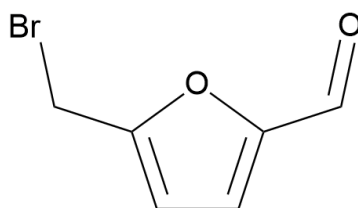


Figure 5: BMF

This marked hydrophobicity makes

5-(halomethyl)furfurals a suitable alternative to 5-HMF since they can be recovered from acidic aqueous reacting systems through the use of apolar organic solvents as soon as they are formed, thus preventing their further decomposition (the so called biphasic systems). 5-HMF limitations are furthermore overcome thanks to a major storage stability offered by this class of molecules<sup>11</sup>.

Relative hydrophobicity of 5-HMF and some of its hydrophobic derivatives is reported in Figure 6<sup>11</sup>.

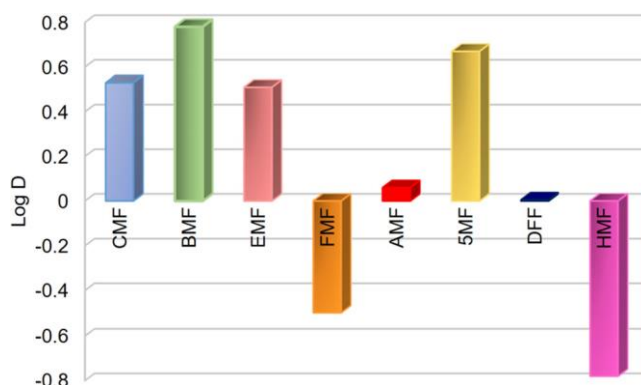


Figure 6: Relative hydrophobicity of 5-HMF and some derivatives<sup>11</sup>

More into detail, in a biphasic system two immiscible solvents are present: the aqueous acidic phase and the apolar phase. In aqueous acidic phase 5-HMF is formed from carbohydrate (biomass, cellulose, glucose or fructose) and subsequently converted to CMF or BMF depending on the acid involved in the process. Once the 5-(halomethyl)furfural is produced it is recovered in the apolar solvent. In such systems the acid has the double role of catalyst for 5-HMF formation and reagent for the nucleophilic substitution of hydroxymethyl group of 5-HMF with halogen, leading to conversion to BMF/CMF<sup>11</sup>.

CMF is the most studied halogenated derivative of 5-HMF. Several studies focused on its preparation from carbohydrates and biomasses and most of the actual protocols involve the use of concentrated HCl.

In 2008, Mascari and Nikitin<sup>12</sup> reported the formation of CMF with high yields formation from cellulose in a biphasic system composed of LiCl solubilised in concentrated HCl and 1,2-dichloroethane. The reacting systems was designed to extract the product in apolar phase that was continuously fed and recovered. The whole process required long times (about 30h), a high quantity of solvent, and repeated addition of HCl and LiCl to achieve satisfactory yields. Further improvements of this reaction were performed by the authors by removing LiCl from reaction media and working in a closed reaction system, reducing the overall reaction time to 3 hours.<sup>13</sup> In the following years several attempts in CMF production improvement were reported by many authors as described in Table 1 (from a comprehensive review by Anchan and Dutta<sup>11</sup>):

Feedstock	Reaction conditions	Yield (%)
Fructose	32% HCl, DCE, 100 °C, 20 min	79
Sucrose	32% HCl, DCE, 130 °C, 20 min	61
Sucrose	37% HCl, DCE, 100 °C, 2.5 min	50
HFCS grade 90	37% HCl, DCE, 100 °C, 1.5 min	85
Fructose	HCl/LiCl, toluene, 65 °C, 3 h	72
Fructose	35% HCl, DCE, 70 °C (MW), 10 min	85
Glucose	35% HCl, DCE, 80 °C (MW), 15 min	39
Inulin		70
Microcrystalline cellulose	35% HCl, DCE, 80 °C (MW), 45 min	71
Fructose	37% HCl+85% H <sub>3</sub> PO <sub>4</sub> , CHCl <sub>3</sub> , 45 °C, 20 h.	46.8
Sorbose		16.4
Cellobiose		19.3
Bamboo pulp	ZnCl <sub>2</sub> -CrCl <sub>3</sub> in HCl, CHCl <sub>3</sub> , 45 °C, 10 h	32.7
Eucalyptus pulp		36.2
Bagasse		50.1
Fructose		80
Fructose	Fructose: ChCl:1:4, AlCl <sub>3</sub> ·6H <sub>2</sub> O, MIBK, 120 °C, 5 h	50.3
Glucose	35% HCl, DCE, BTBAC, 90 °C, 3 h	64
Cellulose		42
Sucrose	LiCl, 37% HCl, DCE replaced every 30 min, 80 °C, 4 h, open batch	35
Cellulose	37% HCl, DCE replaced after 2 h 110 °C, 4 h, closed reactor	82.6

Table 1: CMF production protocols

Noteworthy, in 2013 Breeden et al.<sup>14</sup> reported an high-yield protocol exploiting biphasic systems coupled with MW irradiation that led to satisfactory CMF yields from cellulose in reasonable times with high selectivity. Despite several advancements have been made, most of reported investigations involve simple sugars while more complexes carbohydrates (and biomasses) still need to be properly inquired.<sup>11</sup>

By the other hand, BMF production is even less investigated. Despite that, its production as an alternative to 5-HMF is considered extremely promising because the main reagent involved, HBr, is a better catalyst than HCl, being non-volatile and thus easier to be handled safely<sup>11</sup>.

By critically analysing the works present in literature, two strategies for BMF production can be described, according to the acidic aqueous phase involved:

- Acidic aqueous phases involving LiBr and HBr;
- Acidic aqueous phases involving concentrated HBr (48%).

In 2011, Kumari et al.<sup>15</sup> reported BMF production through the same first protocol developed by Mascall for CMF: different substrates were used (fructose, glucose, cellulose and straw) with concentrated HBr and LiBr. High yields were achieved in long times (up to 48 hours) and continuous extraction of the product was performed by means of different apolar solvents continuously fed to the reactor (Table 2).

Entry	Substrate	Solvent	LiBr (equiv.)	Temperature (°C)	Time (hours)	Yield (%)
1	Fructose	1,2-dichloroethane	20	25	48	68
2	Fructose	Toluene	20	25	48	82
3	Fructose	Tetrahydrofuran	20	25	48	0
4	Fructose	Toluene	2	25	48	70
5	Glucose	Toluene	20	65	48	50
6	Cellulose	Toluene	20	65	28	80
7	Straw	Toluene	20	65	48	68

Table 2: BMF production experiments results, according to Kumari et al.<sup>15</sup>

Few years later, Bredihhin et al.<sup>16</sup> evaluated the performances of different biomasses in BMF production as reported in Table 3, lines 5-9. Similarly as Kumari et al., HBr and LiBr were used in a biphasic system and long reaction times were involved (24 hours).

Some experiments were also conducted by avoiding the use of LiBr, considered neither environmental friendly nor sustainable from an economic point of view: in absence of LiBr a 10% reduction in yield was observed but still promising yields were achieved (Table 3, line 1 vs 2 and line 3 vs 4).

Entry	Substrate	Solvent	LiBr	Temperature (°C)	Time (hours)	Yield (%)
1	Cellulose	1,2-dichloroethane	✓	65	24	59
2	Cellulose	1,2-dichloroethane	X	65	24	48
3	Glucose	1,2-dichloroethane	✓	65	24	64
4	Glucose	1,2-dichloroethane	X	65	24	54
5	Aspen	1,2-dichloroethane	✓	65	24	55
6	Birch	1,2-dichloroethane	✓	65	24	56
7	Alder	1,2-dichloroethane	✓	65	24	50
8	Pine	1,2-dichloroethane	✓	65	24	51
9	Spruce	1,2-dichloroethane	✓	65	24	49

Table 3: BMF production experiments results, according to Bredihhin et al.<sup>16</sup>

Meller et al.<sup>17</sup> were able to perform cellulose conversion to BMF in a closed reaction vessel. This allowed the authors to avoid the use of LiBr and to increase the temperature to values higher than the boiling point of the apolar solvent. Furthermore, reaction times were shortened (4 hours) respect to previously reported studies.

Finally, the molten salt LiBr·3H<sub>2</sub>O coupled with catalytic amounts of HBr were employed to prepare BMF in high yields from cellulose and biomasses by Yoo et al.<sup>18</sup>.

Table 4 (adapted from a comprehensive review by Anchan and Dutta<sup>11</sup>) reports a comparison of the above mentioned studies together with details regarding experimental conditions:



Feedstock	Reaction conditions	Yield (%)	
Fructose	HBr/LiBr, toluene, 65 °C, 3 h	74	Jadhav et al.
Cellulose	HBr, DCE, closed reactor, intermittent extraction, 95 °C, 4 h	74	Meller et al.
Cellulose	aq. HBr, LiBr, DCE, open reactor, continuous extraction, 70 °C, 10 h	37.7	
Fructose	aq. HBr, LiBr, toluene, Na <sub>2</sub> SO <sub>4</sub> (anhyd.), continuous extraction	25 °C, 48 h	82
Glucose		65 °C, 48 h	50
Cellulose		65 °C, 48 h	80
Straw		65 °C, 48 h	68
Glucose	aq. HBr (48%), LiBr, DCE, intermittent extraction	65 °C, 24 h	64
Cellulose		80 °C, 24 h	59
Glucose	aq. HBr, DCE, intermittent extraction, 65 °C, 24 h		54
Cellulose			48
Aspen			41
Cellulose	aq. HBr, LiBr, DCM, 125 °C, 126 min		90
Com Stover			71
Aspen	Al <sub>2</sub> (SO <sub>4</sub> ) <sub>3</sub> , ChBr, MIBK, 120 °C, 5 h		87
Fructose			49
Glucose			20
Starch			19

Table 4: Summary of most notable studies on BMF production, according to Anchan and Dutta

BMF and CMF can be used as intermediates for fuels and chemicals production. BMF and CMF are considered more adequate platform chemicals respect to 5-HMF in Sn2 reactions according to the halomethyl group. BMF is reported to be quite reactive toward weak-nucleophiles, thanks to the Br leaving-group and good stabilisation of  $\alpha$  carbon of furanic ring<sup>15,19</sup>. Most of literature works about conversion of 5-(halomethyl)furfurals involve CMF but, in principle, BMF can take part to the same reactions<sup>11</sup>.

Two main reactive routes for 5-(halomethyl)furfurals conversion to chemicals can be defined: the furanic route and the levulinic route. The first one involves modifications that insist on the furanic structure, while the second one proceeds through 5-(halomethyl)furfural rehydration to levulinic acid, which is considered a fundamental platform chemical. According to Mascall,<sup>20</sup> 5-(halomethyl)furfural chemistry can be described by dividing its products into three “family trees” depending on the intended use of the product.

The three families of products that can be achieved from BMF and CMF are listed below together with some of the most notable examples:

1. Monomers
  - furan-based monomers as 2,5-furandicarboxylic acid and its derivatives involved in PEF (poly(ethylene 2,5-furandicarboxylate)) production. PEF is a furan-based polymer that is considered an alternative to petrochemical PET (poly(ethylene terephthalate)).
  - furan-derived monomers: 5-(halomethyl)furfurals can be converted through a series of subsequent steps into bio-based terephthalic acid for bio-based PET production.
2. Fuels
  - furan-based biofuels: 2,5-dimethylfuran (DMF) is an intermediate in above-mentioned terephthalic acid production from CMF but it can be considered a biofuel in its own right, having an octane number of 101.
3. Chemicals in general: in addition to fuels and monomers production, that are products characterised by high production volume/low income, biorefineries should include in their portfolio also other high added value products to improve their competitiveness.

Furan fatty acids are considered a promising class of molecules due to their antiatherosclerosis activity. Actual synthetic routes for furan fatty acids are characterised by high reagent price and low yields. In 2015 it has been demonstrated furan fatty acid production with high yields from CMF by using cheap and renewable feedstocks<sup>21</sup>. Moreover,  $\delta$ -aminolevulinic acid (herbicide)<sup>22</sup> and ranitidine (antiulcer drug)<sup>23</sup> have been produced from cellulose-derived CMF (Figure 7).

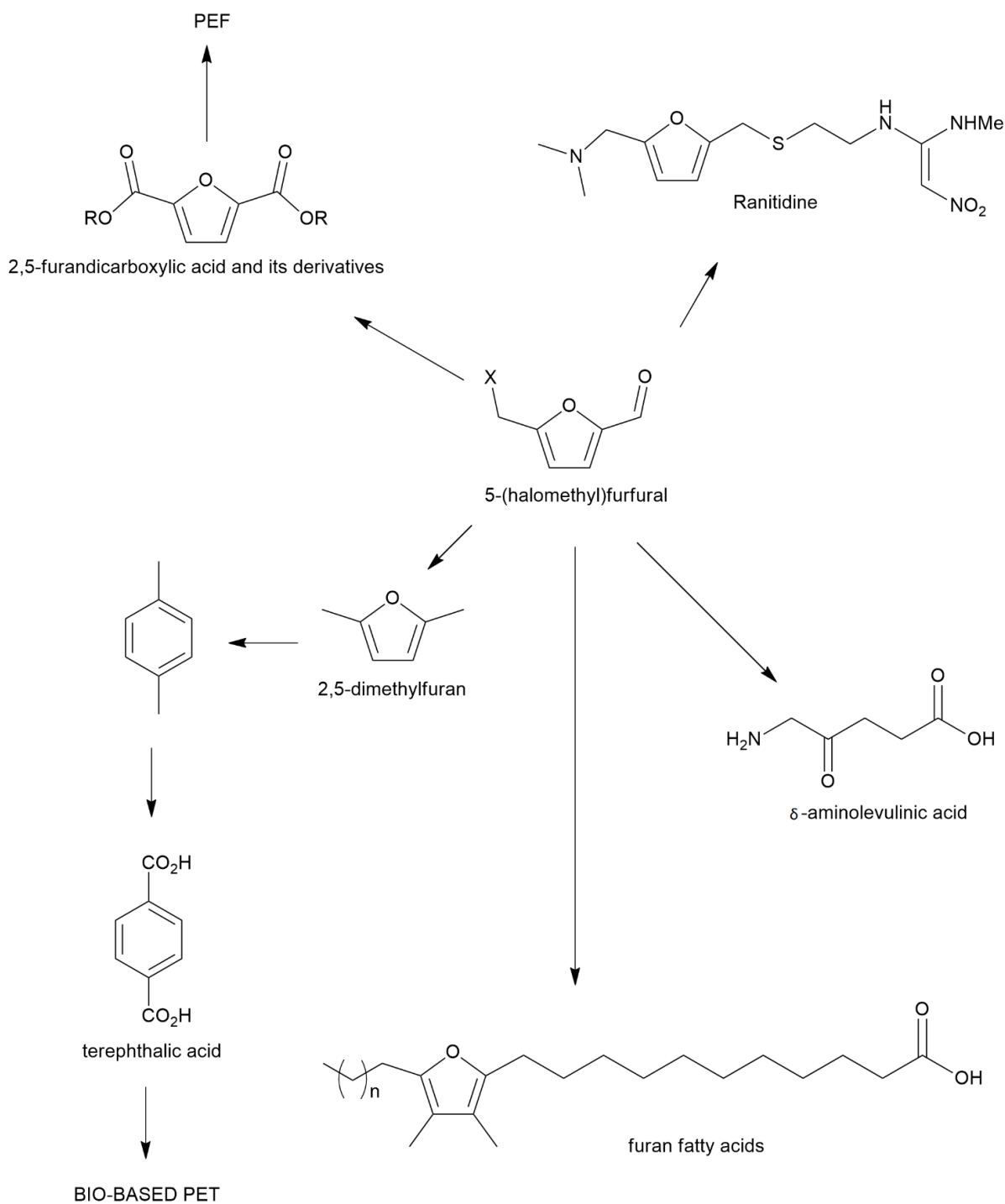


Figure 7: Most notable products derived from 5-(halomethyl)furfurals

### 3.2. RESULTS AND DISCUSSION

In this chapter, the MW-assisted BMF production in biphasic systems from cellulose and biomass is reported (Figure 8).

As previously described, biphasic systems are composed by:

- an aqueous acidic phase where the BMF formation from feedstock takes place,
- an immiscible organic phase (in this case: dichloromethane) that extracts the product once formed, thus removing it from reactive system and preventing its further degradation to humic materials.

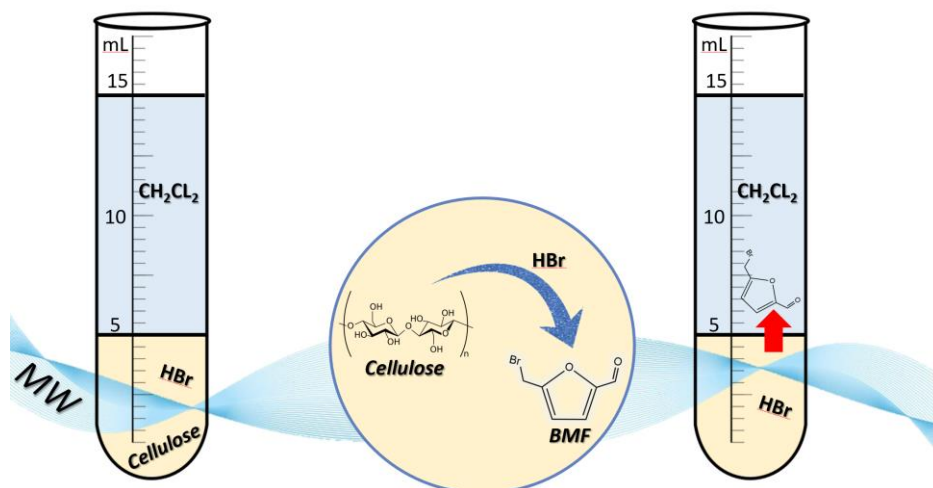


Figure 8: MW-assisted BMF production in biphasic systems from cellulose

Two main aqueous acidic phases, already described in literature were considered:

- LiBr in aqueous solution or in molten salt ( $\text{LiBr} \cdot n\text{H}_2\text{O}$ ) form plus HBr;
- pure concentrated HBr as aqueous phase.

Moreover, considering the possible impact of the different MW field distribution according to the MW configurations (monomode or multimode), two different MW reactors were compared.

The aim of the study was to achieve the best BMF yield through the best combinations of aqueous acidic phase and MW technology, as summarised in Table 5.

To the best of our knowledge this is the first study for BMF production that investigates the effect of MW irradiation.

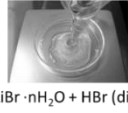

	MW TECHNOLOGY	
AQUEOUS PHASE	Multimode MW reactor Synthwave (Milestone)	Monomode MW reactor Monowave 300 (Anton Paar)
 LiBr · nH <sub>2</sub> O + HBr (dil.)	<b>1</b> Multimode MW reactor LiBr · nH <sub>2</sub> O + HBr (dil.)	<b>2</b> Monomode MW reactor LiBr · nH <sub>2</sub> O + HBr (dil.)
 HBr (Conc.)	<b>4</b> Multimode MW reactor HBr (Conc.)	<b>3</b> Monomode MW reactor HBr (Conc.)

Table 5: summary of planned experiments for MW-assisted BMF production in biphasic systems from cellulose and biomass

Ball-milled cellulose was used as substrate for all the experiments while ball-milled biomass (PHTP) was investigated once the best match of MW technology and aqueous acidic phase was defined.

Ball-milling pre-treatment was performed to reduce the dimensions of raw biomass and cellulose, thus increasing the overall area exposed to reacting system.

Ball-milled cellulose is reported to present significant reduction in crystallinity and thermal stability, thus making it more prone to conversion reactions<sup>24</sup>. Moreover, ball-milling pre-treatment of biomass is reported to be beneficial because it makes carbohydrates fractions more accessible to chemical attack, as it weakens the intramolecular hydrogen bonds with lignin.

The biomass used in this study is post-harvest tomato plant (PHTP), which is made up of tomato plants residues recovered at the end of tomatoes harvesting season. Usually, such biomass is disposed or left in the field without any further valorisation. Its overall chemical composition was investigated by NREL-derived protocol<sup>25</sup> and is reported in Table 3 in section 2.2.1.

Dichloromethane was used as immiscible apolar phase in all the experiments.

At the end of each reaction, dichloromethane BMF-rich phase and acidic aqueous phase were separated from unconverted cellulose/biomass and solid degradation products by means of filtration. Subsequently, liquid-liquid separation was performed in order to separate dichloromethane BMF-rich phase from aqueous acidic phase.

Qualitative analyses of dichloromethane BMF-rich phases were performed in GC-MS and NMR.

Yields were calculated through GC-FID analyses (using pure BMF as standard for external calibration curve) and expressed as % mol of initial anhydroglucose unit content in cellulose,<sup>26</sup> as follows:

$$BMF \text{ yield (mol\%)} = \frac{\text{mol BMF}}{\text{mol anhydroglucose content in cellulose}} \cdot 100$$

When biomass PHTP was used, yields were expressed as % mol of initial anhydroglucose unit content in cellulose fraction (determined with the above-mentioned NREL-derived protocol) of the biomass as follows:

$$BMF \text{ yield (mol\%)} = \frac{\text{mol BMF}}{\text{mol anhydroglucose content in cellulose fraction}} \cdot 100$$

### **3.2.1. Multimode MW reactor and LiBr·nH<sub>2</sub>O + HBr (dil.)**

Molten salt and diluted HBr were tested in a multimode MW reactor (Synthwave, Milestone). Hydration degree of molten salt, time and temperature were investigated to optimise the reaction conditions.

#### Hydration degree of molten salt

Initial reactions were performed at 125°C with LiBr·3H<sub>2</sub>O and diluted HBr in accordance with results reported by Yoo et al.<sup>18</sup> (Table 6)

Reagent	Quantity
Cellulose	0.1000g
LiBr·nH <sub>2</sub> O	5mL
HBr (48%)	0.09mL
CH <sub>2</sub> Cl <sub>2</sub>	10mL

Table 6: experimental conditions applied in multimode MW reactor based on Yoo et al.<sup>18</sup>

Three different reaction times were evaluated (20, 40 and 60 min) and as no substantial improvement in yield were observed from 40 to 60 min, longer times (> 60 min) were not further investigated (Figure 10).

As reported by Kumari et al.<sup>15</sup> and, more into detail by Yoo et al.<sup>18</sup>, molten salt hydration degree is a crucial parameter that strongly affect BMF yield. Indeed, the authors reported 3H<sub>2</sub>O as best hydration degree (Figure 9).

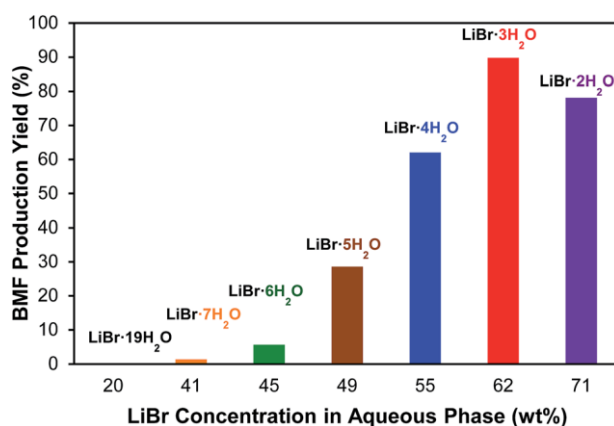


Figure 9: BMF production yield at different hydration degrees according to Yoo et al.<sup>18</sup>

A similar investigation was performed, looking for a possible positive contribution of MW technology in molten salt hydration degree reduction. Therefore, the same reaction was performed using a more hydrated form of molten salt: LiBr·5H<sub>2</sub>O (Figure 10). Despite a marked yield increase over time has occurred from 16.32 to 35.71 mol%, the maximum yield achieved after 60 min, this was considered unsatisfactory if compared with results achieved with LiBr·3H<sub>2</sub>O.

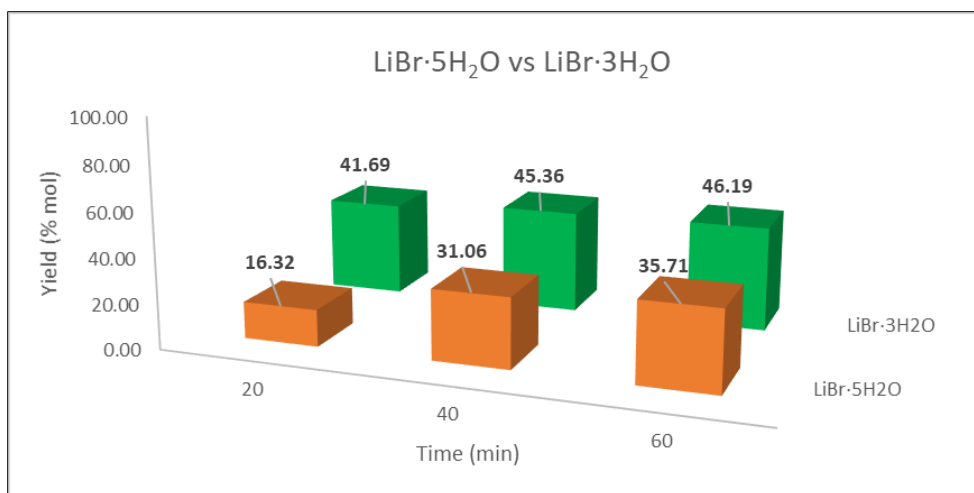


Figure 10: BMF production yield from cellulose at different LiBr hydration degrees in multimode MW reactor at 125°C

According to the mechanism proposed by Yoo et al. (Figure 11), the role of LiBr is crucial:

1. Li<sup>+</sup> and Br<sup>-</sup> improve cellulose swelling and dissolution by disruption of inter- and intra-molecular hydrogen bonds of cellulose by forming Li<sup>+</sup>⋯O-H e Br<sup>-</sup>⋯H-O interactions. Better dissolved cellulose can then be quickly hydrolysed by HBr into glucose;
2. Moreover, Li<sup>+</sup> offers a second reaction pathway (path.2) in isomerisation of glucose to fructose.

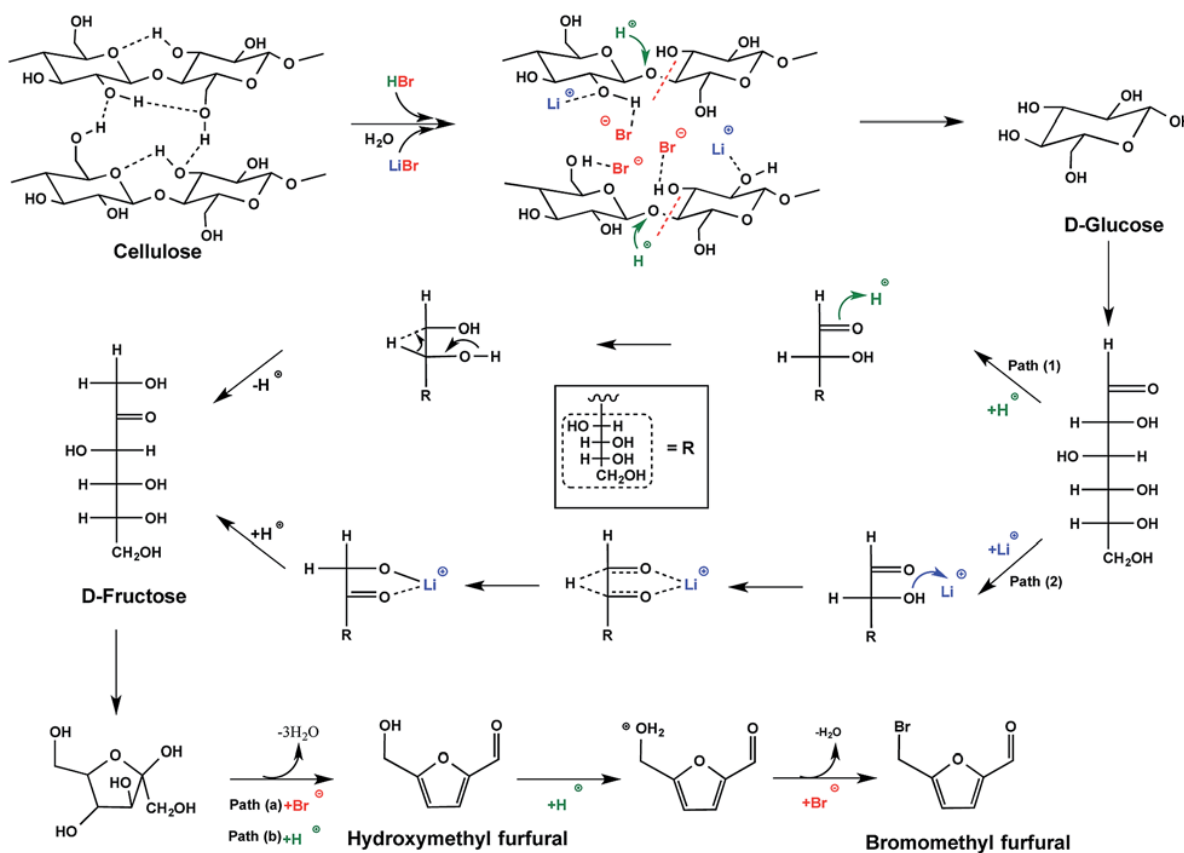


Figure 11: Influence of LiBr in BMF formation according to Yoo et al.<sup>18</sup>

To confirm the crucial role of molten salt, a reaction using deionised water instead of  $\text{LiBr}\cdot n\text{H}_2\text{O}$  was performed in multimode MW reactor at  $125^\circ\text{C}$ : in such case no reaction occurred.

Moreover, a reaction in molten salt without  $\text{HBr}$  (dil.) was performed and no BMF was detected, confirming the synergic effect of molten salt and diluted acid both on cellulose hydrolysis and glucose to fructose isomerisation.

### Temperature screening

Aiming to further optimise the reaction, a  $25^\circ\text{C}$  temperature increase was applied moving from  $125^\circ\text{C}$  to  $150^\circ\text{C}$  (Figure 12).

Such temperature increase showed two beneficial effects: an increase in maximum reaction yield (from 45.36 to 49.66), and a sensible reduction of reaction times (from 40 to only 5 minutes).

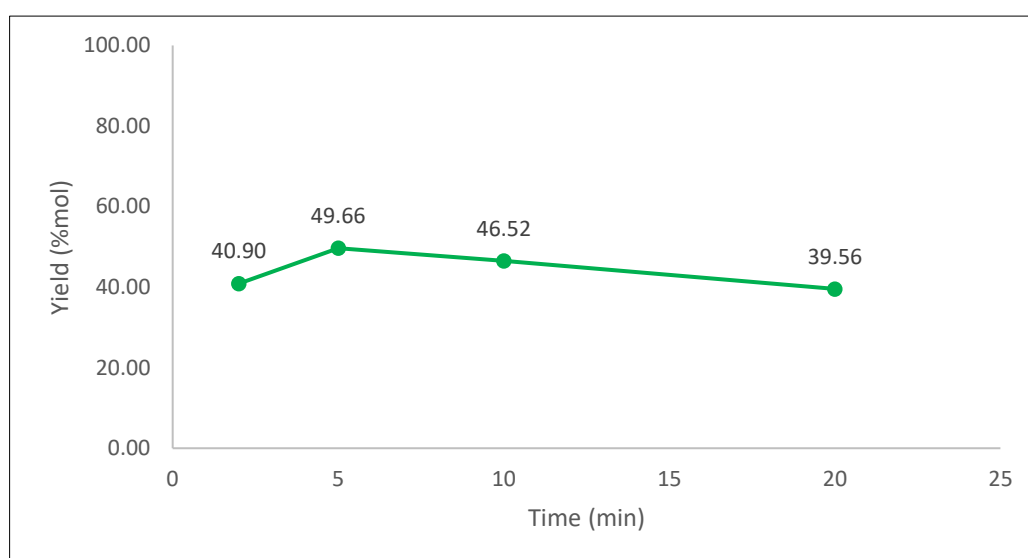


Figure 12: BMF production yield from cellulose in multimode MW reactor at  $150^\circ\text{C}$  using  $\text{LiBr}\cdot 3\text{H}_2\text{O}$

As it is possible to appreciate from Figure 12, at  $150^\circ\text{C}$  the yield increased from 2 to 5 minutes and subsequently decreased with higher reaction times. Yield reduction can be explained considering over-reaction phenomena that led to product degradation and/or direct cellulose degradation to humic materials when exposed to high temperature for long times.

Humins formation (a brownish precipitate recovered on the filter surface during the workup) was observed in all the experiments, but in the ascendent part of the curve BMF formation is the prevailing phenomenon. Over 5 minutes the humins formation becomes more relevant leading to product loss.

A further temperature increase to  $170^\circ\text{C}$  afforded no benefit, leading to massive cellulose degradation to humic materials.

### **3.2.2. Monomode MW reactor and $\text{LiBr}\cdot n\text{H}_2\text{O}$ + $\text{HBr}$ (dil.)**

Aiming to improve the BMF yield, the same reaction system was tested in a monomode microwave reactor (Monowave 300, Anton Paar).

The reaction was initially conducted at  $150^\circ\text{C}$  for 2 minutes, leading to the complete degradation of cellulose and products (Figure 13): no BMF formation was observed.



Figure 13: Degradation products in monomode MW reactor

Subsequently, the temperature was reduced to 100°C, but again, no product was observed, and solid degradation products were recovered. A further temperature reduction to 80°C was performed, but in such case no reaction was detected and starting cellulose remained unmodified in the reaction vial.

The results so far achieved (both in monomode and in multimode MW reactors) can be considered unsatisfactory, if compared with the results reported by Yoo et al.<sup>18</sup> (that reached 90% BMF yield from cellulose in LiBr·3H<sub>2</sub>O reaction environment).

A possible explanation for the lower yields achieved (even in the same conditions reported by Yoo et al.<sup>18</sup>) can be found in the rapid formation of degradation products due to the high MW absorbing capacity of molten salt that can lead to localised high-temperature hot-spots in reaction media, not directly detected by the instrument sensors. This effect is amplified in monomodal reactor, that is characterised by high microwave field density.

### 3.2.3. Monomode MW reactor and HBr (conc.)

Due to the poor results achieved in the monomode reactor (Monowave 300, Anton Paar) coupled with molten salt, the latter was replaced in favour of concentrated HBr.

The absence of molten salt was balanced with an increase in the concentration of HBr, as reported in Table 7:

Reagent	Quantity
Cellulose	0.1000g
HBr (48%)	5mL
CH <sub>2</sub> Cl <sub>2</sub>	10mL

Table 7: experimental conditions applied in monomode MW reactor using HBr (conc.)

In order to promote cellulose dispersion/dissolution in HBr, the reaction system was sonicated in US bath for 1 minute prior to conversion reaction.

After some pre-experiments devoted to defining the experimental pattern, reaction temperature was investigated from 70 to 100°C, and time was investigated in the range 1-15min (Figure 14).



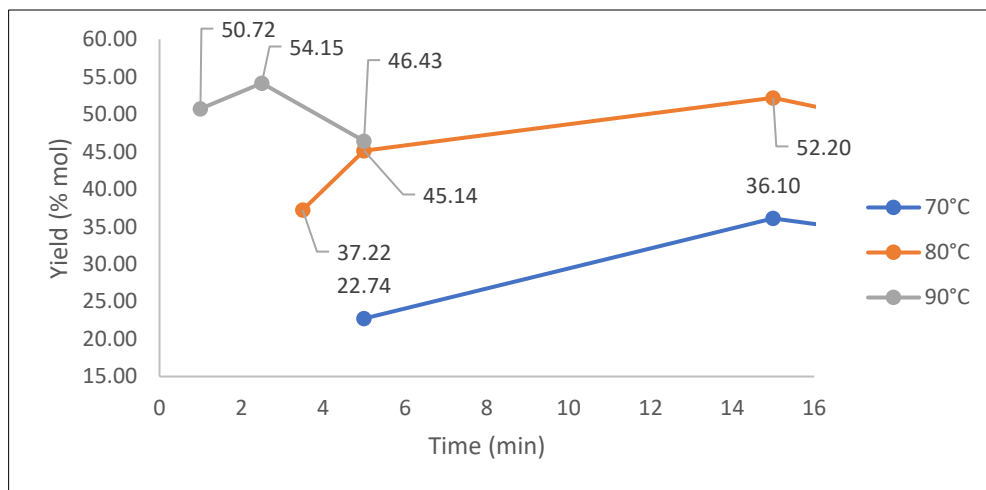


Figure 14: BMF production yield from cellulose at different temperatures in monomode MW reactor using HBr (conc.)

Both for 70°C and 80°C BMF formation was the predominant phenomenon until 15 min, followed by rapid degradation and yield reduction. At 90°C the point of maximum yield was shifted in correspondence of 2'30'' in which the highest BMF yield was achieved, followed by abrupt yield decrease for higher times.

According to these results, the best reaction conditions were defined as reported in Table 8:

Cellulose (g)	0.1000
HBr conc. (mL)	5
CH <sub>2</sub> Cl <sub>2</sub>	10
Temperature (°C)	90
Time (min)	2'30''
<b>Yield (% mol)</b>	<b>54.15</b>

Table 8: best reaction conditions in monomode MW reactor using HBr (conc.)

In such conditions, biomass PHTP was tested as substrate, yielding **37.92% mol BMF**.

#### 3.2.4. Multimode MW reactor and HBr (conc.)

Considering the promising results achieved by coupling monomodal MW reactor with concentrated HBr, the same approach was applied in multimode MW reactor.

Time and temperature were the main parameters investigated. Some pre-experiments were performed to define the experimental pattern and two temperatures were selected as suitable for the optimisation study: 100°C (Figure 15) and 110°C (Figure 16). Lower temperatures gave negligible quantity of BMF, while higher temperatures led to a high quantity of degradation solid by-products.

Thanks to the possibility offered by multimode MW reactor to perform multiple parallel reactions, both cellulose and biomass PHTP were studied at the same time.

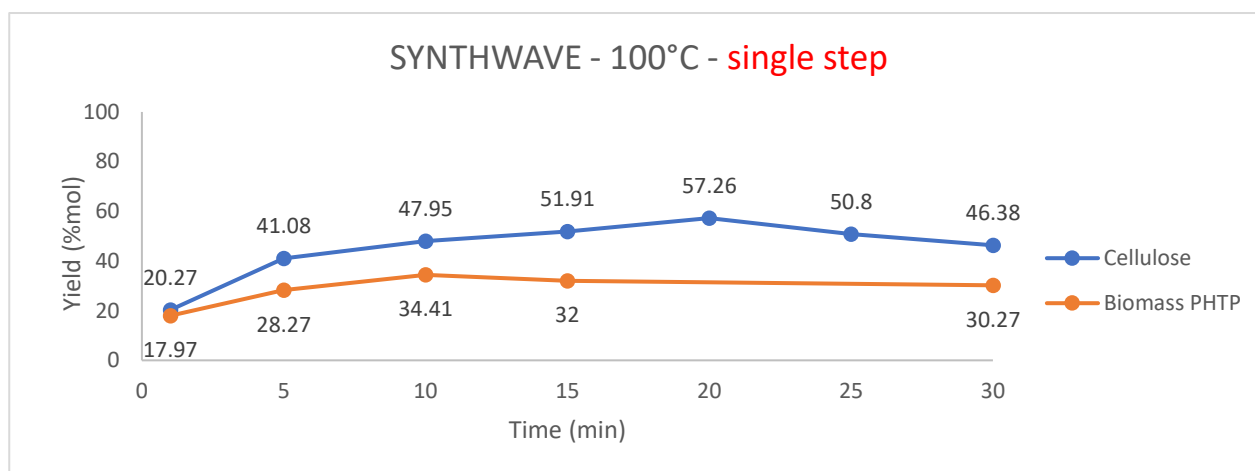


Figure 15: BMF production yield from cellulose and biomass at 100°C in multimode MW reactor using HBr (conc.)

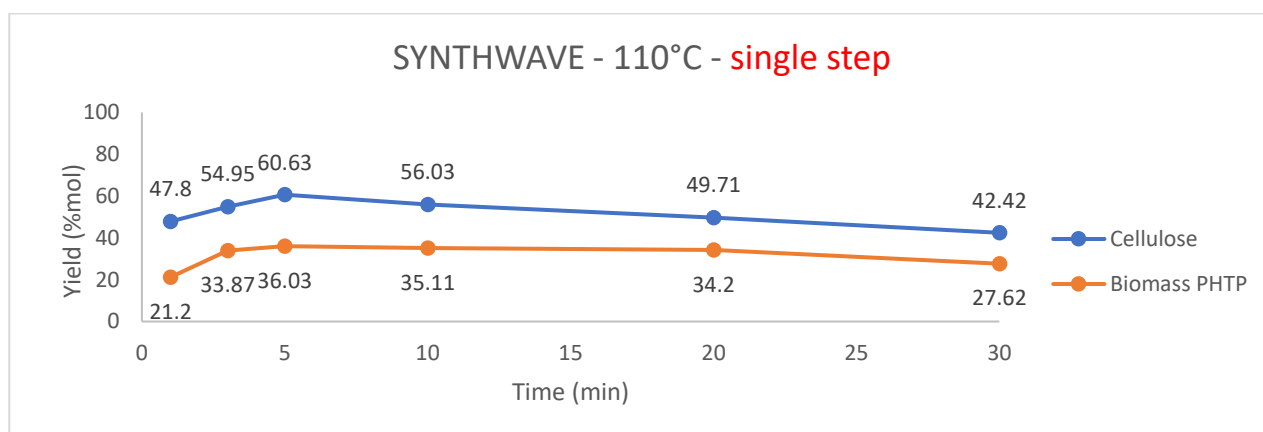


Figure 16: BMF production yield from cellulose and biomass at 100°C in multimode MW reactor using HBr (conc.)

The comparison of the two graphs highlights that the temperature effect is evident: by increasing the temperature of 10°C only, similar yields both for cellulose and biomass can be achieved with a sensible reduction of reaction time.

Indeed, regarding cellulose, at 100°C the yield reaches its maximum at 20 minutes while at 110°C a similar yield can be achieved after only 5 minutes.

When biomass is involved, the maximum yield was achieved at 100°C after 10 minutes, while at 110°C a similar yield was achieved after 5 minutes only.

The difference in achieved yield between cellulose and biomass in both 100°C and 110°C experiments can be explained with the recalcitrance of cellulose contained in the biomass, that is strongly connected with hemicellulose and lignin, and therefore less accessible to HBr reagent.

For both temperatures and both feedstocks the reaction proceeds in a similar way: in the early stage of the reaction BMF formation is the dominant process, then, once the maximum yield is reached, degradation phenomena start to prevail leading to product degradation and yield reduction.

By comparing these BMF yield results with previous experiments, it is evident that multimode MW reactor coupled with concentrated HBr can be considered the best approach for BMF production.

Almost pure BMF was recovered at the end of every reaction. Typical GC-MS spectra of dichloromethane BMF rich phases is reported in Figure 17. The main peak (98% of total GC area) was assigned to BMF according to its MS spectra; some minor impurities (traces) were also detected (Table 9).

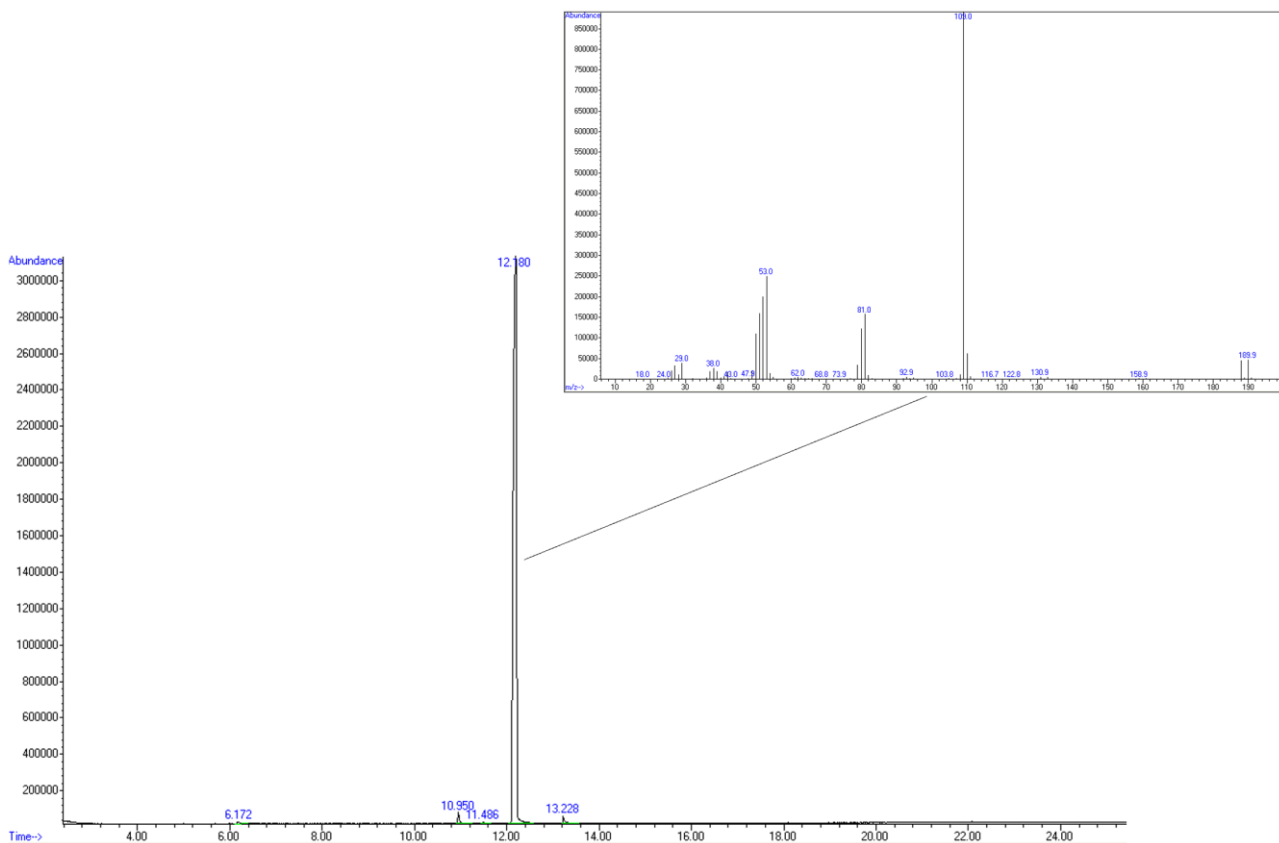


Figure 17: Typical GC-MS spectra of dichloromethane BMF rich phase and detail of BMF MS spectra

r.t. (min)	molecule	GC area (%of total)
6.172	Methylfurfural	0.362
10.950	Undetermined by-product	0.859
11.486	Undetermined by-product	0.128
12.180	BMF	98.089
13.228	Undetermined by-product	0.561

Table 9: r.t. and GC area (% of total) of molecules present GC-MS spectra

Silica-gel column purification was performed, aiming to obtain pure BMF for GC-MS (Figure 18) and  $^1\text{H}$  and  $^{13}\text{C}$  NMR analyses (Figure 19 and Figure 20). In Figure 18 GC-MS spectrum of purified BMF fraction is reported. BMF is the only product detected and its MS spectra is also reported.

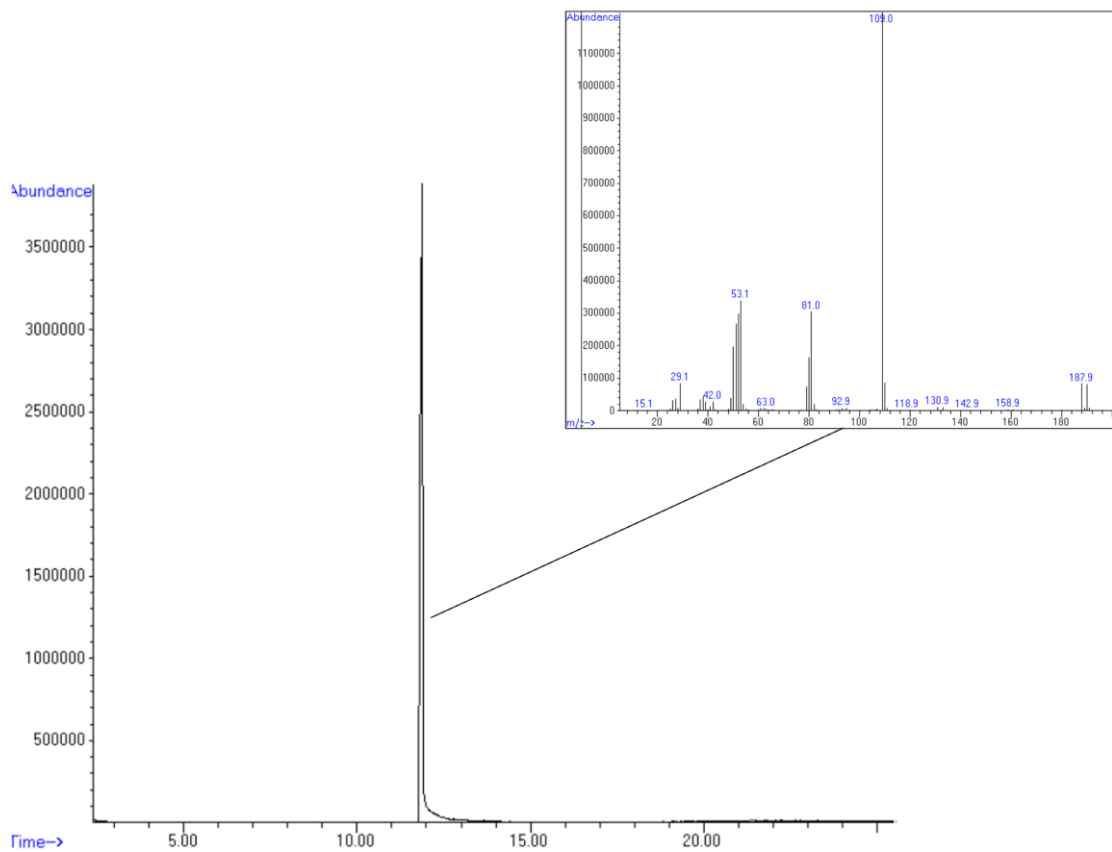


Figure 18: GC-MS spectra of purified BMF

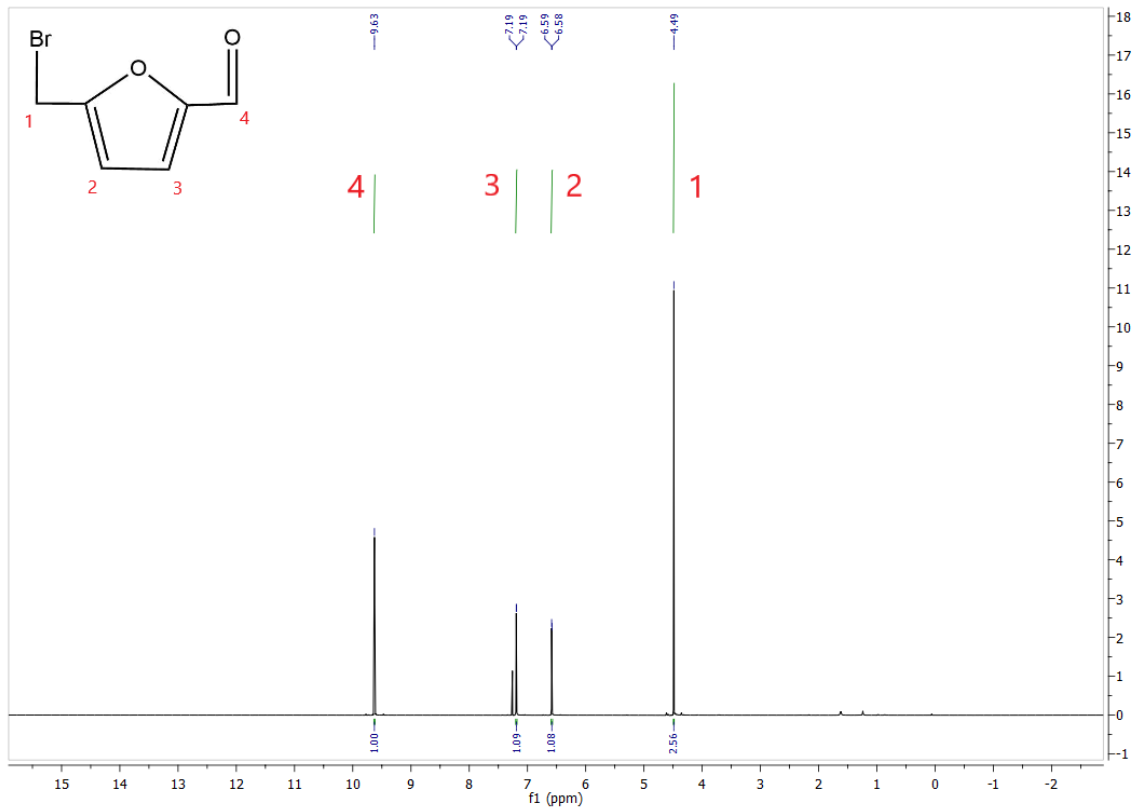


Figure 19: <sup>1</sup>H-NMR of purified BMF

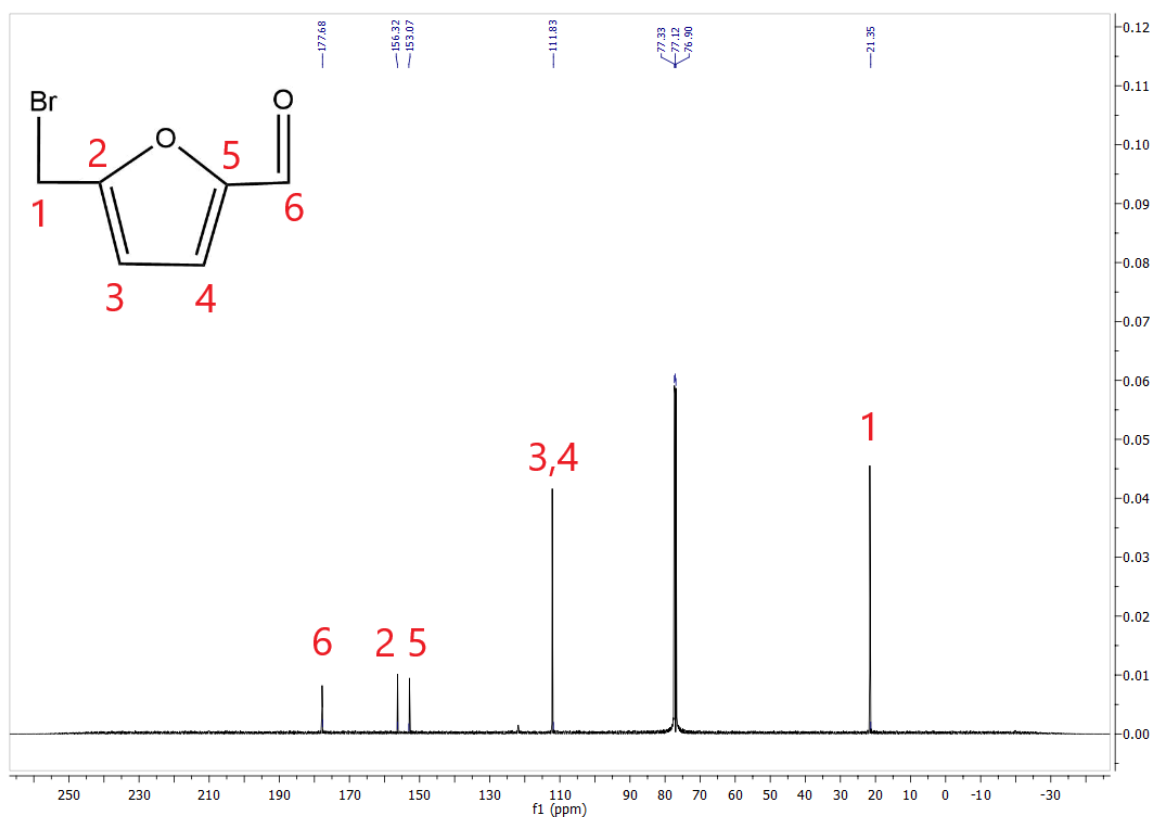


Figure 20:  $^{13}\text{C}$ -NMR of purified BMF

Moving from such positive results, a biphasic multi-step approach was applied, aiming to further improve BMF yield. Biphasic multi-step approach was successfully performed by Breeden et al.<sup>14</sup> in a 6-step CMF production from microcrystalline cellulose.

An overall procedure for multi-step approach can be summarised as follows:

- Reacting system is placed in MW multimode reactor and irradiated for the desired time;
- At the end of the reaction the  $\text{CH}_2\text{Cl}_2$  fraction BMF-rich is removed from concentrated HBr that still contains unconverted reagent and/or reaction intermediates;
- Fresh  $\text{CH}_2\text{Cl}_2$  is then added to the system which will be subjected to a second reaction step;
- The whole procedure can then be repeated for the desired number of steps.

In Figure 21, a scheme of the multi-step approach (3 steps) applied in this work is reported.

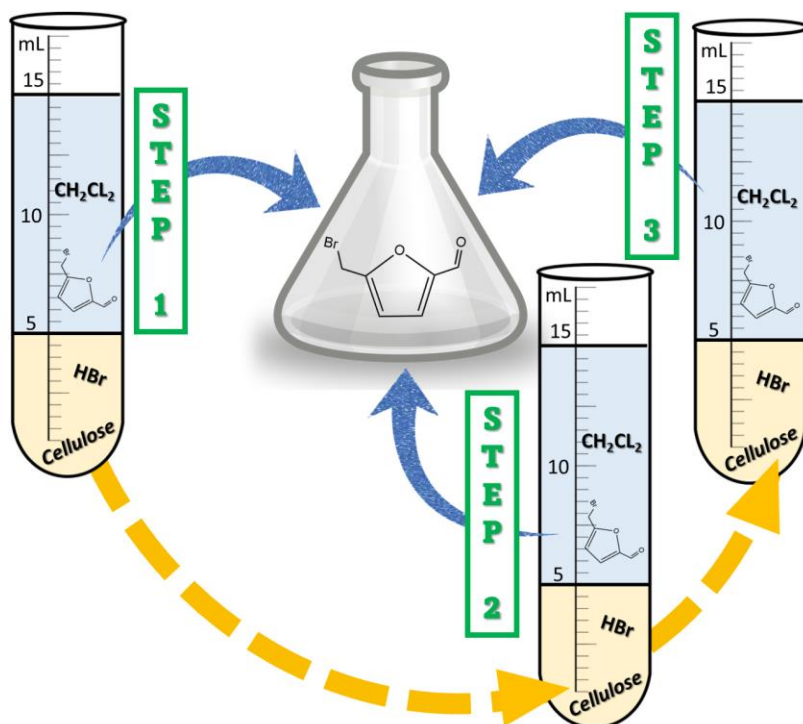


Figure 21: Multi-step approach for BMF MW-assisted production in biphasic systems

Both 100°C and 110°C temperatures and both cellulose and biomass PHTP were investigated. Times for investigation were chosen in correspondence of the ascending points of the curves defined during the single step optimisation. In other words, reactions were performed in correspondence of the times in which BMF production is the prevailing process over degradation. For every time investigated 1-, 2- and 3-step reactions were evaluated, calculating the overall yield achieved by multiple steps.

Multi-step reaction performed at 100°C (Figure 22) showed the highest yield (68.03%mol) for cellulose at 10 minutes, with 3 steps, while for biomass the best result (41.04%mol) was achieved at 5 minutes with 3 steps. By comparing such results with single-step reactions, +10.77% yield was achieved in case of cellulose and +6.63% in case of biomass.

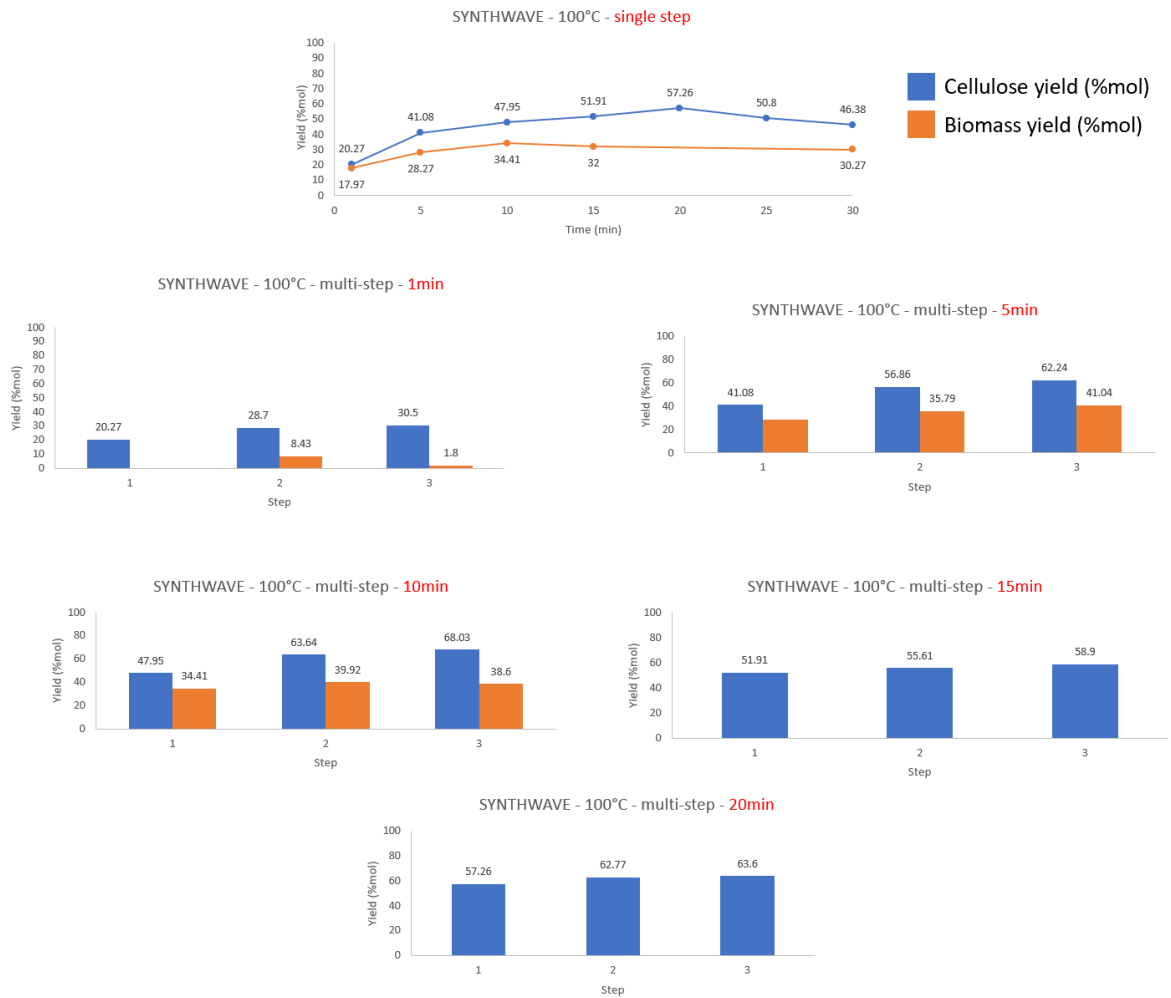


Figure 22: BMF production yield from cellulose and biomass in multi-step reactions at 100°C

Multi-step reaction performed at 110°C (Figure 23) showed the highest yield (64.71%mol) for cellulose at 5 minutes, with 3 steps, while for biomass the best result (45.35%mol) was achieved at 5 minutes with 3 steps. By comparing such results with single-step reactions, +4.08% yield was achieved in case of cellulose and +9.32% yield was achieved in case of biomass.

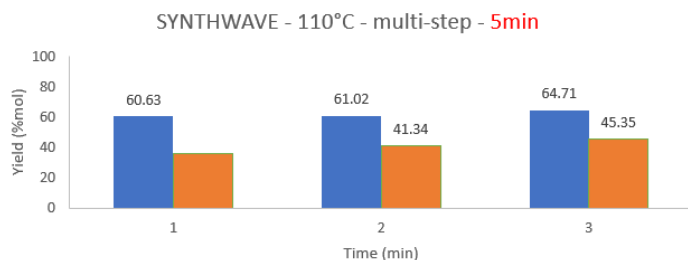
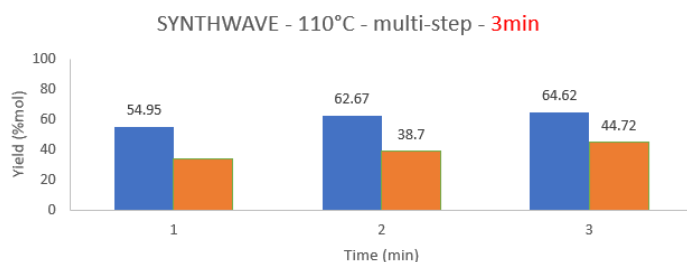
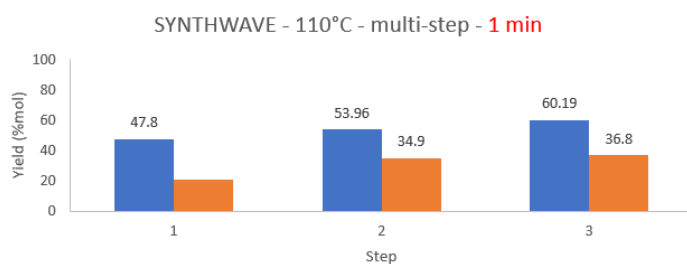
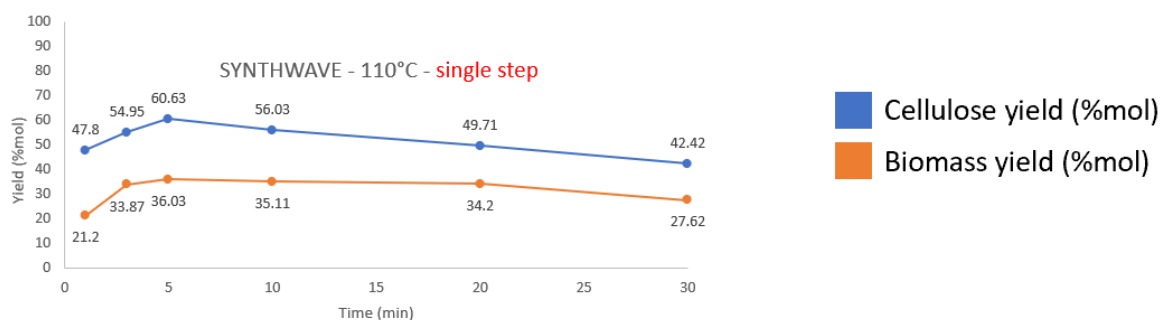


Figure 23: BMF production yield from cellulose and biomass in multi-step reactions at 110°C

According to the results reported, the highest BMF yield from cellulose was achieved at 100°C, 10min with 3 steps while for biomass the highest BMF yield was achieved at 110°C, 5 min with 3 steps, thus confirming that for biomass an increase of temperature is beneficial due to the recalcitrance of this feedstock.

### 3.2.5. CMF production from cellulose and biomass PHTP

CMF was prepared by applying the optimised parameters achieved in single-step multimode MW reactor, with concentrated HCl and dichloromethane. Both 100°C and 110°C temperatures were tested and both cellulose and biomass were used as substrates. Results are reported below in Figure 24



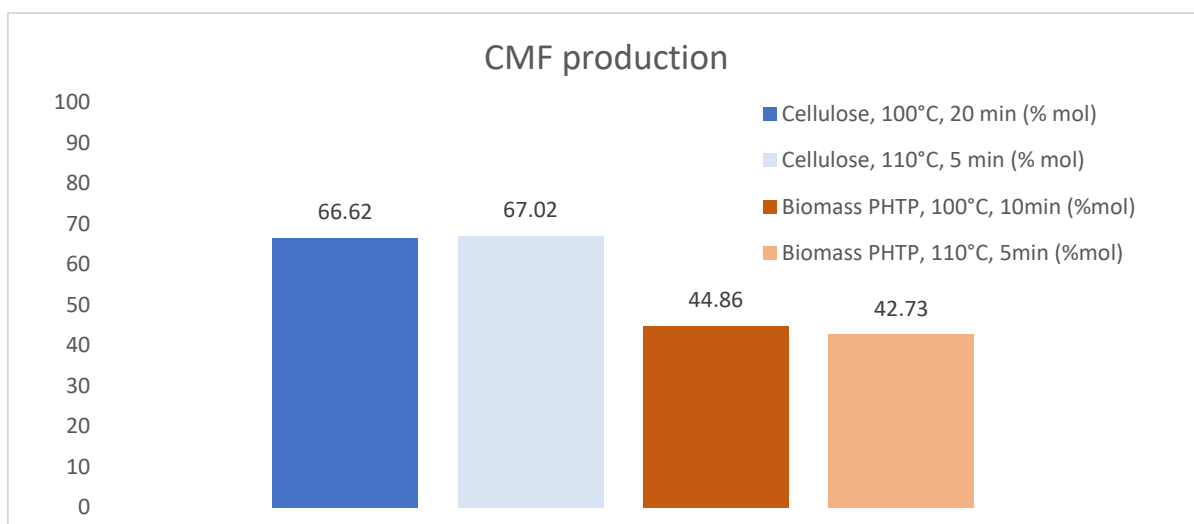


Figure 24: CMF and BMF production yield from cellulose and biomass at 100°C and 110°C in multimode MW reactor

No relevant differences can be seen when temperature was increased from 100°C to 110°C but in all the cases yields achieved for CMF were higher than the homologous results for BMF. Typical chromatogram of CMF crude reaction is reported in Figure 25: CMF was the main product (peak at r.t. 11.009) together with small amounts of other furfurals and undetermined by-products.

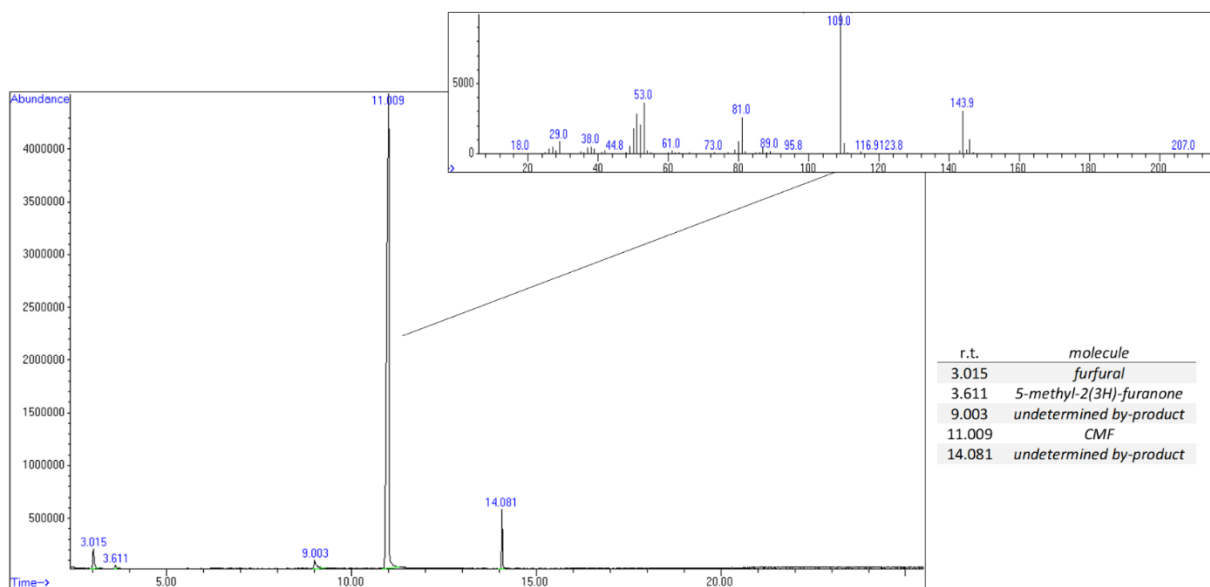


Figure 25: Typical GC-MS spectra of dichloromethane CMF rich phase and detail of CMF MS spectra

### 3.3. CONCLUSIONS

This chapter investigated 5-brominemethylfurfural production in microwave reactors. 5-brominemethylfurfural is considered a valuable alternative to 5-(hydroxymethyl)furfural since its hydrophobicity makes it more suitable for long-term storage, avoiding excessive product degradation. Moreover, also due to its marked hydrophobicity, 5-brominemethylfurfural can be easily recovered in biphasic systems, making its production and recovery more efficient and flexible if compared with 5-(hydroxymethyl)furfural. Theoretically from a biorefinery point of view, 5-brominemethylfurfural chemistry can lead to the same products that can be achieved from 5-(hydroxymethyl)furfural making it an extremely promising platform chemical. Pure cellulose and 2G biomass (PHTP) were used as starting feedstock for the experiments.

The two main strategies reported in literature (LiBr + HBr or concentrated HBr) were coupled with both monomodal and multimode microwave heating.

This approach led to good 5-brominemethylfurfural yields with dramatic reduction of reaction times from days/hours reported in literature (see Table 4) to minutes.

Time reduction exerted by microwave irradiation and relatively low temperatures involved in the protocols are connected with sensible reduction of energy consumption, thus making it more competitive in case of future biorefinery applications.

In Table 10, the best results according to the technology and aqueous phase involved are reported.


	<i>Multimode MW reactor</i>	<i>Monomode MW reactor</i>				
<b>LiBr·nH<sub>2</sub>O + HBr (dil.)</b>	<ul style="list-style-type: none"> <li>Time: 5 min</li> <li>Temperature: 150°C</li> </ul> <p><b>BMF Yield (CELLULOSE): 49.66 %mol</b></p>					
<b>HBr (conc.)</b>	<table border="1"> <tr> <td> <b>SINGLE STEP - CELLULOSE</b> <ul style="list-style-type: none"> <li>Time: 5 min</li> <li>Temperature: 110°C</li> </ul> <p><b>BMF Yield: 60.63 %mol</b></p> </td> <td> <b>SINGLE STEP - BIOMASS</b> <ul style="list-style-type: none"> <li>Time: 5 min</li> <li>Temperature: 110°C</li> </ul> <p><b>BMF Yield: 36.03 %mol</b></p> </td> </tr> <tr> <td> <b>MULTI STEP - CELLULOSE</b> <ul style="list-style-type: none"> <li>Time: 10 min</li> <li>Temperature: 100°C</li> <li>Number of steps: 3</li> </ul> <p><b>BMF Yield: 68.03 %mol</b></p> </td> <td> <b>MULTI STEP - BIOMASS</b> <ul style="list-style-type: none"> <li>Time: 5 min</li> <li>Temperature: 110°C</li> <li>Number of steps: 3</li> </ul> <p><b>BMF Yield: 45.35 %mol</b></p> </td> </tr> </table>	<b>SINGLE STEP - CELLULOSE</b> <ul style="list-style-type: none"> <li>Time: 5 min</li> <li>Temperature: 110°C</li> </ul> <p><b>BMF Yield: 60.63 %mol</b></p>	<b>SINGLE STEP - BIOMASS</b> <ul style="list-style-type: none"> <li>Time: 5 min</li> <li>Temperature: 110°C</li> </ul> <p><b>BMF Yield: 36.03 %mol</b></p>	<b>MULTI STEP - CELLULOSE</b> <ul style="list-style-type: none"> <li>Time: 10 min</li> <li>Temperature: 100°C</li> <li>Number of steps: 3</li> </ul> <p><b>BMF Yield: 68.03 %mol</b></p>	<b>MULTI STEP - BIOMASS</b> <ul style="list-style-type: none"> <li>Time: 5 min</li> <li>Temperature: 110°C</li> <li>Number of steps: 3</li> </ul> <p><b>BMF Yield: 45.35 %mol</b></p>	<ul style="list-style-type: none"> <li>Time: 2'30'' min</li> <li>Temperature: 90°C</li> </ul> <p><b>BMF Yield (CELLULOSE): 54.15 %mol</b> <b>BMF Yield (BIOMASS): 37.92 %mol</b></p>
<b>SINGLE STEP - CELLULOSE</b> <ul style="list-style-type: none"> <li>Time: 5 min</li> <li>Temperature: 110°C</li> </ul> <p><b>BMF Yield: 60.63 %mol</b></p>	<b>SINGLE STEP - BIOMASS</b> <ul style="list-style-type: none"> <li>Time: 5 min</li> <li>Temperature: 110°C</li> </ul> <p><b>BMF Yield: 36.03 %mol</b></p>					
<b>MULTI STEP - CELLULOSE</b> <ul style="list-style-type: none"> <li>Time: 10 min</li> <li>Temperature: 100°C</li> <li>Number of steps: 3</li> </ul> <p><b>BMF Yield: 68.03 %mol</b></p>	<b>MULTI STEP - BIOMASS</b> <ul style="list-style-type: none"> <li>Time: 5 min</li> <li>Temperature: 110°C</li> <li>Number of steps: 3</li> </ul> <p><b>BMF Yield: 45.35 %mol</b></p>					

Table 10: Conclusions

The highest 5-brominemethylfurfural yield both from cellulose and biomass PHTP were achieved using multimode microwave reactor coupled with concentrated HBr, that can be

considered more sustainable if compared with systems involving both HBr and LiBr. Further increase in yields were achieved when multi-step approach was applied.

Some preliminary experiments were also performed using HCl to produce 5-chloromethylfurfural from cellulose and biomass. In this case, the achieved yields were considered competitive with data reported in literature, making the process worth of further optimisations.

A future improvement of the protocol developed so far, can be the substitution of chlorinated apolar solvent with more sustainable and environmental friendly green solvents.

### 3.4. EXPERIMENTAL

#### Reagents

All reagents and solvents, unless otherwise specified, were purchased from Sigma-Aldrich and used without further purification.

#### NREL-derived protocol

NREL-derived protocol was performed as described in chapter 2 section 2.4.

#### Molten salt preparation

The aqueous solution of molten salt was prepared by weighing 61.7g of anhydrous LiBr and adding 38.3g of deionized water, thus obtaining a solution of LiBr · 3H<sub>2</sub>O molten salt (61.7% w / w).

#### Sample analyses

GC-MS analyses were conducted on an Agilent 6890 GC (Agilent Technologies - USA), connected to an Agilent Network 5973 mass detector, using a MEGA-5 MS column (30 m capillary column, 0.25 mm and film thickness of 0.25 μm).

The temperature program was performed as follows:

- initial maintenance in isotherm for 5 minutes at 65°C,
- ramp 10°C / minute up to 100°C
- isotherm at 100°C for 1 minute,
- ramp 20°C / minute up to 230°C
- isotherm 230°C for 1 minute,
- ramp 20°C / minute up to 300°C
- isotherm at 300°C for 5 minutes.

Split injection 1:20, injector temperature 250 ° C, detector temperature 280 ° C. Carrier gas: He.

The GC-FID analyses were conducted on an Agilent 7820A GC (Agilent Technologies - USA), connected to a GC FID detector using a MEGA-5 MS column (capillary column of 30 m, of 0.25 mm and film thickness 0.25 μm).

The temperature program was performed as follows:

- initial maintenance in isotherm for 3 minutes at 50 ° C,
- ramp 3°C / minute up to 80°C,
- ramp 10°C / minute up to 300°C,
- isotherm at 300°C for 10 minutes.

Split injection 1:20, injector temperature 250 ° C, detector temperature 280 ° C. Carrier gas: He.

For quantitative analyses, BMF calibration curve was performed using GC-FID.

Calibration curve is reported Figure 26

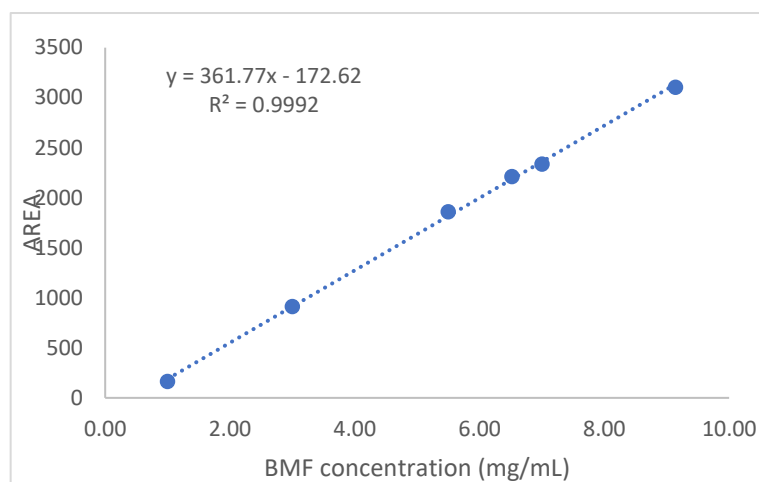


Figure 26: BMF calibration curve

All NMR spectra were recorded with a Jeol 600 ECZ R instrument at 25 °C using  $\text{CDCl}_3$  as a solvent.

#### Ball-mill treatment

Ball-mill treatment for cellulose and biomass was performed in a Restch PM100 ball mill by following the subsequent procedure:

- 5 g of cellulose or biomass PHTP were placed in the medium jar, filled for 1/3 of its volume with medium steel balls,
- 1 hour total treatment time was settled at 550rpm,
- Inversion of rotation direction was settled every 10 minutes.

#### Conversion of cellulose / biomass in monomode MW reactor Monowave 300

Defined quantity of substrate (cellulose or biomass) was weighed in a 30ml vial specific for the Monowave 300 instrument. A magnetic stirring bar was added to the reaction vessel.

- When molten salt  $\text{LiBr} \cdot 3\text{H}_2\text{O}$  was involved, 5ml of molten salt were added to the reaction vial. In order to disperse and homogenize the substrate in the solution, the vial was placed for 1 minute in an ultrasonic bath (Elma Transsonic T460). Subsequently, 0.09 ml of 8.9 M HBr were added to the system. By adding this volume to the reaction vial, a final solution having an HBr concentration equal to 0.16M was obtained. Finally, 10 ml of dichloromethane were to the reaction vial.
- When concentrated HBr was involved, 5mL of 8.9 M HBr were added to the reaction vial. In order to disperse and homogenize the substrate in the solution, the vial was placed for 1 minute in an ultrasonic bath (Elma Transsonic T460). Finally, 10 ml of dichloromethane were to the reaction vial.

Reaction vial was then placed in cavity of the Monowave 300 instrument.

In all reactions, the maximum heating mode “heat as fast as possible” was set for the ramp phase. Desired reaction temperature was settled and stirring speed was settled to 800rpm.

#### Conversion of cellulose / biomass in multimode MW reactor Synthwave

Defined quantity of substrate (cellulose or biomass) was weighed in a 40ml vial specific for the Synthwave instrument. A magnetic stirring bar was added to the reaction vessel.

- When molten salt  $\text{LiBr} \cdot 3\text{H}_2\text{O}$  was involved, 5ml of molten salt were added to the reaction vial. In order to disperse and homogenize the substrate in the solution, the vial was placed for 1 minute in an ultrasonic bath (Elma Transsonic T460). Subsequently 0.09 ml of 8.9 M HBr were added to the system. By adding this volume to the reaction vial, a final solution having an HBr concentration equal to 0.16M was obtained. Finally, 10 ml of dichloromethane were added to the reaction vial.
- When concentrated HBr was involved, 5mL of 8.9 M HBr were added to the reaction vial. In order to disperse and homogenize the substrate in the solution, the vial was placed for 1 minute in an ultrasonic bath (Elma Transsonic T460). Finally, 10 ml of dichloromethane were to the reaction vial.

Reaction vial was placed in Synthwave reactor.

A heating ramp of 3'30'' was settled to reach desired reaction temperature. Desired reaction temperature was settled and stirring speed was settled to 100%.

15bar  $\text{N}_2$  were added to pressurize the reactor avoiding the solvents evaporation/boiling.

#### Multi-step protocol

For some reactions, a multi-step strategy was adopted: at the end of the reaction the crude was filtered in a glass sintered filter under vacuum in order to separate solid residues from the two liquid fractions. Organic phase was recovered, and the remaining aqueous phase was introduced into the reaction vial together with 10 ml of fresh dichloromethane.

Subsequently, the reaction was carried out under the same conditions as the previous step. The procedure was repeated for the desired number of steps.

#### Work-up

At the end of each reaction the following work-up was performed:

- The crude was filtered in a glass sintered filter under vacuum in order to separate solid residues from the two liquid fractions.
- The crude was subsequently placed in a liquid-liquid separation funnel. Dichloromethane BMF-rich phase was recovered and two subsequent extractions with clean dichloromethane were performed.
- Dichloromethane BMF-rich phases were collected and concentrated in rotavapor.
- Concentrated dichloromethane BMF-rich phase was then transferred to a 10mL volumetric flask and dichloromethane was added until 10mL volume was reached.
- 1mL sample was recovered and transferred to a 2 ml vial for GC-MS and / or GC-FID analysis.

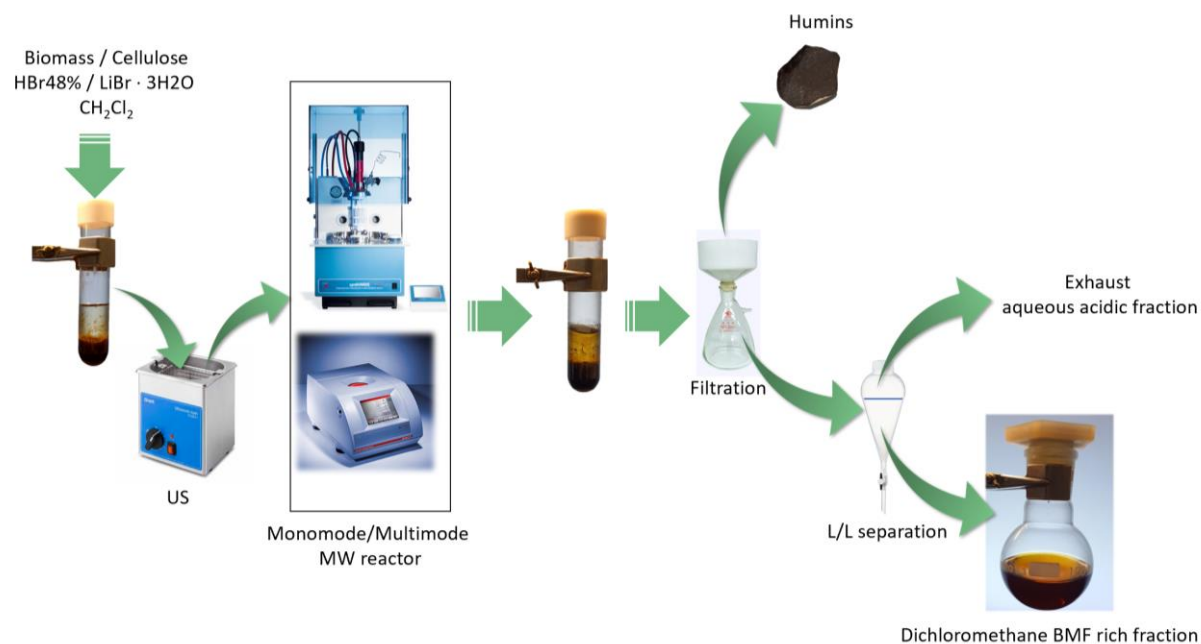


Figure 27: Workup

### BMF purification

Silica column chromatography was performed as a post work-up organic phase purification technique in order to obtain pure BMF. The column was prepared with 30 g of silica suspended in chloroform. Dichloromethane BMF-rich phase was collected in a 50 ml flask and a silica spatula tip was added. The content of the flask was dried in the rotavapor until a dry brownish powder was obtained. This powder was added to the column. The column was performed using dichloromethane as solvent. The various fractions obtained from the chromatographic column were collected in different tubes and analyzed by means of thin layer chromatography (TLC), using chloroform as eluent. Subsequently, BMF-rich fractions were collected together, and the solvent was evaporated under a high flow of N<sub>2</sub> for about 1 hour until pale yellow BMF crystals were obtained.

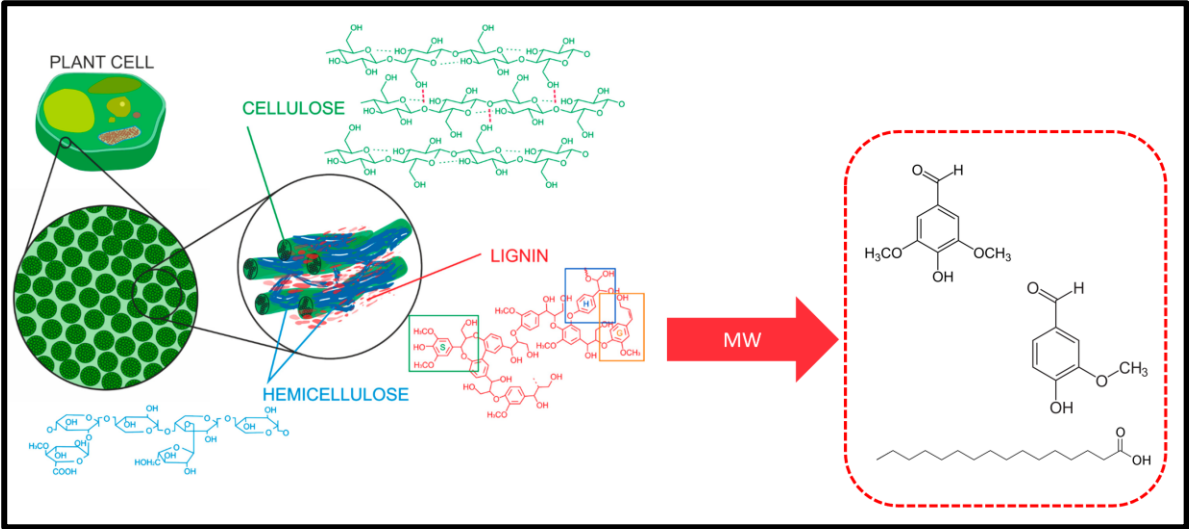
### 3.5. REFERENCES

- (1) Zheng, X.; Gu, X.; Ren, Y.; Zhi, Z.; Lu, X. Production of 5-Hydroxymethyl Furfural and Levulinic Acid from Lignocellulose in Aqueous Solution and Different Solvents. *Biofuels Bioprod. Biorefining* **2016**, *10* (6), 917–931. <https://doi.org/10.1002/bbb.1720>.
- (2) Mukherjee, A.; Dumont, M.-J.; Raghavan, V. Review: Sustainable Production of Hydroxymethylfurfural and Levulinic Acid: Challenges and Opportunities. *Biomass Bioenergy* **2015**, *72*, 143–183. <https://doi.org/10.1016/j.biombioe.2014.11.007>.
- (3) Hu, L.; Wu, Z.; Jiang, Y.; Wang, X.; He, A.; Song, J.; Xu, J.; Zhou, S.; Zhao, Y.; Xu, J. Recent Advances in Catalytic and Autocatalytic Production of Biomass-Derived 5-Hydroxymethylfurfural. *Renew. Sustain. Energy Rev.* **2020**, *134*, 110317. <https://doi.org/10.1016/j.rser.2020.110317>.
- (4) Wang, T.; Nolte, M. W.; Shanks, B. H. Catalytic Dehydration of C<sub>6</sub> Carbohydrates for the Production of Hydroxymethylfurfural (HMF) as a Versatile Platform Chemical. *Green Chem* **2014**, *16* (2), 548–572. <https://doi.org/10.1039/C3GC41365A>.
- (5) Jing, Q.; Lü, X. Kinetics of Non-Catalyzed Decomposition of Glucose in High-Temperature Liquid Water. *Chin. J. Chem. Eng.* **2008**, *16* (6), 890–894. [https://doi.org/10.1016/S1004-9541\(09\)60012-4](https://doi.org/10.1016/S1004-9541(09)60012-4).
- (6) Yu, I. K. M.; Tsang, D. C. W. Conversion of Biomass to Hydroxymethylfurfural: A Review of Catalytic Systems and Underlying Mechanisms. *Bioresour. Technol.* **2017**, *238*, 716–732. <https://doi.org/10.1016/j.biortech.2017.04.026>.
- (7) Dutta, S. Valorization of Biomass-Derived Furfurals: Reactivity Patterns, Synthetic Strategies, and Applications. *Biomass Convers. Biorefinery* **2021**. <https://doi.org/10.1007/s13399-021-01924-w>.
- (8) Galkin, K. I.; Ananikov, V. P. The Increasing Value of Biomass: Moving From C<sub>6</sub> Carbohydrates to Multifunctionalized Building Blocks via 5-(Hydroxymethyl)Furfural. *ChemistryOpen* **2020**, *9* (11), 1135–1148. <https://doi.org/10.1002/open.202000233>.
- (9) Galkin, K. I.; Ananikov, V. P. When Will 5-Hydroxymethylfurfural, the “Sleeping Giant” of Sustainable Chemistry, Awaken? *ChemSusChem* **2019**, *12* (13), 2976–2982. <https://doi.org/10.1002/cssc.201900592>.
- (10) Mascal, M. 5-(Halomethyl)Furfurals from Biomass and Biomass-Derived Sugars. In *Production of Platform Chemicals from Sustainable Resources*; Fang, Z., Smith, R. L., Qi, X., Eds.; Biofuels and Biorefineries; Springer Singapore: Singapore, 2017; pp 123–140. [https://doi.org/10.1007/978-981-10-4172-3\\_4](https://doi.org/10.1007/978-981-10-4172-3_4).
- (11) Anchan, H. N.; Dutta, S. Recent Advances in the Production and Value Addition of Selected Hydrophobic Analogs of Biomass-Derived 5-(Hydroxymethyl)Furfural. *Biomass Convers. Biorefinery* **2021**. <https://doi.org/10.1007/s13399-021-01315-1>.
- (12) Mascal, M.; Nikitin, E. B. Direct, High-Yield Conversion of Cellulose into Biofuel. *Angew. Chem.* **2008**, *120* (41), 8042–8044. <https://doi.org/10.1002/ange.200801594>.
- (13) Mascal, M.; Nikitin, E. B. Dramatic Advancements in the Saccharide to 5-(Chloromethyl)Furfural Conversion Reaction. *ChemSusChem* **2009**, *2* (9), 859–861. <https://doi.org/10.1002/cssc.200900136>.
- (14) Breeden, S. W.; Clark, J. H.; Farmer, T. J.; Macquarrie, D. J.; Meimoun, J. S.; Nonne, Y.; Reid, J. E. S. J. Microwave Heating for Rapid Conversion of Sugars and Polysaccharides to 5-Chloromethyl Furfural. *Green Chem* **2013**, *15* (1), 72–75. <https://doi.org/10.1039/C2GC36290B>.
- (15) Kumari, N.; Olesen, J. K.; Pedersen, C. M.; Bols, M. Synthesis of 5-Bromomethylfurfural from Cellulose as a Potential Intermediate for Biofuel. *Eur. J. Org. Chem.* **2011**, *2011* (7), 1266–1270. <https://doi.org/10.1002/ejoc.201001539>.
- (16) Bredihhin, A.; Mäeorg, U.; Vares, L. Evaluation of Carbohydrates and Lignocellulosic Biomass from Different Wood Species as Raw Material for the Synthesis of 5-Bromomethylfurfural. *Carbohydr. Res.* **2013**, *375*, 63–67. <https://doi.org/10.1016/j.carres.2013.04.002>.



- (17) Meller, E.; Aviv, A.; Aizenshtat, Z.; Sasson, Y. Preparation of Halogenated Furfurals as Intermediates in the Carbohydrates to Biofuel Process. *RSC Adv.* **2016**, *6* (42), 36069–36076. <https://doi.org/10.1039/C6RA06050A>.
- (18) Yoo, C. G.; Zhang, S.; Pan, X. Effective Conversion of Biomass into Bromomethylfurfural, Furfural, and Depolymerized Lignin in Lithium Bromide Molten Salt Hydrate of a Biphasic System. *RSC Adv.* **2017**, *7* (1), 300–308. <https://doi.org/10.1039/C6RA25025D>.
- (19) Le, K.; Zuo, M.; Song, X.; Zeng, X.; Tang, X.; Sun, Y.; Lei, T.; Lin, L. An Effective Pathway for 5-Brominemethylfurfural Synthesis from Biomass Sugars in Deep Eutectic Solvent: An Effective Pathway for 5-Brominemethylfurfural Synthesis. *J. Chem. Technol. Biotechnol.* **2017**, *92* (12), 2929–2933. <https://doi.org/10.1002/jctb.5312>.
- (20) Mascal, M. 5-(Chloromethyl)Furfural (CMF): A Platform for Transforming Cellulose into Commercial Products. *ACS Sustain. Chem. Eng.* **2019**, *7* (6), 5588–5601. <https://doi.org/10.1021/acssuschemeng.8b06553>.
- (21) Chang, F.; Hsu, W.-H.; Mascal, M. Synthesis of Anti-Inflammatory Furan Fatty Acids from Biomass-Derived 5-(Chloromethyl)Furfural. *Sustain. Chem. Pharm.* **2015**, *1*, 14–18. <https://doi.org/10.1016/j.scp.2015.09.002>.
- (22) Mascal, M.; Dutta, S. Synthesis of the Natural Herbicide  $\delta$ -Aminolevulinic Acid from Cellulose-Derived 5-(Chloromethyl)Furfural. *Green Chem* **2011**, *13* (1), 40–41. <https://doi.org/10.1039/C0GC00548G>.
- (23) Mascal, M.; Dutta, S. Synthesis of Ranitidine (Zantac) from Cellulose-Derived 5-(Chloromethyl)Furfural. *Green Chem.* **2011**, *13* (11), 3101. <https://doi.org/10.1039/c1gc15537g>.
- (24) Khan, A. S.; Man, Z.; Bustam, M. A.; Kait, C. F.; Khan, M. I.; Muhammad, N.; Nasrullah, A.; Ullah, Z.; Ahmad, P. Impact of Ball-Milling Pretreatment on Pyrolysis Behavior and Kinetics of Crystalline Cellulose. *Waste Biomass Valorization* **2016**, *7* (3), 571–581. <https://doi.org/10.1007/s12649-015-9460-6>.
- (25) Genevini, P.; Adani, F.; Villa, C. Rice Hull Degradation by Co-Composting with Dairy Cattle Slurry. *Soil Sci. Plant Nutr.* **1997**, *43* (1), 135–147. <https://doi.org/10.1080/00380768.1997.10414722>.
- (26) Rinaldi, R.; Palkovits, R.; Schüth, F. Depolymerization of Cellulose Using Solid Catalysts in Ionic Liquids. *Angew. Chem. Int. Ed.* **2008**, *47* (42), 8047–8050. <https://doi.org/10.1002/anie.200802879>.

# 4. SUSTAINABLE VALORISATION OF LIGNINS



## 4.1. INTRODUCTION

### 4.1.1. Lignin: structure and composition

As previously mentioned, lignin is the second most abundant natural polymer in 2G biomasses. Its main role in plants is to provide structural integrity.

Lignin is composed of three primary “monolignol” units, connected through ether or C-C bonds: sinapyl (3,5-dimethoxy-4 hydroxycinnamyl), coniferyl (3-methoxy-4-hydroxycinnamyl) and *p*-coumaryl (4-hydroxycinnamyl) alcohols; also known as syringyl (S), guaiacyl (G), and *p*-hydroxyphenyl (H) units. Apart such primary monolignol units it should be noted that other “non-canonical” units have been detected such as ferulates, *p*-hydroxybenzoates and *p*-coumarates<sup>1,2,3</sup>.

Abundance of primary units varies widely depending on lignin source and plant type, as reported in Table 1<sup>4</sup>:

Monolignol	Softwood (%)	Hardwood (%)	Non-wood (herbaceous) (%)
<b>Sinapyl alcohol (S)</b>	0-1	50-75	25-50
<b>Coniferyl alcohol (G)</b>	90-95	25-50	25-50
<b><i>p</i>-coumaryl alcohol (H)</b>	0.5-3.4	trace	10-25

Table 1: Monolignol units' abundance in softwood, hardwood and non-wood

Herbaceous plants contain all the three monolignols, hardwoods (or angiosperm lignins) contain high levels of S and G units, while softwoods (or gymnosperm lignins) are extremely rich in G units and their structure is more branched than the others<sup>5</sup>.

Schematic representation of softwood and hardwood lignins together with monolignol units are reported in Figure 1.

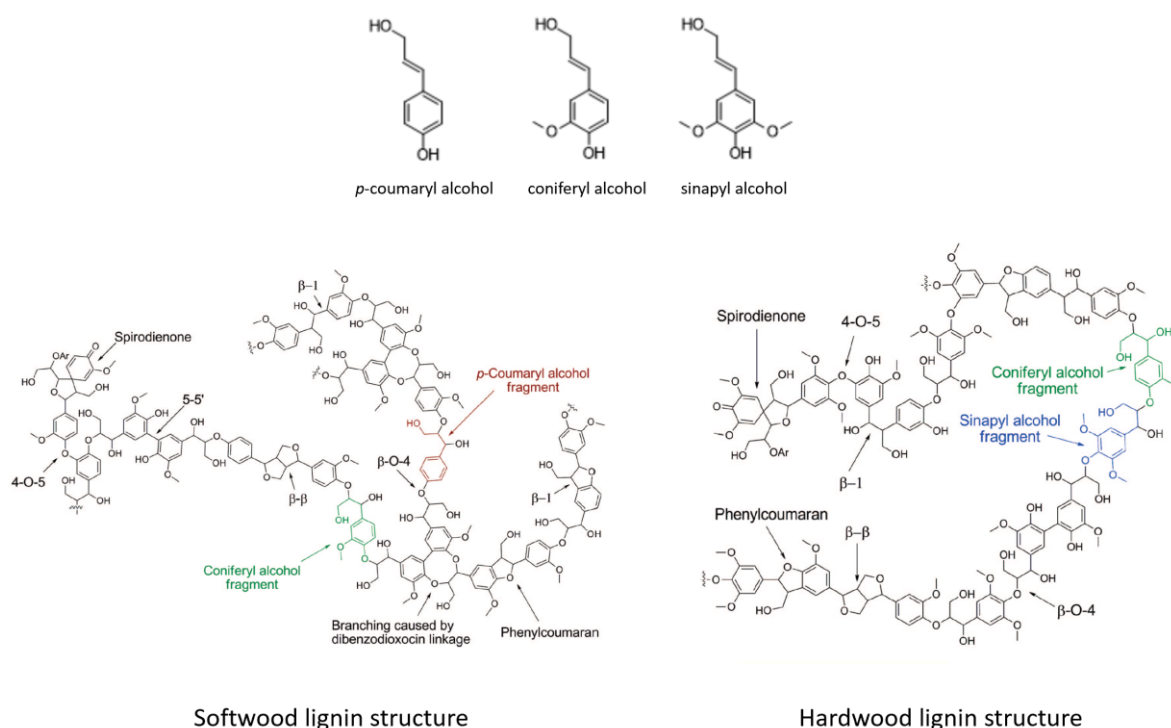


Figure 1: Lignin structure (adapted from Zakzeski et al.)

Monolignol units are connected through a wide variety of linkages such as aryl ether bonds ( $\beta$ -O-4,  $\alpha$ -O-4, 4-O-5) and C-C bonds (5-5',  $\beta$ -5,  $\beta$ -1,  $\beta$ - $\beta$ )<sup>6</sup>.

Apart its intrinsic variability, a fundamental limitation in lignin structure definition relies in the modifications of its original structure exerted by all the isolation/fractionation protocols, making impossible to recover unaltered native lignin (or protolignin, the untreated lignin in plants)<sup>2,1</sup>. Native lignin is covalently cross-linked with hemicellulose, originating an amorphous matrix that surrounds and supports cellulose fibres. Such stabile lignin-carbohydrate linkages are the main obstacle to be overcome when aiming to selectively recover lignin<sup>7</sup>. Consequently, harsh conditions for lignin isolation/fractionation from biomass, can lead to high modification-degrees of native lignin that can strongly influence its further reactivity. Indeed, native lignin is considered highly reactive, while isolated "industrial" or "technical" lignins are reported to be more recalcitrant. During isolation protocols, labile  $\beta$ -O-4 ether bond and ester linkages present in native lignin can be easily cleaved favouring the formation through recondensation of more stable C-C linkages which confer lower reactivity in subsequent valorisation treatments<sup>8</sup>.

#### 4.1.2. Lignin in biorefinery processes

Several biorefinery protocols focused on lignocellulosic feedstock valorisation do not comprise lignin exploitation: carbohydrate fraction is considered the most valuable fraction to be valorised while lignin is usually considered a low value by-product or a cheap energy source that can be burnt to feed the biorefinery process.

Large quantities of technical lignins are produced every year and can be classified into:

- Kraft lignin from the kraft pulping process
- Organosolv lignin from organosolv pulping
- Lignosulfonates from pulping
- Hydrolysis lignin from ethanol production from cellulose

It is estimated that 100million tonnes per year of technical lignins are produced around the world, with 70million tonnes deriving from kraft pulping process. Less than 1-2% of this enormous quantity of lignin is valorised for high-value chemical applications<sup>9</sup>. Aiming to set-up economically feasible biorefinery protocols, lignin valorisation is a fundamental step to be developed alongside with cellulose and hemicellulose valorisation<sup>10,11</sup>.

Owing to its abundance and composition, in recent times, lignin has attracted more and more interest, being considered the largest renewable source of bioaromatics<sup>10</sup>.

Three major approaches for lignin valorisation have been established in past decades<sup>1</sup>:

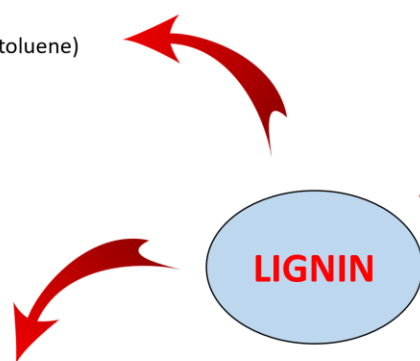
- Power production, green fuels or syngas;
- Use as macromolecule;
- Low molecular weight aromatic compounds production.

Non-energetic uses of lignin have gained increased attention: owing to its complex aromatic structure, lignin can serve as feedstock for bulk or functionalised aromatics.

In 2007 a list of more than 50 products potentially derived from lignin conversions was developed by US Department Of Energy<sup>12</sup>. The main low molecular weight aromatic compounds are summarised in Figure 2<sup>12,7</sup>:

### Hydrocarbons

- BTX (benzene, xylene, toluene)
- Cyclohexane
- Styrenes
- Biphenils



### Phenols

- Phenols
- Substituted phenols
- Catechols, cresols, resorcinols
- Eugenol
- Syringols
- Coniferols
- Guaiacols

### Oxidized products

- Aromatic aldehydes, vanillin, vanillic acid
- Aromatic acids
- Aliphatic acids
- Quinones
- Cyclohexanol
- Beta keto adipate

Figure 2: Main low molecular weight aromatic compounds derived from lignin

The economic potential of some lignin-derived products are illustrated in Figure 3<sup>13</sup>:

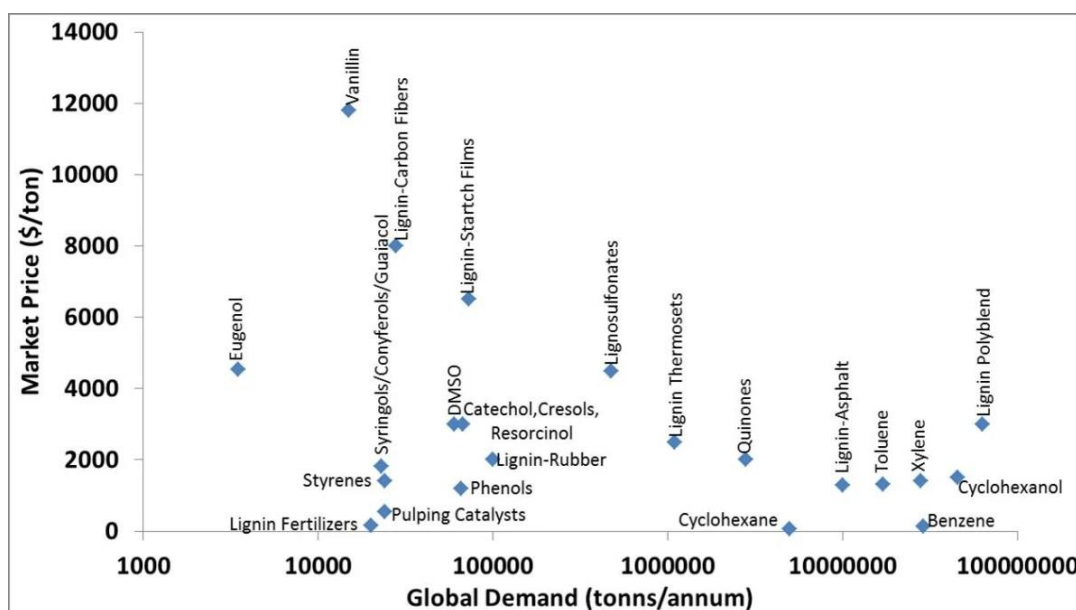


Figure 3: Economic potential of lignin-derived products<sup>13</sup>

#### 4.1.3. Biomass pre-treatments for lignin recovery/isolation

A lot of challenges still remain to be overcome for efficient and profitable lignin valorisation. Indeed, chemical recalcitrance, complex structure and the heterogeneous composition that strongly depends on plant-type and species, make high-value lignin exploitation an ambitious issue<sup>6</sup>. Moreover, as the intrinsic characteristics of technical lignins can vary widely, particular attention should be focused in the choice of their valorisation protocol<sup>7</sup>.

The importance of lignin recovery and valorisation increased so much that led, in recent years, to the so called "lignin-first" approach, which states the lignin valorisation as primary step to be performed before any other carbohydrate valorisation during biorefinery treatments<sup>14</sup>.

Several studies are focused on development of new approaches (pre-treatments) for lignin isolation/fractionation that aim to achieve high purity lignins with good reactivity<sup>15</sup>. Indeed,

methods for lignin isolation can be divided in two groups, according to the degree of structural modification of resulting lignin (Figure 4)<sup>11</sup>:

- Methods resulting in significant structural modifications (pulsing methods such as Kraft, Sulfite, Alkaline and Klason). Such methods are focused in pure-cellulose recovery, while lignin is obtained as side-stream product. As previously described, harsh conditions can heavily impact lignin structure with negative consequences in terms of reactivity. Moreover, Kraft, Klason and Sulphite methods produce sulphur-enriched lignins whose application can be limited by sulphur presence.
- Methods resulting in mild structural modifications (Björkman process, cellulytic enzymatic and enzymatic mild acidolysis, ionic liquid treatment and organosolv process). These methods induce lower extent lignin modifications but technical and economic limitations in their applicability remain relevant.

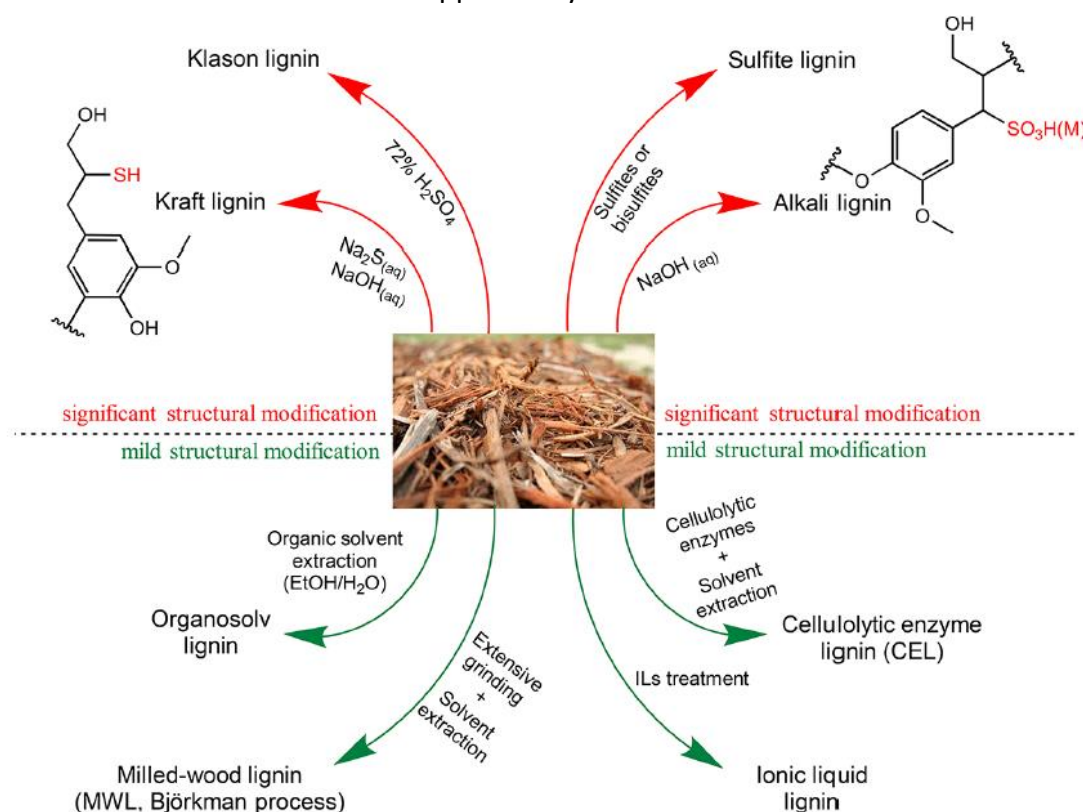


Figure 4: Lignin isolation methods<sup>11</sup>

#### 4.1.4. Oxidative valorisation of lignin

Once the lignin has been recovered through biomass pre-treatment protocols, it can be chemically valorised to produce valuable products. Several lignin valorisation strategies can be classified as<sup>3</sup>:

- Lignin cracking/hydrolysis;
- Reduction reactions that aim to de-functionalise lignin monomers to form simpler phenols, benzene, toluene, xylene;
- Oxidation reactions that aim to convert monomers to chemicals characterized by extensive functionality that can serve as platform chemicals or directly as fine chemicals.

Among these, lignin oxidation is reported in literature as a valuable approach that allows production of highly functionalised molecules.

Both model compounds and real lignins were investigated in oxidative conditions. Model compounds were usually employed to validate the protocols before moving to real-case lignins<sup>16</sup>. Several catalysts and oxidising agents (chlorine, chlorine oxide, oxygen, hydrogen peroxide, ozone and peroxyacids) were tested to improve oxidation results<sup>17,16,8,10</sup>.

Among oxidising agents, oxygen is considered one of the most promising because of low price, availability, and sustainability.

Despite the exact mechanism involved in alkaline oxidation remains unclear, Gierer et al.<sup>18</sup> and Tarabanko et al.<sup>19–21</sup> proposed two radical reaction mechanisms.

According to Gierer et al., in alkaline conditions phenolic hydroxyl groups are ionised to phenolate ions and proceeds with phenoxy radical formation. Alkaline conditions are required to favour -OH ionisation.

Phenoxy radicals can be subjected to oxygen addition in ortho, para or C $\beta$  positions forming peroxy anions. Peroxy anion species can undergo to several subsequent reactions leading to:

- 1) C $_4$ -C $_{\alpha}$  bond cleavage, forming p-quinones
- 2) Oxirane structure formation
- 3) Aromatic ring cleavage, leading to carboxylic acids formation
- 4) C $_{\alpha}$ -C $_{\beta}$  bond cleavage, yielding phenolic aldehydes

In alkaline conditions, lignin conversion to phenolic monomers is reported to be the main route<sup>22</sup>.

Owing to the radical nature of the reaction, recondensation of lignin fragments should also be considered, leading to biphenyl structures characterised by high resistance to oxygen oxidation. Despite that, in alkaline conditions reactions is reported to tend to yield mainly aldehydic products.

According to Schutyser et al.<sup>10</sup> reaction mechanism proposed by Gierer et al. can be summarised as reported in the scheme below (Figure 5):

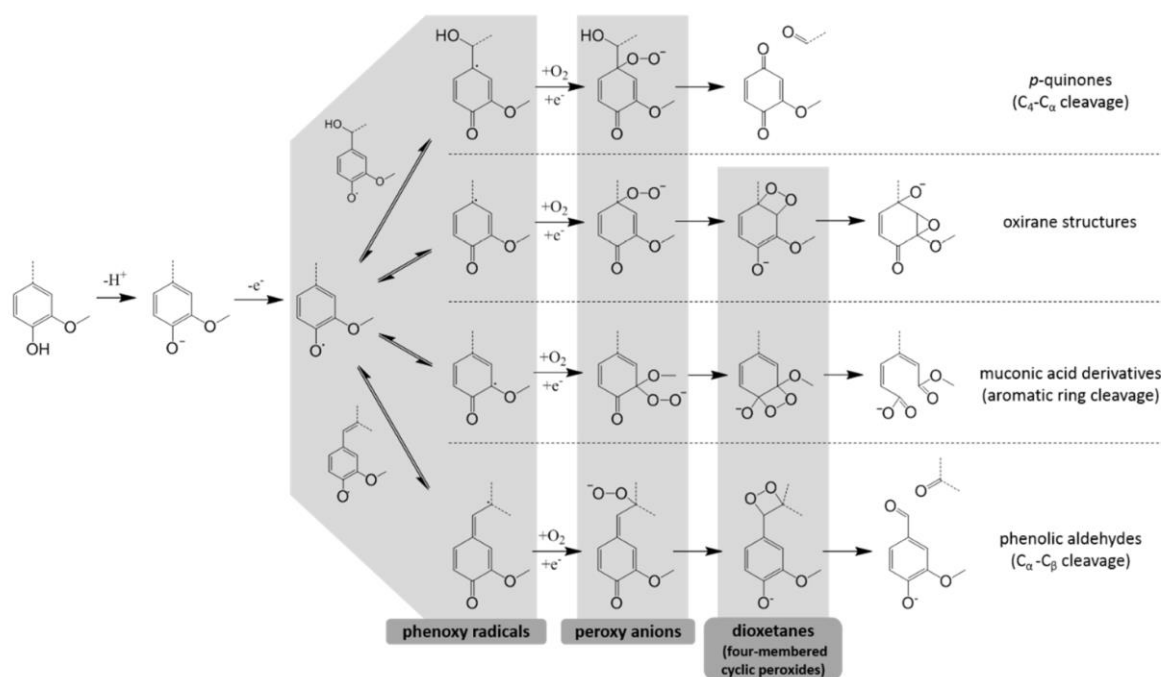


Figure 5: Mechanism of alkaline oxidation of lignin according to Gierer et al.<sup>10,18</sup>

According to the mechanism reported, it should be noted that a possible parallel route can lead to aromatic ring cleavage, yielding carboxylic acids, explaining bio aromatics degradation

to carboxylic acids. Several studies are focused on parameters optimisation for carboxylic acid production (the so called partial wet oxidation)<sup>23,24</sup>.

If bio-aromatics are targeted, particular care should be devoted to reaction condition optimisation, since it was demonstrated that aromatic aldehydes (in particular: vanillin) can be further degraded after their formation, depending on pH, vanillin concentration, temperature and oxygen concentration<sup>25</sup>.

Presumable mechanism of vanillin degradation was deeply investigated by Zhu et al. (Figure 6)<sup>26</sup>

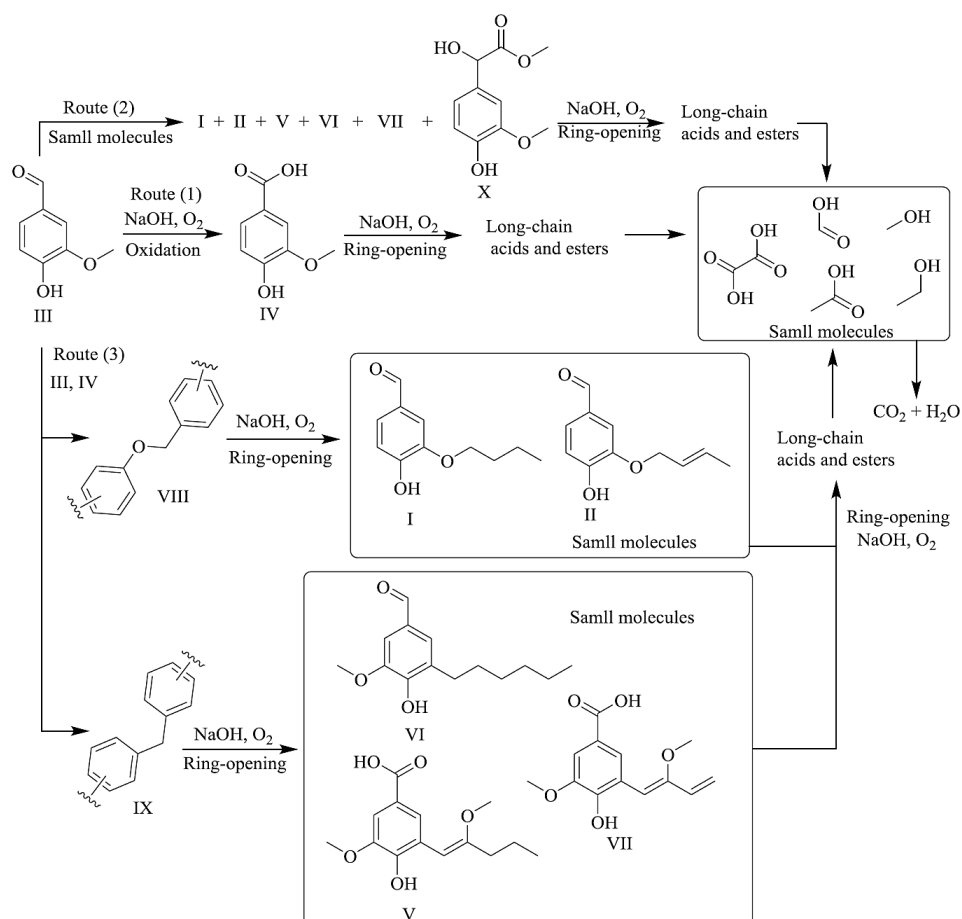


Figure 6: Vanillin degradation mechanism according to Zhu et al.

Adequate tuning of reaction parameters is therefore mandatory also because of the different reactivity of different lignins. Maximum aromatic aldehydes yield from lignin results from a balance of reactions of formation, degradation and competing reactions<sup>27</sup>.

Tarabanko et al. reported an alternative mechanism for alkaline lignin oxidation not involving direct oxygen addition but instead a second oxidation (electron abstraction) of phenoxy radicals with cinnamaldehyde-like intermediate formation and subsequent cleavage of C<sub>α</sub>-C<sub>β</sub> bond through retro aldol reaction (Figure 7).



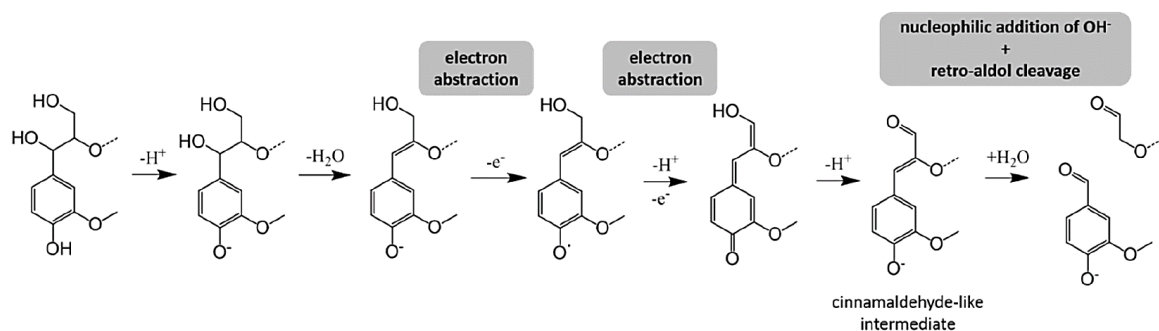


Figure 7: Mechanism of alkaline oxidation of lignin according to Tarabanko et al.

Aiming to improve reaction efficiency and selectivity, several catalysts (inorganic metal-based, organometallics and organocatalysts) were studied, and a complete discussion about catalysed lignin oxidation together with proposed reaction mechanisms was reported by Ma et al.<sup>22</sup>

Nowadays, Borregaard company (Norway) is the only producer in the world that produces wood-based (bio) vanillin through a sustainable process that results in 90%  $CO_2$  emission reduction (information by the company) if compared with vanillin production from petro-based guaiacol process<sup>28</sup>.

## 4.2. RESULTS AND DISCUSSION

### 4.2.1. Sustainable microwave-assisted aerobic oxidation of tomato plant waste into bio-aromatics and organic acids

In this section, an alkaline, oxidative, microwave-assisted, catalyst-free strategy for native lignin valorisation (i.e. lignin in raw biomass) is reported.

Whole raw post-harvest tomato plant biomass was investigated as feedstock for the proposed protocol, aiming to contemporarily valorise lignin and carbohydrates in a one-pot approach without any isolation or fractionation pre-treatment.

Aiming to simplify the system, no catalyst was used, and sustainable oxidising agents (oxygen, air) were employed. Bio-aromatics and carboxylic acids were recovered respectively from lignin and carbohydrates fraction of the raw biomass (Figure 8).

The whole protocol was optimised targeting the maximisation of bio-aromatics recovery.

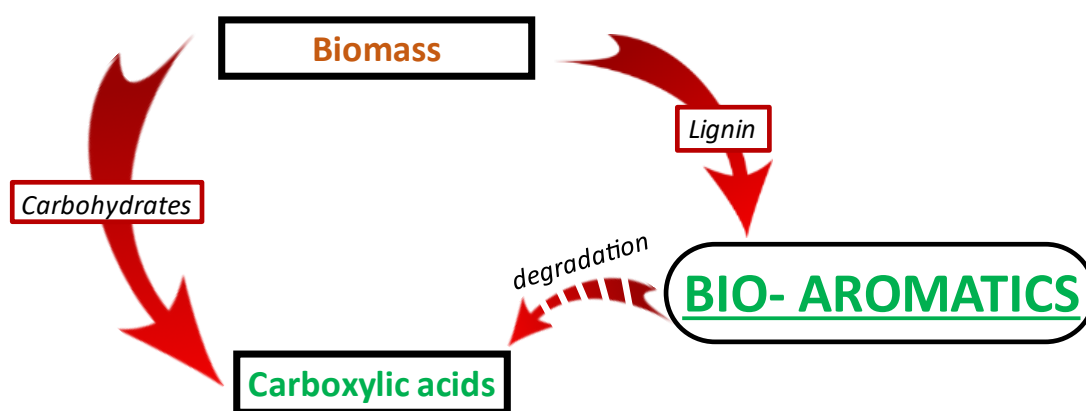


Figure 8: An overview of the proposed protocol for MW-assisted aerobic oxidation of tomato plant waste

#### Post-harvest tomato plants

The biomass used in this study is post-harvest tomato plant (PHTP) waste, which is made up of tomato plants residues recovered at the end of harvesting season. Usually, such biomass is disposed or left in the field without any further valorisation.

PHTP belongs to angiosperms and is classified as hardwood. Its overall chemical composition was investigated by following NREL-derived protocol and is reported in Table 3, section 2.2.1. Being PHTP an angiosperm (hardwood), its lignin content is lower if compared with gymnosperms (softwoods). Moreover, its main monolignols are the S and G units while H unit is present only in traces.

#### PHTP alkaline oxidation towards bio-aromatics and organic acids

Vanillin from G unit and syringaldehyde from S unit are expected to be the main bio-aromatics achieved from the alkaline oxidation of PHTP lignin fraction.

The MW multimode reactor was employed because of its positive effect exerted in reaction control, energy efficiency, reaction time reduction and selectivity improvement. Consequently, according to the complex structure of lignin, characterised by recalcitrant chemical bonds, the use of MW technology is expected to improve the results of the protocol, simplifying the cleavage of C-C and  $\beta$ -O-4 ether bonds<sup>29</sup>. In a detailed study, Ouyang et al.<sup>30</sup>, demonstrated the positive contribution of MW irradiation in wheat straw alkali lignin: labile ether bonds (characterised by low bond energy) are easily cleaved yielding small amounts of

monophenol compounds and higher amounts of lignin oligomeric phenols linked by C-C bonds. Such high bond energy linkages can be easily cleaved thanks to the thermal MW effect (i.e. homogeneous temperature). Moreover, according to the authors, improved stable bonds cleavage can be explained with specific non-thermal (or athermal) effects of MW that can increase pre-exponential factor and decrease activation energy in Arrhenius equation. Despite being highly controversial<sup>31,32</sup>, non-thermal effects combined with undoubted thermal ones can result in a more performative cleavage of C-C bonds if compared with conventional heating, leading to an increased formation of monophenolic products. The authors of the study observed overall yield increase in monophenolics from 0.92% to 13.61% if compared with conventional reactions in identical time, temperature, and catalyst conditions. A decrease in monophenols was observed when excessive time and temperature conditions were applied, due to recondensation phenomena, suggesting the crucial role of parameters optimisation when MW are applied.

PHTP oxidation was conducted in alkaline conditions (NaOH, 2M) using oxygen or air as sustainable oxidising agents without the use of any catalyst (Table 2). As previously mentioned, alkaline environment is reported to favour bio-aromatics production<sup>8</sup>. Reaction conditions were optimised aiming to maximise vanillin yield, as vanillin is the most valuable product that can be achieved from lignin oxidation. Organic acids were recovered as added-value by-products of the one-pot reaction and separated from the bio-aromatics in the downstream processing of the crude reaction by simple pH variation via liquid-liquid extraction. A scheme summarising the protocol (reaction + downstream processing) is reported in Figure 9.

<b>Time (min)</b>	15 / 30	
<b>Temperature (°C)</b>	170 / 180	
<b>Oxidising agent</b>	<i>Oxygen</i> (bar)	15
	<i>Air</i> (bar)	15 / 72

Table 2: Experimental conditions

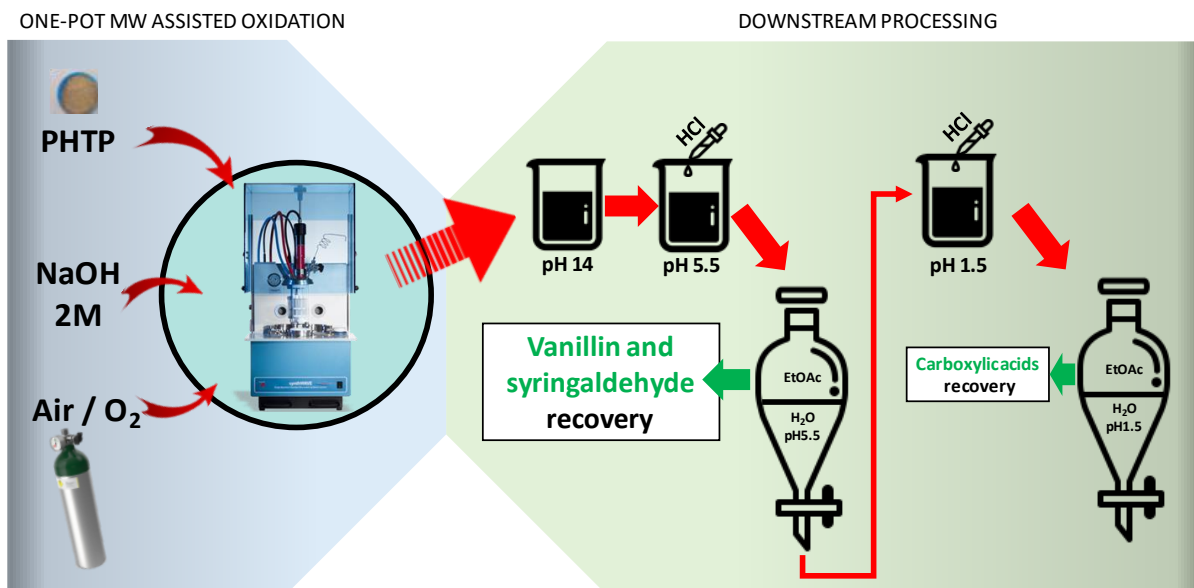


Figure 9: Reaction and workup

At the end of the reaction, the crude was separated from the unconverted biomass and acidified to pH 5.5 to allow the recovery of bio-aromatics through liquid-liquid extraction using ethyl acetate. Further acidification to pH 1.5 and liquid-liquid extraction using ethyl acetate allowed carboxylic acids recovery.

Biomass conversion was monitored and vanillin and syringaldehyde yields were established through GC-FID analysis. Qualitative analysis of bio-aromatic rich fraction and carboxylic acids rich fraction were conducted through GC-MS.

Using oxygen as oxidising agent (15 bar), two temperatures were investigated (170 – 180°C). Conversion, total carboxylic acid yield and vanillin/syringaldehyde yield are reported in Table 3.

Entry	Temperature (°C)	Time (min)	Vanillin (wt % IL)	Syringaldehyde (wt % IL)	Total carboxylic acids (wt % BOC)	Biomass conversion (%)
1	170	15	7.1	11.9	22.1	62.1
2	170	30	8.7	9.6	20.1	72.6
3	180	15	5.8	10.7	35.7	62.2
4	180	30	6.1	6.1	30.7	64.8

Table3: Results of oxidation experiments (oxygen, 170-180°C)

The highest vanillin yield (entry 2) was achieved in correspondence of 170°C and 30 min. As expected, (Figure 10), in bio-aromatics rich fraction vanillin and syringaldehyde were detected as the two main bio-aromatics and some traces of *p*-hydroxybenzaldehyde were also observed. Moreover, some traces of the aceto-derivative of vanillin (acetovanillone) were found while, quite surprisingly, no traces of aceto-derivative of syringaldehyde were observed.

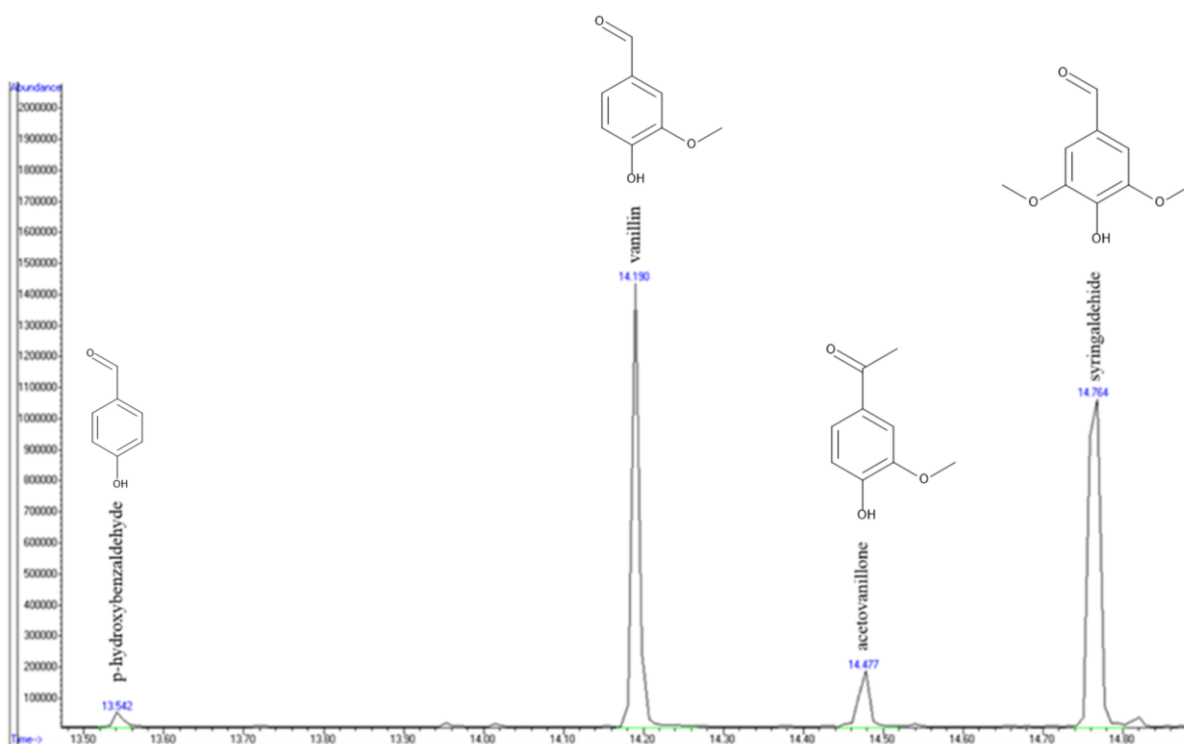


Figure 10: Typical GC-MS of bio-aromatics rich fraction

PHTP was treated in the same conditions of entry 2, without oxygen. Surprisingly, no bio aromatics were recovered, suggesting a crucial role of the oxygen in PHTP treatment for bio aromatics production.

Aiming to further improve sustainability of the process, the same reactions were performed using air as oxidising agent at two different pressures: 15 bar and 72 bar.

The first air pressure value was chosen to be equal to the pressure of previous pure oxygen experiments, while the second one was chosen to provide the same pressure of oxygen of previous pure oxygen experiments, being the partial pressure of oxygen at 72 bar equal to 15 bar.

Entry	Pressure (bar)	Temperature (°C)	Time (min)	Vanillin (wt % IL)	Syringaldehyde (wt % IL)	Total carboxylic acids (wt % BOC)	Biomass conversion (%)
1'	15	170	15	4.7	15.7	29.9	66.9
2'		170	30	6.7	15.1	36.3	52.1
3'		180	15	5.6	13.1	31.3	69.4
4'		180	30	5.9	6.4	38.4	66.4
1''	72	170	15	6.9	9.8	31.3	66.9
2''		170	30	8.2	9.0	18.1	53.3
3''		180	15	4.8	1.5	15.8	66.7
4''		180	30	6.2	6.2	31.4	64.6

Table 4: Results of oxidation experiments (air 15-72 bar, 170-180°C)

Vanillin yields with 72 bar of air were very similar to those achieved using pure oxygen (Table 3 entry 2 and Table 4 entry 2''), despite conversions were lower. Therefore, the sustainability of the process can be improved by using air instead of oxygen.

When lower air pressure was applied, vanillin yield decreased sensibly, while syringaldehyde yield increased. Such results demonstrate that tuning of experimental conditions is crucial: indeed, reaction parameters can be modified targeting different platform chemicals (vanillin, syringaldehyde or carboxylic acids)

Carboxylic acids rich fractions presented several different acids namely lactic acid, acetic acid, 2-hydroxybutanoic acid, levulinic acid, 2-hydroxypentanoic acid, succinic acid, maleic acid, malic acid and 2-hydroxypentanedioic acid (Figure 11).

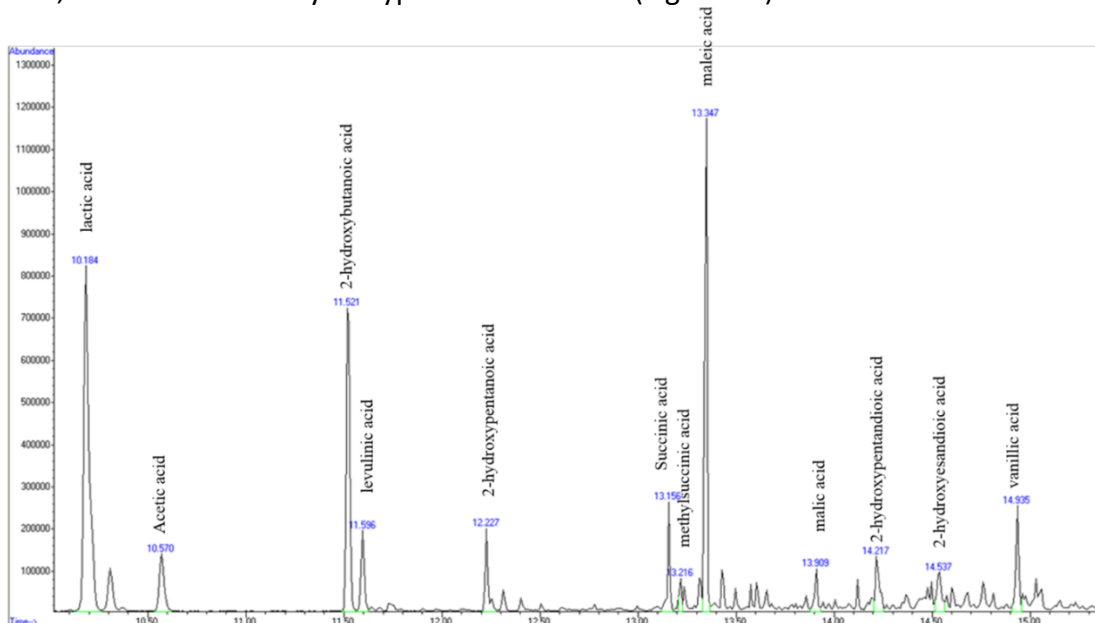


Figure 11: Typical GC-MS of carboxylic acid rich fraction

Such carboxylic acids are reported to derive from alkaline degradation of glucose, cellobiose, cellulose and hemicellulose; carbohydrates degradation in alkaline conditions were extensively reviewed by Knill and Kennedy<sup>33</sup>. Moreover, carboxylic acids can also derive from lignin, through parallel pathways involving aromatic ring-opening of phenolic monomers as hypothesized by Gierer et al.<sup>18</sup> and through degradation reactions of bio-aromatics as described by Zhu et al.<sup>26</sup>.

NREL protocol was performed on residual, unconverted PHTP (RPHTP) recovered after the oxidation. Both RPHTP from oxygen and air (72 bar) oxidation were investigated.

As reported in Table 5, both lignin and carbohydrate fractions were depauperated during the reaction, thus confirming their conversion into phenols and carboxylic acids (conversion are expressed as conversion % of the quantity of each single component contained in initial PHTP). Among carboxylic acids, also vanillic acid was detected, probably derived from partial further oxidation of vanillin<sup>26</sup>.

<b>Components</b>	<b>170°C, 30min, 15bar O<sub>2</sub></b>		<b>170°C, 30min, 72bar Air</b>	
	RPHTP composition (W%)	Conversion (%)	RPHTP composition (W%)	Conversion (%)
<b>Organic feed</b>	26.7	90.6	27.0	83.8
<b>Cellulose</b>	4.7	96.7	11.6	86.1
<b>Hemicellulose</b>	12.0	84.3	3.3	92.7
<b>Lignin</b>	8.1	85.1	12.0	62.7
<b>Protein, lipids</b>	1.5	86.2	0.1	98.4

Table 5: Composition of PHTP residues recovered after the oxidation experiments

Organic feed in oxygen reaction showed higher conversion if compared with air reaction. Also, lignin and cellulose conversions were slightly higher in case of oxygen reaction, while hemicellulose conversion was higher in case of air reaction. Despite that, as already mentioned, vanillin, syringaldehyde and carboxylic acids recovery in optimised conditions both for air and oxygen yielded similar results (Table 3 entry 2 and Table 4 entry 2'').

#### 4.2.2. Sustainable microwave-assisted aerobic oxidation of lignins from grape stalks into bioaromatics and long chain fatty acids

In this section, grape stalks (GS) were investigated for lignin extraction through combination of natural deep eutectic solvents (NaDES) and non-conventional technologies (US and MW). Recovered lignins were subsequently valorised through the above discussed alkaline, oxidative, MW-assisted, catalyst free reaction yielding bio-aromatics and long chain fatty acids.

##### GS characterisation

Raw GS lignin content was chemically characterised by following two different NREL-derived protocols. Results are compared and summarised in Table 6:

Composition	NREL-derived protocol 1 (%wt.)	NREL-derived protocols2 (%wt.)
Lignin	27.81 ± 1.57	32.92 ± 0.58

Table 6: Lignin content of raw GS

Both NREL-derived protocols led to coherent results in lignin quantification: non-negligible amounts of lignin were detected, making GS a promising substrate for lignin isolation and subsequent valorisation.

The percentage of lignin contained in GS was assumed to be an average of the results achieved in the two protocols, equal to 30.37%.

At the end of both protocols, lignin samples were recovered and stored for further valorisation experiments.

##### GS delignification and lignin recovery

Coherently with the “lignin first” approach, pre-treatment for lignin recovery from GS was performed exploiting non-conventional technologies such as multimode MW reactor and ultrasound.

Aiming to enhance sustainability of the whole process, non-conventional technologies were combined with two different NaDES<sup>34</sup>:

1. a bicomponent NaDES or “NaDES 1” (ChLA, choline chloride + lactic acid (1:10 mol))
2. a tricomponent NaDES or “NaDES 2” (ChLaGly, choline chloride + lactic acid + glycerol, (1:1:1) mol).
3. For sake of comparison alkaline extractions involving NaOH were investigated in the same conditions. Indeed, as reported by many authors,<sup>35,36</sup> alkaline extractions can lead to high delignification degree in several biomasses.

NaDESs are innovative solvents derived from the mixture of natural compound. Such compounds, when mixed in specific molar ratios, led to the formation of a solvent characterised by melting points lower than the melting points of their components and below room temperature<sup>37</sup>. The synthesis of these compounds is carried out by combining hydrogen bonding donors (HBDs), such as glycerol or lactic acid, and hydrogen bonding acceptors (HBAs), especially quaternary ammonium salts such as choline chloride.

Being composed of natural compounds, NaDES fully meets the principles of green chemistry, being sustainable, readily available, economic, easy to be prepared, with low toxicity<sup>38,39</sup>.



At the end of every extraction, the liquid fraction rich in solubilised lignin was separated from the remaining GS. Subsequently, the lignin solubilised in the liquid fraction was precipitated by adding water in case of NaDES1 and NaDES2 or by adding HCl in case of NaOH.

Entry	Solvent	Technology	Time (min)	Temperature (°C)	Delignification (%wt.)
1	NaOH (10%)	MAE	60	50	28.81 ± 1.40
2	NaOH (10%)	MAE	30	120	46.06 ± 6.48
3	NaDES1	MAE	30	120	79.44 ± 5.88
4	NaDES2	MAE	30	120	76.40 ± 1.47
5	NaOH (10%)	UAE	60	50	34.48 ± 6.05
6	NaDES1	UAE	120	50	51.32 ± 6.35
7	NaDES2	UAE	120	50	65.40 ± 0.00

Table 7: Delignification degree

In Table 7 delignification degree of MW-assisted and US-assisted lignin extractions are reported:

- By comparing entry 2,3 and 4 it is clear that a significant improvement in delignification was achieved by using NaDES with respect to NaOH. Higher temperature was applied in order to decrease NaDES' viscosity and improve mass transfer.
- By comparing entry 1 and 2 the effect of a temperature increase is clearly evident for alkaline extraction, leading to higher delignification in shorter times. In 120°C experiment, time was reduced from 60 to 30 minutes aiming to avoid excessive exposition of GS to high temperatures that could led to partial degradation of the extracted lignin. These results indicate that temperature is a crucial parameter when performing microwave-assisted delignification with NaOH.
- When NaDES1 and NaDES2 were coupled with US, despite high delignification degrees were achieved, no lignins were recovered in the subsequent precipitation step.

From lignin extraction 5 lignins were therefore recovered, while 2 other lignins were recovered at the end on the two NREL-derived protocols (Table 8). Each lignin was ball-milled aiming to achieve a more reactive and uniform sample. FT-IR analyses were performed (Figure 12).

Lignin	Conditions
Lignin 1	NREL 1
Lignin 2	NREL 2
Lignin 3	NaOH (10 %) 50°C, 60 min, UAE
Lignin 4.1.	NaOH (10 %) 50°C, 60 min, MAE
Lignin 4.2.	NaOH (10 %) 120°C, 30 min, MAE
Lignin 5	NaDES 1, 120°C, 30 min, MAE
Lignin 6	NaDES 2, 120°C, 30 min, MAE

Table 8: List of recovered lignins

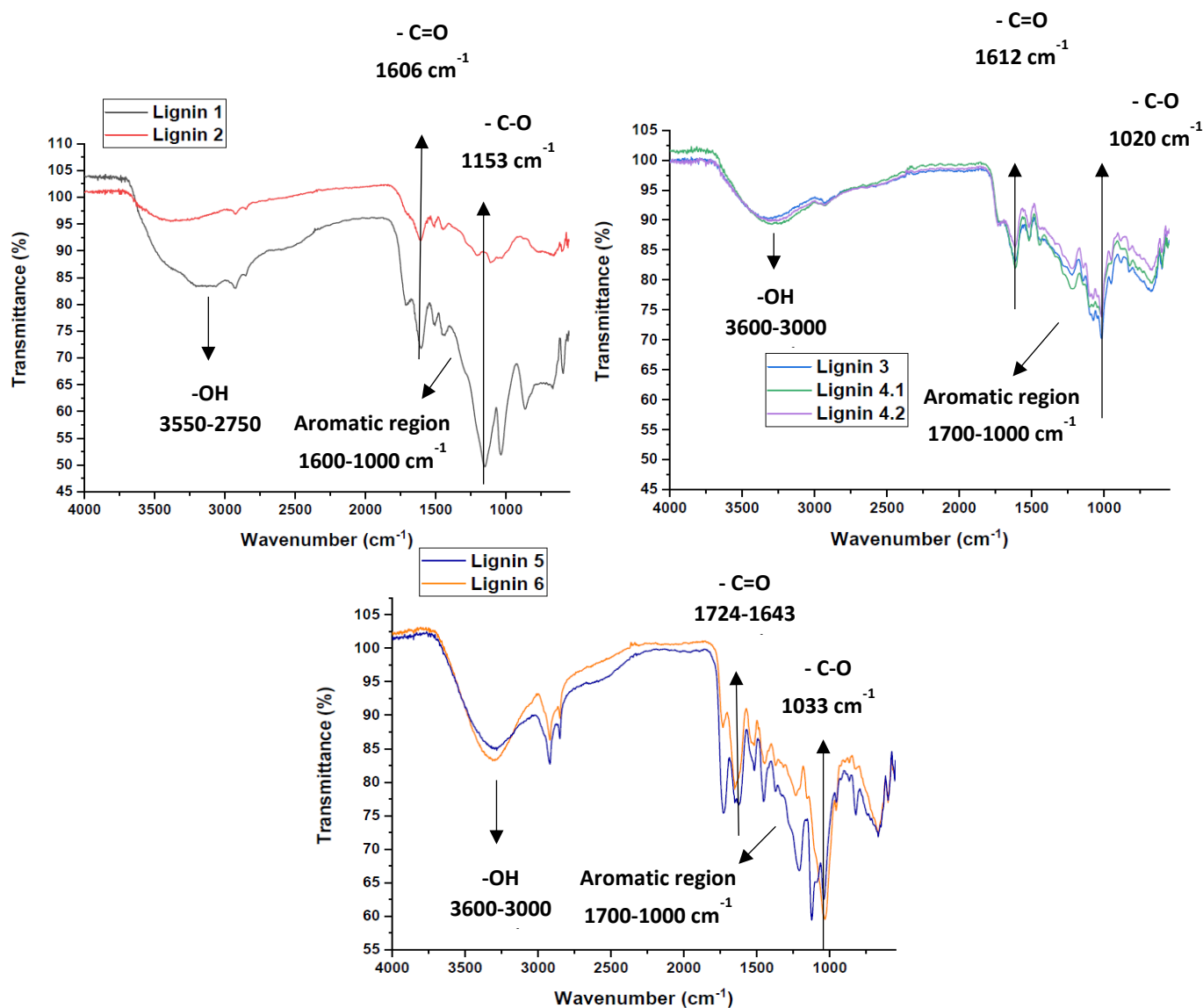


Figure 12: FTIR spectra of lignins

The analysis of the spectra allowed some considerations on structural modifications of lignins after the extractions under different conditions:

- Lignins from NaOH treatment presented a weak cross-linked structure, as it is possible to observe by the aromatic region in Lignin 3, Lignin 4.1. and Lignin 4.2., where the bands related to C=C vibration of the aromatics ( $1700-1000\text{ cm}^{-1}$ )<sup>40-42</sup> are less intense compared to both NREL and NaDES lignins. This behaviour can be explained by considering the possible structural modifications exerted in native lignin by alkaline conditions<sup>11</sup>. Furthermore, the amount of ether linkages seems to be lower if compared with other lignins, indeed the carbonyl and C-O bands present lower intensity if compared with the other kind of lignins.
- NaDES allowed recovery of less modified lignin, with a high cross-linked structure, as confirmed by both aromatic region and C=O and C-O sharp bands ( $1724-1643$  and  $1033\text{ cm}^{-1}$ , respectively). It can be concluded that NaDES can interact with free phenolic groups through hydrogen bond interactions, leading to a milder delignification with less structural modifications respect to NaOH.
- NREL lignins presented high cross-linked structure, probably due to the harsh acidic conditions that led to more condensed fragments.

#### Raw GS and lignin oxidation

MW-assisted catalyst free oxidation was conducted on raw GS and on lignin 4.2 (derived from NaOH MAE), lignin 5 (derived from NaDES1 MAE) and 6 (derived from NaDES2 MAE). Reaction conditions were derived from previous section for PHTP oxidation:  $170^{\circ}\text{C}$ , 30 min, 15 bar of oxidizing agent (air or  $\text{O}_2$ ) and NaOH 2M.

Results are summarised in Table 9 (expressed as area % of total).

MOLECULE	Area % of total							
	GS1 oxygen	GS1 air	4.2.1 oxygen	4.2.2 air	5.1 oxygen	5.2 air	6.1 oxygen	6.2 air
<b>BIOAROMATICS</b>	<b>67.1</b>	<b>58.0</b>	11.0	16.9	<b>34.2</b>	<b>37.4</b>	8.5	12.0
<b>LCFA</b>	15.4	23.9	3.8	4.3	<b>46.6</b>	<b>43.8</b>	<b>31.0</b>	<b>52.0</b>
<b>LCH/LCA</b>	13.0	16.0	<b>77.0</b>	<b>78.8</b>	14.5	18.8	<b>46.2</b>	<b>31.1</b>
<b>CARBOXYLIC ACIDS</b>	4.5	2.0	8.3	---	4.6	---	14.3	4.9

Table 9: Main product classes detected in oxidation experiments

According to the lignin type, different behaviours were observed:

- When raw GS were used, coherently with what previously observed for PHTP, the main products observed were bioaromatics. Conversely, the recovery of carboxylic acids was very low. In addition, minor quantities of long chain fatty acids (LCFA) and alkenes were detected.
- When lignin isolated through NaDES1 MAE was used, the main detected products were LCFA together with significant amounts of bioaromatics.
- When lignin isolated through NaDES2 MAE was used the main detected products were LCFA and long chain hydrocarbons (LCH): when oxygen was involved, alkenes were the most abundant products while when air was used LCFA were predominant.

- When lignin isolated from NaOH MAE was used, the main detected products were LCH with minor quantities of LCFA and/or bioaromatics.

Long chain di acids formation was previously observed by Zhang et al.<sup>43</sup> during lignin and lignin-derived model compounds three-phase-three-dimensional electro-Fenton oxidation reaction.

Hexadecanoic and octadecanoic acid were the main LCFA detected by the authors, but the results varied widely according to the lignin type. Same similar behaviour was observed in oxidation reactions herein described (see Table 9). A possible explanation to LCFA formation was provided by Zhu et al.<sup>26</sup> (Figure 6, route 3) describing monophenols degradation phenomena in alkaline oxidation. Indeed, according to the authors, monophenols can condense into dimers and subsequently decompose into complex phenols that undergo ring-opening reactions forming long chain acids. Similar mechanism was proposed by Zhang et al.: as reported in Figure 13 at the beginning of the process, lignin is degraded into small fragments that are immediately converted into dicarboxylic acids through ring-opening reactions. Finally dicarboxylic acids are converted to LCFA through Kolbe synthesis.

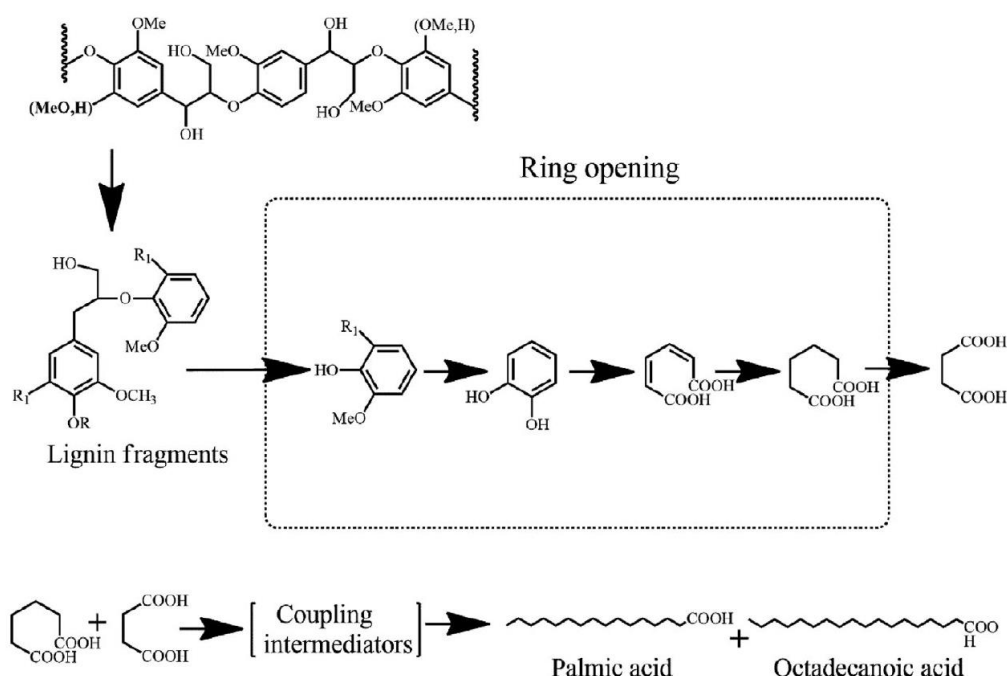


Figure 13: LCFA formation according to Zhang et al.<sup>40</sup>

LCFA have been investigated as bio-diesel precursors thanks to the high energy density possessed by this class of molecules. Several studies focused on their use as fuel both at unprocessed state (characterised by several advantages such as renewability, high heat content, lower sulfur content, lower aromatic content, and biodegradability) or at processed state (in a form more compatible with actual combustion engines).

The possibility to derive biodiesel precursors from non-edible feedstocks could allow to overcome ethical issues deriving from the use of food-crops such as seeds<sup>44</sup>.

Despite being previously reported, formation of LCH remains unclear: Bentivenga et al.<sup>45</sup> reported LCH formation (octadecene, octadecane, eicosanol) during singlet-oxygen-mediated degradation of steam-exploded lignin.

The complete list of the products achieved during the oxidation experiments is reported in Table 10. Abundance of each compound is expressed as area % of total.

molecule	feedstock							
	Area % of total							
	GS1 oxygen	GS2 air	lignin 4.2.1 oxygen	lignin 4.2.2 air	lignin 5.1 oxygen	lignin 5.2 air	lignin 6.1 oxygen	lignin 6.2 air
2-hydroxypropanoic acid	1.6	2.0	0.0	0.0	4.6	0.0	6.2	4.9
2-hydroxy-butanoic acid	0.8	0.0	0.0	0.0	0.0	0.0	0.0	0.0
4-oxo-pentanoic acid	0.8	0.0	8.3	0.0	0.0	0.0	8.1	0.0
2-hydroxy-butanoic acid	0.8	0.0	0.0	0.0	0.0	0.0	0.0	0.0
butanedioic acid	0.5	0.0	0.0	0.0	0.0	0.0	0.0	0.0
benzoic acid	0.4	0.0	0.0	0.0	0.0	0.0	5.0	0.0
4-hydroxy-benzaldehyde (p-hydroxybenzaldehyde)	0.8	0.0	0.0	0.0	0.0	0.0	0.0	0.0
2,6-dimethoxyphenol	0.4	0.0	0.0	0.0	0.0	0.0	0.0	0.0
4'-hydroxy-acetophenone	0.3	0.0	0.0	0.0	0.0	0.0	0.0	0.0
4-hydroxy-3-methoxy-benzaldehyde (vanillin)	15.1	6.5	0.0	0.0	11.3	2.7	0.0	0.0
3-hydroxy-benzoic acid or 4-hydroxy-benzoic acid	1.0	0.8	0.0	0.0	0.0	0.0	0.0	0.0
cetene	2.5	1.8	11.0	13.2	0.0	3.0	0.0	4.3
2,4-hydroxy-benzaldehyde	1.1	1.4	0.0	0.0	0.0	0.0	0.0	0.0
4'-hydroxy-3'-methoxy-acetophenone (acetophenone)	7.4	6.9	0.0	0.0	4.7	2.9	0.0	0.0
3,5-dimethoxy-4-hydroxy-benzaldehyde (syringaldehyde)	16.2	10.5	0.0	0.0	7.4	0.0	0.0	0.0
1-(4-hydroxy-3,5-dimethoxyphenyl)-ethanone (acetosyringone)	0.0	0.0	0.0	3.7	0.0	0.0	0.0	0.0
3-hydroxy-4-methoxy-benzoic acid (vanillic acid)	8.8	9.1	0.0	0.0	5.6	0.0	0.0	0.0
3,5-hydroxy-benzoic acid	0.0	1.1	0.0	0.0	0.0	0.0	0.0	0.0
3-vanilpropanol	1.4	1.4	0.0	0.0	0.0	0.0	0.0	0.0
3,5-dimethoxy-4-hydroxybenoic acid (syringic acid)	2.6	4.6	0.0	0.0	0.0	0.0	0.0	0.0
p-(hydroxy)-cinnamic acid	6.2	9.1	0.0	0.0	0.0	0.0	0.0	0.0
p-hydroxyphenyl hydroxy acrylate	0.0	0.0	0.0	0.0	0.0	4.6	0.0	4.1
4-hydroxy-3-methoxy-cinnamic acid	2.9	4.7	0.0	0.0	0.0	0.0	0.0	0.0
3-hydroxy-3-(4'-hydroxy-3'methoxyphenil)propionic acid	0.0	0.0	0.0	0.0	5.2	11.0	0.0	3.5
p-hydroxyphenyl hydroxy acrylate	0.0	0.0	0.0	0.0	0.0	13.3	3.5	0.0
tetradecene	0.4	0.0	0.0	0.0	0.0	0.0	0.0	0.0
1-Octadecene	4.4	5.3	24.9	25.0	7.2	7.8	12.9	13.0
(E)-5-eicosene	2.6	3.5	20.5	23.5	3.9	5.0	7.4	7.7
1-docosene	1.9	2.7	14.5	17.6	3.4	3.5	6.3	6.3
1-nonadecene	1.4	1.8	11.4	8.0	0.0	2.6	3.9	4.1
9-hexacosene	2.2	2.8	5.6	0.0	0.0	0.0	15.6	0.0
Z-12-pentacosene	0.0	0.0	0.0	4.7	0.0	0.0	0.0	0.0
decanoic acid	0.5	0.5	0.0	0.0	0.0	0.0	0.0	0.0
octanoic acid	1.5	2.4	0.0	0.0	0.0	0.0	0.0	0.0
hexadecanoic acid	2.7	3.3	3.8	4.3	13.2	19.9	12.8	16.9
9,12-octadecadienoic acid	0.3	3.7	0.0	0.0	9.2	0.0	6.7	9.7
octadecanoic	1.4	1.2	0.0	0.0	4.2	5.7	4.0	5.2
alpha-linolenic acid	1.7	2.2	0.0	0.0	7.4	6.4	0.0	0.0
octadecadienoic acid	0.7	0.7	0.0	0.0	2.9	3.7	0.0	0.0
hexadecandioic acid	6.1	9.9	0.0	0.0	9.6	8.1	0.0	13.8
docosanoic acid	0.0	0.0	0.0	0.0	0.0	0.0	7.5	6.4
octadecanedioic acid	0.4	0.0	0.0	0.0	0.0	0.0	0.0	0.0

Table 10: Detailed list of products detected in oxidation experiments

Considering the high amounts of bioaromatics achieved in GS1 oxidation, vanillin and syringaldehyde yields were quantified via q-NMR analyses, that reported a 7.68 wt% vanillin yield and a 7.70 wt% syringaldehyde yield

Presence of LCFA was also confirmed by NMR analysis (Figure 14).

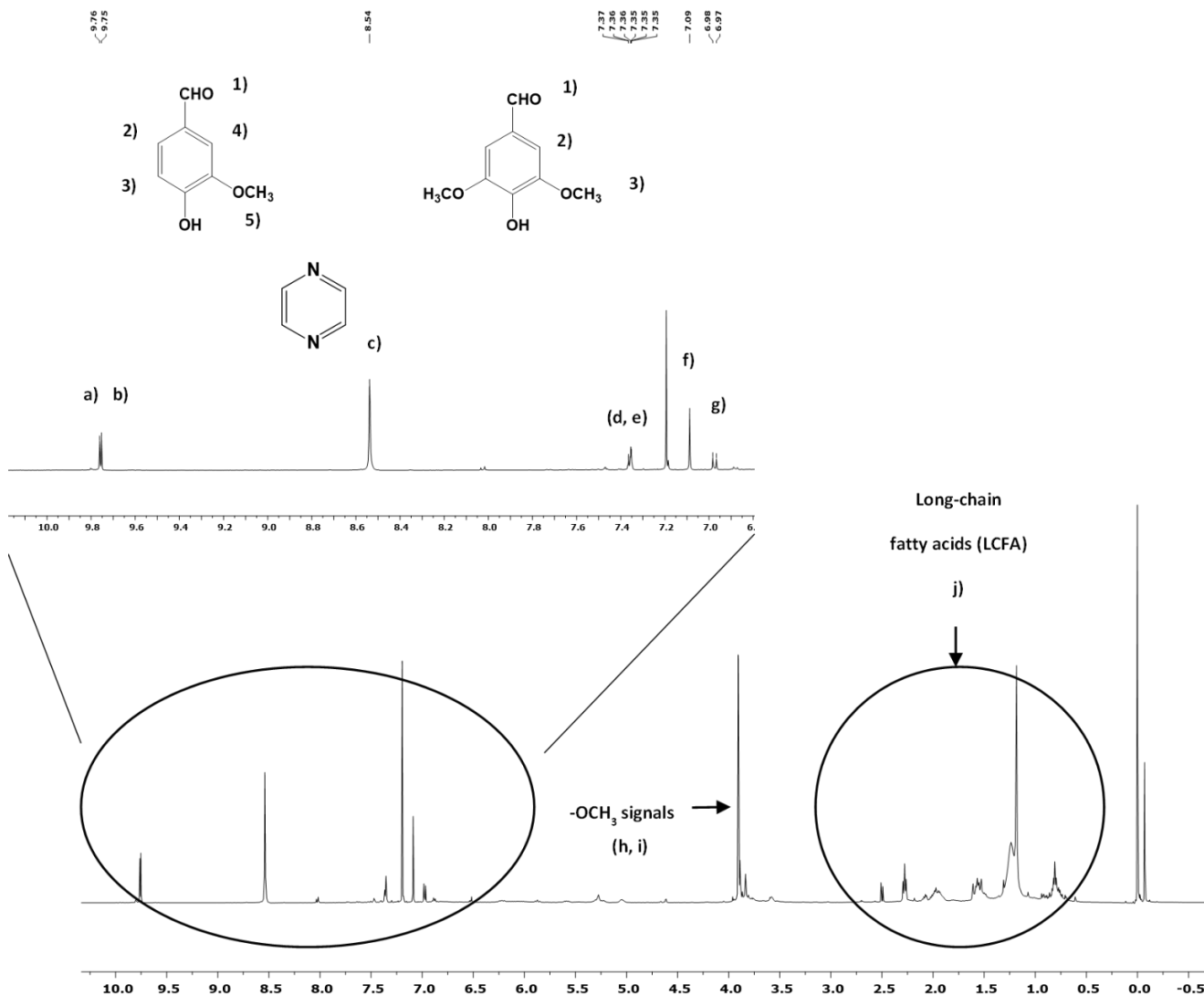


Figure 14:  $^1\text{H-NMR}$  of GS1

### 4.3. CONCLUSIONS

An efficient protocol for catalyst free, microwave assisted oxidation of raw biomass and lignin was settled-up in the present chapter. In the first part of the work raw post-harvest tomato plant was used as feedstock, yielding bioaromatics (vanillin and syringaldehyde) and carboxylic acids with good conversion degree. Sustainability of the protocol was improved by using air as oxidising agent. According to the results, reaction conditions can be tuned and optimised targeting different products (vanillin, syringaldehyde or carboxylic acids) by the conversion of all biomass' components. In the second part of the work, different lignins were extracted from grape stalks using a non-conventional approach involving two different NaDES coupled with microwave irradiation and compared with lignin from the same feedstock using alkaline microwave-assisted extraction. NaDES led to higher delignification degrees (around 80%) compared to NaOH, probably owing to their ionic structure, that strongly interact with microwaves through ionic conduction, prompting the breaking of intramolecular hydrogen bonds.

Recovered lignins and raw grape stalks were oxidated using the previously defined protocol for alkaline, microwave assisted oxidation. According to the feedstock involved (raw grape stalks, NaDES-extracted lignin or NaOH-extracted lignin) different main reaction products were identified such as long chain fatty acid and long chain hydrocarbons (considered biofuels precursors and valuable platform chemicals) in case of extracted lignins, and bioaromatics in case of raw grape stalks.

## 4.4. EXPERIMENTAL

### Reagents

All reagents and solvents, unless otherwise specified, were purchased from Sigma-Aldrich and used without further purification.

### PHTP and GS analyses

PHTP chemical characterisation was performed according to previously reported protocol (see chapter 2 paragraph 2.4)

The chemical characterization of GS was carried out by following two analytical and standard procedures: the first protocol (NREL1) was performed as reported by Sluiter et al. and Álvarez et. al. while the second protocol (NREL2) was the same performed on PHTP (see chapter 2 paragraph 2.4)

### PHTP, GS and lignin ball-milling pre-treatment

PHTP, GS or lignin were ball milled in a planetary ball mill (PM100, Restch, GmbH).

5g raw PHTP was poured into a stainless-steel single ball milling beaker (125mL volume) and 25 stainless steel milling balls (10mm diameter) were added.

PHTP was milled in such system for 60 minutes, at 550 rpm. Every 10 minutes rotation direction was inverted.

### Microwave assisted catalyst-free oxidation

According to the type of starting material different quantities were involved:

200mg in case of PHTP

100mg in case of extracted lignin

350mg in case of GS

The starting material was laced in a 40mL round bottomed vial and 20mL NaOH 2N were added to the biomass/lignin. The system was placed in a high-pressure MW reactor (SynthWave, Milestone Srl, MLS GmbH, Bergamo Italy) and appropriate pressure of oxygen or air was added. Reaction was conducted under stirring (max.). At the end of the reaction MW reactor was chilled to room temperature.

Crude reaction was filtered under vacuum on paper filter in order to separate unconverted biomass/lignin from the liquid fraction. Filter was washed with 30mL distilled water.

Unconverted biomass/lignin was recovered and dried in 40°C oven and subsequently weighted to establish conversion.

Liquid fraction recovered after the filtration was acidified with HCl 2N until pH 5.5 was reached. Liquid-liquid extraction was performed in separating funnel using 30mL ethyl acetate aiming to recover bio-aromatics from the crude. Liquid-liquid extraction was performed 3 times. Ethyl acetate fraction was collected in 100mL balloon and evaporated in rotatory evaporator under vacuum and stored for GC-MS and GC-FID analysis.

The remaining aqueous phase was then acidified to reach pH 1.5 using HCl 2N and subsequently extracted using ethyl acetate. Liquid-liquid extraction was performed 3 times. Ethyl acetate fraction was collected in 100mL balloon and evaporated in rotatory evaporator under vacuum and stored for GC-MS and GC-FID analysis.

All GC-MS analyses were performed after derivatisation of the sample: 2mg of sample were solubilized in 1 mL of chloroform. Then, 100  $\mu$ L of BSTFA (N,O-bis(trimethylsilyl)trifluoroacetamide) were added to the solution. The mixture was heated for 45 min at 60 °C under magnetic stirring.



### GS delignification

MAE was performed in a high-pressure professional multimode MW reactor, SynthWave (Milestone Srl). NaOH experiments took place at 50°C for 60 min or 120°C for 30 min.

5 g of GS were placed in five 40 ml microwave glass vials. NaOH solution (400 mg of NaOH in 80 mL of deionized H<sub>2</sub>O) was prepared and added to the vials, keeping the solid:liquid ratio equals to 1:20. After the extraction, the crude was separated by centrifugation (Rotofix 32, Hettich Zentrifugen, Tuttlingen, Germany) (4000 rpm, 30 min), washing the solid two times with NaOH solution and subsequently with deionized H<sub>2</sub>O.

Solid fraction was dried in a oven at 40 °C and weighted to evaluate the delignification.

Liquid fraction was recovered and pertinent volume of HCl 2M was added to immediately promote the precipitation of lignin at pH =1-2. This last mixture was filtered under vacuum, washing the recovered lignin with deionized H<sub>2</sub>O until neutrality.

NaDES experiments took place at 120°C for 30 min: 2.5 g of GS were placed in five 40 ml microwave glass reactor (20 ml maximum volume). Suitable volume of NaDESs was added, keeping solid:liquid ratio in 1:50.

The crude was separated by centrifugation (4000 rpm, 45 min), washing the solid with a NaDES solution.

Solid fraction (was washed with a high volume of deionized H<sub>2</sub>O to remove the NaDES. After that, it was freeze-dried and weighted to know the delignification yield.

Considering the liquid phase recovered after centrifugation, approximately 2L of deionized H<sub>2</sub>O were added to this fraction as the antisolvent, thus promoting the lignin precipitation after 12-16h at 4°C. After that, the mixture was filtered under vacuum. The recovered lignins were ball-milled for a further oxidation.

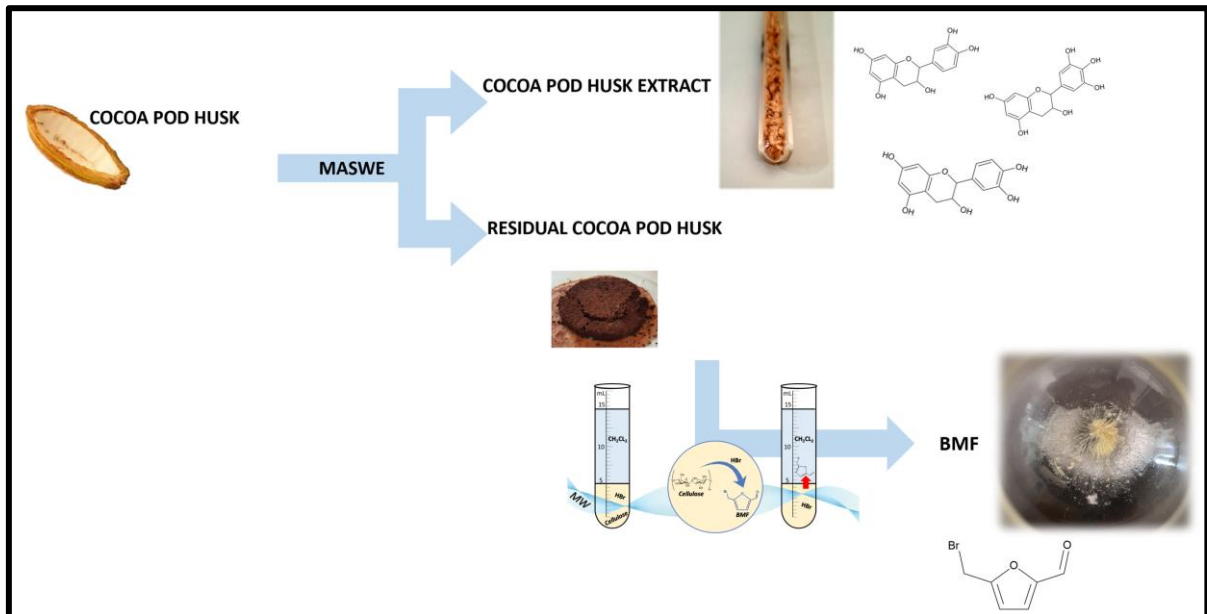
## 4.5. REFERENCES

- (1) Gillet, S.; Aguedo, M.; Petitjean, L.; Morais, A. R. C.; da Costa Lopes, A. M.; Łukasik, R. M.; Anastas, P. T. Lignin Transformations for High Value Applications: Towards Targeted Modifications Using Green Chemistry. *Green Chem.* **2017**, *19* (18), 4200–4233. <https://doi.org/10.1039/C7GC01479A>.
- (2) Liu, C.; Wu, S.; Zhang, H.; Xiao, R. Catalytic Oxidation of Lignin to Valuable Biomass-Based Platform Chemicals: A Review. *Fuel Process. Technol.* **2019**, *191*, 181–201. <https://doi.org/10.1016/j.fuproc.2019.04.007>.
- (3) Zakzeski, J.; Bruijninx, P. C. A.; Jongerius, A. L.; Weckhuysen, B. M. The Catalytic Valorization of Lignin for the Production of Renewable Chemicals. *Chem. Rev.* **2010**, *110* (6), 3552–3599. <https://doi.org/10.1021/cr900354u>.
- (4) Li, C.; Zhao, X.; Wang, A.; Huber, G. W.; Zhang, T. Catalytic Transformation of Lignin for the Production of Chemicals and Fuels. *Chem. Rev.* **2015**, *115* (21), 11559–11624. <https://doi.org/10.1021/acs.chemrev.5b00155>.
- (5) Ragauskas, A. J.; Beckham, G. T.; Bidy, M. J.; Chandra, R.; Chen, F.; Davis, M. F.; Davison, B. H.; Dixon, R. A.; Gilna, P.; Keller, M.; Langan, P.; Naskar, A. K.; Saddler, J. N.; Tschaplinski, T. J.; Tuskan, G. A.; Wyman, C. E. Lignin Valorization: Improving Lignin Processing in the Biorefinery. *Science* **2014**, *344* (6185), 1246843–1246843. <https://doi.org/10.1126/science.1246843>.
- (6) Costa, C. A. E.; Vega-Aguilar, C. A.; Rodrigues, A. E. Added-Value Chemicals from Lignin Oxidation. *Molecules* **2021**, *26* (15), 4602. <https://doi.org/10.3390/molecules26154602>.
- (7) Yuan, T.-Q.; Xu, F.; Sun, R.-C. Role of Lignin in a Biorefinery: Separation Characterization and Valorization: Separation, Characterization, and Valorization of Lignin for Biorefinery. *J. Chem. Technol. Biotechnol.* **2013**, *88* (3), 346–352. <https://doi.org/10.1002/jctb.3996>.
- (8) Vangeel, T.; Schutyser, W.; Renders, T.; Sels, B. F. Perspective on Lignin Oxidation: Advances, Challenges, and Future Directions. *Top. Curr. Chem.* **2018**, *376* (4), 30. <https://doi.org/10.1007/s41061-018-0207-2>.
- (9) Xu, C. C.; Dessbesell, L.; Zhang, Y.; Yuan, Z. Lignin Valorization beyond Energy Use: Has Lignin's Time Finally Come? *Biofuels Bioprod. Biorefining* **2021**, *15* (1), 32–36. <https://doi.org/10.1002/bbb.2172>.
- (10) Schutyser, W.; Renders, T.; Van den Bosch, S.; Koelewijn, S.-F.; Beckham, G. T.; Sels, B. F. Chemicals from Lignin: An Interplay of Lignocellulose Fractionation, Depolymerisation, and Upgrading. *Chem. Soc. Rev.* **2018**, *47* (3), 852–908. <https://doi.org/10.1039/C7CS00566K>.
- (11) Sun, Z.; Fridrich, B.; de Santi, A.; Elangovan, S.; Barta, K. Bright Side of Lignin Depolymerization: Toward New Platform Chemicals. *Chem. Rev.* **2018**, *118* (2), 614–678. <https://doi.org/10.1021/acs.chemrev.7b00588>.
- (12) Holladay, J. E.; White, J. F.; Bozell, J. J.; Johnson, D. *Top Value-Added Chemicals from Biomass - Volume II—Results of Screening for Potential Candidates from Biorefinery Lignin*; PNNL-16983, 921839; 2007; p PNNL-16983, 921839. <https://doi.org/10.2172/921839>.
- (13) Varanasi, P.; Singh, P.; Auer, M.; Adams, P. D.; Simmons, B. A.; Singh, S. Survey of Renewable Chemicals Produced from Lignocellulosic Biomass during Ionic Liquid Pretreatment. *Biotechnol. Biofuels* **2013**, *6* (1), 14. <https://doi.org/10.1186/1754-6834-6-14>.
- (14) Korányi, T. I.; Fridrich, B.; Pineda, A.; Barta, K. Development of 'Lignin-First' Approaches for the Valorization of Lignocellulosic Biomass. *Molecules* **2020**, *25* (12), 2815. <https://doi.org/10.3390/molecules25122815>.
- (15) Xu, J.; Li, C.; Dai, L.; Xu, C.; Zhong, Y.; Yu, F.; Si, C. Biomass Fractionation and Lignin Fractionation towards Lignin Valorization. *ChemSusChem* **2020**, *13* (17), 4284–4295. <https://doi.org/10.1002/cssc.202001491>.
- (16) Dai, J.; Patti, A. F.; Saito, K. Recent Developments in Chemical Degradation of Lignin: Catalytic Oxidation and Ionic Liquids. *Tetrahedron Lett.* **2016**, *57* (45), 4945–4951. <https://doi.org/10.1016/j.tetlet.2016.09.084>.
- (17) Gao, R.; Li, Y.; Kim, H.; Mobley, J. K.; Ralph, J. Selective Oxidation of Lignin Model Compounds. *ChemSusChem* **2018**, *11* (13), 2045–2050. <https://doi.org/10.1002/cssc.201800598>.

- (18) Gierer, J. Chemistry of Delignification: Part 2: Reactions of Lignins during Bleaching. *Wood Sci. Technol.* **1986**, *20* (1), 1–33. <https://doi.org/10.1007/BF00350692>.
- (19) V. E. Tarabanko, Y. V. Hendogina, D. V. Petuhov and E. P. Pervishina, Reaction Kinetics and Catalysis Letters, 2000, 69, 361-368.
- (20) V. E. Tarabanko and D. V. Petukhov, Chemistry for Sustainable Development, 2003, 11, 655-667.
- (21) V. E. Tarabanko, D. V. Petukhov and G. E. Selyutin, Kinetics and Catalysis, 2004, 45, 569-577.
- (22) Ma, R.; Xu, Y.; Zhang, X. Catalytic Oxidation of Biorefinery Lignin to Value-Added Chemicals to Support Sustainable Biofuel Production. *ChemSusChem* **2015**, *8* (1), 24–51. <https://doi.org/10.1002/cssc.201402503>.
- (23) Xiang, Q.; Lee, Y. Y. Oxidative Cracking of Precipitated Hardwood Lignin by Hydrogen Peroxide. *Appl. Biochem. Biotechnol.* **2000**, *84*, 10.
- (24) Demesa, A.; Laari, A.; Sillanpää, M.; Koiranen, T. Valorization of Lignin by Partial Wet Oxidation Using Sustainable Heteropoly Acid Catalysts. *Molecules* **2017**, *22* (10), 1625. <https://doi.org/10.3390/molecules22101625>.
- (25) Fargues, C.; Mathias, Á.; Silva, J.; Rodrigues, A. Kinetics of Vanillin Oxidation. *Chem. Eng. Technol.* **1996**, *19* (2), 127–136. <https://doi.org/10.1002/ceat.270190206>.
- (26) Zhu, Y.; Liu, J.; Liao, Y.; Lv, W.; Ma, L.; Wang, C. Degradation of Vanillin During Lignin Valorization Under Alkaline Oxidation. *Top. Curr. Chem.* **2018**, *376* (4), 29. <https://doi.org/10.1007/s41061-018-0208-1>.
- (27) Rodrigues Pinto, P. C.; Borges da Silva, E. A.; Rodrigues, A. E. Insights into Oxidative Conversion of Lignin to High-Added-Value Phenolic Aldehydes. *Ind. Eng. Chem. Res.* **2011**, *50* (2), 741–748. <https://doi.org/10.1021/ie102132a>.
- (28) <https://www.borregaard.com/Product-Areas/Biovanillin/>.
- (29) Yunpu, W.; Leilei, D.; Liangliang, F.; Shaoqi, S.; Yuhuan, L.; Roger, R. Review of Microwave-Assisted Lignin Conversion for Renewable Fuels and Chemicals. *J. Anal. Appl. Pyrolysis* **2016**, *119*, 104–113. <https://doi.org/10.1016/j.jaap.2016.03.011>.
- (30) Ouyang, X.; Zhu, G.; Huang, X.; Qiu, X. Microwave Assisted Liquefaction of Wheat Straw Alkali Lignin for the Production of Monophenolic Compounds. *J. Energy Chem.* **2015**, *24* (1), 72–76. [https://doi.org/10.1016/S2095-4956\(15\)60286-8](https://doi.org/10.1016/S2095-4956(15)60286-8).
- (31) de la Hoz, A.; Díaz-Ortiz, Á.; Moreno, A. Microwaves in Organic Synthesis. Thermal and Non-Thermal Microwave Effects. *Chem Soc Rev* **2005**, *34* (2), 164–178. <https://doi.org/10.1039/B411438H>.
- (32) Stuerger, D. A. C.; Gaillard, P. Microwave Athermal Effects in Chemistry: A Myth's Autopsy: Part I: Historical Background and Fundamentals of Wave-Matter Interaction. *J. Microw. Power Electromagn. Energy* **1996**, *31* (2), 87–100. <https://doi.org/10.1080/08327823.1996.11688299>.
- (33) Knill, C. J.; Kennedy, J. F. Degradation of Cellulose under Alkaline Conditions. *Carbohydr. Polym.* **2003**, *51* (3), 281–300. [https://doi.org/10.1016/S0144-8617\(02\)00183-2](https://doi.org/10.1016/S0144-8617(02)00183-2).
- (34) Calcio Gaudino, E.; Tabasso, S.; Grillo, G.; Cravotto, G.; Dreyer, T.; Schories, G.; Altenberg, S.; Jashina, L.; Telysheva, G. Wheat Straw Lignin Extraction with Bio-Based Solvents Using Enabling Technologies. *Comptes Rendus Chim.* **2018**, *21* (6), 563–571. <https://doi.org/10.1016/j.crci.2018.01.010>.
- (35) Gazliya, N.; Aparna, K. Microwave-Assisted Alkaline Delignification of Banana Peduncle. *J. Nat. Fibers* **2021**, *18* (5), 664–673. <https://doi.org/10.1080/15440478.2019.1645786>.
- (36) Harahap, A. F. P.; Rahman, A. A.; Sadrina, I. N.; Gozan, M. Optimization of Pretreatment Conditions for Microwave-Assisted Alkaline Delignification of Empty Fruit Bunch by Response Surface Methodology. *Int. J. Technol.* **2019**, *10* (8), 1479. <https://doi.org/10.14716/ijtech.v10i8.3431>.
- (37) Vanda, H.; Dai, Y.; Wilson, E. G.; Verpoorte, R.; Choi, Y. H. Green Solvents from Ionic Liquids and Deep Eutectic Solvents to Natural Deep Eutectic Solvents. *Comptes Rendus Chim.* **2018**, *21* (6), 628–638. <https://doi.org/10.1016/j.crci.2018.04.002>.

- (38) Gdansk University of Technology, 11/12 Narutowicza St., 80-233 Gdansk, Poland; Owczarek, K.; Szczepanska, N.; Gdansk University of Technology, 11/12 Narutowicza St., 80-233 Gdansk, Poland; Plotka-Wasyłka, J.; Gdansk University of Technology, 11/12 Narutowicza St., 80-233 Gdansk, Poland; Rutkowska, M.; Gdansk University of Technology, 11/12 Narutowicza St., 80-233 Gdansk, Poland; Shyshchak, O.; Lviv Polytechnic National University, 12 S.Bandery St., 79013 Lviv, Ukraine; Bratychak, M.; Lviv Polytechnic National University, 12 S.Bandery St., 79013 Lviv, Ukraine; Namiesnik, J.; Gdansk University of Technology, 11/12 Narutowicza St., 80-233 Gdansk, Poland. Natural Deep Eutectic Solvents in Extraction Process. *Chem. Chem. Technol.* **2016**, *10* (4s), 601–606. <https://doi.org/10.23939/chcht10.04si.601>.
- (39) Satlewal, A.; Agrawal, R.; Bhagia, S.; Sangoro, J.; Ragauskas, A. J. Natural Deep Eutectic Solvents for Lignocellulosic Biomass Pretreatment: Recent Developments, Challenges and Novel Opportunities. *Biotechnol. Adv.* **2018**, *36* (8), 2032–2050. <https://doi.org/10.1016/j.biotechadv.2018.08.009>.
- (40) Lorente, A., Remón, J., Salgado, M., Huertas-Alonso, A.J., Sánchez-Verdú, P., Moreno, A., Clark, J.H. 2020. Sustainable Production of Solid Biofuels and Biomaterials by Microwave-Assisted, Hydrothermal Carbonization (MA-HTC) of Brewers' Spent Grain (BSG). *ACS Sustainable Chemistry & Engineering*, *8*(51), 18982-18991.
- (41) Sevilla, M., Maciá-Agulló, J.A., Fuertes, A.B. 2011. Hydrothermal Carbonization of Biomass as a Route for the Sequestration of CO<sub>2</sub> : Chemical and Structural Properties of the Carbonized Products. *Biomass and Bioenergy*, *35*(7), 3152-3159.
- (42) Xiao, X., Chen, B., Zhu, L. 2014. Transformation, Morphology, and Dissolution of Silicon and Carbon in Rice Straw-Derived Biochars under Different Pyrolytic Temperatures. *Environmental Science & Technology*, *48*(6), 3411-3419.
- (43) Zhang, S.; Zhang, Z.; Ge, M.; Liu, B.; Chen, S.; Zhang, D.; Gao, L. Converting Lignin into Long-chain Fatty Acids with the Electro-Fenton Reaction. *GCB Bioenergy* **2021**, *13* (8), 1290–1302. <https://doi.org/10.1111/gcbb.12859>.
- (44) Lestari, S.; Maki-Arvela, P.; Beltramini, J.; Lu, G. Q. M.; Murzin, D. Transforming Triglycerides and Fatty Acids into Biofuels. *ChemSusChem* **2009**, *2* (12), 1109–1119. <https://doi.org/10.1002/cssc.200900107>.
- (45) Bentivenga, G.; Bonini, C.; D'Auria, M.; De Bona, A.; Mauriello, G. Fine Chemicals from Singlet-Oxygen-Mediated Degradation of Lignin — a GC/MS Study at Different Irradiation Times on a Steam-Exploded Lignin. *J. Photochem. Photobiol. Chem.* **2000**, *135* (2–3), 203–206. [https://doi.org/10.1016/S1010-6030\(00\)00287-2](https://doi.org/10.1016/S1010-6030(00)00287-2).

## 5. COCOA BY-PRODUCT VALORISATION: A BIOREFINERY APPROACH



## 5.1. INTRODUCTION

Increasing demand of cocoa related products has led cocoa industry to massive production levels. Facing an ever-growing cocoa bean request, developing countries governments, have encouraged farmers to plant additional trees<sup>1</sup>. As direct consequence, an enormous quantity of wastes and by-products are generated along the cocoa production chain, posing serious sustainability issues.

Even though they are considered wastes, cocoa pod husk (CPH) and cocoa bean shell (CBS) (the two main by-products of cocoa industry) still contain interesting amounts of biologically active compounds (polyphenols), dietary fibre, lignin, and carbohydrates. This makes cocoa wastes perfect feedstock candidates for biorefinery<sup>2</sup> (Figure 1).

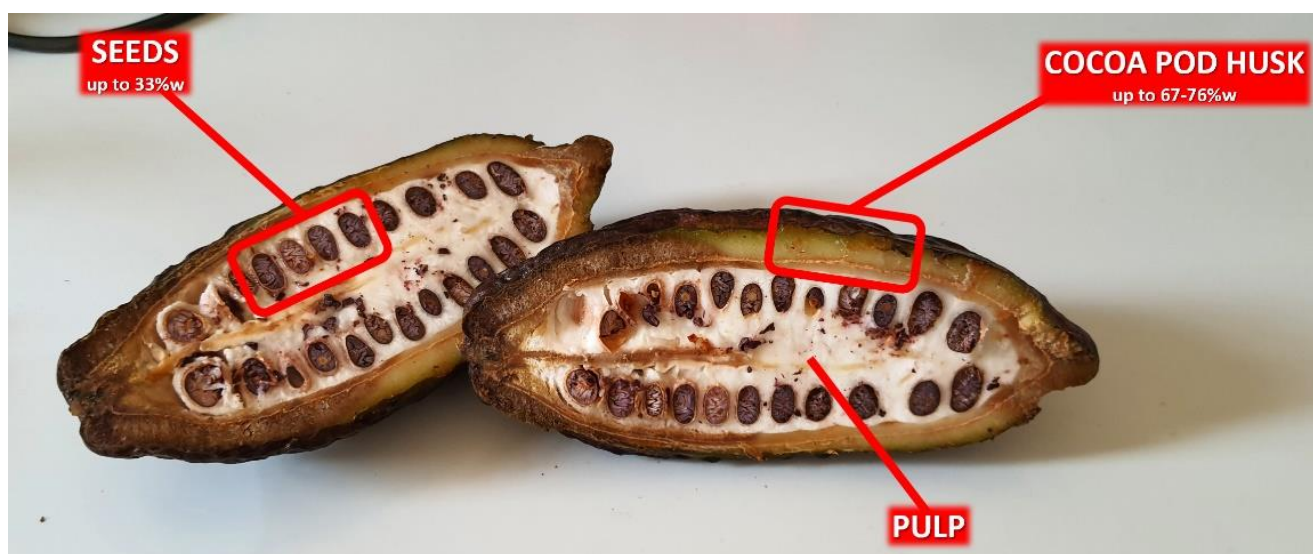


Figure 1: Opened cocoa fruit

Cocoa (*Theobroma cacao* L.) is a tree native to Central and South America. Widely cultivated in tropical regions, it is recognised as a fundamental source of economic profit for several countries. Seven countries (Côte d'Ivoire, Ghana, Indonesia, Nigeria, Cameroon, Brazil and Ecuador) are the main world producers (up to 90% of global cocoa-bean production) with an export value of 9.94 billion USD estimated in 2018<sup>3-6</sup>. Cocoa beans market forecast reports an annual growth rate of 7.3% from 2019 to 2025<sup>7,8</sup>.

Cocoa fruit is a pod whose weight ranges from 0.2 to more than 1kg. Cocoa fruits are composed by an external husk containing a mucilage with beans dispersed into it. About 40 beans are contained in every pod, accounting up to 33% weight of the whole fruit. Cocoa beans are the only part of cocoa fruit exploited in cocoa industry for food production<sup>3,9,10</sup>. Beans are surrounded by an external layer, the shell, that is discarded in the later processing stage. When fruits reach the adequate ripeness, they are collected and opened. CPH is discarded, and the beans are recovered and conveyed to the first stage for cocoa production.

Considering that husk account for 67-76% of the fruit's weight<sup>2</sup>, and considering the data regarding world production, an enormous quantity of waste is produced in the early stages of cocoa industry chain. Usually discarded husks are left to rotten trough the borders of plantation without any further valorisation.

In Figure 2 a flowchart of cocoa industry is represented, highlighting steps that involve organic waste production<sup>9,11</sup>.

Inappropriate treatment of cocoa husk can endanger the plantation, potentially propagating diseases such as pod rot, black pod and cocoa pod borer. Such diseases can cause severe crop losses from 20 to 30% of the annual crop, endangering the supply chain and subsistence of local farmers<sup>2,12,13</sup>.

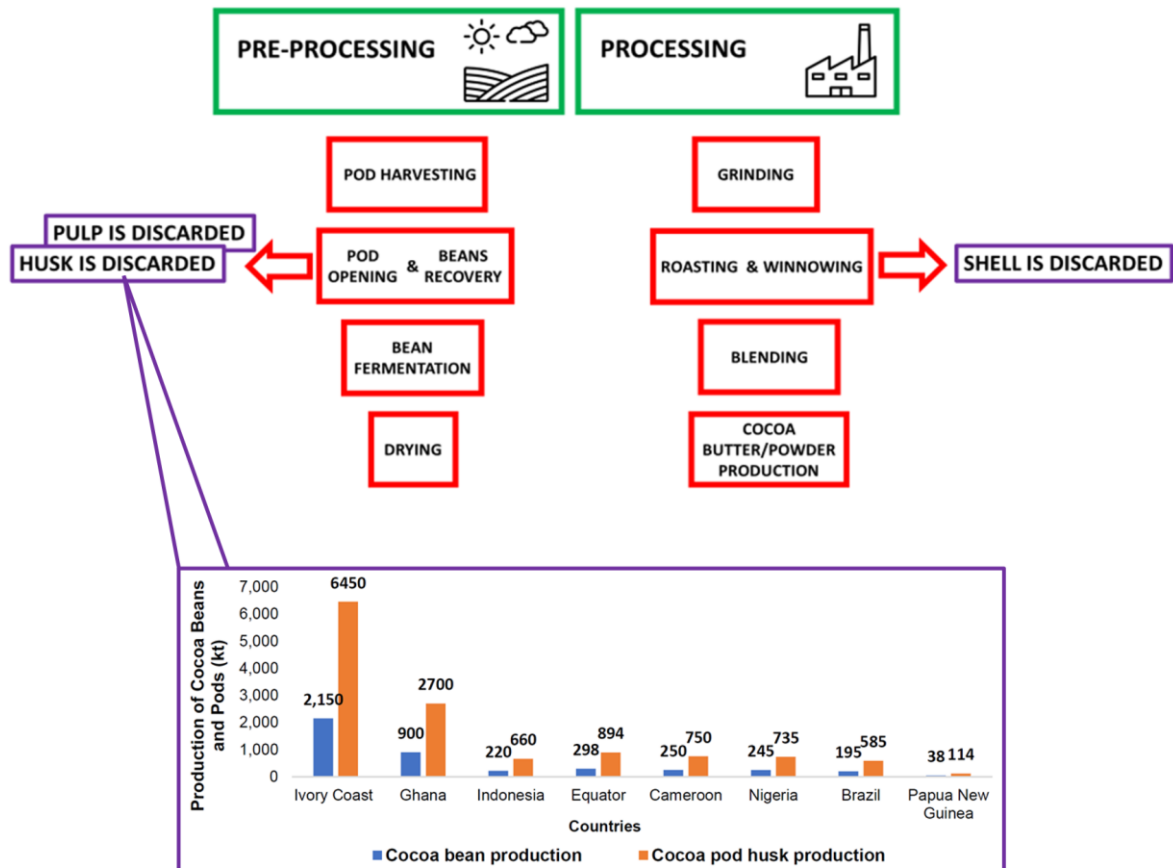


Figure 2: Cocoa production chain and CPH waste worldwide production

### 5.1.1.1. Cocoa pod husk composition

CPH composition was investigated by many researchers and average composition is reported in Table 1<sup>2,12</sup>.

<b>Protein</b>	2.9 – 9.1
<b>Ash</b>	5.9 – 13.0
<b>Lipid</b>	0.6 – 4.7
<b>Total carbohydrates</b>	17.4 – 47.0
<b>Lignin</b>	14.7 – 38.8
<b>Total dietary fibers</b>	18.3 – 59.0
<b>Pectin</b>	6.1 – 12.6
<b>Polyphenols</b>	4.6 – 6.9 g GAE/100g

Table 1: CPH composition

Given the chemical composition here reported, it is clear that CPH still contain high quantities of valuable compounds. In particular from a biorefinery point of view, the high quantity of polyphenols makes CPH a perfect candidate for extraction pre-treatments before any other valorisation strategy. Several studies focused on CPH valorisation, from low-value application as soil fertiliser to high value application as feedstock for pectin and polyphenols, as summarised in Figure 3<sup>14</sup>.

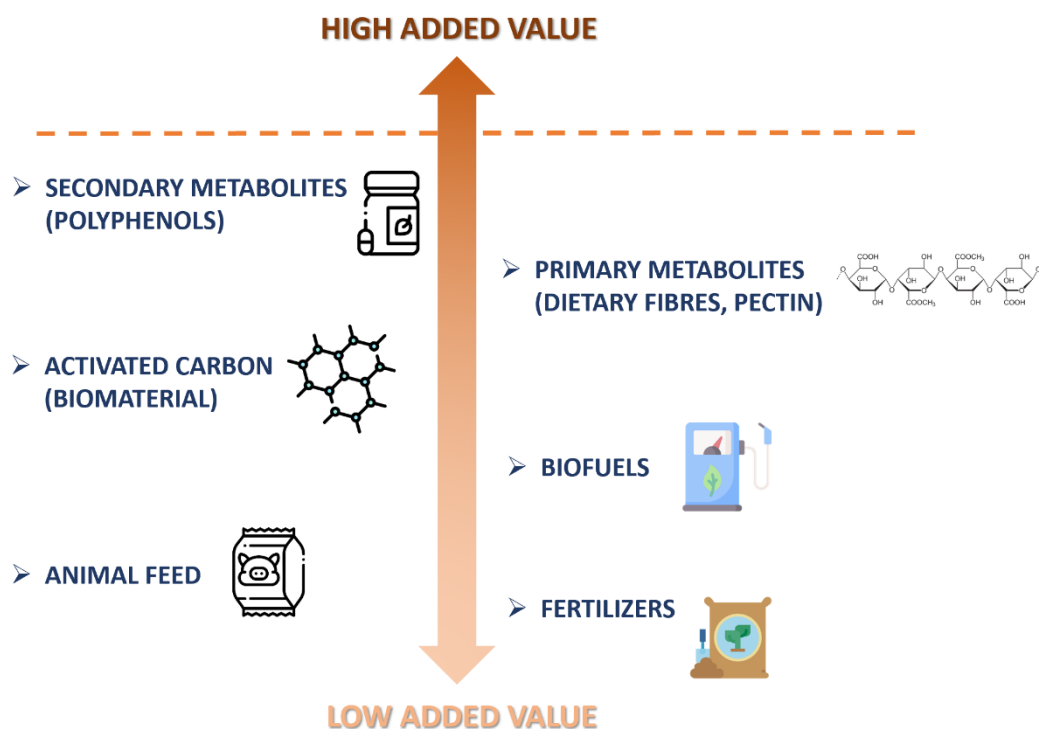


Figure 3: CPH valorisation strategies

### 5.1.2. Secondary metabolites from cph: polyphenols

Secondary metabolites produced by plants such as polyphenols, terpenes, tocopherols and alkaloids were intensely studied in recent years because of their possible positive effects on human health<sup>15,16</sup>. Polyphenols are a class of secondary metabolites that protect plants against parasites, pathogens, UV light, reactive oxygen, and nitrogen species. Moreover, polyphenols are involved in plant-plant interference and defence against plant predators<sup>17,18</sup>.

The main structural unit of polyphenols is the phenolic ring and thousands of polyphenols have been detected in nature: several classes of polyphenols were defined as summarised in Figure 4<sup>19</sup>.

Such classification is based on the number of phenolic rings involved in the overall structure and the structural moieties that bind them<sup>20,21</sup>.

Due to their potential health benefits, global polyphenols market is constantly growing: in 2018, it

was valued at USD 1.28 billion and is expected to grow further. Indeed, polyphenols are widely employed in functional foods, beverages, and cosmetic and pharmaceutical formulations.

Biological effects that polyphenols can exert on human health have been extensively reviewed<sup>21</sup>:



Polyphenols are characterised by strong antioxidant activity, allowing them to scavenge various types of oxygen, nitrogen, and chlorine species and consequently lowering the oxidative-stress damage<sup>16,22</sup>.

Reactive oxygen radicals can originate during respiration and metabolism. Their generation increases during stress-situations, in aging, and during exposure to environmental pollution. Those highly reactive radicals can damage DNA, lipids and proteins<sup>23</sup> and several studies suggests that polyphenols can have an important role in prevention of such damages<sup>22,23</sup>.

- Epidemiological studies and human trials investigated the positive effect exerted by a polyphenolic-rich diet that can reduces the risks of cardiovascular diseases and coronary diseases<sup>20</sup>,
- Prevention of atherosclerosis has been related to the inhibition of low density-lipoprotein (LDL) oxidation,
- Polyphenols can reduce or inhibit enzyme activity involved in the release of glucose into the gastrointestinal tract and can delay glucose transfer from the stomach to the small intestine thus exerting an anti-diabetic action
- Some investigations suggest that polyphenols can interact with neuronal and glial pathways, modulate gene expression, and arrest cell-apoptosis mechanisms thus preventing neurodegenerative diseases, such as Alzheimer's disease, Parkinson's disease, neuro-inflammation, and glutamatergic excitotoxicity, Flavonoids can regulate protein and lipid kinase signalling pathways and thus cause a neuro-inflammatory response in the central nervous system<sup>24</sup>.
- Chemo-protective effects were also ascribed to polyphenols, in particular, in the gastrointestinal system, thanks to their interactions with nutrients, reactive metabolites, activated carcinogens and mutagens. Moreover polyphenols can influence the expression of many genes that are associated with cancer, and modulate the activity of key proteins that control cell proliferation<sup>20</sup>

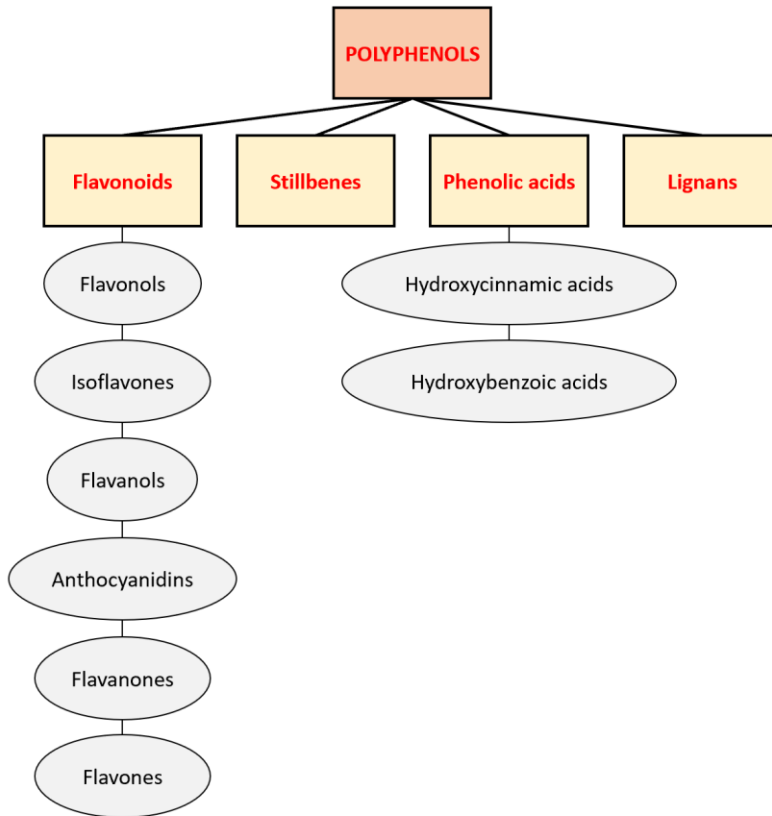


Figure 4: Main polyphenols classes

Felice et al.<sup>25</sup> tested CPH extracts antioxidant activity on endothelium of blood vessels cells showing enhanced viability. Moreover, owing to the excellent stability in a physiological environment, CPH extracts, showed a good permeability across rat intestine. These recent results may prompt further research on extracts application in the prevention of cardiovascular diseases

Rachmawaty et al.<sup>26</sup> have performed research on the activity of CPH polyphenol-rich extracts against pathogenic fungus *Fusarium oxysporum*, and suggested that a correlation exists between the antifungal activity of the CPH extract and the presence of polyphenols.

Santos et al.<sup>27</sup>, 2014 have tested the antimicrobial activity of a CPH extract obtained via spontaneous fermentation. The extract showed antimicrobial activity against medically important *Pseudomonas aeruginosa* and *Salmonella choleraesuis*. The extract was fractionated, and all the bioactive fractions contained phenols, steroids and terpenes.

## 5.2 RESULTS AND DISCUSSION

The aim of the work presented in this chapter was to set up environmentally friendly protocol for sustainable polyphenols extraction/recovery and subsequently integrate the protocol in broader bio-refinery model for CPH valorisation, exploiting BMF production protocol reported in Chapter 2.

### 5.2.1 cocoa pod husk extraction

#### Cocoa pod husk characterisation

Blade milled dry cocoa pod husk from Ecuador was chemically characterised by NREL-derived protocol<sup>28</sup>.

Inorganic fraction in CPH accounts for 7.27% W, moisture accounts for 10.40%W while organic fraction accounts for 83.08% W.

Organic fraction was characterised in term of its main constituents with an uncertainty of 2.88% W. Results are summarised in Figure 5.

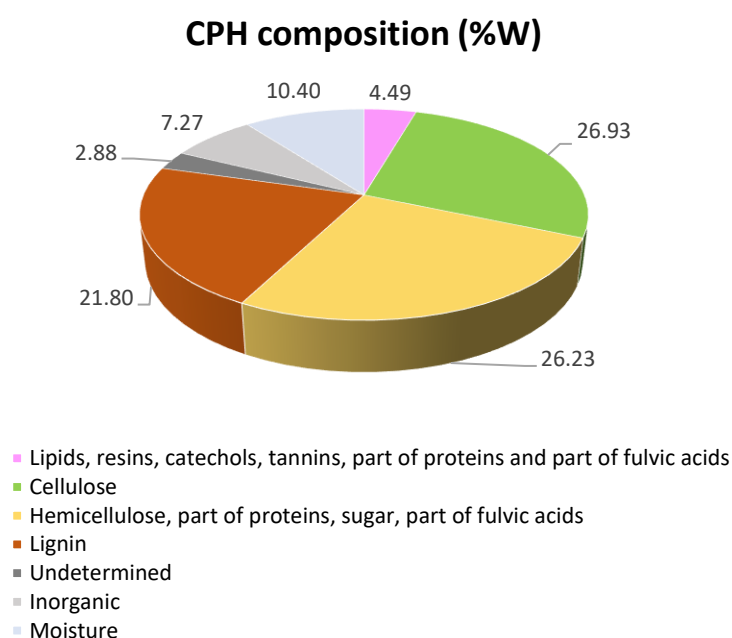


Figure 5: CPH composition (%W)

Data achieved through NREL-derived protocol are in accordance with data reported in literature, but it should be noted that literature data can vary widely, as reported in Table 2 for cellulose, hemicellulose and lignin<sup>11</sup>.

Discrepancies in literature reported data, can be due to different factors such as variety, geographic factors, collection period, storage conditions, and method of analysis<sup>11</sup>.

<b>Cellulose (%W)</b>	18.42 – 44.69
<b>Hemicellulose (%W)</b>	11.97 – 38.08
<b>Lignin(%W)</b>	12.06 – 34.82

Table 2: Cellulose, hemicellulose and lignin content in CPH according to literature<sup>11</sup>

Achieved data show promising values of carbohydrates and lignin, making CPH an interesting feedstock for valorisation studies.

Moreover, several authors<sup>12,2</sup> reported interesting levels of phenolic content in CPH (4.6 – 6.9g /100g CPH).

Following a bio-refinery approach, high added-value components should be recovered prior to apply other valorisation strategies, therefore, aiming to better define the overall polyphenols content in CPH, exhaustive-conventional extraction (ECE) protocol was planned and performed.

Low-molecular-weight flavanols such as catechins and proanthocyanidins oligomers together with flavonols, anthocyanins and flavones, are reported to be easily extracted by means of hydroalcoholic mixtures. Also non-phenolic compounds (organic acids, sugars) can be extracted in such conditions. Due to hydrogen bonds and hydrophobic interactions with insoluble cell-wall fractions, polymerised proanthocyanidins recovery is not possible through hydroalcoholic mixtures: acetone/water mixtures are required to disrupt such weak energy linkages<sup>29</sup>. Therefore, ECE involves the use of methanol/water and acetone/water mixtures preceded by a defatting step in hexane. Several steps are involved, and every step was repeated twice, for an overall extraction time of 20hours as reported in Table 3.

Step	Solvent	Temperature	Time	Repetitions
Defatting	Hexane	50°C	2	2
1	<b>Methanol/water 80/20</b>	Room temperature	2	2
2	<b>Acetone/water 70/30</b>	Room temperature	2	2
3	<b>Methanol/water 80/20</b>	Reflux	2	2
4	<b>Acetone/water 70/30</b>	Reflux	2	2

Table 3: ECE protocol

Overall extraction yield (defatting + step 1 to 4) was estimated to be 27.1% of the CPH initial weight.

Total polyphenols content in CPH at the end of the protocol (step 1-4) was estimated to be 54.1 mg GAE/ g CPH (Figure 6).

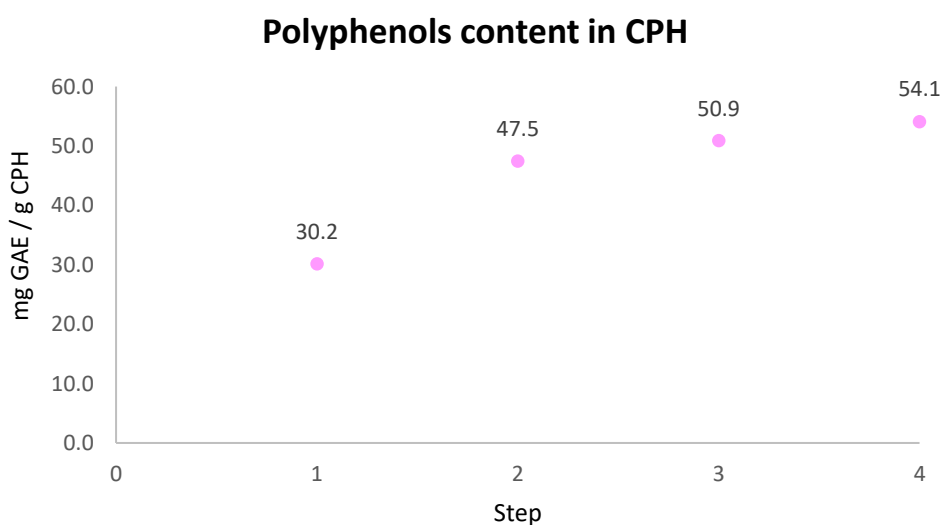


Figure 6: Polyphenols content in CPH vs step

Technology screening and optimisation for sustainable polyphenols extraction from CPH

Both UAE and MASWE were investigated aiming to define and subsequently optimise, the best technology for sustainable polyphenols extraction from cocoa pod husk.

UAE (20kHz, 500W) was investigated, using two solvent systems: pure water and ethanol/water 70/30 mixture, in a time range from 0 to 60 minutes, at room temperature. Solid/liquid ratio was kept constant equals to 1/20.

In both cases comparison with silent extraction was performed.

Results were monitored by Folin-Ciocalteu assay and expressed as mg GAE / g dry CPH as reported in Figure 7 and 8

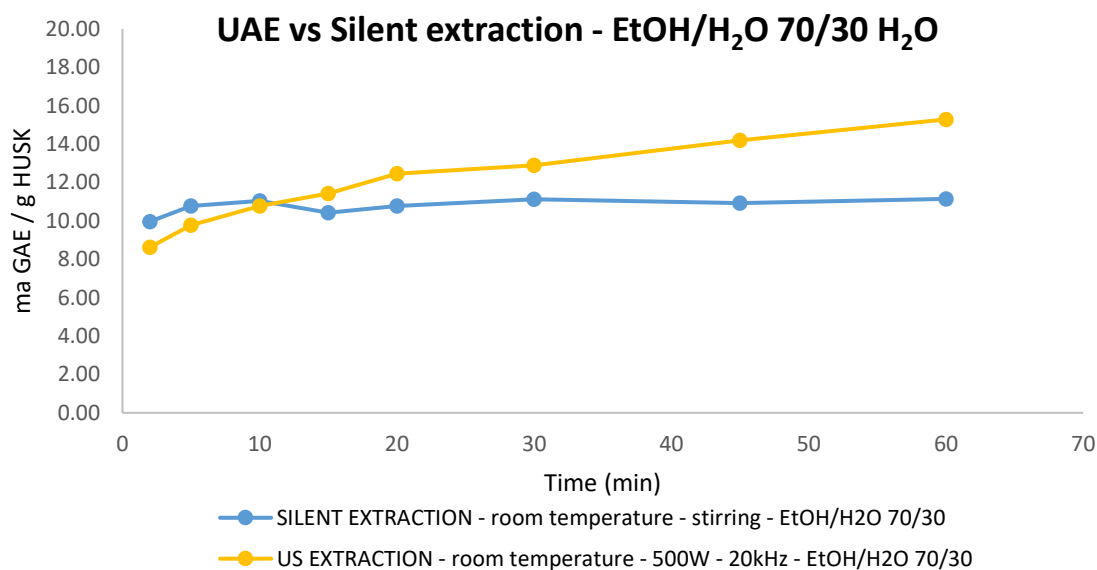


Figure 7: UAE vs silent extraction

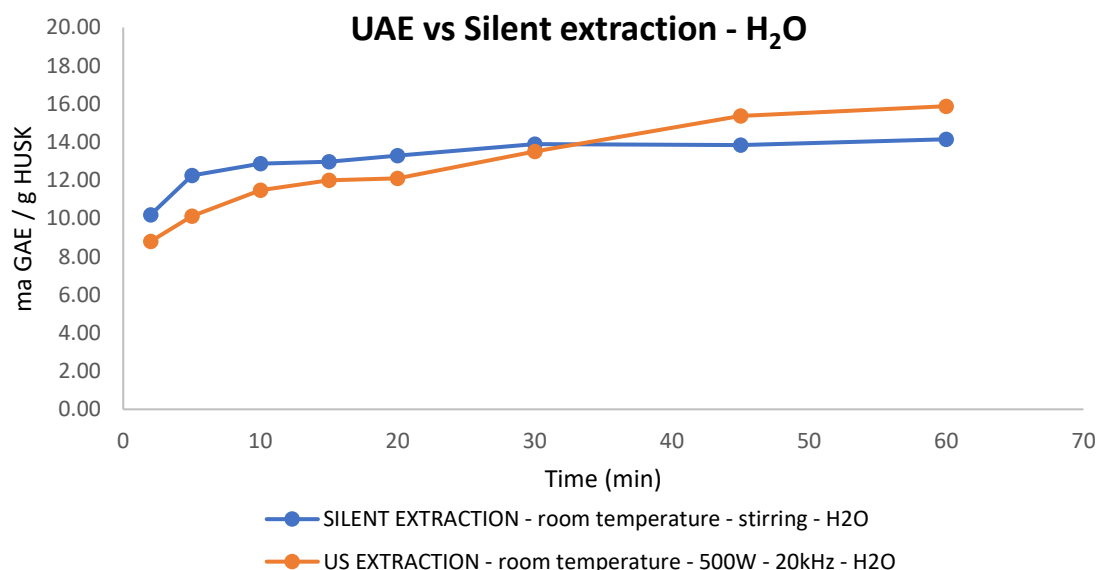


Figure 8: UAE vs silent extraction

In both solvent systems UAE showed a slight benefit when compared with silent extraction when time exceeded 10min in case of ethanol/water and 30min in case of pure water.

Despite this, UAE yields achieved in both solvent systems can be considered unsatisfactory, very far from results achieved in conventional-exhaustive extraction (around 15 mg GAE / g dry CPH both for pure water and ethanol/water and 54.1 mg GAE / g dry CPH for conventional-exhaustive extraction).

Therefore, no further investigations were performed in UAE.

Microwave-assisted subcritical water extraction (MASWE) was investigated as valuable strategy for polyphenols extraction from CPH. Higher benefit was expected from MASWE being the extraction conditions harsher, if compared with UAE.

Water was therefore used as solvent and extraction was investigated in a time range from 0 to 45 minutes.

Extractions were performed in a multimode MW reactor (SYNTHWAVE, Milestone) as summarised in Table 4

<b>Time (min)</b>	0 – 45
<b>Temperature (°C)</b>	150
<b>S/L ratio</b>	1 to 10

Table 4: MASWE experimental conditions

Overall extraction yield (Figure 9), quantity of extracted polyphenols (Figure 10) and total polyphenols content in extract, were monitored.

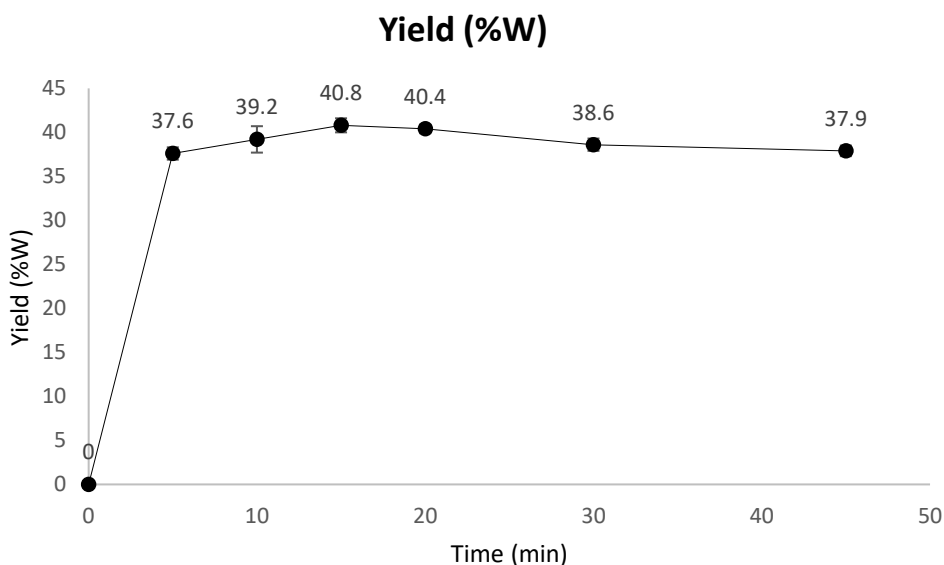


Figure 9: Yield (%W) of MASWE

The best overall extraction yield was reached at only 15 minutes (40.8%w). Comparing this data with ECE (26.4% w) is evident the positive effect exerted from MASWE in overall extraction yield, due to higher mass-transfer and improved solubility. Total polyphenols were also estimated in the range 0 – 45 minutes:

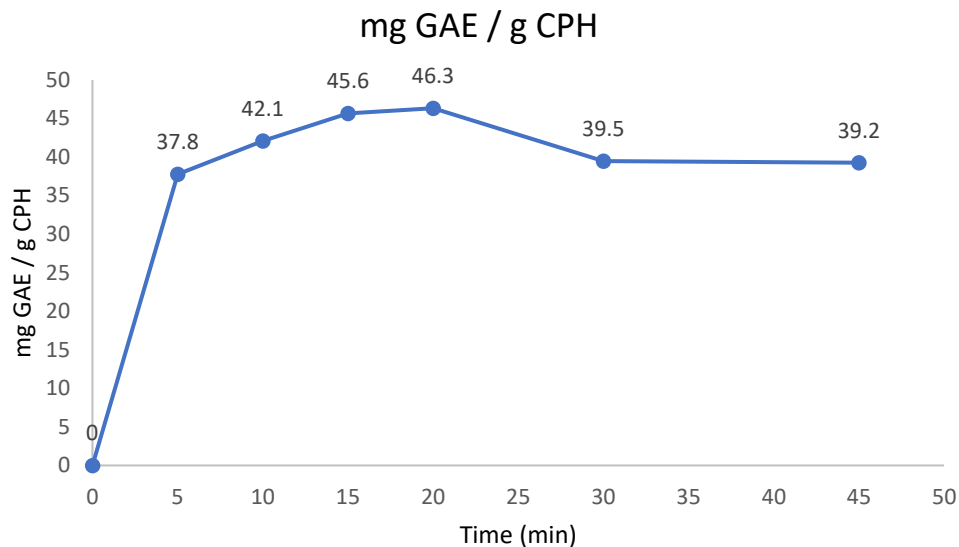


Figure 10: mg GAE/g CPH

After 20 minutes, extracted polyphenols reached the maximum value of 46.3 mg GAE / g CPH corresponding to 85.6% of total polyphenols estimated by ECE.

Polyphenols content in the extract was estimated to be 114.7 mg GAE / g extract.

For higher times (> 20 minutes), the quantity of extracted polyphenols decreased at values around 39 mg GAE / g CPH. This behaviour can be due to partial degradation of 125hermos-labile polyphenols that can undergo to degradation because of exposition to harsh temperature conditions for prolonged times<sup>30</sup>.

#### Conventional subcritical water extraction (SWE)

Identified MASWE conditions were transposed to a conventional Parr pressure reactor. After 20min at 150°C and s/l ratio 1/10, 40.6mg GAE/ CPH were recovered. Slight decrease in polyphenols recovery (40.6 vs 46.3 mg GAE/g CPH) can be due to less efficient heating and cooling that required longer times respect to MASWE, leading to less efficient extraction or partial degradation phenomena.

Despite that, conventional subcritical water seems to be satisfactory, leading to 106.3 mg GAE/ g extract and 76.6% recovery of total polyphenols estimated by ECE, confirming a good transposability from microwave reactor to conventional reactor for subcritical water extraction.

#### Further MASWE optimisation

Aiming to reach almost complete polyphenols extraction in MASWE, the solid/liquid ratio was increased from 1 to 10 to 1 to 20, at 20 minutes, 150°C. An increase in water involved was expected to be beneficial in mass transfer improvement. As expected in such conditions 42.6% W yield was achieved and 54.4 mg GAE / g HUSK was obtained, finally equalling ECE results for polyphenols extraction. Polyphenols content in the extract was estimated to be 128.0 mg GAE / g extract.

A temperature increase was also investigated from 150°C to 170°C reaching 56.3 mg GAE / g HUSK, demonstrating no substantial benefits in temperature increase.

For sake of comparison room temperature extraction in water (maceration) and reflux extraction (100°C) were performed, confirming the undoubted benefits of subcritical water extraction technology for polyphenols extraction from CPH (Figure 11).

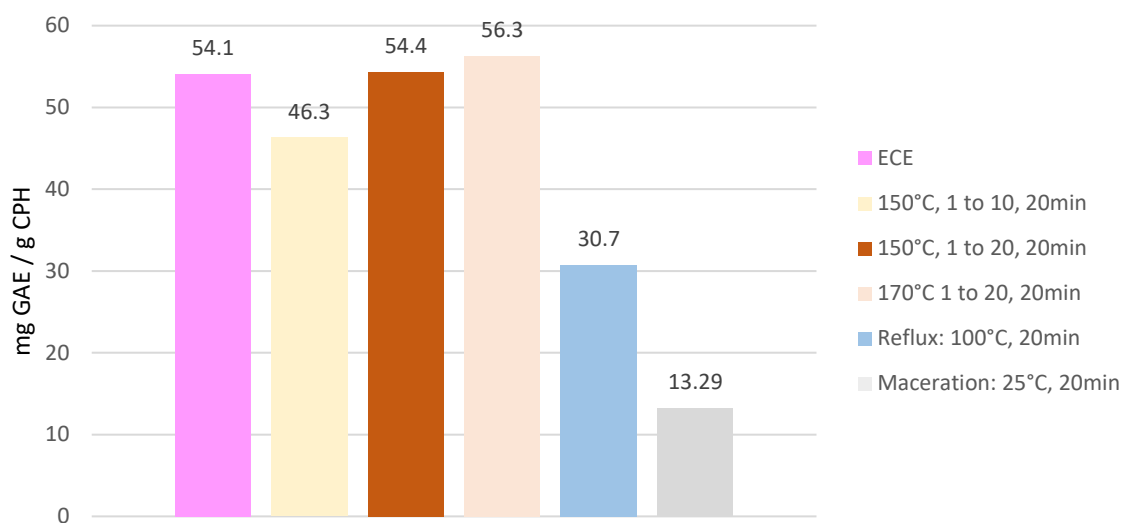


Figure 11: MASWE optimisation

#### Scaling-up & polyphenols purification from MASWE extracts

According to previously optimised results, a MASWE scaling up from 2g to 25g was performed (Table 5).

<b>DRY HUSK (g)</b>	25
<b>H<sub>2</sub>O (mL)</b>	500
<b>s/l ratio</b>	1 to 20
<b>Temperature (°C)</b>	150
<b>Time (min)</b>	20

Table 5: conditions for MASWE scaling-up

Extraction was performed directly in 800mL vessel of microwave reactor (Synthwave, Milestone).

41%W overall extraction yield was achieved with extracted polyphenols reaching the value of 51.7 g GAE / g HUSK and polyphenols content in the extract equals to 126.1 mg GAE / g extract, confirming the perfect scalability to 25g.

After the extraction, residual husk was recovered, dried, and saved for future valorisation investigations.

As previously described in Chapter 1, despite the beneficial effects exerted in improved mass transfer and matrix wetting that ensure complete polyphenols extraction, subcritical water lacks selectivity due to severe temperature conditions, increasing the recovery of co-extracted molecules.

Aiming to recover almost pure polyphenols a downstream protocol was settled using SEPABEADS SP207 adsorbent resins for polyphenols recovery from the extract<sup>31</sup>.

Resin adsorption is a very common technique for polyphenols isolation/recovery from extracts. Such downstream process is quite simple and inexpensive: adsorption resins are characterised by extended durability, high adsorption capacity, easy regenerability, and high



chemical stability. The only relevant cost is connected to the ethanol involved for resin regeneration/polyphenols recovery. High selectivity is another characteristic that makes adsorption resins a valuable and interesting strategy for polyphenols isolation<sup>32</sup>.

4g of raw extract recovered after the scaling-up test were therefore treated and two fractions were recovered at the end of the protocol: a co-extractives-rich fraction, and a polyphenols-rich fraction.

Polyphenols-rich fraction accounts for 15.49%W of raw extract and co-extracts rich fraction accounts for 80.13%W. A loss of 4.38%W based on initial extract was observed during resin treatment.

Polyphenols-rich fraction was analysed by means of Folin-Ciocalteu test and high efficiency of polyphenols recovery was observed: 88.4% of polyphenols present in the raw extract were recovered, with purity degree of 71.9%W. Such results demonstrate the feasibility of adsorbent resins treatment for downstream processes of polyphenols isolation from raw extracts with high content of co-extracts.

### 5.2.2. Valorisation of residual husk

Remaining husk (residual cocoa pod husk, RCPH) recovered at the end of the extraction was investigated by means of NREL-derived protocol (Figure 12).

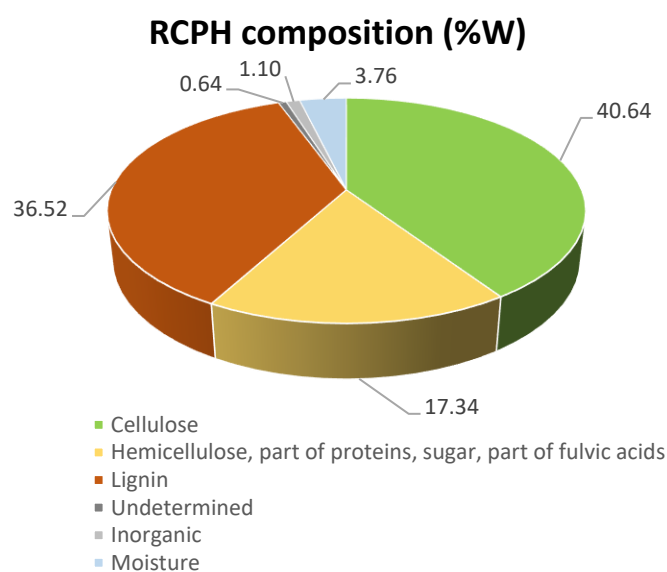


Figure 12: RCPH composition

Starting from these data, mass balance referred to cellulose, hemicellulose and lignin was analysed.

100g of CPH were used as base of calculation, results are summarised in Table 6 and Figure 13

	<b>CPH composition (g)</b>	<b>RCPH composition (g)</b>
Cellulose	26.93	23.97
Hemicellulose	26.23	10.23
Lignin	21.8	21.55
Other	25.04	3.25
<b>TOT. (g)</b>	<b>100</b>	<b>59</b>

Table 6: CPH and RCPH composition

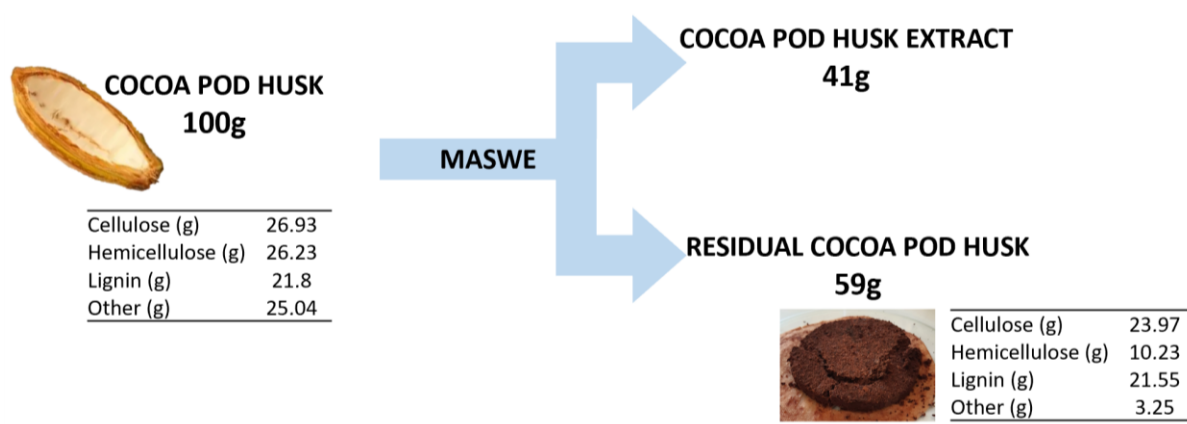


Figure 13: Mass balance of MASWE

While a sensible quantity of hemicellulose was depauperated, mass balance shows non-negligible quantities of cellulose and lignin present RCPH that can be valorised according to biorefinery and CE principles. Indeed, according to the calculations, cellulose and lignin seems to be almost non depauperated in RCPH recovered at the end of MASWE.

FTIR ATR spectres of lignins recovered at the end of NREL-derived protocol for CPH and RCPH were recorded and compared: the two spectra are very similar confirming the hypothesis that lignin remains almost unmodified after MASWE.

Previously reported optimised protocols for cellulose valorisation to BMF was therefore applied to RCPH. For sake of comparison same protocols were applied to raw CPH.

#### RCPH and CPH conversion to BMF

RCPH and CPH were subjected to previously reported optimised conditions for biomass conversion to BMF.

Single step and multi-step experiments were conducted at 110°C and 100°C.

Reported results are expressed as %mol referred to anhydroglucose units present in the cellulose fraction contained in CPH or RCPH (Table 7).

Matrix	Step	Temperature (°C)	Time (min)	Yield %mol	g BMF / 100g raw CPH
RCPH	Single step	100°C	10	54.08	11.56
CPH			10	57.89	13.90
RCPH	Single step	110°C	5	43.83	9.37
CPH			5	46.25	11.10
RCPH	Multi step	100°C	5+5+5	51.47	11.00
CPH			5+5+5	52.23	12.54
RCPH	Multi step	110°C	5+5+5	46.02	9.84
CPH			5+5+5	70.73	16.98

Table 7: RCPH and CPH conversion to BMF

Multi-step approach for CPH lead to surprising results at 110°C: in such conditions cellulose is converted to BMF with 70.73% mol yield. By the other hand RCPH showed best result in single step treatment, in 10 min at 100°C. In such conditions 54.08% mol yield BMF was achieved, equals to 11.56g BMF / 100g raw CPH, demonstrating that BMF can be easily achieved from RCPH following a biorefinery approach that firstly aims to recover high added

value secondary metabolites through extraction and subsequently converts the remaining matrix to BMF.

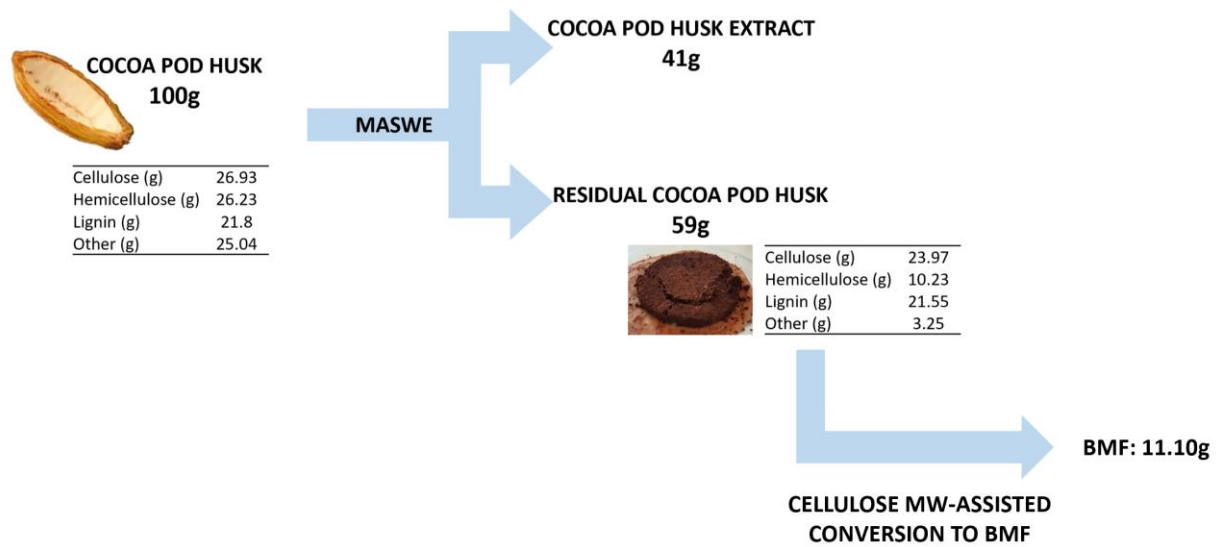


Figure 14: Mass balance MASWE + BMF production

According to the scheme reported in Figure 14, a protocol coherent with biorefinery approach was therefore settled-up. 100g of CPH can be pre-treated by means of MASWE, leading to 41g of polyphenols-rich extract. Remaining solid RCPH can be further converted to 11.10g of BMF leading to valorisation of cellulose fraction.

### 5.3. CONCLUSIONS

Cocoa pod husk was successfully used as starting feedstock for biorefinery valorisation protocol. In the first part of the work cocoa pod husk was investigated as source of high-added value polyphenols by means of non-conventional extractions. ultrasound-assisted extractions showed low benefit in polyphenols extraction while microwave-assisted subcritical water extraction showed engaging performances in polyphenols recovery allowing quantitative extraction of polyphenols contained in the feedstock. The protocol was scaled-up from few grams to 25g. Recovered extract was subsequently treated using adsorption resins aiming to recover high-purity polyphenols fraction.

Aiming to fully valorise cocoa pod husk, coherently with biorefinery approach, exhaust matrix (residual cocoa pod husk) recovered at the end of the extraction process, was subsequently subjected to 5-brominemethylfurfural production by following the optimised protocol described in chapter 3.

5-brominemethylfurfural was achieved in satisfactory yield, thus demonstrating the integrability of the two protocols.

## 5.4. EXPERIMENTAL

### Reagents

All reagents and solvents, unless otherwise specified, were purchased from Sigma-Aldrich and used without further purification.

### Plant material

Dry CPH from Ecuador were blade-milled in a lab blender. Particles dimensions range from 0.5 to 1.5mm.

### NREL-derived protocol

NREL-derived protocol was performed as described in chapter 2 section 2.4.

### Exhaustive-conventional extraction (ECE)

-8g of DVP were extracted in 160mL hexane (solid to liquid ratio 1g:20mL) at 50°C (reflux in oil bath) for 2h under stirring. The extract was then filtered and residual CPH was recovered and subjected to a second extraction step in hexane. The aim of this step was to remove lipophilic content of CPH.

-Residual CPH recovered after hexane extraction was extracted at room temperature under stirring, using 160mL methanol/water 80/20, for 2h. The extract was then filtered and residual CPH was recovered and subjected to a second methanol/water 80/20 extraction step.

- Residual CPH recovered after previous extraction steps was extracted at room temperature under stirring, using 160mL acetone/water 70/30, for 2h. The extract was then filtered and residual CPH was recovered and subjected to a second acetone/water extraction step.

-Methanol/water and acetone/water extractions were repeated in same above-reported conditions in an oil bath at reflux.

In conclusion 5 samples deriving by consecutive extractions of CPH were recovered. Solvents were evaporated and methanol/water and acetone/water fractions were analysed through Folin-Ciocalteu test for total polyphenols content.

### Ultrasound assisted extractions (UAE)

UAEs were performed using stainless steel immersion horn sonotrode 20kHz, 500W (HNG-20500-SP, Hainertec, Suzhou, China).

10g of CPH were placed in a 500mL round bottom vial. 200mL water or ethanol/water 70/30 were added to CPH (s/l ratio 1g to 20mL) and subjected to US irradiation.

8 extract samples (0.5mL) were recovered in time range from 0 to 60 minutes. 0.5mL of appropriate solvent were added to the extraction vial every time a sample was recovered, in order to keep total volume constant.

Polyphenols content in each sample was estimated through Folin-Ciocalteu test for total polyphenols.

Temperature was kept constant around 30°C by an ice bath.

Experimental conditions are summarised in Table 8.

<b>Power (W)</b>	500
<b>Frequency (kHz)</b>	20
<b>CPH (g)</b>	10
<b>Solvent, water or ethanol/water 70/30 (mL)</b>	200
<b>s/l ratio g/mL</b>	1/20
<b>Time (min)</b>	0 – 60
<b>Temperature (°C)</b>	30

Table 8

#### Silent extractions

Silent extraction for comparison with UAE experiments were conducted in 500mL flat bottom balloon. 10g of CPH were placed in the balloon and 200mL water or ethanol/water 70/30 were added (s/l ratio 1g to 20mL). 8 extract samples (0.5mL) were recovered in time range from 0 to 60 minutes. Polyphenols content in each sample was estimated through Folin-Ciocalteu test for total polyphenols.

Experimental conditions are summarised in Table 9

<b>CPH (g)</b>	10
<b>Solvent, water or ethanol/water 70/30 (mL)</b>	200
<b>s/l ratio g/mL</b>	1/20
<b>Time (min)</b>	0 – 60
<b>Temperature (°C)</b>	30

Table 9

#### Microwave-assisted subcritical water extraction (MASWE)

1-2g of CPH were added to 40mL glass vial. Appropriate volume of water (10-20mL) was added. The system was subjected to microwave irradiation in a microwave reactor Synthwave, Milestone in a time range from 5 to 45 minutes under stirring. 15bar N<sub>2</sub> were added to the reactor in order to keep water in its liquid state.

<b>CPH (g)</b>	1 - 2
<b>Solvent, water</b>	20
<b>s/l ratio g/mL</b>	1/10 - 1/20
<b>Time (min)</b>	0 – 45
<b>Temperature (°C)</b>	150, 170
<b>N<sub>2</sub> (bar)</b>	15

Table 10

Extract was recovered by means of centrifugation at 4500rpm in 15mL falcon. Water was removed through freeze drying. Overall extraction yield was determined by gravimetric analysis of raw extract, polyphenols content was determined by means of Folin-Ciocalteu test for total polyphenols and expressed as mg GAE / g extract and mg GAE / g CPH.

#### Subcritical conventional extraction

2g CPH were placed in Parr pressure reactor. Extraction was performed for 20min at 150°C and s/l ratio 1/10. Extract was recovered by means of centrifugation at 4500rpm in 15mL falcon. Water was removed through freeze drying. Overall extraction yield was determined by gravimetric analysis of raw extract, polyphenols content was determined by means of Folin-Ciocalteu test for total polyphenols and expressed as mg GAE / g extract and mg GAE / g CPH

#### Room temperature and 100°C CPH extraction, conventional

2g CPH were placed in 250mL glass balloon.

-100°C extraction was performed in an oil bath (reflux) under stirring for 20min and s/l ratio 1/20.

-Room temperature extraction was performed under stirring for 20min and s/l ratio 1/20. Extract were recovered by means of centrifugation at 4500rpm in 15mL falcon. Water was removed through freeze drying. Overall extraction yield was determined by gravimetric analysis of raw extract, polyphenols content was determined by means of Folin-Ciocalteu test for total polyphenols and expressed as mg GAE / g extract and mg GAE / g CPH

#### Polyphenols recovery from raw extract

Diaon Sepabeads 207 was used for polyphenols recovery from raw MASWE extract.

According to polyphenols content in raw extract and adsorption capacity of the resin (2.5 mg polyphenols/g resin<sup>31</sup>) an appropriate quantity of resin was weighted.

The resin is first regenerated with ethanol in glass baker and then transferred in glass column and washed with 3 bed volumes (BV) of deionized water.

4g of raw extract were solubilised in 100mL deionised water and passed trough the resin.

The column was then washed with 3 BV of deionized water in order to eluate the compounds not adsorbed on the resin. Obtained water fraction is rich in carbohydrates. The column was then washed with 3 BV of 75 % (vol/vol) ethanol in order to desorb compounds (polyphenols) adsorbed on the resin. Thus, ethanol fraction is rich in polyphenols. After eluation and desorption process, resin was regenerated with 3 BV of deionized water for further application.

Carbohydrates-rich fraction and polyphenols-rich fraction were evaporated and freeze-dried in glass balloon. The two fractions were weighted and polyphenols content in polyphenols-rich fraction was determined by means of Folin-Ciocalteu test.

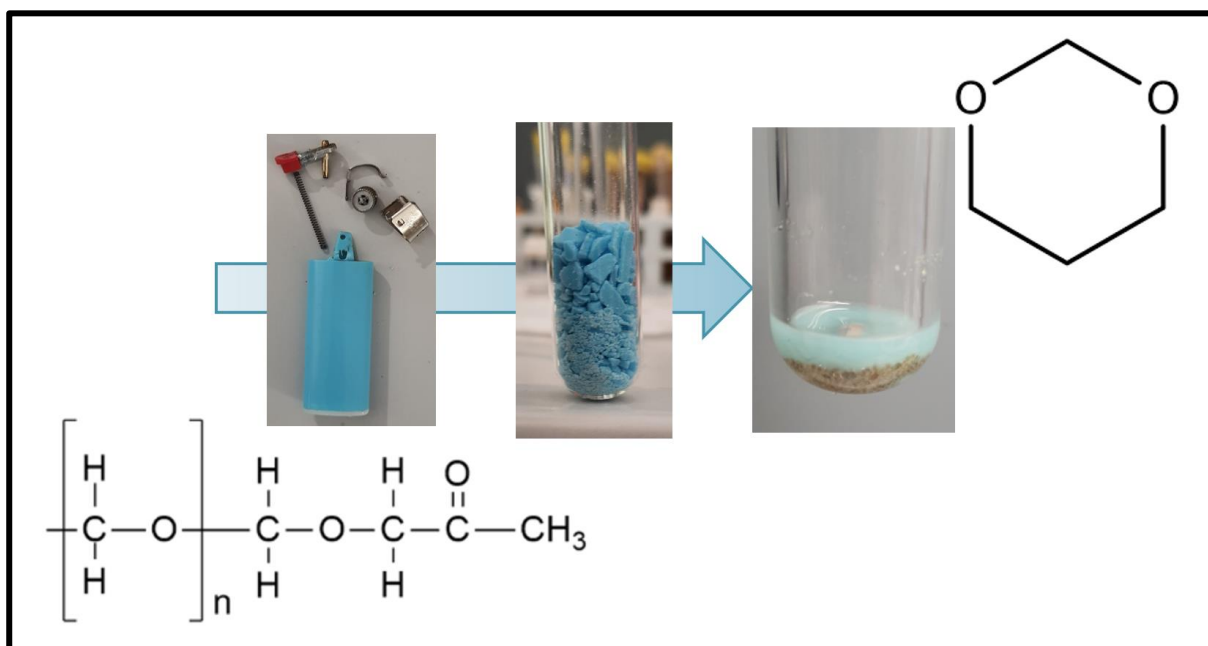
## 5.5. REFERENCES

- (1) Uy, J. R.; Careo, N. D.; Llarena, D.; Barajas, J. R. Optimization of Furfural Extraction from *Theobroma Cacao* Wastes Using Response Surface Methodology. *MATEC Web Conf.* **2019**, *268*, 06010. <https://doi.org/10.1051/mateconf/201926806010>.
- (2) Lu, F.; Rodriguez-Garcia, J.; Van Damme, I.; Westwood, N. J.; Shaw, L.; Robinson, J. S.; Warren, G.; Chatzifragkou, A.; McQueen Mason, S.; Gomez, L.; Faas, L.; Balcombe, K.; Srinivasan, C.; Picchioni, F.; Hadley, P.; Charalampopoulos, D. Valorisation Strategies for Cocoa Pod Husk and Its Fractions. *Curr. Opin. Green Sustain. Chem.* **2018**, *14*, 80–88. <https://doi.org/10.1016/j.cogsc.2018.07.007>.
- (3) Beckett, S. T. *The Science of Chocolate*, Repr., twice.; RSC paperbacks; Royal Society of Chemistry: Cambridge, 2006.
- (4) Figueroa, K. H. N.; García, N. V. M.; Vega, R. C. Cocoa By-products. In *Food Wastes and By-products*; Campos-Vega, R., Oomah, B. D., Vergara-Castañeda, H. A., Eds.; Wiley, 2020; pp 373–411. <https://doi.org/10.1002/9781119534167.ch13>.
- (5) Okiyama, D. C. G.; Navarro, S. L. B.; Rodrigues, C. E. C. Cocoa Shell and Its Compounds: Applications in the Food Industry. *Trends Food Sci. Technol.* **2017**, *63*, 103–112. <https://doi.org/10.1016/j.tifs.2017.03.007>.
- (6) [Http://www.fao.org/faostat/en/#data/QC](http://www.fao.org/faostat/en/#data/QC).
- (7) [Https://www.grandviewresearch.com/industry-analysis/cocoa-beans-market](https://www.grandviewresearch.com/industry-analysis/cocoa-beans-market).
- (8) [Https://www.lisd.org/library/ssi-global-market-report-cocoa](https://www.lisd.org/library/ssi-global-market-report-cocoa).
- (9) Afoakwa, E. O. *Chocolate Science and Technology*; Wiley-Blackwell: Chichester, U.K. ; Ames, Iowa, 2010.
- (10) Sobamiwa, O.; Longe, O. G. Utilization of Cocoa-Pod Pericarp Fractions in Broiler Chick Diets. *Anim. Feed Sci. Technol.* **1994**, *47* (3–4), 237–244. [https://doi.org/10.1016/0377-8401\(94\)90127-9](https://doi.org/10.1016/0377-8401(94)90127-9).
- (11) Ouattara, L. Y.; Kouassi, E. K. A.; Soro, D.; Soro, Y.; Yao, K. B.; Adouby, K.; Drogui, A. P.; Tyagi, D. R.; Aina, P. M. Cocoa Pod Husks as Potential Sources of Renewable High-Value-Added Products: A Review of Current Valorizations and Future Prospects. *BioResources* **2020**, *16* (1), 1988–2020. <https://doi.org/10.15376/biores.16.1.Ouattara>.
- (12) Campos-Vega, R.; Nieto-Figueroa, K. H.; Oomah, B. D. Cocoa (*Theobroma Cacao* L.) Pod Husk: Renewable Source of Bioactive Compounds. *Trends Food Sci. Technol.* **2018**, *81*, 172–184. <https://doi.org/10.1016/j.tifs.2018.09.022>.
- (13) Martínez, R.; Torres, P.; Meneses, M. A.; Figueroa, J. G.; Pérez-Álvarez, J. A.; Viuda-Martos, M. Chemical, Technological and in Vitro Antioxidant Properties of Cocoa (*Theobroma Cacao* L.) Co-Products. *Food Res. Int.* **2012**, *49* (1), 39–45. <https://doi.org/10.1016/j.foodres.2012.08.005>.
- (14) Mariatti, F.; Gunjević, V.; Boffa, L.; Cravotto, G. Process Intensification Technologies for the Recovery of Valuable Compounds from Cocoa By-Products. *Innov. Food Sci. Emerg. Technol.* **2021**, *68*, 102601. <https://doi.org/10.1016/j.ifset.2021.102601>.
- (15) De Filippis, L. F. Plant Secondary Metabolites: From Molecular Biology to Health Products. In *Plant-Environment Interaction*; Azooz, M. M., Ahmad, P., Eds.; John Wiley & Sons, Ltd: Chichester, UK, 2015; pp 263–299. <https://doi.org/10.1002/9781119081005.ch15>.
- (16) Rasouli, H.; Farzaei, M. H.; Khodarahmi, R. Polyphenols and Their Benefits: A Review. *Int. J. Food Prop.* **2017**, 1–42. <https://doi.org/10.1080/10942912.2017.1354017>.
- (17) Brglez Mojzer, E.; Knez Hrnčič, M.; Škerget, M.; Knez, Ž.; Bren, U. Polyphenols: Extraction Methods, Antioxidative Action, Bioavailability and Anticarcinogenic Effects. *Molecules* **2016**, *21* (7), 901. <https://doi.org/10.3390/molecules21070901>.
- (18) Ferrazzano, G.; Amato, I.; Ingenito, A.; Zarrelli, A.; Pinto, G.; Pollio, A. Plant Polyphenols and Their Anti-Cariogenic Properties: A Review. *Molecules* **2011**, *16* (2), 1486–1507. <https://doi.org/10.3390/molecules16021486>.
- (19) Oliver, S.; Vittorio, O.; Cirillo, G.; Boyer, C. Enhancing the Therapeutic Effects of Polyphenols with Macromolecules. *Polym. Chem.* **2016**, *7* (8), 1529–1544. <https://doi.org/10.1039/C5PY01912E>.



- (20) Abbas, M.; Saeed, F.; Anjum, F. M.; Afzaal, M.; Tufail, T.; Bashir, M. S.; Ishtiaq, A.; Hussain, S.; Suleria, H. A. R. Natural Polyphenols: An Overview. *Int. J. Food Prop.* **2017**, *20* (8), 1689–1699. <https://doi.org/10.1080/10942912.2016.1220393>.
- (21) El Gharra, H. Polyphenols: Food Sources, Properties and Applications - a Review: **Nutraceutical Polyphenols**. *Int. J. Food Sci. Technol.* **2009**, *44* (12), 2512–2518. <https://doi.org/10.1111/j.1365-2621.2009.02077.x>.
- (22) Petti, S.; Scully, C. Polyphenols, Oral Health and Disease: A Review. *J. Dent.* **2009**, *37* (6), 413–423. <https://doi.org/10.1016/j.jdent.2009.02.003>.
- (23) Khurana, S.; Venkataraman, K.; Hollingsworth, A.; Piche, M.; Tai, T. Polyphenols: Benefits to the Cardiovascular System in Health and in Aging. *Nutrients* **2013**, *5* (10), 3779–3827. <https://doi.org/10.3390/nu5103779>.
- (24) Sharma, R. Polyphenols in Health and Disease. In *Polyphenols in Human Health and Disease*; Elsevier, 2014; pp 757–778. <https://doi.org/10.1016/B978-0-12-398456-2.00059-1>.
- (25) Felice, F.; Fabiano, A.; De Leo, M.; Piras, A. M.; Beconcini, D.; Cesare, M. M.; Braca, A.; Zambito, Y.; Di Stefano, R. Antioxidant Effect of Cocoa By-Product and Cherry Polyphenol Extracts: A Comparative Study. *Antioxidants* **2020**, *9* (2), 132. <https://doi.org/10.3390/antiox9020132>.
- (26) Rachmawaty; Mu'nisa, A.; Hasri; Pagarra, H.; Hartati; Maulana, Z. Active Compounds Extraction of Cocoa Pod Husk (*Thebroma Cacao* L.) and Potential as Fungicides. *J. Phys. Conf. Ser.* **2018**, *1028*, 012013. <https://doi.org/10.1088/1742-6596/1028/1/012013>.
- (27) Santos, R. X.; Oliveira, D. A.; Sodré, G. A.; Gosmann, G.; Brendel, M.; Pungartnik, C. Antimicrobial Activity of Fermented Theobroma Cacao Pod Husk Extract. *Genet. Mol. Res.* **2014**, *13* (3), 7725–7735. <https://doi.org/10.4238/2014.September.26.10>.
- (28) Genevini, P.; Adani, F.; Villa, C. Rice Hull Degradation by Co-Composting with Dairy Cattle Slurry. *Soil Sci. Plant Nutr.* **1997**, *43* (1), 135–147. <https://doi.org/10.1080/00380768.1997.10414722>.
- (29) *Handbook of Analysis of Active Compounds in Functional Foods*, 0 ed.; Nollet, L. M. L., Toldra, F., Eds.; CRC Press, 2012. <https://doi.org/10.1201/b11653>.
- (30) Sólyom, K.; Solá, R.; Cocero, M. J.; Mato, R. B. Thermal Degradation of Grape Marc Polyphenols. *Food Chem.* **2014**, *159*, 361–366. <https://doi.org/10.1016/j.foodchem.2014.03.021>.
- (31) Soto, M. L.; Conde, E.; González-López, N.; Conde, M. J.; Moure, A.; Sineiro, J.; Falqué, E.; Domínguez, H.; Núñez, M. J.; Parajó, J. C. Recovery and Concentration of Antioxidants from Winery Wastes. *Molecules* **2012**, *17* (3), 3008–3024. <https://doi.org/10.3390/molecules17033008>.
- (32) Hellwig, V.; Gasser, J. Polyphenols from Waste Streams of Food Industry: Valorisation of Blanch Water from Marzipan Production. *Phytochem. Rev.* **2020**, *19* (6), 1539–1546. <https://doi.org/10.1007/s11101-020-09663-y>.

## 6. CYCLIC ACETALS PRODUCTION FROM RENEWABLE DIOLS AND POLYOXYMETHYLENE PLASTIC WASTE



## 6.1. INTRODUCTION

Since 1950s plastics had rapid worldwide diffusion, boosting in an unprecedented way the progress of humanity. Nowadays, plastics are ubiquitous materials characterised by unique and versatile mechanical properties, low production costs, easy manufacturing, lightness, and extreme durability.

In 2017, the total volume of plastics produced since the early years of their commercialisation was estimated to be equals to 8300 million metric tons<sup>1</sup>. Widely employed for single-use packaging applications, due to its resistance to decomposition, an enormous percentage of plastics has accumulated in landfills or, even worse, in the environment (Figure 1<sup>1</sup>).

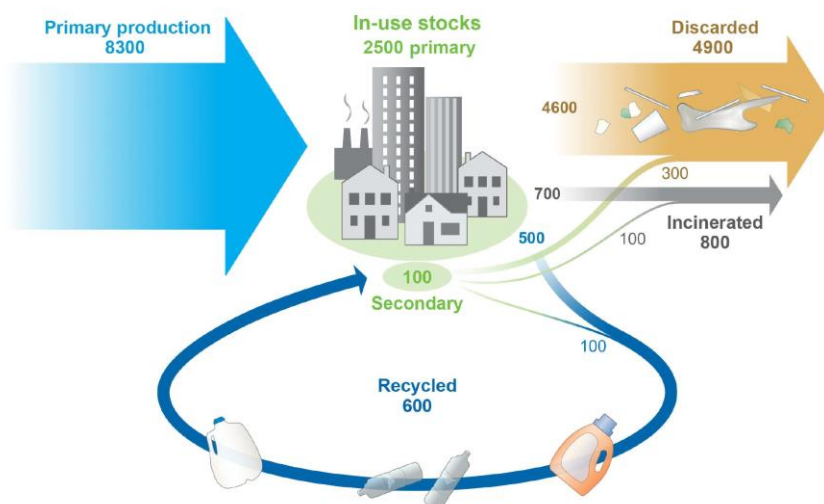


Figure 1: Global production, use, and fate of polymer resins, synthetic fibres, and additives (1950 to 2015; in million metric tons).

Despite the recycling and recovery rates of packaging and other plastics are increasing in the EU<sup>2,3</sup>, discard rate still remains high thus confirming that plastics economy is to date, mainly linear.

In 2016, 150Mt of plastics were estimated to circulate in marine environment, with deleterious effects on marine flora and fauna and also on human health<sup>4,5</sup>.

High disposal rates without any further recycle or valorisation imply more production of virgin materials thus increasing depletion of fossil resources.

According with CE principles, re-valorisation of already circulating plastics should be strongly promoted through recycling, aiming to reduce landfilling and pollution and minimising dependence on fossil resources<sup>6</sup>.

### 6.1.1. Recycling processes for plastic wastes

Four types of recycling processes can be defined<sup>6,7,8</sup>:

1. *Primary recycling* or “closed loop recycling”, contemplates the recovery of discarded plastic product and its re-manufacturing into the same original product, ideally without losing its properties. A small quantity of virgin material can be added to the new products, depending on the necessity.
2. *Secondary recycling* or “open loop recycling” contemplates re-processing of polymer waste leaving intact the chemical identity of the macromolecule, but the final product can be different from the original one. In contrast to what is commonly thought, such

approach does not imply that properties of new products are necessarily lower than the original one.

3. *Tertiary recycling* or “*chemical recycling*” contemplates chemical processes that exploit plastic waste as feedstock for monomer recovery or fuels and chemicals production. Chemical recycling can be achieved through different technologies/processes as follows (Table 1)<sup>8,9</sup>:

Process	Advantages	Limitations/Challenges
<i>Chemolysis</i>	-pure value-added products generated	-only suitable for condensation polymers -high volumes required for economical sustainability
<i>Pyrolysis (thermal cracking)</i>	-suitable for heterogeneous mixtures of plastics or plastics difficult to depolymerise -simple technology easily optimisable	-high energy required -complex reactions involved -contaminants are a problem -PVC not suitable - efficiency and profitability dependent of feedstock mix and quality
<i>Fluid catalytic cracking (pyrolysis process improved by catalyst addition)</i>	-catalyst addition allows temperature reduction -catalyst addition can improve quality of products -high conversion and yields	-not suitable for mixed wastes (catalyst sensitive to chloride and nitrogen contaminants)
<i>Hydrogen technologies (Hydrocracking)</i>	-products quality - suitable for heterogeneous mixtures of plastics	-cost of hydrogen
<i>Gasification</i>	-hydrocarbons and syngas produced -inexpensive gasifying agent (air) -well known technology	- syngas quality should be improved to make it suitable for different applications -production of by-products (tar and char)

Table1: Chemical recycling of plastics

4. *Quaternary recycling* contemplates incineration of the polymer aiming to recover some quantity of energy. Such approach should only be performed when previously illustrated strategies can't be applied.

#### 6.1.1.1. Microwave-assisted plastic waste recycling

Microwave technology can be efficiently used for plastic recycling: in recent year microwave assisted pyrolysis (MAP) of plastic waste emerged as a promising chemical recycling strategy. Plastic polymers can be decomposed into low molecular weight products that can serve as energy or material source.

Several advantages are shown by MAP that make it a promising alternative to conventional heating pyrolysis:

- Thanks to the selective heating of MW, plastic mixtures can be heated avoiding the problems of conventional pyrolysis. Indeed, when PVC is present in the mixture, during conventional pyrolysis, HCl gases can be released, thus forming chlorinated hydrocarbons with polyolefin-based plastics. Instead, when MAP is applied, PVC is suddenly and selectively heated thanks to its high dielectric loss factor, allowing separation of dehydrochlorination reactions of PVC from thermal decomposition of other plastics.
- When MW adsorbents are added to the plastic waste, heating rate can be improved, making the process less energy consumptive and improving the heating rate in respect to conventional processes. Despite some plastics are MW-transparent, the addition of adsorbents can allow the process to reach high temperatures (up to 1000°C in few minutes). Microwave adsorbents dispersed in the bulk of plastic mixture can act as a heating source improving homogeneity and uniformity of heating<sup>10-12</sup>.

In addition to pyrolysis, some chemical recycling processes have been investigated: PET waste aminolysis to terephthalimides to be used as plasticisers was performed with good results in MW in very short times<sup>13</sup>. LDPE was converted to functional chemicals in MW oxidative protocol<sup>14</sup>. Some low-temperature applications of MW for plastic recycling were also reported: terephthalic acid was recovered in mild conditions from PET at 85°C in 40minutes<sup>15</sup>. MW combined to zeolites allowed efficient terephthalic acid recovery from PET<sup>16</sup>.

### 6.1.2. Polyoxymethylene: production and recycling

First discovered in 1920, and industrially produced since 1960s, polyoxymethylene (POM), also called acetal, polyacetal or polyformaldehyde is an engineering thermoplastic material characterised by good mechanical properties, high resistance to solvents, chemicals, and fuels. It presents low friction and wear characteristics. POM is successfully used in a wide range of applications from automotive (main application field) to food industry, from life sciences to manufacturing industries.

POM is mainly processed by molding, injection and extrusion and can be produced as acetal homopolymer or acetal copolymer with comonomer addition every 70-100 units (Figure 2)<sup>17,18</sup>.

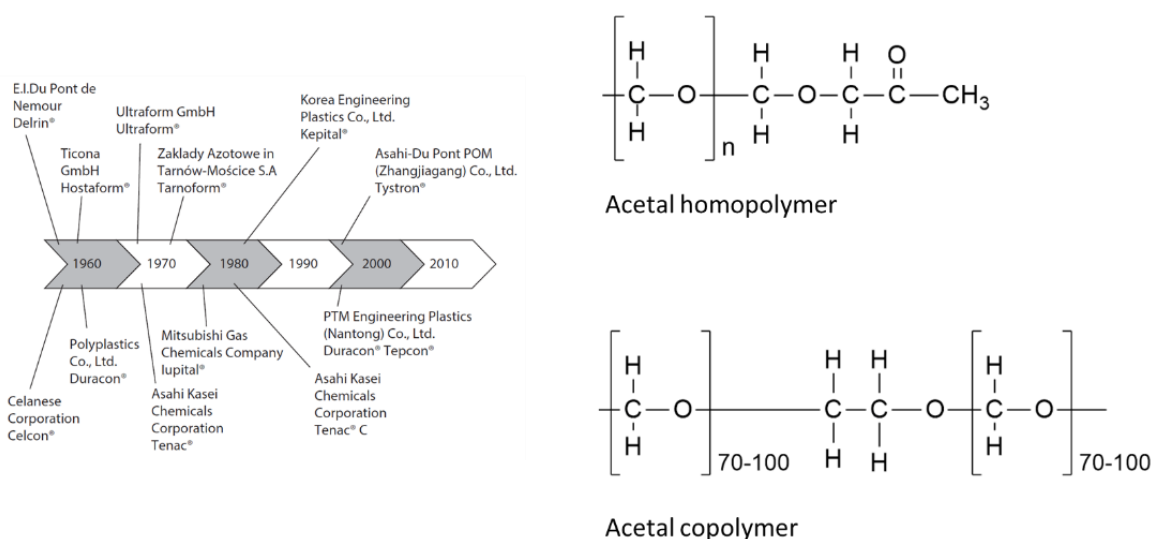


Figure 2: History and structure of POM

Since 1980s POM consumption has almost increased continuously, year by year, as shown in Figure 3<sup>17</sup>.

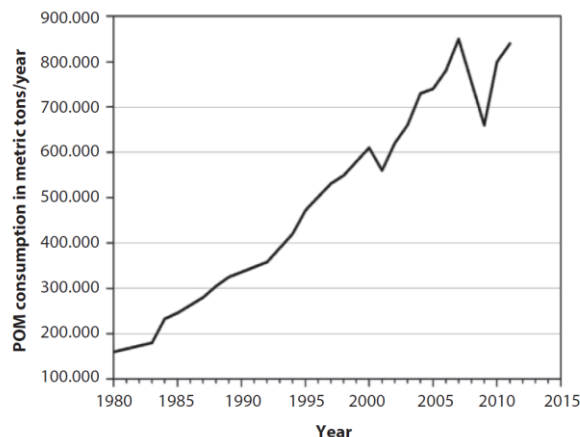


Figure 3: POM consumption per year since 1980

Up to now, chemical recycling of POM waste towards chemical products has been poorly investigated.

According to K. Beydoun and J. Klankermayer<sup>19</sup> POM can be successfully converted into value-added cyclic acetals by catalytic depolymerisation and reaction with bio-based renewable diols (Figure 4). Cyclic acetals have wide applications as solvents, fuel additives, pharmaceutical intermediates, and monomers.

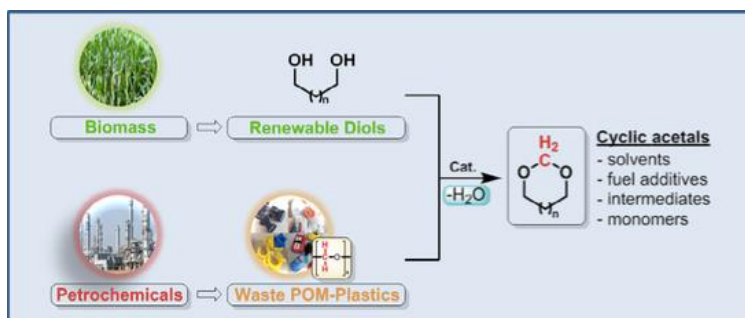


Figure 4: Cyclic acetals production from POM according to K. Beydoun and J. Klankermayer<sup>19</sup>

### 6.1.3. C2-C4 diols production from renewable feedstocks

C2-C4 diols are important platform chemicals widely employed in polymers, fuels, solvents, pharmaceuticals and cosmetics areas. 1,3-propanediol is one of the major building blocks involved in PET, PBT and PTT production. 18 million tons of C2-C4 diols are produced every year from fossil feedstocks. In recent times, production of such diols from renewable sources has attracted interests of scientific community as valuable sustainable alternatives. Some C3-C4 diols isomers can be easily produced through biological approach while production of some other isomers is extremely challenging due to the lack of natural synthetic pathways, requiring therefore studies on modification of such natural pathways<sup>21</sup>. DuPont and Genencor established recombinant *Escherichia coli* protocol for 1,3PDO production from glucose that is

unanimously recognised as a milestone in this field. Commercial-scale production through such protocol was successfully developed<sup>22</sup>.

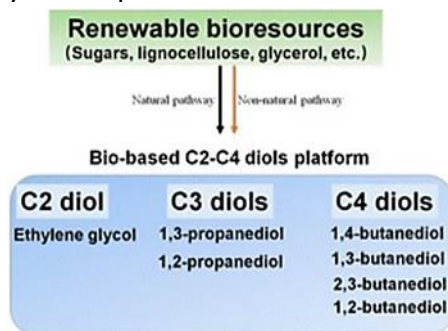


Figure 5: Bio-based renewable diols

## 6.2. RESULTS AND DISCUSSION

The aim of the work described in this chapter is to improve the efficiency and sustainability of the above-mentioned K. Beydoun and J. Klankermayer protocol for POM conversion to 1,3-dioxane with renewable diols.

As reported by the two authors, the reaction can be performed in presence of solvent 1,4-dioxane and 1% mol metal triflate catalyst (in particular,  $\text{Bi}(\text{OTf})_3$ ) by reacting POM with 1,3-propanediol excess (1.2 equivalents) as illustrated below:

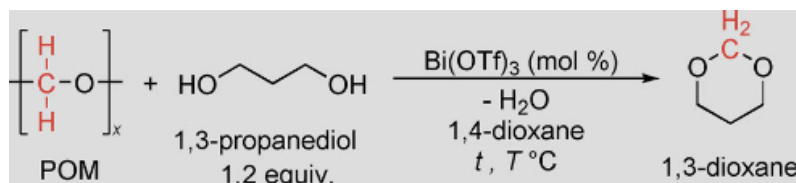


Figure 6: POM conversion to 1,3-dioxane in presence of 1,4-dioxane solvent

At 100°C, after 40 minutes, 99% mol 1,3-dioxane yield was achieved.

Moreover, neat reaction, not involving harmful solvent 1,4 dioxane, was reported with satisfactory yields but in longer times (up to 16 hours).  $\text{Bi}(\text{OTf})_3$  loading was reduced to 0.2% mol. In such conditions 86% mol 1,3-dioxane yield was achieved (Figure 7).

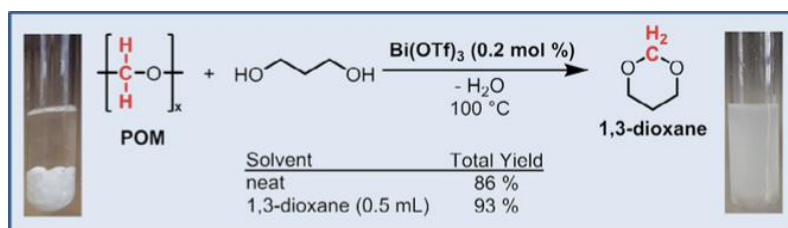


Figure 7: POM conversion to 1,3-dioxane (neat reaction)

Defined protocol was finally tested by the authors in real-case experiment by using waste POM (Figure 8).

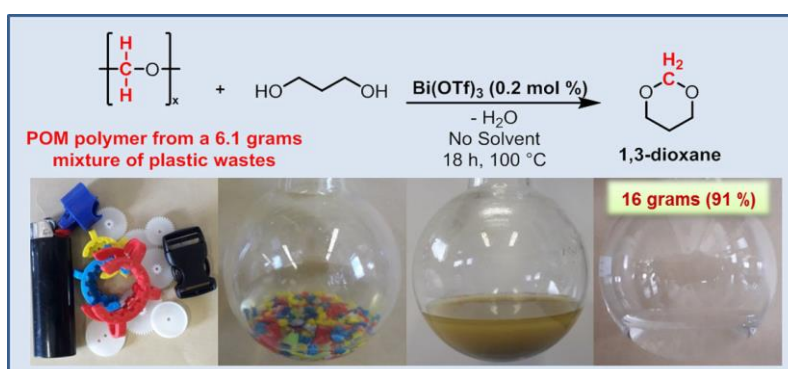


Figure 8: Real-case waste POM conversion to 1,3-dioxane (neat reaction)

All the reported reactions were performed under conventional conditions, using heavy walled sealed vials under magnetic stirring in heating block.

Improvement of the proposed protocol sustainability could be achieved by:



- using MW monomode reactor (Figure 9, reaction time shortening, energy consumption reduction);
- the adoption of low-cost solid-acid catalysts instead of homogeneous high-price metal triflate catalysts. The adoption of solid-acid heterogeneous catalysts could also positively impact the overall protocol by easing catalyst recovery by simple filtration from reaction mixture.

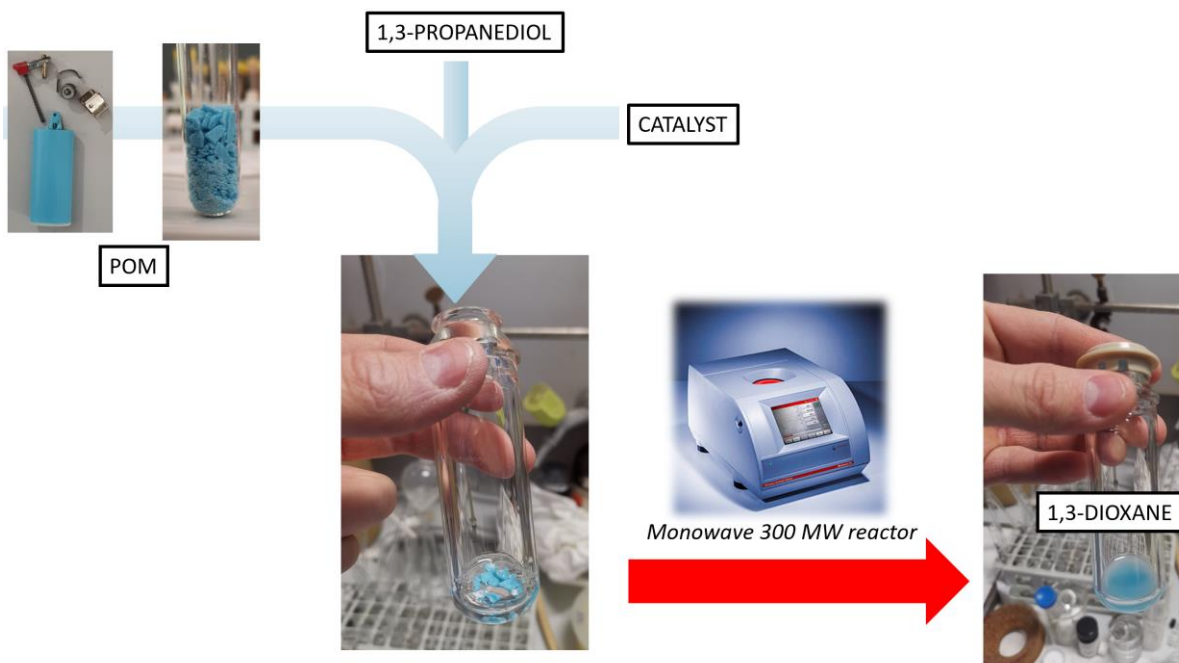


Figure 9: Scheme of the proposed protocol

### 6.2.1. Metal triflate catalysts

As the protocol developed by K. Beydoun and J. Klankermayer involves the use of metal triflates catalysts, in the early stage of this work,  $\text{Bi}(\text{OTf})_3$  was used in neat condition.

The aim of this procedure was therefore to reduce the time of the solvent-less (neat) treatment from hours (16) to minutes through the adoption of monomode MW (Monowave 300) reactor.

#### Time screening

Reaction time was monitored in the range 5 to 40 minutes, no solvent was employed (neat reaction), and the reaction temperature was kept constant and equals to the one used by K. Beydoun and J. Klankermayer.

Also  $\text{Bi}(\text{OTf})_3$  loading was kept equals to the loading reported by the authors (0.2%mol). Differently, 1,3-PDO loading was kept in 1:1 mol ratio with formaldehyde units' content in POM, aiming to avoid excessive reagent loss (authors performed reaction in 1,3-PDO excess, equals to 1.2:1 mol respect to formaldehyde units' content in POM). Virgin POM was employed during the investigation. Experiment conditions are summarised in Table 2:

<b>virgin POM (g)</b>	0.2000g
<b>1,3PDO loading</b>	1:1 mol respect to formaldehyde units' content in POM
<b>Bi(OTf)<sub>3</sub> loading</b>	0.2mol % respect to formaldehyde units' content in POM
<b>Temperature (C°)</b>	100
<b>Stirring (rpm)</b>	300
<b>Time (min)</b>	5 - 40

Table 2: Experimental conditions for reaction conducted with Bi(OTf)<sub>3</sub>

As 1 mole of 1,3-dioxane can be formed from 1 mole of formaldehyde units' content in POM, yield was expressed as mol % of formaldehyde units content in POM, as reported in the equation below:

$$1,3 - dioxane \text{ yield } (\%mol) = \frac{\text{mol } 1,3 - dioxane}{\text{mol formaldehyde units in POM}} * 100$$

Conversion was expressed by weighting the residual unconverted material recovered at the end of the reaction as reported in the equation below:

$$\text{Conversion } (W\%) = \frac{\text{unconverted POM } (g)}{\text{initial POM loading } (g)} * 100$$

Reactions were quantitatively monitored through GC-FID, while qualitative analyses were conducted through GC-MS and NMR. Results are reported in Figure 10:

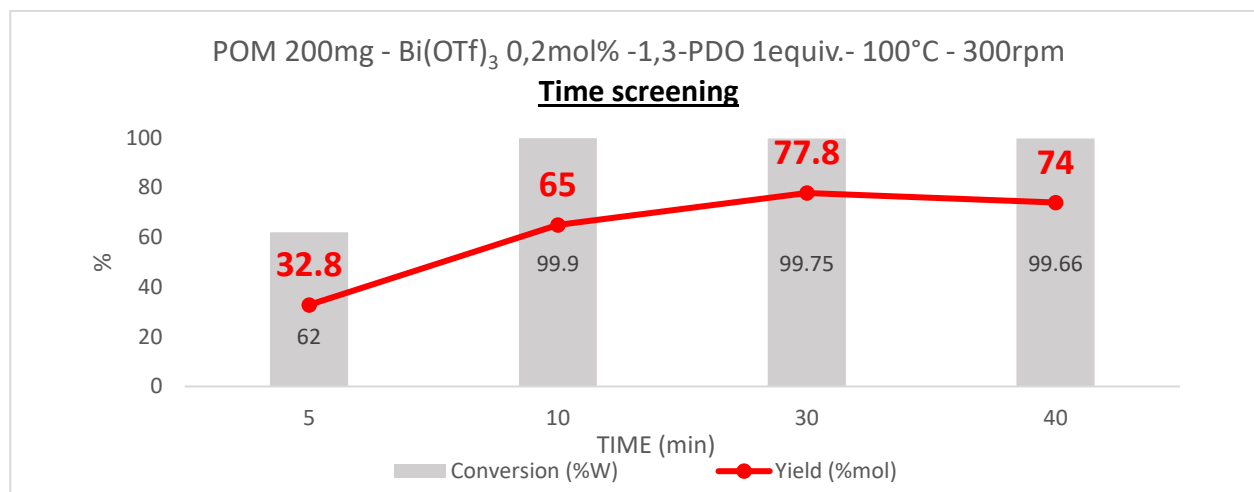


Figure 10: Time screening (Bi(OTf)<sub>3</sub>)

Almost complete conversion was achieved after only 10 minutes, and the yield reached his maximum at 30 minutes (77.8% mol).

Control experiment was conducted in the same conditions (30 minutes) to confirm the positive role of MW, performing the same experiment in an oil bath, yielding 6.2%mol with only 28.37% conversion.

It can be concluded that MW have a fundamental contribution in yield increase and time reduction, due to the fast and homogeneous heating provided.

The positive effect acted by MW in time reduction is also clearly evident if results are compared with those by K. Beydoun and J. Klankermayer that reported 86%mol yield from virgin POM in neat conditions in 16 hours.

POM type: virgin POM vs real case waste POM

Reaction using real waste POM derived from end of life lighter was performed in previously reported MW conditions, resulting in 78.8 mol% yield and almost complete conversion after 30 minutes.

Comparing the results, in optimised conditions no relevant differences can be found between virgin POM and waste POM, confirming the transferability of conditions identified in virgin POM to real-case waste POM (Figure 11).

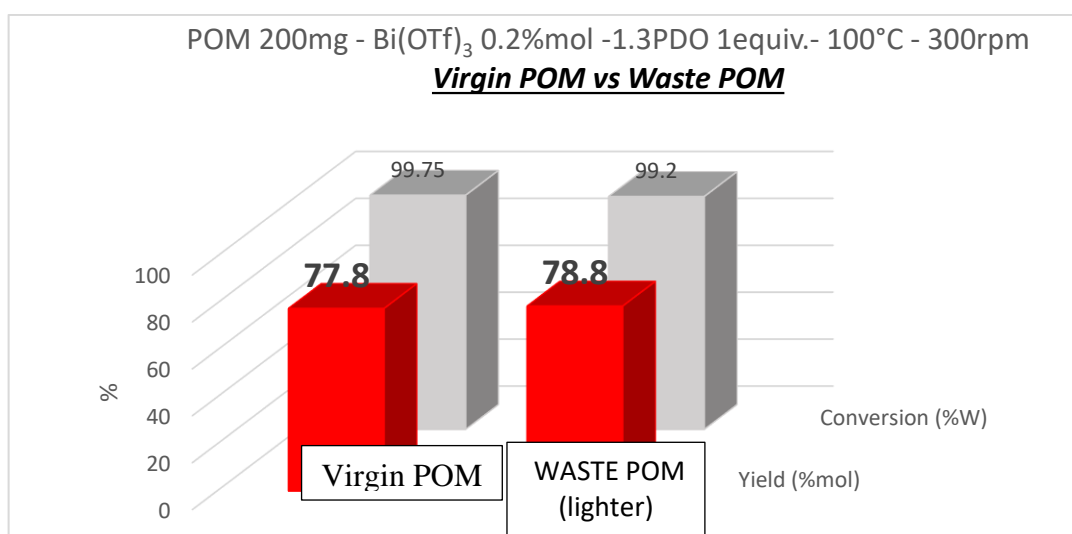


Figure 11: Virgin POM vs waste POM (Bi(OTf)<sub>3</sub>)

1,3-PDO loading effect

Slight difference in yield with K. Beydoun and J. Klankermayer (77.8 mol% vs 86 mol%), can be explained considering that 1,3-PDO was used in excess by the authors, while previously described MW experiments were conducted in equimolar conditions in order to avoid excessive use of reagent.

In a following experiment 1,3-PDO quantity was increased from 1:1 to 1.2:1 mol respect to formaldehyde units' content in POM, reaching 81.4% mol yield, very close to results reported in literature (Table 3).

	Present work 1 1,3-PDO equivalents	Present work 1.2 1,3-PDO equivalents	K. Beydoun & J. Klankerm 1.2 1,3-PDO equivalents
Time	30min	30min	16h
Temperature (°C)	100	100	100
Yield (%mol)	77.8	81.4	86
Conversion (% w)	99.75	99.90	Not reported

Table 3: Experimental results compared with literature

### *Bi(OTf)<sub>3</sub> loading reduction*

Finally, a reduction in catalyst loading was performed from 0.2% to 0.1% mol respect to formaldehyde units' content in POM, reaching a satisfactory 79.9% yield.

In Figure 12 and Figure 13, typical <sup>1</sup>H-NMR and <sup>13</sup>C-NMR spectra of reaction on virgin POM is reported. The main peaks were assigned to the product 1,3-dioxane and to unreacted reagent 1,3-propanediol.

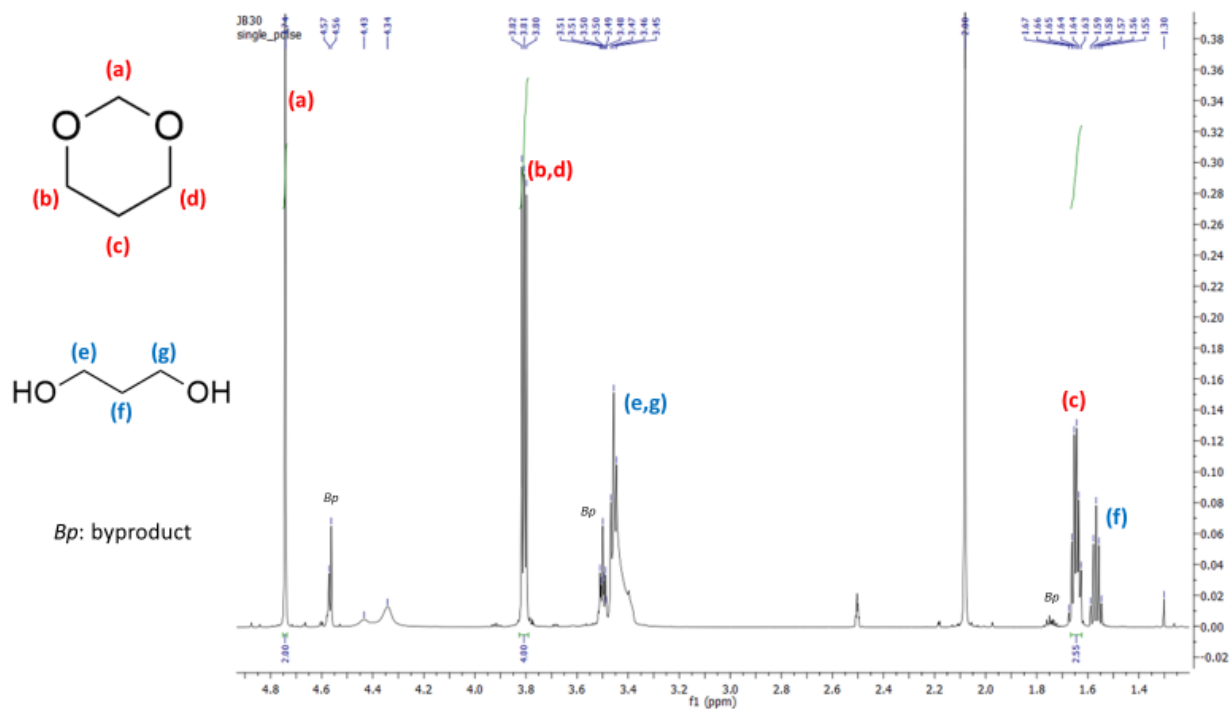


Figure 12: <sup>1</sup>H-NMR of reaction conducted using Bi(OTf)<sub>3</sub>

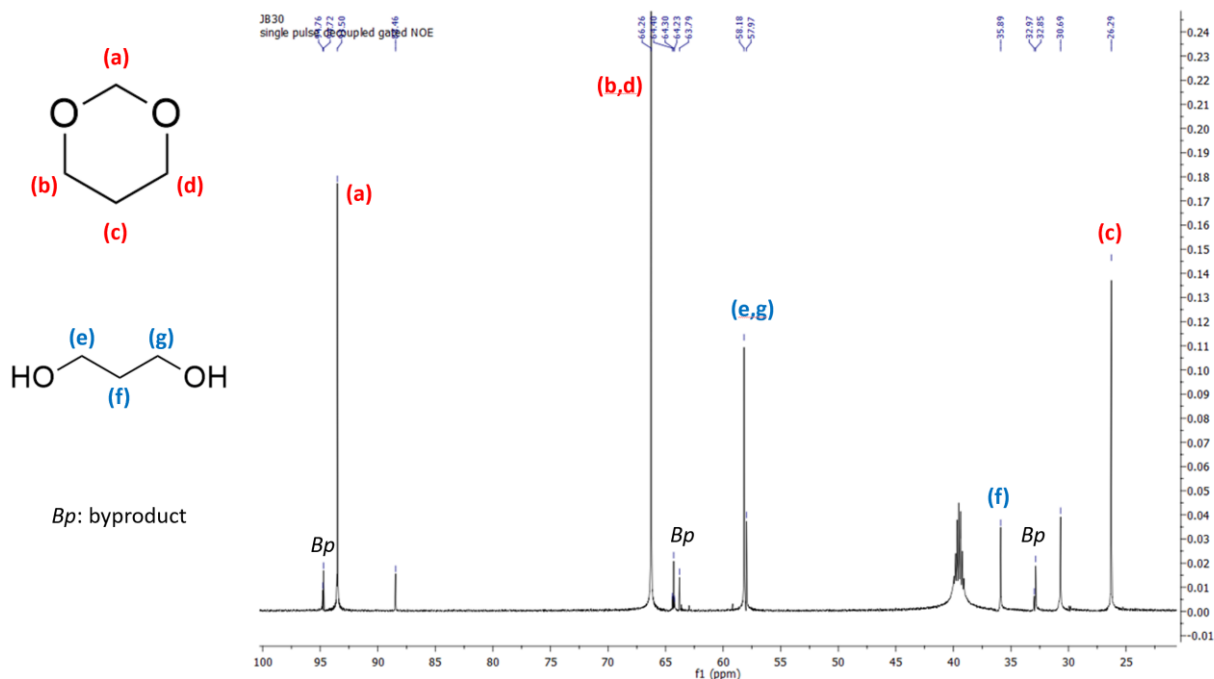


Figure 13:  $^{13}\text{C}$ -NMR of reaction conducted using  $\text{Bi}(\text{OTf})_3$

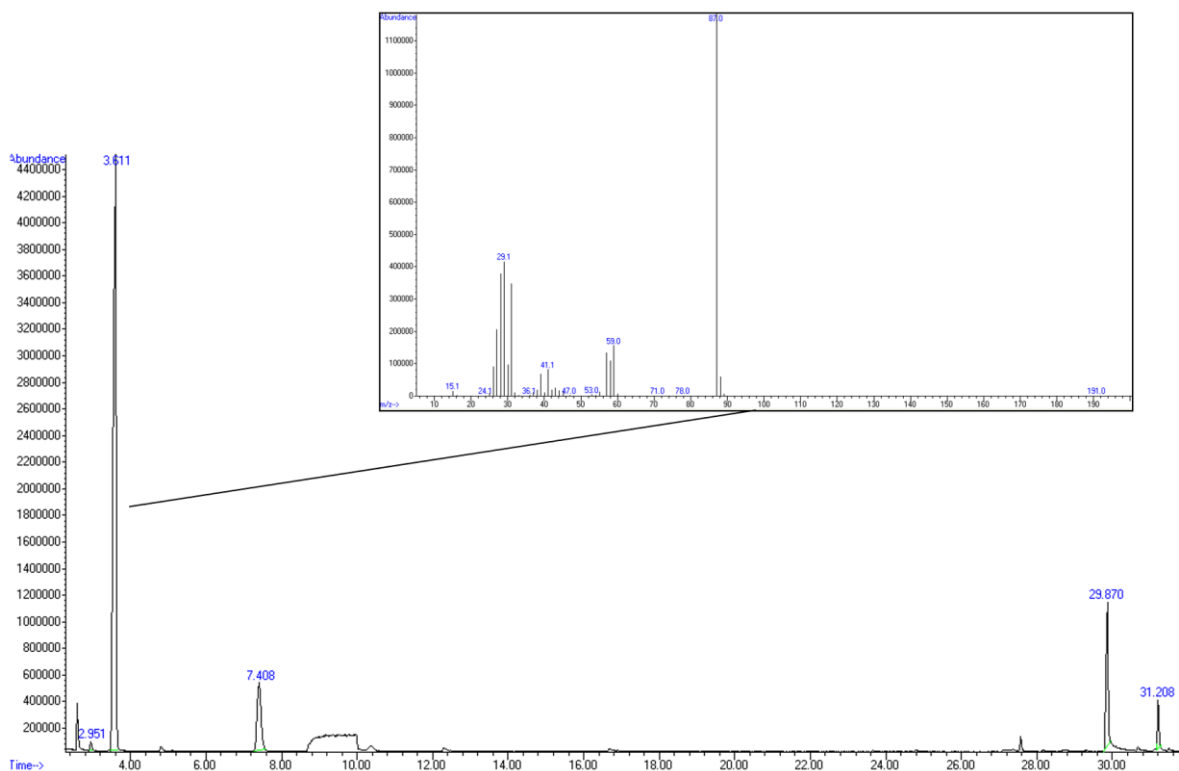


Figure 14: GC-MS of reaction conducted using  $\text{Bi}(\text{OTf})_3$

r.t.(min)	molecule	GC area (%of total)
2.951	2,2-dimethyl-1,3-dioxolane	0.656
3.811	1,3-dioxane	73.214
7.408	2,2,4-trimethyl-1,3-dioxolane	11.277
29.870	1,3,5-trioxane	12.182
31.208	2-ethyl-4-methyl-1,3-dioxolane	2.671

Table 4: Detected products in GC-MS spectra

In Figure 14 a typical GC-MS of the crude reaction is also reported. The main peak was assigned to 1,3-dioxane according to its MS spectra. 1,3-dioxane was the main product detected together with lower amounts of other cyclic acetals that can be formed during the reaction (Table 4). The presence of such molecules is also confirmed by NMR analyses and can be originated by the presence of co-monomers present in POM.

### **Sc(OTf)<sub>3</sub>**

Scandium triflate (0.2mol% respect to POM formaldehyde units' content in POM) was also investigated with commercial POM and 1.2 equivalents of 1,3-PDO (neat reaction).

77.3% yield and 99.8% conversion were achieved.

Interestingly, K. Beydoun and J. Klankermayer reported very low yield using this catalyst in solvent-assisted conditions (6% mol), thus confirming the fundamental contribution of MW to reaction.

### **6.2.2. Solid-acid catalysts**

Considering the above promising results and aiming to further improve the sustainability of the protocol, different heterogeneous catalysts were tested.

Advantages of heterogeneous catalysts rely in the easy recovery of the catalyst at the end of the reaction by simple filtration.

According to the possible reaction mechanism, the cyclic acetal is formed from formaldehyde units through acid-catalysed cyclization after POM depolymerisation. Cyclic acetals formation with solid acid catalysts was investigated by Deutsch et al. in presence of glycerol and paraformaldehyde (a POM with low polymerisation degree)<sup>23</sup>. Different types of solid-acid catalysts were therefore tested during this work phase: 3 zeolites at different Si/Al ratios and 3 different acid ion-exchange resins plus Si-propylsulphonic acid (Table 5).

<b>Solid-acid catalyst</b>		<b>SiO<sub>2</sub> : Al<sub>2</sub>O<sub>3</sub> ratio</b>
<b>Zeolite</b>	β	360 : 1
	HY	30 : 1
	HY	5.1 : 1
<b>Solid-acid catalyst</b>		<b>Exchange capacity</b>
<b>Acid ion-exchange resin</b>	Amberlite IR 120 (H) gel Sulphonic acid	1.8 (eq/L)
	Culligan Cullex gel Sulphonic acid	2 (eq/L)
	Relite RPS macroporous Sulphonic acid	2 (eq/L)
<b>Si-propylsulphonic acid</b>		0.8 meq/g

Table 5: Solid-acid catalysts investigated in this work

#### **6.2.2.1. Zeolites**

Neat reaction was studied and optimized on zeolite β with SiO<sub>2</sub>:Al<sub>2</sub>O<sub>3</sub> ratio 360:1 and once the optimised conditions were achieved two other zeolites (HY 30 :1 and HY 5.1 : 1) were tested.

### Temperature screening

Preliminary experiments devoted to define the experimental field were performed keeping as starting point the optimised time and temperature conditions previously defined for the homogeneous catalyst Bi(OTf)<sub>3</sub> as reported in Table 6

<b>POM (g)</b>	0.4000
<b>1,3-PDO loading</b>	2:1 mol respect to formaldehyde units' content in POM
<b>ZEOLITE β 360 loading</b>	1:4 zeolite:POM
<b>TEMPERATURE (°C)</b>	100
<b>TIME (min)</b>	30
<b>STIRRING (rpm)</b>	500

Table 6: Conditions for temperature screening (zeolite)

Being the catalyst heterogeneous, an excess of 1,3-PDO was used (2:1 mol respect to formaldehyde units' content in POM): indeed, the increase in liquid 1,3-PDO could be beneficial for the reaction kinetics, favouring mass transfer and improving mixing, being two out of three components of the reacting system in the solid state.

Despite promising POM conversion, 1,3-Dioxane yield was negligible in such conditions.

A temperature increase from 100°C to 130°C was therefore investigated, leading to 76.5 mol% 1,3- dioxane yield and almost complete conversion, as described in Figure 15.

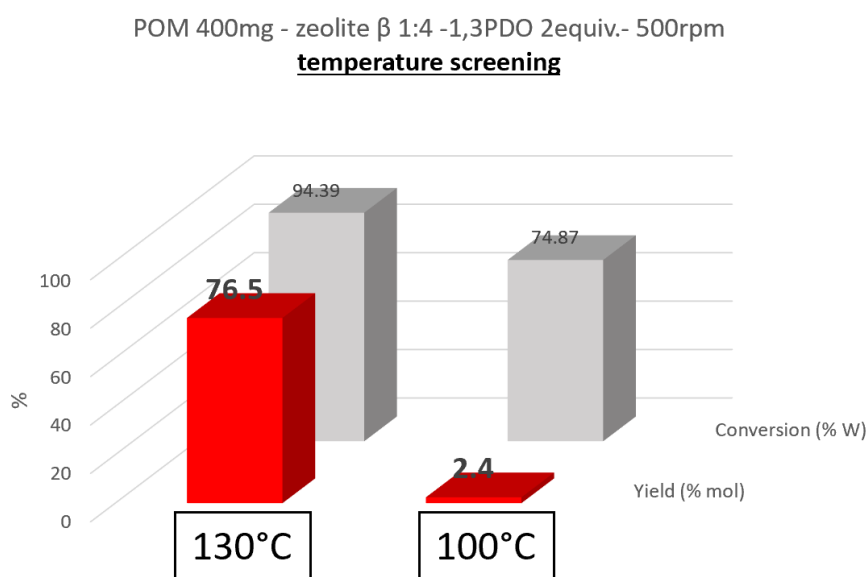


Figure 15: Temperature screening (zeolite)

Moreover, the optimal catalyst loading was defined testing 1:4 and 1:2 zeolite:POM ratios. This catalyst amount increase afforded the same yield, demonstrating that 1:4 zeolite:POM ratio was enough (Table 7).

<b>Zeolite:POM ratio</b>	<b>1,3 dioxane yield (% mol)</b>
1:4	76.5
1:2	76.4

Table 7: 1,3 dioxane yields according to different zeolite:POM ratios

Time screening

Reaction time was investigated. Appreciable yields were already obtained starting from 5 minutes, reaching the maximum at 30 min with >90% conversion and surprisingly 76.5 mol% 1,3-dioxane yield (Figure 16).

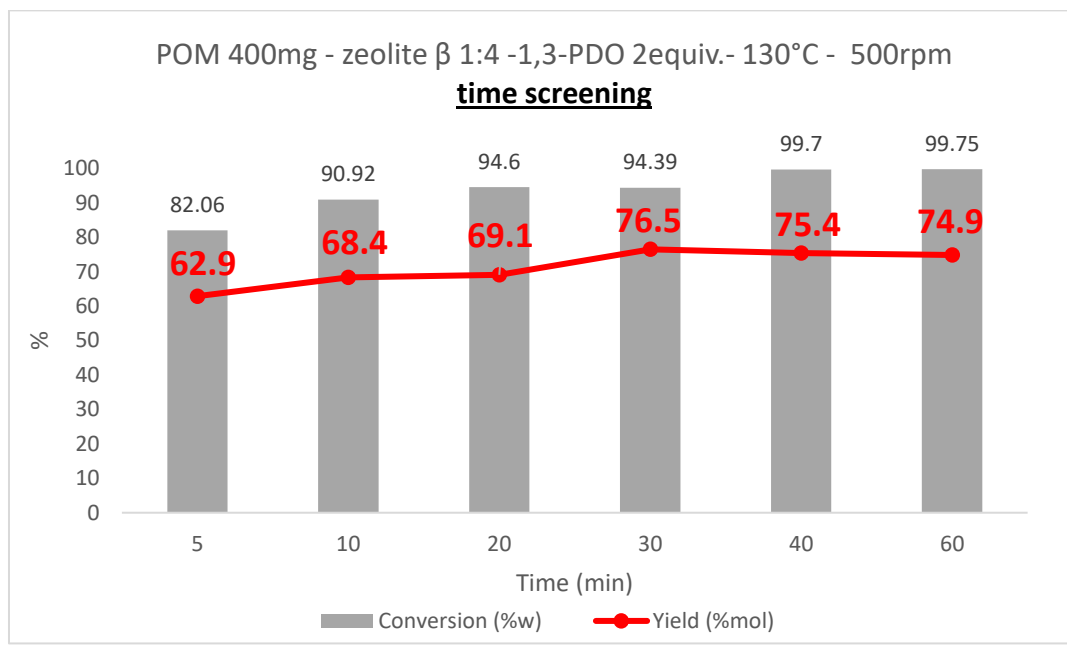


Figure 16: Time screening (zeolite)

1,3-PDO loading

Finally, 1,3-PDO loading was optimised, aiming to reduce reagent excess at minimum (Figure 17).

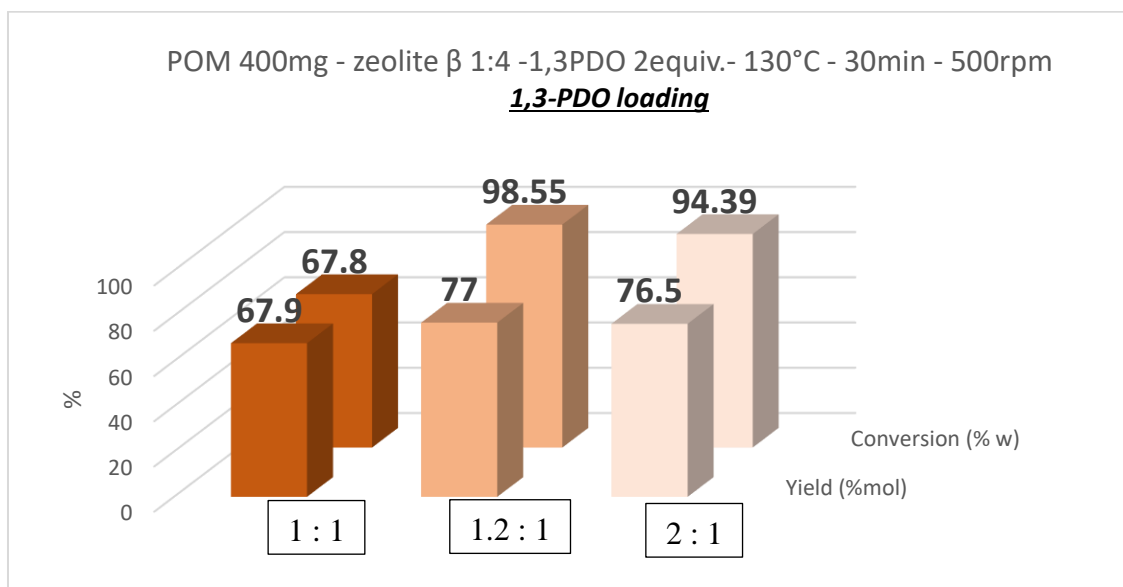


Figure 17: 1,3-PDO loading (zeolite)



As can be seen from Figure 17, 1,3-PDO excess can be reduced to 1.2 equivalents without any loss in yield.

A subsequent reduction to equimolar amount with POM led to 10% yield reduction and approx. 30% lower conversion, probably due to inefficient mixing of the system.

Final optimised condition can be summarised as follows (Table 8):

<b>POM (g)</b>	0.4000
<b>1,3 PDO loading</b>	1.2:1 mol respect to formaldehyde units' content in POM
<b>ZEOLITE <math>\beta</math> 360 loading</b>	1:4 zeolite:POM
<b>TEMPERATURE (<math>^{\circ}</math>C)</b>	130
<b>TIME (min)</b>	30
<b>STIRRING (rpm)</b>	500

Table 8: Optimised conditions (zeolite)

### Zeolite screening

Optimised reaction conditions were applied by changing the zeolite type and by using both commercial grade virgin POM and real waste POM derived from end of life lighter.

As can be seen in Figure 18, both zeolite  $\beta$  with  $\text{SiO}_2:\text{Al}_2\text{O}_3$  ratio 360:1 and zeolite Y with  $\text{SiO}_2:\text{Al}_2\text{O}_3$  ratio 30:1 showed similar performances with comparable results both on virgin POM and on waste POM. Zeolite Y with  $\text{SiO}_2:\text{Al}_2\text{O}_3$  ratio 5.1:1 showed lower performances.

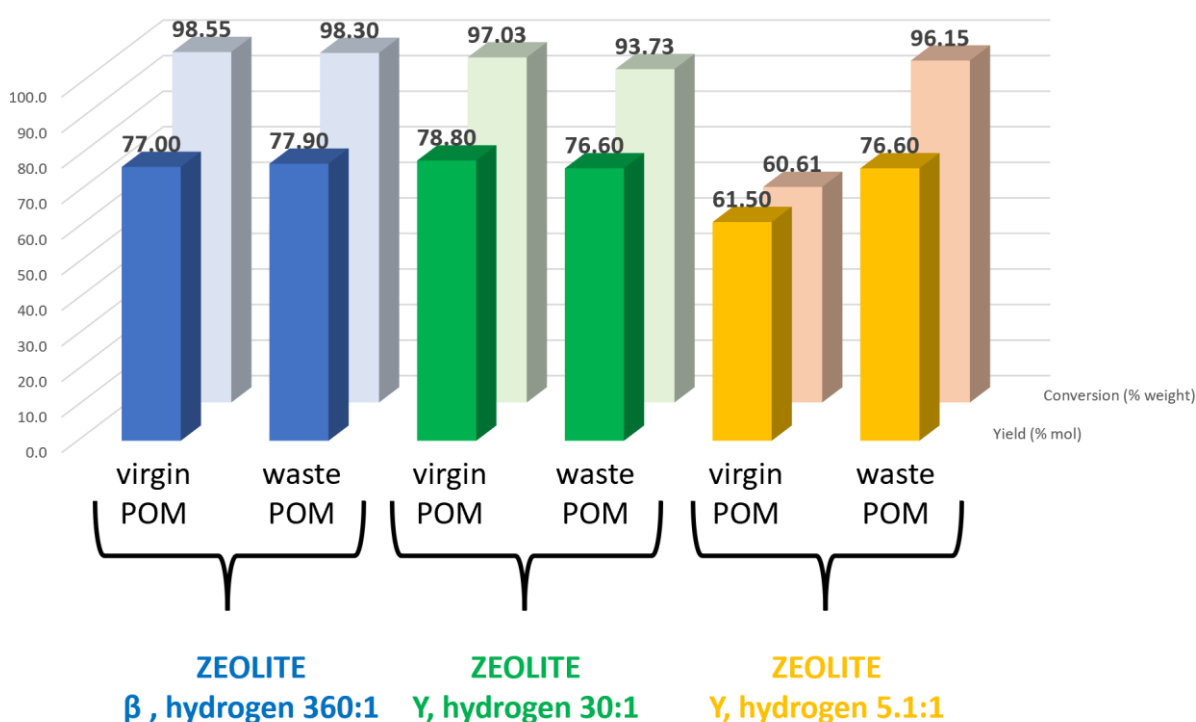


Figure 18: Zeolite screening

### Catalyst recycle

Finally, catalyst recycle experiments were performed: zeolite  $\beta$  was recovered by simple filtration at the end of the optimised reaction with virgin POM, washed with acetone and dried

for 4 hours in oven at 400°C. Zeolite was then re-used in a second reaction cycle, yielding 75.7% mol 1,3-dioxane yield and 96% conversion.

As the results of the second reaction cycle are very similar to those achieved in the first one (77.0% mol yield and 98.55% w conversion), it can be concluded that zeolites can be proficiently used as easy-recyclable catalysts for high-yield 1,3-dioxane production from POM materials.

#### 6.2.2.2. Ion exchange resins

Neat reaction was then studied and optimized on Amberlite IR 120 (H) ion exchange resin and once the optimised conditions were achieved two other ion exchange resins (Relite RPS and Culligan Cullex) were tested.

##### Temperature screening

Optimal temperature was defined in preliminary experiments: both 100°C (previously optimised temperature for metal triflate catalysts) and 130°C (previously optimised temperature for zeolites catalysts) were investigated.

Again, 1,3-PDO was kept in 2:1 mol ratio respect to formaldehyde units' content in POM and time was kept constant to 30 minutes. Resin loading was kept equals to 1:2 ratio with POM (Table 9).

<b>POM (g)</b>	0.4000
<b>1,3 PDO</b>	2:1 mol respect to formaldehyde units' content in POM
<b>Amberlite IR 120 (H)</b>	1:2 resin:POM
<b>TEMPERATURE (°C)</b>	100 - 130
<b>TIME (min)</b>	30
<b>STIRRING (rpm)</b>	500

Table 9: Conditions for temperature screening (resin)



Figure 19: Resin degradation phenomena during the reaction conducted at 130°C

The product recovered at 130°C showed light yellow colour, thus suggesting resin degradation phenomena during the reaction (Figure 19). Therefore, 100°C was selected as the optimised temperature for subsequent reaction optimisation.

### Time screening

Reaction time was investigated from 5 to 60 minutes (Figure 20).

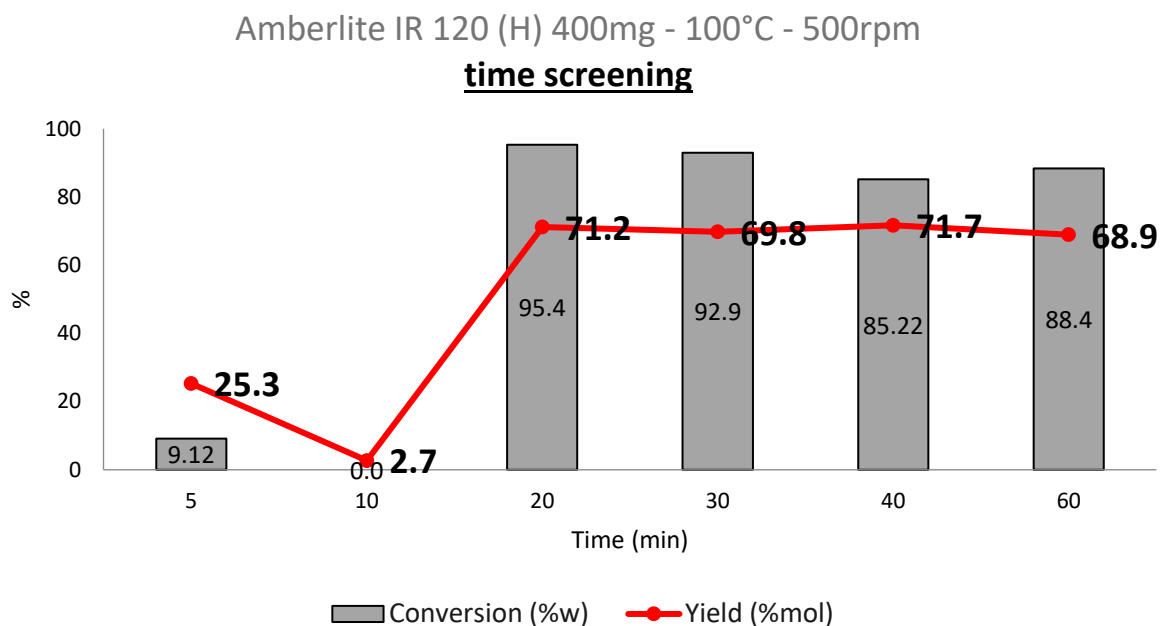


Figure 20: Time screening (resin)

The highest yield (71.2% mol) was achieved at 20 minutes with 95.4% conversion. Lower times (5, 10 minutes) lead to inconclusive results because in such conditions reaction is in the very early stage and most of POM remains unconverted: catalysts, reagents and products remain incorporated in unconverted, melted POM thus making impossible to properly evaluate yield and conversion.

Resin loading was investigated in optimised conditions (20 minutes, 100°C, 1,3-PDO 2:1 mol ratio respect to formaldehyde units' content in POM).

Resin:POM ratio	1,3 dioxane yield (% mol)
1:4	38
1:2	71.2
1:1	71.5

Table 10: 1,3 dioxane yields according to different resin:POM ratios

When 1:2 and 1:1 resin:POM ratios were used similar results were achieved, meanwhile a reduction to 1:4 resin:POM ratio led to lower yields. The optimal Resin:POM ratio was therefore established equals to 1:2.

### 1,3-PDO loading

Finally, 1,3-PDO loading was optimised, aiming to reduce reagent excess at minimum.

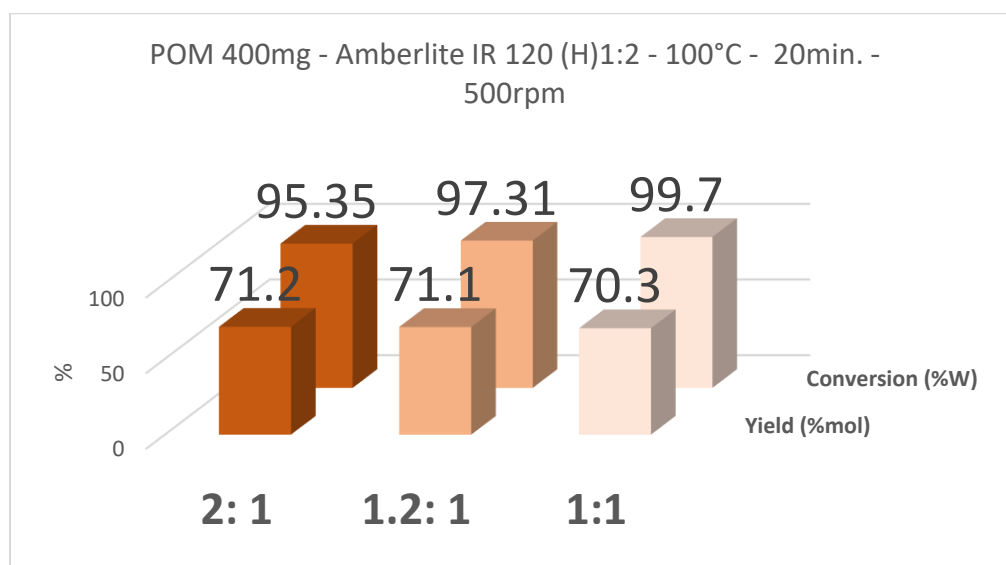


Figure 21: 1,3-PDO loading (resin)

As can be seen from the graph, 1,3-PDO excess can be reduced from 2:1 to equimolar without any loss in yield (Figure 21).

### POM type: virgin POM vs real case waste POM

Reaction using waste POM derived from end of life lighter was performed in previously reported MW conditions, resulting in 75.1% mol yield and almost complete conversion (99%).

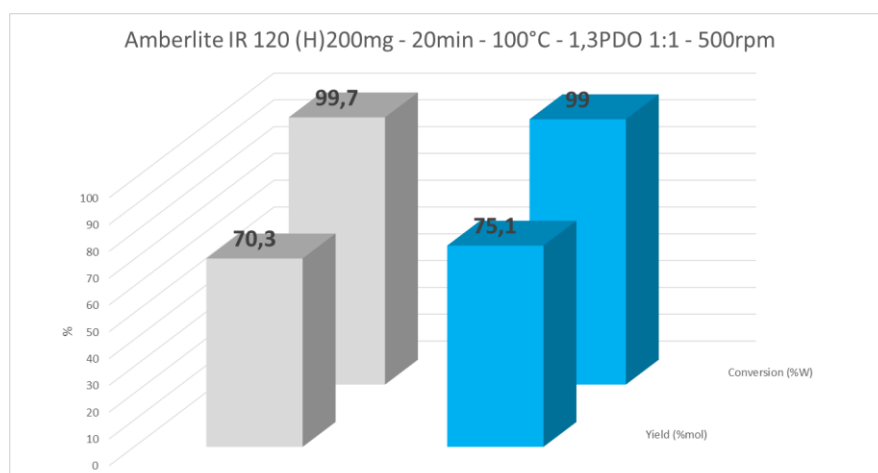


Figure 22: Virgin POM vs waste POM (resin)

By comparing the results, it is evident that in optimised conditions no relevant differences can be found between virgin POM and waste POM, confirming the transferability of conditions identified in virgin POM to real-case waste POM.

Final optimised conditions are summarised in Table 11.

<b>POM (g)</b>	0.4000
<b>1,3-PDO loading</b>	1.2:1 mol respect to formaldehyde units' content in POM
<b>Resin loading</b>	1:4 resin:POM
<b>TEMPERATURE (°C)</b>	130
<b>TIME (min)</b>	30
<b>STIRRING (rpm)</b>	500

Table 11: Optimised conditions (resin)

Resin screening

The optimised reaction conditions were applied for a screening of suitable resins and by using both commercial grade virgin POM and real waste POM derived from end of life lighter. The three resins showed similar results, despite IR120 was confirmed as the best one (Figure 23).

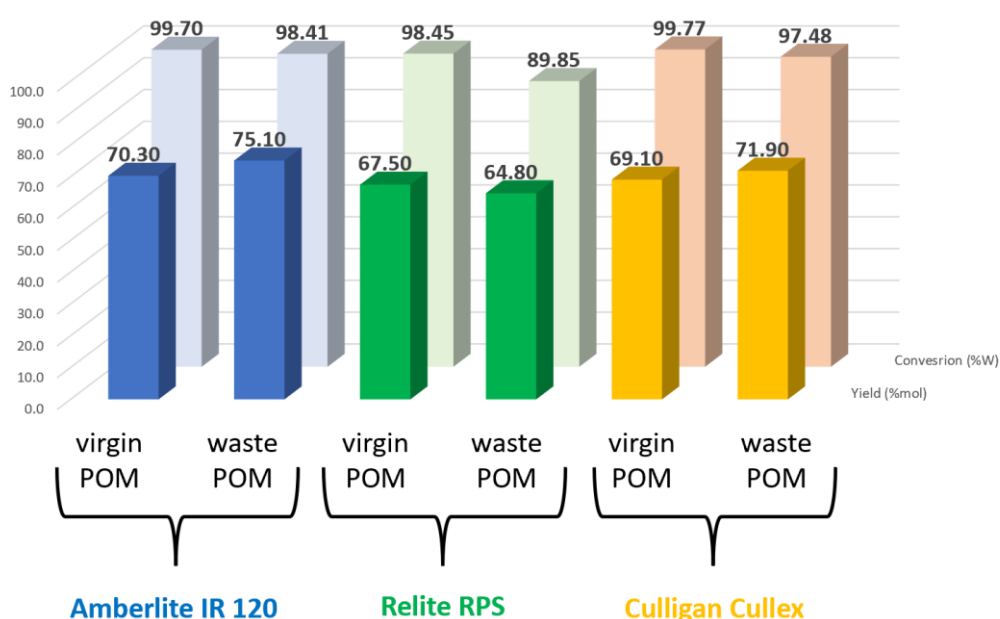


Figure 23: Resin screening

Si-propylsulphonic acid

Si-propylsulphonic acid was investigated as solid catalyst by adopting the same resin optimised conditions. Both virgin POM and real waste POM derived from end of life lighter were used as substrates (Figure 24).

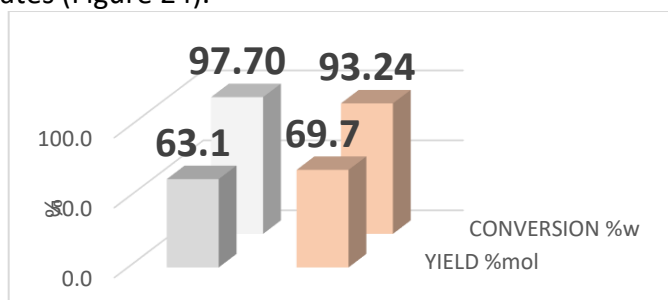


Figure 24: virgin POM vs waste POM

### 6.3. CONCLUSIONS

In this chapter, an already existing protocol for polyoxymethylene chemical recycle was improved through the use of monomode microwave reactor and various types of catalysts. 1,3-dioxane was achieved as main product in satisfactory yields.

In the first part of the work a substantial reduction of solvent-less reaction time respect to literature, from 16 hour to 30 minutes, was possible thanks to the efficient and homogeneous microwave heating. Reduction of reaction time can be considered a fundamental step for future industrialisation of the protocol, lowering the energy consumption.

Moreover, a 50% reduction of catalyst loading (from 0.2 to 0.1% mol) was possible without any negative impact in yield. A second metal triflate catalyst ( $\text{Sc}(\text{Otf})_3$ ) was tested in optimised conditions achieving engaging yield.

Both virgin and waste polyoxymethylene were tested with similar results, thus demonstrating the effective feasibility of the protocol for chemical recycling.

In the second part of the work, homogeneous metal triflates catalysts were substituted with less expensive solid acid catalysts such as zeolites, resins and Si-propylsulphonic acid. The use of low-price solid acid catalysts allowed achievement of yields comparable to literature-reported yields with the advantage of easier catalyst recovery. Indeed, among all solid acid catalysts tested, zeolite  $\beta$  360 and zeolite Y 30 showed the best performances (both virgin and waste polyoxymethylene) leading to results very close to results reported in case of  $\text{Bi}(\text{Otf})_3$  homogeneous catalyst. These catalysts proved reusable in a second cycle, affording almost the same yields as the first one.

The involvement of renewable, biomass-derived 1,3-propanediol demonstrates the possibility to include biorefinery products in a chemical recycling protocol, thus increasing its sustainability.

As main future perspective, a scaling-up of the protocol should be evaluated, moving from monomode microwave reactor (suitable for lab-scale experiments) to multimode microwave reactor (more suitable when higher amounts of materials are treated).

## 6.4. EXPERIMENTAL

### Reagents

All reagents used in this work were used without any further purification.

Virgin POM 3mm granules were purchased from GoodFellow (Cambridge, UK);

Bi(OTf)<sub>3</sub> (CAS:88189-03-1) was purchased from Alfa Aesar;

Sc(OTf)<sub>3</sub> (CAS:144026-79-9) was purchased from Sigma-Aldrich;

1.3 propanediol (CAS:504-63-2) was purchased from Alfa Aesar.

### Sample analyses

GC-MS analyses were conducted on an Agilent 6890 GC (Agilent Technologies - USA), connected to an Agilent Network 5973 mass detector, using a MEGA-5 MS column (30 m capillary column, 0.25 mm and film thickness of 0.25 μm).

The temperature program was performed as follows:

- initial maintenance in isotherm for 5 minutes at 65°C,
- ramp 10°C / minute up to 100°C
- isotherm at 100°C for 1 minute,
- ramp 20°C / minute up to 230°C
- isotherm 230°C for 1 minute,
- ramp 20°C / minute up to 300°C
- isotherm at 300°C for 5 minutes.

Split injection 1:20, injector temperature 250 ° C, detector temperature 280 ° C. Carrier gas: He.

The GC-FID analyses were conducted on an Agilent 7820A GC (Agilent Technologies - USA), connected to a GC FID detector using a MEGA-5 MS column (capillary column of 30 m, of 0.25 mm and film thickness 0.25 μm).

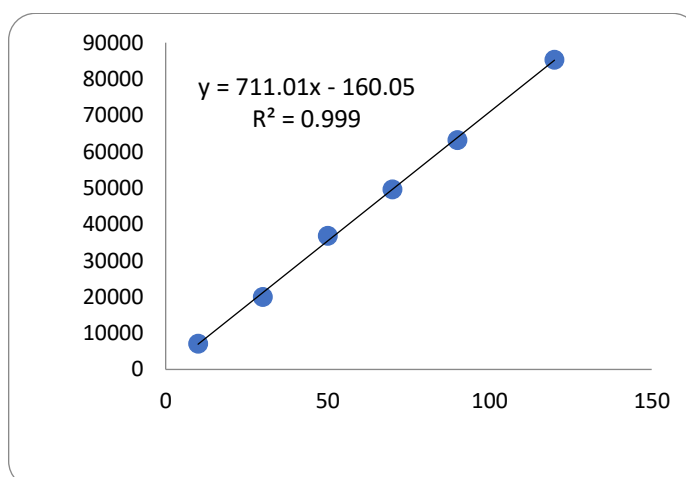
The temperature program was performed as follows:

- initial maintenance in isotherm for 3 minutes at 50 ° C,
- ramp 3°C / minute up to 80°C,
- ramp 10°C / minute up to 300°C,
- isotherm at 300°C for 10 minutes.

Split injection 1:20, injector temperature 250 ° C, detector temperature 280 ° C. Carrier gas: He.

For quantitative analyses, BMF calibration curve was performed in GC-FID.

Calibration curve is reported below:



#### MW-assisted reaction using metal triflate catalyst

200mg of virgin/waste POM were weighted and placed in a 10mL vial. Proper quantities of 1,3-PDO and metal triflate catalyst ( $\text{Bi}(\text{OTf})_3$  or  $\text{Sc}(\text{OTf})_3$ ) were added. Magnetic stirrer was performed, and the vial was closed with cap.

Vial was placed in the cavity of monomode MW reactor (Monowave 300, Anton Paar) and heated to reach desired temperature. "heat as fast as possible" heating mode was selected to reach desired temperature in minor time possible. Stirring was kept constant equals to 300rpm.

At the end of the reaction, vial was removed from the reactor and the crude reaction was transferred in an Eppendorf tube. This was then subjected to centrifugation (1 min, 21000rpm), aiming to separate non converted solid granules of POM from liquid fraction containing product 1,3-dioxane.

Liquid fraction was recovered. The whole procedure was repeated three times washing the reaction vial with acetone in order to quantitatively recover the product and unconverted POM.

The crude was filtered through a celite pad, aiming to remove catalyst, and transferred in a 10mL volumetric flask for further GC-FID and GC-MS analysis.

#### MW-assisted reaction using solid-acid catalysts

400mg of virgin/waste POM was weighted in a 30mL vial. Proper quantities of 1,3-PDO and of the solid acid catalyst were added to the vial. The vial was closed with a cap, and the magnetic stirrer was added.. The vial was placed in a monomode MW reactor (Monowave 300, Anton Paar) and heated to reach the desired temperature. "heat as fast as possible" heating mode was selected to reach desired temperature in minor time possible. Stirring was kept constant equals to 300rpm.

At the end of the reaction, the vial was removed from the reactor and crude was transferred in an Eppendorf tube. This was then subjected to centrifugation (1 min, 21000rpm), aiming to separate the non-converted solid granules of POM and the solid acid catalyst from liquid fraction containing product 1,3-dioxane.

Liquid fraction was recovered. The whole procedure was repeated three times washing reaction vial with acetone in order to quantitatively recover the product and unconverted POM.

After centrifugation crude was finally transferred in a 10mL volumetric flask for further GC-FID and GC-MS analysis.



## 6.5. REFERENCES

- (1) Geyer, R.; Jambeck, J. R.; Law, K. L. Production, Use, and Fate of All Plastics Ever Made. *Sci. Adv.* **2017**, *3* (7), e1700782. <https://doi.org/10.1126/sciadv.1700782>.
- (2) <https://ec.europa.eu/eurostat/web/products-eurostat-news/-/Ddn-20210113-1>.
- (3) [https://ec.europa.eu/eurostat/statistics-explained/index.php?Title=Packaging\\_waste\\_statistics#Waste\\_generation\\_by\\_packaging\\_material](https://ec.europa.eu/eurostat/statistics-explained/index.php?Title=Packaging_waste_statistics#Waste_generation_by_packaging_material).
- (4) Schmaltz, E.; Melvin, E. C.; Diana, Z.; Gunady, E. F.; Rittschof, D.; Somarelli, J. A.; Virdin, J.; Dunphy-Daly, M. M. Plastic Pollution Solutions: Emerging Technologies to Prevent and Collect Marine Plastic Pollution. *Environ. Int.* **2020**, *144*, 106067. <https://doi.org/10.1016/j.envint.2020.106067>.
- (5) World Economic Forum, 2016. The New Plastics Economy: Rethinking the Future of Plastics. World Economic Forum.
- (6) Schyns, Z. O. G.; Shaver, M. P. Mechanical Recycling of Packaging Plastics: A Review. *Macromol. Rapid Commun.* **2021**, *42* (3), 2000415. <https://doi.org/10.1002/marc.202000415>.
- (7) Thiounn, T.; Smith, R. C. Advances and Approaches for Chemical Recycling of Plastic Waste. *J. Polym. Sci.* **2020**, *58* (10), 1347–1364. <https://doi.org/10.1002/pol.20190261>.
- (8) Ragaert, K.; Delva, L.; Van Geem, K. Mechanical and Chemical Recycling of Solid Plastic Waste. *Waste Manag.* **2017**, *69*, 24–58. <https://doi.org/10.1016/j.wasman.2017.07.044>.
- (9) Solis, M.; Silveira, S. Technologies for Chemical Recycling of Household Plastics – A Technical Review and TRL Assessment. *Waste Manag.* **2020**, *105*, 128–138. <https://doi.org/10.1016/j.wasman.2020.01.038>.
- (10) Zhou, N.; Dai, L.; Lv, Y.; Li, H.; Deng, W.; Guo, F.; Chen, P.; Lei, H.; Ruan, R. Catalytic Pyrolysis of Plastic Wastes in a Continuous Microwave Assisted Pyrolysis System for Fuel Production. *Chem. Eng. J.* **2021**, *418*, 129412. <https://doi.org/10.1016/j.cej.2021.129412>.
- (11) Kumagai, S.; Nakatani, J.; Saito, Y.; Fukushima, Y.; Yoshioka, T. Latest Trends and Challenges in Feedstock Recycling of Polyolefinic Plastics. *J. Jpn. Pet. Inst.* **2020**, *63* (6), 345–364. <https://doi.org/10.1627/jpi.63.345>.
- (12) Aishwarya, K. N.; Sindhu, N. Microwave Assisted Pyrolysis of Plastic Waste. *Procedia Technol.* **2016**, *25*, 990–997. <https://doi.org/10.1016/j.protcy.2016.08.197>.
- (13) Bäckström, E.; Odellius, K.; Hakkarainen, M. Ultrafast Microwave Assisted Recycling of PET to a Family of Functional Precursors and Materials. *Eur. Polym. J.* **2021**, *151*, 110441. <https://doi.org/10.1016/j.eurpolymj.2021.110441>.
- (14) Bäckström, E.; Odellius, K.; Hakkarainen, M. Trash to Treasure: Microwave-Assisted Conversion of Polyethylene to Functional Chemicals. *Ind. Eng. Chem. Res.* **2017**, *56* (50), 14814–14821. <https://doi.org/10.1021/acs.iecr.7b04091>.
- (15) Myren, T. H. T.; Stinson, T. A.; Mast, Z. J.; Huntzinger, C. G.; Luca, O. R. Chemical and Electrochemical Recycling of End-Use Poly(Ethylene Terephthalate) (PET) Plastics in Batch, Microwave and Electrochemical Reactors. *Molecules* **2020**, *25* (12), 2742. <https://doi.org/10.3390/molecules25122742>.
- (16) Kang, M. J.; Yu, H. J.; Jegal, J.; Kim, H. S.; Cha, H. G. Depolymerization of PET into Terephthalic Acid in Neutral Media Catalyzed by the ZSM-5 Acidic Catalyst. *Chem. Eng. J.* **2020**, *398*, 125655. <https://doi.org/10.1016/j.cej.2020.125655>.
- (17) DuPont Delrin Acetal Copolymer White Paper.Pdf.
- (18) *Polyoxymethylene Handbook: Structure, Properties, Applications and Their Nanocomposites*; Luftl, S., P. M., V., Sarathchandran, C., Eds.; John Wiley & Sons, Scrivener Publishing: Hoboken, New Jersey : Salem, MA, 2014.
- (19) Beydoun, K.; Klankermayer, J. Efficient Plastic Waste Recycling to Value-Added Products by Integrated Biomass Processing. *ChemSusChem* **2020**, *13* (3), 488–492. <https://doi.org/10.1002/cssc.201902880>.
- (20) Chopade, S. P.; Sharma, M. M. Acetalization of Ethylene Glycol with Formaldehyde Using Cation-Exchange Resins as Catalysts: Batch versus Reactive Distillation. 9.
- (21) Zhang, Y.; Liu, D.; Chen, Z. Production of C2–C4 Diols from Renewable Bioresources: New Metabolic Pathways and Metabolic Engineering Strategies. *Biotechnol. Biofuels* **2017**, *10* (1), 299. <https://doi.org/10.1186/s13068-017-0992-9>.
- (22) Xu, B.; Ma, C. Advances in the Production of 1, 3-Propanediol by Microbial Fermentation; Hangzhou City, China, 2019; p 020048. <https://doi.org/10.1063/1.5110842>.
- (23) Deutsch, J.; Martin, A.; Lieske, H. Investigations on Heterogeneously Catalysed Condensations of Glycerol to Cyclic Acetals. *J. Catal.* **2007**, *245* (2), 428–435. <https://doi.org/10.1016/j.jcat.2006.11.006>.

## **GENERAL CONCLUSIONS**

The present PhD thesis showcased different successful strategies for full biomass valorisation. Cellulose, hemicellulose, lignin, and secondary metabolites were properly extracted and/or converted by means of non-conventional technologies (microwaves and ultrasounds) aiming to obtain high added value products, consistently with circular economy principles and biorefinery concept. Each strategy proposed in this manuscript required particular attention in the choice of the appropriate technology and overall approach, aiming to maximise product yield, minimise reaction times and at the same time keeping the protocols as versatile and simple as possible.

It is hoped that this manuscript could give a contribution, albeit small, to the development of a new perspective, towards a more sustainable future.

## APPENDIX

### Publications

- **Process intensification technologies for the recovery of valuable compounds from cocoa by-products**

Francesco Mariatti, Veronika Gunjević, Luisa Boffa, Giancarlo Cravotto  
*Innovative Food Science & Emerging Technologies*, Vol. 68, March 2021, 102601  
<https://doi.org/10.1016/j.ifset.2021.102601>

- **A smart use of biomass derivatives to template an: Ad hoc hierarchical SAPO-5 acid catalyst**

Francesco Mariatti, Ivana Miletto, Geo Paul, Leonardo MarcheseSilvia Tabasso, Maela Manzoli,  
Giancarlo Cravotto , Enrica Gianotti  
*RSC advances*, issue 63, 2020  
<https://doi.org/10.1039/D0RA06353C>

- **Effect of different non-conventional extraction methods on the antibacterial and antiviral activity of fucoidans extracted from *Nizamuddinina zanardinii***

Mehdi Alboofetileh, Masoud Rezaei, Mehdi Tabarsa, Massimo Rittà, Manuela Donalisio,  
Francesco Mariatti, Sang Guan You, David Lembo, Giancarlo Cravotto  
*International Journal of Biological Macromolecules*, Vol. 124, 1March 2019, pp 131-137  
<https://doi.org/10.1016/j.ijbiomac.2018.11.201>

- **Subcritical water extraction as an efficient technique to isolate biologically-active fucoidans from *Nizamuddinina zanardinii***

Mehdi Alboofetileh, Masoud Rezaei, Mehdi Tabarsa, Sang Guan You, Francesco Mariatti,  
Giancarlo Cravotto  
*International Journal of Biological Macromolecules*, Vol. 128, 1May 2019, pp 244-253  
<https://doi.org/10.1016/j.ijbiomac.2019.01.119>

- **Sustainable Microwave-Assisted Aerobic Oxidation of Tomato Plant Waste into Bioaromatics and Organic Acids**

Silvia Tabasso, Francesco Mariatti, Giorgio Grillo, Luisa Boffa, Pier Silvio Tibaldi, Giancarlo Cravotto  
*Industrial & Engineering Chemistry Research*, 2019, 58, 20, 8578–8584  
<https://pubs.acs.org/doi/10.1021/acs.iecr.9b01330>

- **Pilot scale cavitation reactors and other enabling technologies to design the industrial recovery of polyphenols from agro-food by-products, a technical and economical overview**

Giancarlo Cravotto, Francesco Mariatti, Veronika Gunjevic, Massimo Secondo, Matteo Villa,  
Jacopo Parolin, Giuliano Cavaglià  
*Foods* 2018 Sep; 7(9): 130.  
[10.3390/foods7090130](https://doi.org/10.3390/foods7090130)

## ACKNOWLEDGEMENTS

Grazie,

Al mio tutor, professor Giancarlo Cravotto, per avermi trasmesso ed insegnato con il suo prezioso esempio l'entusiasmo e la passione per la ricerca. Per le enormi opportunità di crescita che mi ha sempre offerto, permettendomi di arrivare fino a qui. Per essere sempre stato punto di riferimento e fonte inesauribile di ispirazione. Non avrei potuto sperare in un tutor migliore. Grazie.

Alla mia co-tutor, professoressa Silvia Tabasso, per la sua preziosa guida, per tutto l'aiuto, il supporto e la disponibilità ad un continuo confronto, scambio di opinioni ed idee che mi hanno permesso di raggiungere questo importante traguardo.

Alla mia famiglia: a mia madre Ivana, a mio padre Valerio a mia sorella Cecilia.

Per avermi trasmesso quei valori profondi che mi permettono, ogni giorno, di scegliere da che parte stare.

Per avermi insegnato ed aiutato in ogni modo a credere in me.

Perché spesso avete creduto in me più di quanto lo facessi io stesso.

A voi dedico la fatica di questo lavoro e di questi anni, sperando di rendervi sempre orgogliosi di me.

A Francesca, che è energia allo stato puro.

Perché io quella sera lo sapevo da subito. Lo sapevo e basta.

Per ogni piccolo passo fatto insieme che poi messi uno dietro l'altro, fanno passi da gigante.

Perché mi spingi ad essere ogni giorno un uomo migliore.

Perché sorridi sempre e sei sempre di buon umore, e così mi fai stare bene.

Per il futuro, luminoso, che ci aspetta.

Ti amo.

A Maria Vittoria, nonna Maria, zio Giovanni, Cecilia, Andrea.

Persone autentiche dal cuore grande.

Per avermi accolto nella vostra casa con naturalezza, serenità ed affetto.

A Case e Denna, gli Amici di tutta una vita, insostituibili perché c'erano, ci sono e ci saranno sempre.

Al tutto mio gruppo di ricerca composto di persone fantastiche e brillanti.

A Giorgio, perché se avere un collega così è una fortuna, averlo come amico lo è ancor di più.

Non so neanche più per quanti anni abbiamo condiviso questo percorso. Da organica 1 al dottorato. Un percorso infinito fatto di infiniti momenti di confronto, caffè, risate, ragionamenti, scherzi, pranzi, cene, aperitivi, studio, esperimenti. Potrei continuare all'infinito. Spero basti dirti Grazie, Bro!

A Veronika, per essere sempre stata propositiva e positiva, per il tuo prezioso ed inestimabile rigore e per la tua competenza. Lavorare con te è sempre stato naturale e spontaneo. Se una parte importante di questa tesi esiste, è anche grazie a te.

A Federico, prima tesista, poi collega, anzi di più, amico. Per le nostre infinite ore passate “in ufficio” a fare infinite ipotesi, ragionamenti ed analisi sul nostro lavoro.

A Bellu ed Elisa, che ringrazio insieme e loro sanno il perché. Siete stati amici preziosi e supporto fondamentale nei momenti difficili. Per avermi dato sempre sostegno, che fosse con chiacchierate e discussioni infinite o con un semplice scherzo: grazie!

Ai mitici Stefano e Robertino, sempre disponibili e sempre di buon umore. Dire che siete una presenza fondamentale in laboratorio è dire poco!

A Fabio con il quale ho condiviso il faticoso percorso del dottorato (fatto di corsi, convegni e summer school) ma anche la decisamente meno faticosa passione per gli incontri di MMA.

A Lorenzo, perché parlare di Toro di fronte ad un caffè ed una siga è stato appuntamento fisso per parecchi lunedì.

Ai ragazzi che ho avuto l'onore di seguire nei loro percorsi di tesi: a Jimmy, dotato di una manualità fuori dal comune; a Mirko, per il suo rigore e per la bella amicizia che è nata nei seppur pochi mesi passati a lavorare insieme; ad Alessio per la sua infinita pazienza e dedizione al lavoro.

Il vostro contributo è stato a dir poco fondamentale.

Lavorare con voi mi ha permesso di crescere.

Grazie anche a (in ordine sparso): Clelia, Sasi, Katia, Domenico, Lollo from baladin, Luisa, la professoressa Maela Manzoli e la professoressa Emanuela Calcio Gaudino.